



The University of  
**Nottingham**

**Identification and analysis of the  
synergistic targets of TBX5 and GATA-4**

**Bhakti R. Patel, BSc**

**MEDICAL LIBRARY**  
QUEENS MEDICAL CENTRE

**Thesis submitted to the University of Nottingham  
for the degree of Doctor of Philosophy**

**September 2010**

## DECLARATION

I declare that this thesis has not, whether in the same or different form, been presented to this or any other university in support of an application for any degree other than that for which I am now a candidate.

## TABLE OF CONTENTS

DECLARATION.....	ii
TABLE OF CONTENTS.....	iii
INDEX OF FIGURES.....	xiii
INDEX OF TABLES.....	xvii
LIST OF ABBREVIATIONS.....	xx
ACKNOWLEDGEMENTS.....	xxiii
ABSTRACT.....	1
CHAPTER 1: INTRODUCTION.....	2
1.1 Cardiac Development.....	2
1.1.1 Pre-gastrulation and gastrulation.....	2
1.1.2 Formation of the primary heart field.....	3
1.1.3 Formation of the linear heart tube.....	4
1.1.4 Looping of the heart.....	6
1.1.5 Chamber formation.....	9
1.1.6 Endocardial cushion formation and function.....	11
1.1.7 Septation.....	11
1.1.7.1 Atrial septation.....	11
1.1.7.2 Atrioventricular septation.....	12
1.1.7.3 Outflow tract septation.....	13
1.1.7.4 Ventricular septation.....	13
1.1.8 Valve development.....	16
1.1.9 The cardiac conduction system.....	18
1.2 Congenital heart defects.....	19
1.2.1 Cardiac septation defects.....	19
1.2.2 Conotruncal and aortic arch defects.....	20
1.3 Growth factor signalling in cardiac development.....	22
1.3.1 TGF- $\beta$ type receptor signalling.....	22
1.3.1.1 BMPs.....	23

1.3.2 Receptor tyrosine kinase signalling.....	24
1.3.2.1 Fibroblast growth factors.....	24
1.3.2.2 Vascular Endothelial Growth Factor.....	25
1.3.2.3 Epidermal Growth Factors.....	26
1.3.2.4 Cytokine signalling.....	26
1.3.3 Wnt signalling.....	27
1.4 Transcriptional regulation of cardiogenesis and gene regulatory networks.....	29
1.4.1 Nkx2.5.....	31
1.4.2 The T-box family of transcription factors.....	32
1.4.2.1 TBX5.....	33
1.4.3 The GATA family of transcription factors.....	34
1.4.3.1 GATA-4.....	35
1.4.3.2 GATA-5.....	37
1.4.3.3 GATA-6.....	37
1.4.4 The MADS family of transcription factors.....	38
1.4.4.1 Serum Response Factor (SRF).....	38
1.4.4.2 The myocyte enhancer factor family of transcription factors.....	39
1.4.4.2.1 MEF2C.....	39
1.4.4.2.2 MEF2A.....	40
1.4.5 The HAND family of transcription factors.....	40
1.5 Co-operative activity of cardiac transcription factors.....	42
1.6 The extracellular matrix.....	46
1.7 The contractile apparatus.....	49
1.7.1 Myosin heavy chains.....	51
1.7.2 Myosin light chains.....	51
1.7.3 Actins.....	52
1.7.4 Tropomyosin.....	52
1.7.5 Troponins.....	53
1.8 Cardiac model systems relevant to this thesis.....	54
1.8.1 The P19 cell line as a model of cardiomyocyte differentiation.....	54

1.8.2 The developing chick as a model of cardiogenesis .....	54
1.9 Background to this thesis.....	55
1.10 Aims and objectives.....	59
<b>CHAPTER 2: MATERIALS AND METHODS.....</b>	<b>60</b>
2.1 Materials.....	60
2.1.1 Molecular Methods.....	60
2.1.2 Microbial techniques.....	61
2.1.3 DNA purification techniques.....	61
2.1.4 Whole mount in situ hybridisation (WISH).....	61
2.1.5 Western Blotting.....	63
2.1.6 Morpholino knockdown.....	64
2.2 Methods.....	70
2.2.1 Molecular methods.....	70
2.2.1.1 Genomic DNA extraction.....	70
2.2.1.2 RNA extraction.....	70
2.2.1.3 Nucleic acid quantification.....	70
2.2.1.4 Reverse Transcription.....	71
2.2.1.5 Primer design.....	71
2.2.1.6 Polymerase chain reaction (PCR).....	72
2.2.1.6.1 HotStar Taq.....	72
2.2.1.6.2 PfuUltra 11 Fusion HS DNA Polymerase.....	72
2.2.1.7 Agarose Gel Electrophoresis.....	72
2.2.1.8 DNA sequencing.....	73
2.2.1.9 Quantitative PCR (QPCR) for validation of mouse targets.....	73
2.2.1.9.1 Methodology.....	72
2.2.1.9.2 Assay design.....	72
2.2.1.10 QPCR for expression analysis in the chick.....	75
2.2.1.10.1 Assay design.....	75
2.2.1.10.2 Amplification conditions.....	75
2.2.1.10.3 Comparative C <sub>T</sub> vs Relative Standard Curve method.....	75

2.2.1.10.4	Specification of experimental parameters.....	75
2.2.1.10.5	Preparation of standard curves.....	76
2.2.1.11	Microarray expression analysis.....	76
2.2.2	Microbial techniques.....	78
2.2.2.1	A-tailing procedure for cloning into the pGEM-T Vector.....	78
2.2.2.2	Ligation of vector – insert.....	78
2.2.2.3	Transformation.....	78
2.2.2.4	Colony PCR.....	79
2.2.2.5	Overnight cultures.....	79
2.2.2.6	Preparation of glycerol stocks.....	79
2.2.2.7	Plasmid DNA isolation (Miniprep).....	79
2.2.2.8	Plasmid DNA isolation (Maxiprep).....	80
2.2.2.9	Plasmid linearization by restriction digestion.....	81
2.2.2.10	Introduction of restriction sites by PCR amplification for subcloning into the pGL3-Basic and pGL3-Promoter vectors.....	81
2.2.2.11	Restriction digestion and vector dephosphorylation.....	81
2.2.3	DNA purification techniques.....	82
2.2.3.1	Shrimp Alkaline Phosphatase / ExonucleaseI treatment.....	82
2.2.3.2	Column purification of PCR products.....	82
2.2.3.3	DNA extraction from agarose gels.....	82
2.2.3.4	Ethanol precipitation of DNA.....	83
2.2.4	Chick embryo techniques.....	84
2.2.4.1	General care and conditions.....	84
2.2.4.2	Embryo staging.....	84
2.2.5	Chick expression studies.....	85
2.2.5.1	Collection of chick embryonic tissue for RT-PCR, QPCR, and microarray expression analysis.....	85
2.2.5.2	Whole mount in situ hybridisation (WISH).....	85
2.2.5.2.1	Embryo collection and preparation.....	85
2.2.5.2.2	Probe synthesis and digoxigenin (DIG) labelling.....	86

2.2.5.2.3 Probe purification and quantification.....	86
2.2.5.2.4 <i>In situ</i> hybridisation.....	86
2.2.5.3 Western blotting.....	87
2.2.5.3.1 Collection of tissue.....	87
2.2.5.3.2 Preparation of tissue lysates.....	88
2.2.5.3.3 HeLa cell growth and isolation.....	88
2.2.5.3.4 Preparation of HeLa cell lysates.....	88
2.2.5.3.5 Protein quantification.....	89
2.2.5.3.6 SDS PAGE and western blotting.....	89
2.2.5.3.7 Conditions tested for antibody optimisation.....	89
2.2.6 Morpholino knockdown.....	91
2.2.6.1 Morpholino knockdown technology.....	91
2.2.6.2 Identification of target regions for morpholino design.....	91
2.2.6.3 Morpholino design and preparation.....	91
2.2.6.4 Morpholino delivery.....	92
2.2.6.5 Application of morpholino via F127 pluronic gel to embryos in ovo....	93
2.2.7 Phenotypic analysis of embryos.....	94
2.2.7.1 Embryo isolation and processing.....	94
2.2.7.2 Embedding and sectioning.....	94
2.2.7.3 Haemulum staining and mounting of slides.....	94
2.2.7.4 Photography and analysis.....	95
<b>CHAPTER 3: IDENTIFICATION OF DOWNSTREAM TARGETS OF TBX5 and</b>	
<b>GATA-4 IN THE MOUSE P19 CELL LINE.....</b>	<b>96</b>
3.1 Aims.....	96
3.2 Results.....	97
3.2.1 QPCR validation of microarray data.....	97
3.2.1.1 Assay design.....	97
3.2.1.2 Selection of endogenous controls.....	97
3.2.1.2.1 Analysis of endogenous control variation across study	
samples.....	98

3.2.1.2.2 Test normalisation using short-listed endogenous control genes.....	100
3.2.1.3 Analysis of target and control gene amplification efficiency.....	100
3.2.1.4 Expression analysis.....	103
3.2.2 Selection of genes for further study.....	107
3.2.2.1 Relative expression of candidate genes in TBX5 / GATA-4 overexpression cell lines.....	107
3.2.2.2 Relative expression of candidate genes in wild type differentiating P19 cells.....	107
3.2.3 Candidate genes.....	108
3.2.3.1 TPM1.....	108
3.2.3.2 Fibronectin.....	108
3.2.3.3 Desmin.....	109
3.2.3.4 PETA-3.....	109
3.2.3.5 PA2.26.....	110
3.2.3.6 FUCA1.....	110
3.2.3.7 RBMS1.....	111
3.2.4 Bioinformatic identification of conserved TBX5 and GATA-4 binding sites within putative targets.....	112
3.2.5 Cloning of RBMS1 fragments for functional analysis of evolutionarily conserved regions (ECRs) in RBMS1.....	119
3.2.5.1 Identification of regions of the RBMS1 gene for further study.....	119
3.2.5.2 Primer design and PCR amplification.....	121
3.2.5.3 Destination vectors.....	123
3.2.5.3.1 pGL3-Basic vector with ANF minimal promoter.....	123
3.2.5.3.2 pGL3-Promoter vector.....	123
3.2.5.4 Cloning of the RBMS1 intron 1 fragment.....	126
<b>CHAPTER 4: STUDY OF CANDIDATE GENES IN THE EMBRYONIC CHICK.....</b>	<b>127</b>
4.1 Aims.....	127
4.2 Results.....	128

4.2.1 Investigation of candidate gene temporal expression profiles by RT-PCR...	128
4.2.2 Development of an in ovo model of TBX5 and GATA-4 knockdown.....	130
4.2.2.1 Morpholino position and design.....	130
4.2.2.2 Selection and design of specificity controls.....	130
4.2.2.4 Selection of a developmental window for morpholino application.....	134
4.2.2.5 Morpholino application and assessment of uptake.....	134
4.2.2.6 Preliminary testing of targeting and control morpholinos in ovo.....	136
4.2.2.7 External phenotypic analysis of single and double knockdown embryos.....	138
4.2.2.7.1 Whole body analysis.....	138
4.2.2.7.2 Cardiac analysis.....	140
4.2.2.8 Histological analysis of embryos.....	142
4.2.3 QPCR expression analysis of candidate genes in TBX5 / GATA-4 double knockdown embryos.....	147
4.2.3.1 Sample collection and preparation.....	147
4.2.3.2 QPCR assay design.....	147
4.2.3.3 Comparative CT method ( $\Delta\Delta CT$ ) versus Relative Standard Curve Method.....	148
4.2.3.5 Selection of an endogenous control for relative quantification.....	148
4.2.3.5.1 Preparation of standard curves.....	149
4.2.3.5.2 Analysis of variation of endogenous control expression levels in study samples.....	152
4.2.3.6 QPCR expression analysis of candidate genes.....	153
<b>CHAPTER 5: INVESTIGATION OF THE ROLE OF RBMS1 IN CARDIAC DEVELOPMENT.....</b>	<b>157</b>
5.1 Introduction.....	157
5.1.2 $\alpha$ -Smooth muscle actin, a transcriptional target of RBMS1.....	158
5.1.3 Transcriptional regulation of $\alpha$ -smooth muscle actin.....	159
5.1.4 $\alpha$ -Cardiac and $\alpha$ -skeletal actin.....	160
5.2 Aims.....	160

5.3 Results.....	161
5.3.1 Bioinformatic identification and characterisation of the chicken RBMS1 gene.....	161
5.3.2 Investigation of RBMS1 expression in the developing chick.....	168
5.3.2.1 RT-PCR.....	168
5.3.2.2 Whole mount in situ hybridisation.....	170
5.3.3 RBMS1 morpholino knockdown studies.....	176
5.3.3.1 Design of splice-junction targeting morpholinos.....	176
5.3.3.2 Preliminary testing of morpholinos in ovo.....	178
5.3.3.3 Selection of an alternative control of specificity.....	178
5.3.3.4 External phenotypic analysis of RBMS1 knockdown embryos.....	181
5.3.3.5 Histological analysis of RBMS1 knockdown embryos.....	183
5.3.4 Characterisation of morpholino effects on splicing.....	188
5.3.4.1 RBMS1 E2I2 morpholino.....	188
5.3.4.1.1 Sample collection and preparation.....	188
5.3.4.1.2 Primer placement for detection of alternatively spliced transcripts.....	188
5.3.4.1.3 RT-PCR amplification and sequencing of mRNA transcripts..	189
5.3.4.2 RBMS1 E8I8 morpholino.....	191
5.3.4.2.1 Sample collection and preparation.....	191
5.3.4.2.2 Primer placement for detection of alternatively spliced transcripts.....	191
5.3.4.2.3 RT-PCR amplification and sequencing of mRNA transcripts..	191
5.3.5 QPCR analysis of morpholino effects on mRNA levels.....	193
5.3.5.1 Validation of RPLPO as an appropriate endogenous control.....	193
5.3.5.2 QPCR analysis of RBMS1 in morpholino treated embryos.....	195
5.3.6 Bioinformatic promoter analysis of the $\alpha$ -actin genes.....	197
5.3.7 QPCR expression analysis of the actin genes in RBMS1 E2I2 morpholino treated animals and controls.....	198
5.3.7.1 QPCR assay design.....	198

5.3.7.2 Expression analysis.....	200
<b>CHAPTER 6: Microarray expression analysis of TBX5 / GATA-4 double knockdown embryos.....</b>	<b>202</b>
6.1 Aims.....	202
6.2 Results.....	203
6.2.1 Morpholino knockdown and tissue collection.....	203
6.2.2 Assessment of RNA quality.....	203
6.2.3 Microarray expression study.....	207
6.2.3.1 Analysis of data.....	207
6.2.4 Genes identified in microarray analysis of TBX5 and GATA-4 knockdown..	221
6.2.4.1 Reliability of data and general considerations.....	221
6.3.5 Gene expression analysis using GEISHA.....	223
6.3.6 RT-PCR expression analysis.....	225
<b>CHAPTER 7: DISCUSSION.....</b>	<b>228</b>
7.1 TBX5 and GATA-4 in cardiac development.....	228
7.2 Identification of targets of TBX5 and GATA-4 in the mouse P19 cell line.....	229
7.2.1 Validation of gene expression and preliminary bioinformatic analysis.....	230
7.2.2 Candidate genes.....	231
7.3 Development of a model system for assessment of the responsiveness of candidate genes to TBX5 and GATA-4.....	233
7.3.1 Development of an <i>in ovo</i> model of TBX5 and GATA-4 knockdown.....	233
7.3.2 Candidate gene responsiveness to combined knockdown of TBX5 and GATA-4.....	235
7.4 Investigation of the role of RBMS1 in cardiac development.....	236
7.4.1 RBMS1 expression.....	237
7.4.2 Morpholino knockdown of RBMS1.....	238
7.4.3 Characterisation of morpholino effects.....	239
7.5 Identification of new synergistic targets of TBX5 and GATA-4.....	240
7.6 Summary of findings and implications of this research.....	243
7.7 Limitations of this approach.....	244

<b>REFERENCES.....</b>	<b>246</b>
<b>APPENDIX A: An overview of cardiac development in the chick.....</b>	<b>304</b>
<b>APPENDIX B: QPCR assays designed to candidate genes in the mouse.....</b>	<b>306</b>
<b>APPENDIX C: IUPAC-IUB consensus nucleotide definitions.....</b>	<b>308</b>
<b>APPENDIX D: Cell transfection and luciferase reporter assays.....</b>	<b>309</b>
<b>APPENDIX E: Negative RT controls performed in parallel to expression profiling of candidate genes in the chick heart.....</b>	<b>311</b>
<b>APPENDIX F: Relative sizes of products amplified for expression profiling of candidate genes in the chick heart.....</b>	<b>312</b>
<b>APPENDIX G: Standard amino acid abbreviations.....</b>	<b>313</b>
<b>APPENDIX H: Map of the pGEM T Easy vector.....</b>	<b>314</b>
<b>APPENDIX I: Genes identified in microarray expression analysis of TBX5 / GATA-4 double knockdown embryos.....</b>	<b>315</b>
<b>APPENDIX J: Negative RT controls performed in parallel to expression profiling of candidate genes chick embryonic segments at HH16, HH19 and HH24.....</b>	<b>323</b>

## INDEX OF FIGURES

### CHAPTER 1

Figure 1.1	Embryonic origin of the heart.....	5
Figure 1.2	Cardiac looping.....	8
Figure 1.3	Representation of ballooning of the heart.....	10
Figure 1.4	Human atrial and ventricular septation.....	15
Figure 1.5	Cardiac valve formation.....	17
Figure 1.6	Stages of heart development and associated defects.....	21
Figure 1.7	Transcriptional networks involved in heart development.....	30
Figure 1.8	Human mutations in sarcomeric and Z-disc proteins .....	50

### CHAPTER 3

Figure 3.1	Relative expression of candidate genes in TBX5 / GATA4 overexpression cell lines G10 and G20.....	105
Figure 3.2	Relative expression of candidate genes in wild type differentiating wild type cells.....	106
Figure 3.3	Mulan analysis of candidate genes in human, mouse and chicken.	114
Figure 3.4	Mulan analysis of the RBMS1 gene in human and mouse.....	120
Figure 3.5	PCR amplification of the conserved region within intron 1 of RBMS1.....	120
Figure 3.6	pGL3-Basic Vector circle map and schematic displaying position of inserts.....	122
Figure 3.7	pGL3-Promoter Vector circle map and schematic displaying position of insert.....	124

### CHAPTER 4

Figure 4.1	RT-PCR expression profiles of candidate genes in the chick heart	129
------------	--	-----

Figure 4.2	TBX5 targeting morpholino sequence and target region.....	132
Figure 4.3	GATA-4 targeting morpholino sequence and target region.....	133
Figure 4.4	Assessment of morpholino uptake.....	135
Figure 4.5	External phenotypic analysis of embryos treated with 5-mismatch morpholinos in comparison to standard control-treated and wild type embryos.....	137
Figure 4.6	External whole body analysis of TBX5 / GATA-4 single and double knockdown embryos.....	139
Figure 4.7	External cardiac analysis of TBX5 / GATA-4 single and double knockdown embryos.....	141
Figure 4.8	Histological analysis of the three control groups.....	144
Figure 4.9	Histological analysis of TBX5 and GATA-4 knockdown embryos...	145
Figure 4.10	GAPDH amplification plot (A) and resulting standard curve (B).....	150
Figure 4.11	TBP amplification plot (A) and resulting standard curve (B).....	150
Figure 4.12	EEF1A1 amplification plot (A) and resulting standard curve (B).....	151
Figure 4.13	RPLPO amplification plot (A) and resulting standard curve (B).....	151
Figure 4.14	Relative expression of candidate genes in TBX5 / GATA-4 knockdown animals and controls.....	156

## CHAPTER 5

Figure 5.1	Synteny of the chicken and human RBMS1 genes.....	162
Figure 5.2	Multispecies conservation of the RBMS1 gene.....	163
Figure 5.3	Multispecies alignment of RBMS1 protein sequences.....	164
Figure 5.4	ClustalW alignment of the two chicken RBMS1 mRNA transcripts..	165
Figure 5.5	Representation of the two chicken RBMS1 mRNA transcripts and EST coverage.....	167
Figure 5.6	RT-PCR expression analysis of RBMS1.....	169
Figure 5.7	Amplicons used for RNA probe synthesis.....	172
Figure 5.8	In situ hybridisation expression analysis of RBMS1 in the HH16	

	and HH19 chick embryo using the 5F/10R probe.....	173
Figure 5.9	In situ hybridisation expression analysis of RBMS1 in the HH24 chick embryo using the 1F/5R probe.....	174
Figure 5.10	In situ hybridisation expression analysis of RBMS1 in the HH24 chick embryo using the 5F/10R probe.....	175
Figure 5.11	RBMS1 E2I2 and control morpholino sequences and predicted effects on mRNA splicing.....	177
Figure 5.12	External phenotypic analysis of embryos treated with RBMS1 E2I2 and 5-mismatch morpholinos in comparison to standard control-treated and wild type embryos.....	179
Figure 5.13	RBMS1 E8I8 morpholino sequence and predicted effect on splicing.....	180
Figure 5.14	Altered cardiac morphology of RBMS1 knockdown embryos.....	182
Figure 5.15	Histological analysis of altered cardiac morphology of RBMS1 knockdown embryos at HH19.....	185
Figure 5.16	Characterisation of the effect of the RBMS1 E2I2 morpholino on mRNA splicing.....	190
Figure 5.17	Characterisation of the effect of the RBMS1 E8I8 morpholino on mRNA splicing.....	192
Figure 5.18	QPCR expression analysis of RBMS1 in E2I2 morpholino treated animals and controls.....	196
Figure 5.19	QPCR expression analysis of RBMS1 in E8I8 morpholino treated animals and controls.....	196
Figure 5.20	QPCR assays used for expression analysis of the three actin genes.....	199
Figure 5.21	QPCR expression analysis of the three actin genes in RBMS1 E2I2 morpholino treated animals and controls.....	201

**CHAPTER 6**

Figure 6.1	Bioanalyser analysis of RNA samples prior to microarray analysis	206
Figure 6.2	Genes differentially regulated in microarray analysis of TBX5 and GATA-4 single and double knockdown.....	208
Figure 6.3	RT-PCR expression analysis of nine candidate genes.....	227

## INDEX OF TABLES

### CHAPTER 1

Table 1.1	Genes down-regulated in microarray expression analysis of TBX5 / GATA-4 overexpression cell lines.....	57
Table 1.2	Genes up-regulated in microarray expression analysis of TBX5 / GATA-4 overexpression cell lines.....	58

### CHAPTER 2

Table 2.1	Primers used for PCR amplification of mouse genomic regions of RBMS1.....	65
Table 2.2	Primers used for introduction of SacI restriction sites.....	65
Table 2.3	QPCR assays designed to candidate genes in the chick.....	66
Table 2.4	Primers designed to the chicken RBMS1 gene.....	67
Table 2.5	QPCR assays designed to the $\alpha$ -actin genes in the chick.....	67
Table 2.6	Primers used in RT-PCR expression analysis of genes identified in microarray analysis of TBX5 / GATA-4 double knockdown embryos.....	68
Table 2.7	Morpholinos used in the TBX5 / GATA-4 knockdown study.....	69
Table 2.8	Morpholinos used in the RBMS1 knockdown study.....	69

### CHAPTER 3

Table 3.1	Relative expression of six candidate endogenous control genes in study samples.....	99
Table 3.2	Relative expression of FUCA1 when normalised against candidate endogenous control genes tmem131 and dynactin.....	100
Table 3.3	Target and endogenous control real time assay linearity and efficiency.....	102
Table 3.4	Relative expression of candidate genes in TBX5 / GATA4	

	overexpression cell lines and wild type differentiating wild type cells, measured by QPCR.....	104
<b>CHAPTER 4</b>		
Table 4.1	Summary of abnormalities seen in TBX5 / GATA-4 single and double knockdown embryos and controls.....	146
Table 4.2	Summary of endogenous control gene assay properties.....	152
Table 4.3	Mean CT and $\Delta$ CT values of EEF1A1 and RPLPO in study Samples.....	153
Table 4.4	QPCR expression analysis of candidate genes in TBX5 / GATA-4 knockdown animals and controls.....	155
<b>CHAPTER 5</b>		
Table 5.1	Summary of heart abnormalities seen in RBMS1 knockdown embryos in comparison to controls.....	186
Table 5.2	Mean CT and $\Delta$ CT values of RPLPO in study samples.....	194
Table 5.3	QPCR expression analysis of RBMS1 in E2I2 and E8I8 morpholino treated animals and controls.....	195
Table 5.4	QPCR expression analysis of actin genes in RBMS1 E2I2 morpholino treated animals and controls.....	200
<b>CHAPTER 6</b>		
Table 6.1	RNA concentration, purity, and integrity of samples used for microarray expression analysis.....	205
Table 6.2	Genes differentially regulated in microarray analysis of TBX5 / GATA-4 double knockdown chick embryos.....	209
Table 6.3	Genes differentially regulated in microarray analysis of TBX5 single knockdown chick embryos.....	211
Table 6.4	Genes differentially regulated in microarray analysis of GATA-4	

	single knockdown chick embryos.....	214
Table 6.5	Genes differentially regulated in microarray analysis of TBX5 / GATA-4 double knockdown, TBX5 single knockdown, and GATA- 4 single knockdown chick embryos.....	216
Table 6.6	Genes differentially regulated in microarray analysis of TBX5 / GATA-4 double knockdown and TBX5 single knockdown and chick embryos.....	217
Table 6.7	Genes differentially regulated in microarray analysis of TBX5 / GATA-4 double knockdown and GATA-4 single knockdown and chick embryos.....	219
Table 6.8	Genes differentially regulated in microarray analysis of TBX5 single knockdown and GATA-4 single knockdown chick embryos..	220
Table 6.9	Gene expression data from GEISHA.....	224

## LIST OF ABBREVIATIONS

<b>ANF</b>	Atrial natriuretic factor
<b>ASD</b>	Atrial septal defect
<b>AV</b>	Atrioventricular
<b>AVSD</b>	Atrioventricular septal defect
<b>BAF</b>	Brahma-associated factor
<b>BCIP</b>	5-bromo-4-chloro-3-indolyl phosphate
<b>BLAST</b>	Basic local alignment search tool
<b>BNP</b>	Brain natriuretic peptide
<b>BSA</b>	Bovine serum albumin
<b>CAD</b>	Coronary artery disease
<b>cDNA</b>	Complementary cDNA
<b>CHD</b>	Congenital heart defect
<b>CNC</b>	Cardiac neural crest
<b>DCM</b>	Dilated cardiomyopathy
<b>DEPC</b>	Diethylpyrocarbonate
<b>DIG</b>	Digoxygenin
<b>DMEM</b>	Dulbecco's minimum essential media
<b>DMF</b>	Dimethylformamide
<b>DNA</b>	Deoxyribonucleic acid
<b>dNTP</b>	Deoxynucleotide triphosphate
<b>DORV</b>	Double outlet right ventricle
<b>E.coli</b>	Eschericia coli
<b>ECL</b>	Enhanced chemiluminescence
<b>ECM</b>	Extracellular matrix
<b>ECR</b>	Evolutionarily conserved region
<b>EDTA</b>	Ethylenediaminetetraacetic acid
<b>EMT</b>	Epithelial to mesenchymal transition
<b>EST</b>	Expressed sequence tag
<b>Exol</b>	Exonuclease I

<b>FAM</b>	Fluorescein amidite
<b>FDR</b>	False discovery rate
<b>HBSS</b>	Hank's buffered salt solution
<b>HCM</b>	Hypertrophic cardiomyopathy
<b>HH</b>	Hamburger and Hamilton
<b>HOS</b>	Holt-Oram syndrome
<b>HRP</b>	Horseradish peroxidase
<b>IDC</b>	Idiopathic dilated cardiomyopathy
<b>KD</b>	Knockdown
<b>LB</b>	Luria-Bertani
<b>MMD</b>	Moyamoya disease
<b>NBT</b>	Nitroblue tetrazolium
<b>NMD</b>	Nonsense-mediated decay
<b>OFT</b>	Outflow tract
<b>PBS</b>	Phosphate buffered saline
<b>PBST</b>	Phosphate buffered saline with 0.1% Triton X-100
<b>PCR</b>	Polymerase chain reaction
<b>PDA</b>	Patent ductus arteriosus
<b>PFA</b>	Paraformaldehyde
<b>PMSF</b>	Phenylmethylsulfonyl fluoride
<b>PTA</b>	Persistent truncus arteriosus
<b>PTC</b>	Premature termination codon
<b>QPCR</b>	Quantitative polymerase chain reaction
<b>RAE</b>	Retinoic acid embryopathy
<b>RIN</b>	RNA integrity number
<b>RIPA buffer</b>	Radioimmunoprecipitation assay buffer
<b>RNA</b>	Ribonucleic acid
<b>RT-PCR</b>	Reverse-transcriptase polymerase chain reaction
<b>SAP</b>	Shrimp alkaline phosphatase
<b>SDS PAGE</b>	Sodium dodecyl sulphate polyacrylamide gel electrophoresis

<b>SGBS</b>	Simpson-Golabi-Behmel syndrome
<b>SMC</b>	Smooth muscle cell
<b>SOC</b>	Super optimal broth with catabolite repression
<b>SRE</b>	Serum response element
<b>SSC</b>	Saline sodium citrate
<b>TAAD</b>	Thoracic aortic aneurysms and dissections
<b>TBS</b>	Tris buffered saline
<b>TBST</b>	Tris buffered saline with 0.1% Tween20
<b>TGA</b>	Transposition of the great arteries
<b>TOF</b>	Tetralogy of Fallot
<b>VSD</b>	Ventricular septal defect
<b>VSMC</b>	Vascular smooth muscle cell
<b>WISH</b>	Whole mount in situ hybridisation
<b>WT</b>	Wild type

## ACKNOWLEDGEMENTS

Firstly, I would like to thank my supervisors David and Siobhan, and all of the members of both research groups, for their help and advice over the years. David has been the most wonderful supervisor and I cannot thank him enough for his patience, optimism and support. I would also like to thank Peter Shaw for his early insights into this research, and Sheila Gardener who was acting postgraduate tutor for a period of my study, and was a great help in this role.

I am very grateful to Jonathan Ronksley, whose idea for his own PhD project formed the basis of this thesis, and whom it was a joy to work with. Many thanks also to Chris Moore, Daphne Goh, Eddy Sun, Tushar Ghosh, Sarah Buxton, Thelma Robinson, Aziza Alibhai, Diji Kuriakose, and Sue Willington for all the help and generosity with their time. Thanks also to Andy Bennett and Marcus Marvin for their immensely helpful advice on QPCR. I would also like to acknowledge all of my fellow postgraduates and former running club members, in particular, Ben, Sapna, James, and Rachel. These people have been an absolute pleasure to know and made my time in Nottingham enjoyable.

Prior to my PhD I had the pleasure of working for Professor Nilesh Samani and Professor Richard Trembath, and would like thank them for having me as a member of their research groups where I learnt many of the fundamental skills to becoming a good researcher. Thanks also to Laurence Hall who was a brilliant mentor, and my former colleagues and friends Andrea and Jas, who I can always depend on.

Lastly, I would like to thank my close friends and family who have done so much. Serena has given me continued support over the years. I was lucky enough to meet Ugljesa during this PhD, and he has been there for me since. Special thanks to my wonderful siblings Kalpesh, Shila, and Ketan for everything. Finally, I would like to thank my mother and late father for their hard work, support, and encouragement. It is to them I dedicate this thesis.

## ABSTRACT

Cardiac development is a complex multi-step process involving a diverse network of genes. Defects in cardiac genes can lead to congenital heart defects (CHDs), and understanding the processes involved in normal cardiogenesis is crucial in elucidating the pathogenesis of disease. Mutations in a number of cardiac transcription factors have been associated with CHDs, including TBX5 and GATA-4. These transcription factors are high in the regulatory hierarchy and form a complex that is thought to direct and synergistically regulate common cardiac pathways. However, little is currently known about their joint targets. This study aimed to identify and analyse genes important in cardiogenesis, with focus on the combined targets of TBX5 and GATA-4. Microarray expression analysis of TBX5 / GATA-4 double overexpression P19 cell lines led to the identification of a large number of genes, of which seven were selected for study; *PA2.26*, *PETA-3*, *FUCA1*, *FN*, *TPM1*, *DES*, and *RBMS1*. Expression of these was confirmed in the embryonic chick heart at Hamburger and Hamilton (HH) stages 12 – 26. The cell cycle regulator and transcription factor RBMS1 was selected for investigation of its role in cardiac development. Morpholino knockdown of RBMS1 expression in the developing chick resulted in defects in cardiac looping and atrial septation. Whilst further work is required to strengthen this data, this is a novel finding and opens up possibilities for future research into cardiac transcriptional networks. Microarray expression analysis using an *in ovo* model of TBX5 and GATA-4 double knockdown led to the identification of a number of interesting putative targets, including *TFAP2B*, *GPC3*, and *CRABP1*, which have known roles in cardiac development. *TFAP2B* is of particular interest as mutations in this gene are associated with the heart-hand disorder Char syndrome. *LOC420770*, a novel gene of unknown function, was also identified and displayed expression indicative of a heart-limb profile. Further studies to attempt elucidation of the function of this gene may provide a novel candidate gene for CHD. Investigation of these genes will form the basis of future research, contributing to our current knowledge of the vast network of genes involved in development of the heart.

# CHAPTER 1

## INTRODUCTION

### 1.1 CARDIAC DEVELOPMENT

The heart is the first organ to form in embryogenesis, developing by a complex and precisely co-ordinated process involving heart specification, formation of the linear heart tube, looping, and maturation to ultimately form a four-chambered structure [Martinsen, 2005]. Processes such as septation, valve development and coronary vasculature formation occur in parallel and are crucial. Cardiac development is regulated by a vast network of genes encoding growth factors, transcription factors, co-factors and regulators, signalling proteins, and structural molecules, some of which will be described here. Perturbations in the developmental process can lead to heart malformations, and understanding the molecular processes involved in normal cardiac development is important in elucidating the pathogenesis of congenital heart defects. The anatomical development of the heart has been widely studied in a number of organisms including human (Carnegie Stages / CS), mouse (Embryonic days / E), and chick (Hamburger and Hamilton stages / HH), and is detailed below. Processes that differ between mammals and the chick (namely atrial septation) are discussed.

#### 1.1.1 Pre-gastrulation and gastrulation

At the pre-primitive streak stage, cardiac precursor cells are identifiable in the epiblast cell layer [Yutzey and Kirby, 2002]. The primitive streak is a triangular region found in the midline of the long axis of the oval disc in the area pellucida, darker than its surroundings due to cell ingression to this region before outward cell migration begins. At the onset of primitive streak formation, cardiac progenitor cells exist in the postero-lateral epiblast [Hatada and Stern, 1994; Yatskievych et al., 1997]. Interaction between the postero-lateral epiblast and hypoblast is required for anterior lateral plate mesoderm formation, and this region gives rise to the heart [Ehrman and Yutzey,

1999]. The intermediate primitive streak extends from the posterior into the centre of the area pellucida and contains precardiac cells in the anterior [Rawles, 1943] (Figure 1.1A). The definitive primitive streak extends over most of the area pellucida.

Gastrulation, where the three embryonic germ layers are established, is one of the first morphogenetic events to occur in development. Migration of cells from the upper layer of the primitive streak gives rise to the ectoderm, the earliest layer to form and the outermost. The endoderm is formed by inward migration of cells along the archenteron from the inner layer of the gastrula. The mesoderm, an additional layer between the ectoderm and endoderm, is formed from some of the cells migrating to form the endoderm. Each germ layer gives rise to specific body tissues.

### **1.1.2 Formation of the primary heart field**

Precardiac cells are found in the anterior mesoderm and either side of the node [Linask and Lash, 1986]. The anterior intestinal portal, head process and head fold develop, and the cells that will form the heart move into two bilateral regions in the anterolateral region of the embryo called the primary heart field, first identified by Rawles in 1943 [Rawles, 1943] (Figure 1.1B). This region gives rise to the myocardium and endocardium. Cardiac precursor cells (not yet fully committed) segregate into the splanchnic mesoderm layer during migration into the primary heart fields. This layer is adjacent to the endoderm, which is thought to induce differentiation of myocardial cells [Abu-Issa et al., 2004]. Definition of the avian embryonic heart forming region (HFR) has been attempted through the use of early cardiac markers such as Nkx2.5 and GATA-4, and by cell lineage tracing studies [Redkar et al., 2001]. The two methods yielded differing results, as with many previous studies, and the extent of the heart forming region remains unclear. As cardiac precursor cells reach a higher level of commitment, expression of cardiac genes is initiated [van den Hoff et al., 2004]. The prospective heart forming regions migrate to form the cardiac crescent (Figure 1.1C) (week 2 of human gestation / E7.5

in mouse), whilst the neural plate forms from the ectoderm, and folds to become the neural tube.

### **1.1.3 Formation of the linear heart tube**

The cardiac crescent moves towards the embryonic neck and the cardiac plate folds into the primary heart tube at the embryonic ventral midline (Figure 1.1D) [Moorman et al., 2003], connected to the body by a posterior inflow (venous pole) and anterior outflow (arterial pole). The linear heart tube comprises two concentric layers of cells separated by an extensive matrix of cardiac jelly; the outer layer is made up of myocardial cells, and the inner layer consists of endocardial cells [Brutsaert, 2003]. This structure, together with the remainder of the heart forming regions, takes the shape of an inverted Y. At this pre-looping phase, the heart is centrally positioned and undergoes rapid elongation along the craniocaudal axis of the embryo to form a long nearly symmetrical tube [Moorman et al., 2003]. The primitive tubular heart begins to beat spontaneously soon after it is formed, at CS 10 (22 – 23 days) in humans, E8 in mouse, and HH10 in the chick [Franco et al., 1998].

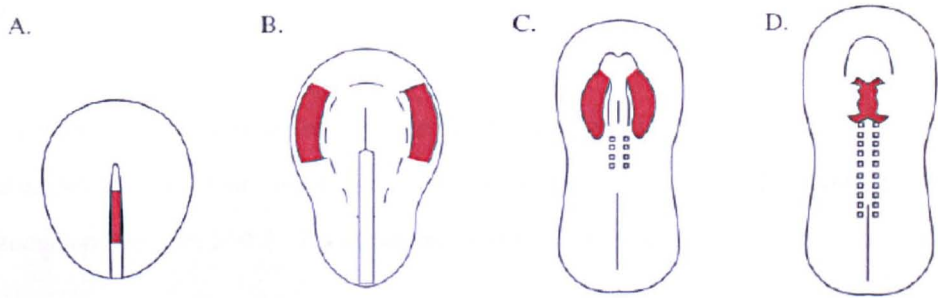


**Figure 1.1 Embryonic origin of the heart.** Heart forming regions are displayed in red. A) Heart progenitor cells are located in the upper region of the primitive streak, under Hensen's node. B) Bilateral heart primordia are present in the anterior lateral plate mesoderm. C) Formation of the cardiac crescent following fusion of the anterior end of the two heart fields. D) Fusion of heart primordia to form a beating heart tube at the embryonic midline. *Adapted from Yutzey et al., 2002*

#### 1.1.4 Looping of the heart

The looping process can be subdivided into four phases following pre-looping (as described in 1.1.3); dextral-looping to form the c-shaped loop, transformation from the c-shaped loop to the s-shaped loop (early and late phases), and the positional changes which occur mainly in the primitive outflow tract (OFT) during cardiac septation [Manner, 2000]. These are represented in Figure 1.2.

During dextral looping, the linear heart tube loops to the right to become c-shaped and asymmetric (Figure 1.2, 1). This process is essential in ventricle orientation and connection to the appropriate vessels, and is dependent on asymmetric signalling cascades [Kathiriya and Srivastava, 2000]. The right lateral furrow flattens, the left deepens, and the diameter of the heart tube increases particularly at the caudal end (an early manifestation of the thinner outflow portion (primitive conus) and thicker primitive ventricular region) [Manner, 2000]. The primitive ventricular region, composed of the primordia of the apical trabeculated regions of the left and right ventricles, bends to the right resulting in the ventral and dorsal sides of the heart tube becoming the convex right and concave left sides of the bend [Manner, 2000]. Myocardial precursor cells from the posterior region of the primary heart field contribute to the atria forming region, and cells from a second population of heart precursor cells in the pharyngeal mesoderm termed the secondary heart field, migrate into the cranial (arterial) pole of the heart, supporting growth of the outflow tract and right ventricle forming regions [Abu-Issa et al., 2004; Kelly et al., 2001; Kelly and Buckingham, 2002; Mjaatvedt et al., 2001; Moorman et al., 2007; Waldo et al., 2001]. Cardiac neural crest (CNC) cells undergo epithelial-to-mesenchymal transition (EMT) and migrate away from the neural tube into the heart via the outflow tract and pharyngeal arch arteries [Boot et al., 2003]. CNC cells are essential for correct outflow tract septation, cardiac innervation, aortic arch repatterning, and myocardial function [Kirby, 2002].

Cardiac looping continues transforming the heart from a c-shape to an s-shaped structure via an early and late phase (Figure 1.2, 2-3). In the early phase, the caudal wall of the primitive conus, and cranial wall of the primitive atria move closer together, and the primitive ventricular bend shifts from a cranial to caudal position from the atria [Manner, 2009; Martinsen, 2005]. This transforms the heart to an immature s-shaped structure. In the late phase of s-looping, the proximal part of the outflow tract shifts to the left and ballooning of the chambers also occurs (described in 1.1.5) [Manner, 2009]. The epicardium, myocardium, endocardium and cardiac jelly heart layers have also developed upon completion of this process.

The last phase of looping is often referred to as the cardiac septation phase, since this is the main anatomical event occurring at this stage. A number of morphological changes occur resulting in positional changes of cardiac regions (Figure 1.2, 4). The proximal two thirds of the outlet section of the outflow tract shifts from a position lateral to the atria, to a position ventral to the right atrium, and the outflow tract and inner curvature of the ventricular bend are remodelled [Manner, 2009].

8

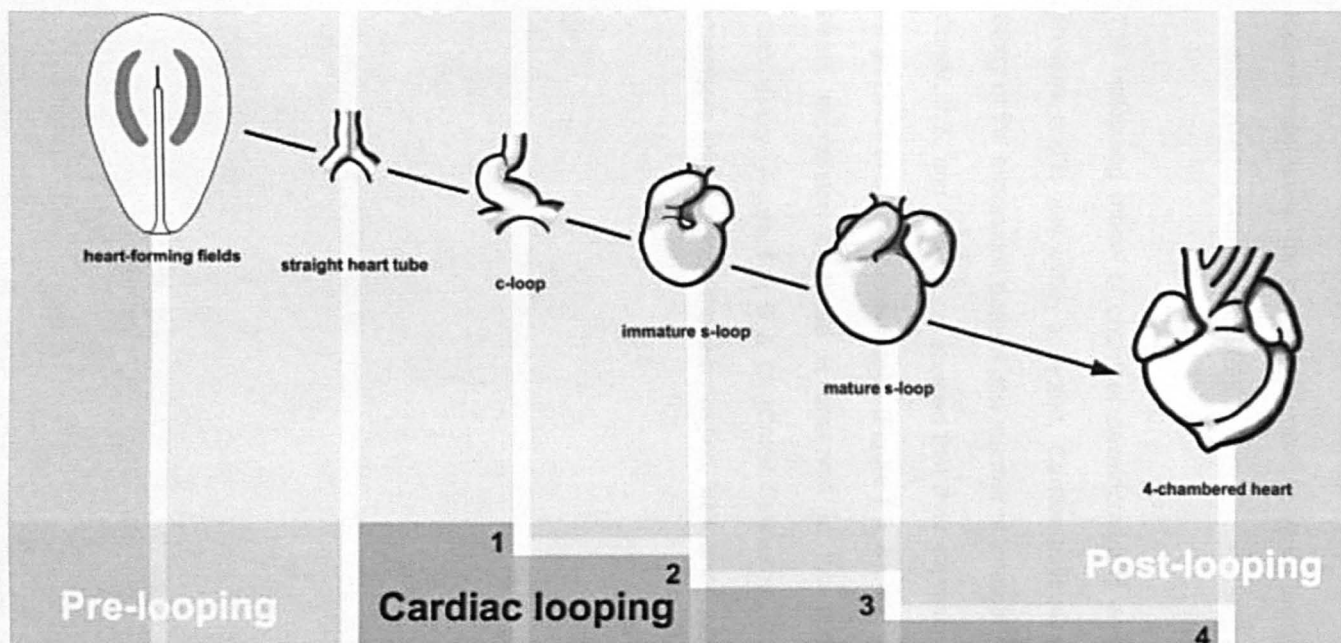


**Figure 1.2 Cardiac looping**

Looping of the heart is represented in four phases. 1) Dextral-looping, where the linear heart tube loops to the right to become c-shaped and asymmetric. 2) Early phase s-looping, where the heart is transformed to an immature s-shaped structure. 3) Late phase s-looping, where the proximal part of the outflow tract shifts to the left and the heart is transformed to a mature s-shaped structure. 4) Cardiac septation, where a number of positional changes of cardiac regions occur, mainly in the primitive outflow tract. *Adapted from Manner, 2009*

### 1.1.5 Chamber formation

There have been two main theories about how the cardiac chambers form – the segmental theory, and the ballooning theory. According to the segmental model, the cardiac chambers form from segmental primordia along the anteroposterior axis of the heart tube, and this has been supported by apparent segmental expression of various cardiac genes [Franco et al., 1998]. The heart tube contains caudal atrial and cranial ventricular regions which will give rise to the cardiac chambers (separated by the atrioventricular canal), and a cranial outflow tract. In this model, the outer curve of the looped heart gives rise to the right ventricle, whilst the inner bend gives rise to the left ventricle [De La Cruz et al., 1989].

The ballooning model of chamber development is an alternative theory behind this process, and is now widely accepted. Cardiac ballooning is represented in Figure 1.3. Study of the expression pattern of a number of 'chamber specific' cardiac genes (ANF, Chisel, *Irx5*, and SERCA2a) showed that their expression is spatially restricted to the ventral side of the linear heart tube (Figure 1.3, A), and in the looped heart and mature heart, expression of these is observed in the outer curvature and chambers respectively (Figure 1.3, B & C) [Christoffels et al., 2000]. This demonstrates the chambers originate from the outer region, 'ballooning' out from the heart tube.

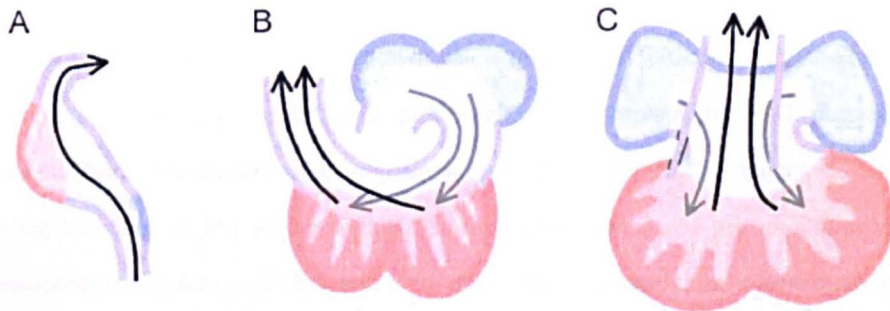


**Figure 1.3 Representation of ballooning of the heart**

Prospective ventricular and atrial myocardium regions are shown in pink and blue respectively. Arrows denote the direction of blood-flow; grey arrows indicate blood-flow into the ventricles, and black arrows indicate blood-flow through the outflow tract. Three phases of development are represented, A) the linear heart tube, B) the mature s-looped heart, and C) the four chambered heart. The chambers originate from the outer region of the heart tube, 'ballooning' out. *Adapted from Christoffels et al., 2000*

### **1.1.6 Endocardial cushion formation and function**

Endocardial cushions are cell masses which initially appear as swellings in the cardiac jelly that form by EMT of the endothelial cell layer. In this process, endothelial cells delaminate, invade the cardiac jelly, proliferate, and complete the EMT process to differentiate into mesenchymal cells [Runyan and Markwald, 1983]. Cushions form in specific locations of the atrioventricular and conus regions, and are crucial in valve development and fusion of the septa to divide the chambers, atrioventricular (AV) canal, and outflow tract for formation of the aortic and pulmonary channels [Markwald et al., 1977].

### **1.1.7 Septation**

Septation divides the heart into four distinct chambers, and separates the outflow tract region into the pulmonary and aortic channels. This compartmentalisation is critical in establishing and maintaining separate pulmonary and systemic circulations. Defects in septation, when left uncorrected, can lead to pulmonary vascular disease, atrial enlargement with a resulting predisposition to atrial arrhythmias, ventricular dilation, and a shortened life expectancy [Garg, 2006].

#### **1.1.7.1 Atrial septation**

Development of the interatrial septum, which separates the left and right atria, begins with downward growth of the septum primum from the dorsal cranial wall of the common atrium into the atrial lumen, towards the endocardial cushions in the AV canal [Anderson et al., 2003] (Figure 1.4A). The interatrial septum is identifiable from CS 13. The primary atrial opening (or foramen) between the septum primum and endocardial cushions is termed the ostium primum. The septum primum harbours a mesenchymal cap which becomes fused with the superior and inferior endocardial cushions in the AV canal (which also become fused with one another), closing the ostium primum [Wessels et al., 2000]. In parallel, perforations form in the upper part of the septum as a result of apoptosis, and these coalesce to form a secondary atrial foramen termed the ostium secundum [Abdulla et al., 2004] (Figure 1.4B).

Development of an additional septum, the septum secundum, begins from the roof of the atrium wall and alongside the remnants of the septum primum [Lamers and Moorman, 2002] (Figure 1.4C). This leaves an opening called the foramen ovale. Following breakdown of the upper portion of the septum primum, the remaining part acts as a valve in this region and is termed the valve of foramen ovale [Anderson et al., 2003]. Once lung circulation begins postnatally, increased pressure in the left atrium results in fusion of the foramen ovale valve with the septum secundum to close the foramen ovale and complete atrial septation [Anderson et al., 2003] (Figure 1.4D).

As mentioned, the process of atrial septation in the chick differs to that of mammals, and formation of the septum secundum does not occur. In the chick, the septum primum begins downward growth from the inner atrial wall at HH14 [Anderson et al., 2003]. It becomes fused with dorsal and ventral endocardial cushions in the AV canal at HH 24 (4 days), and small perforations (foramina secunda) form in the mid-dorsal portion of the septum primum in parallel, maintaining communication between the atria [Hendrix and Morse, 1977]. These increase in number and size from days 5 to 8, creating cords of endocardium covered tissue [Morse and Hendrix, 1980]. This cord tissue thickens during days 8 to 15, reducing the size of the foramina secunda. By day 2 post hatching, the interatrial perforations are closed, and atrial septation is complete [Hendrix and Morse, 1977]. This variation between species means that particular atrial septal defects which arise from disturbances in septum secundum formation cannot be modelled in the chick (discussed in section 1.2). Cardiac development in the chick is discussed further in Chapter 4.

#### **1.1.7.2 Atrioventricular septation**

The atrioventricular septum separates the atria and ventricles. Atrioventricular cushions form at the superior and inferior borders of the AV canal, and lateral cushions form on the left and right borders in parallel. The superior and inferior cushions continue to grow and extend into the lumen, becoming fused with one another and developing into the mature AV septum [Sadler, 2006].

### **1.1.7.3 Outflow tract septation**

The aorticopulmonary septum divides the common outflow tract (truncus arteriosus) and conus region into aortic and pulmonary channels. Migration of cardiac neural crest cells (CNCs) into the outflow tract region via the pharyngeal arches contributes to the formation of cushions in this region [Kirby, 1987; Waldo et al., 1998]. A pair of opposing ridges termed the left and right superior truncus swellings form in the truncus, and distal growth of these towards one another results in fusion to form the aorticopulmonary septum [Sadler, 2006]. In parallel, cushions also form on the right dorsal and left ventral walls of the conus region. These grow distally, and towards one another to join with the truncus septum, dividing the conus into anterolateral and posteromedial portions [Sadler, 2006]. The vessels rotate to connect with the appropriate chamber, with the aorta joining the left ventricle, and the pulmonary artery connecting to the right ventricle, generating separate pulmonary and systemic circulations. Alignment and fusion of the aorticopulmonary septum, ventricular septum, AV septum, and base of the atrial septum occurs to produce a four-chambered heart.

### **1.1.7.4 Ventricular septation**

The muscular interventricular septum, which separates the left and right ventricles, forms as a result of growth between the inlet and outlet regions of the ventricular section [Lamers et al., 1992] (Figure 1.4C-D). The ventricular medial walls become apposed and merge, giving rise to the muscular portion of the interventricular septum which is identifiable from week 5 (CS 15) [Lamers and Moorman, 2002]. At this stage, communication between the two ventricles via the interventricular foramen can still occur. Proliferation of the conus cushions and completion of conus septation (described in section 1.1.7.3) results in shrinkage of the interventricular foramen. Outgrowth from the inferior endocardial cushion to the muscular interventricular septum occurs, closing the interventricular foramen. The right and left conus cushion and inferior endocardial cushion proliferations form the membranous portions of the

interventricular septum. Ventricular septation is complete by CS 23 [Lamers et al., 1992].

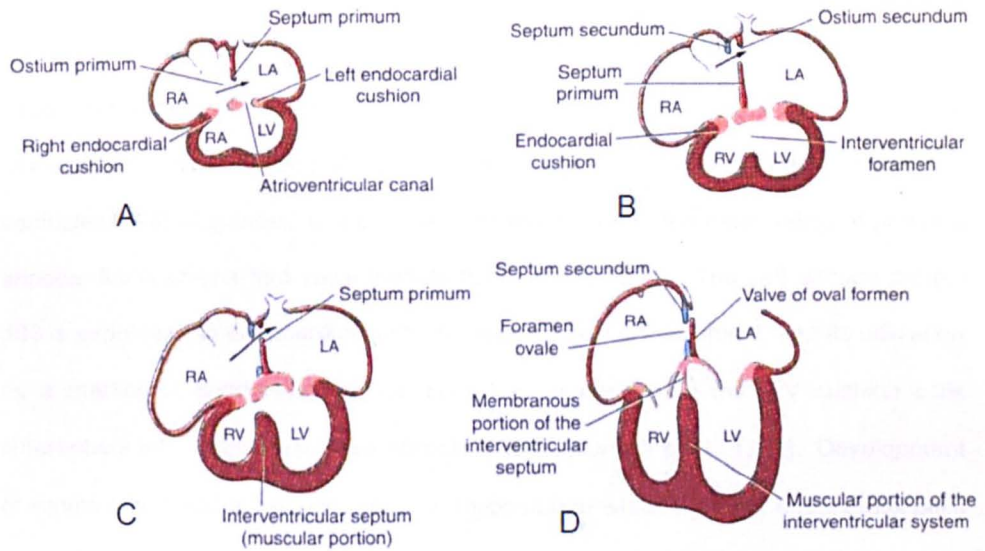


**Figure 1.4 Human atrial and ventricular septation**

A) 30 day embryo. The septum primum grows from the roof of the atrial chamber and extends towards the AV canal. The space between the septum primum and endocardial cushions is termed the ostium primum. B) 33 day embryo. The septum primum fuses with the endocardial cushions in the AV canal, resulting in closure of the ostium primum. The ostium secundum forms as a result of perforations in the septum primum. Development of the septum secundum, also from the roof of the atrial chamber, begins. This does not occur in the chick. C) 37 day embryo. Growth of the septum secundum towards the valve of foramen ovale occurs. The ventricular medial walls become apposed and merge, giving rise to the muscular portion of the interventricular septum. D) Newborn. The septum secundum and valve of foramen ovale fuse to divide the atria. Outgrowth from the inferior endocardial cushion to the muscular interventricular septum occurs, closing the interventricular foramen. The conus cushion and inferior endocardial cushion proliferations form the membranous portions of the interventricular septum. *Adapted from Langman's Medical Embryology, 10<sup>th</sup> Edition*

### 1.1.8 Valve development

Cardiac valves are thin fibrous structures which open and close in a precise manner, allowing unidirectional blood flow through the heart. Two sets of valves form in the heart; the semilunar valves (aortic and pulmonary) form in the outflow tract, and atrioventricular (AV) valves (tricuspid and mitral) in the AV canal between the atria and ventricles. Valvulogenesis is a complex process involving the remodelling of primitive endocardial cushions into valve leaflets [Chin et al., 1992]. The cell surface protein JB3 is expressed in endocardial cushion tissue early in development, and its utilisation as a marker of endothelial derived cells has demonstrated that AV cushion cells differentiate into connective tissue fibroblast cells [Wunsch et al., 1994]. Development of valves is initiated by signals from the myocardium which promote endocardial cells to undergo EMT forming endocardial cushions composed of proliferative valve progenitor cells in an extracellular matrix [Armstrong and Bischoff, 2004]. Endocardial cushions become cellularised by proliferation of mesenchymal cells, they elongate and are remodelled to form functional valves composed of three main layers – the atrialis (elastin-rich), spongiosa (proteoglycan-rich), and fibrosa (collagen-rich) [Hinton et al., 2006]. This is represented in Figure 1.5. Valve remodelling is characterised by this increase in ECM organisation and complexity, and also by a decrease in endocardial cushion cell proliferation [Hinton et al., 2006; Lincoln et al., 2004]. Altered expression of specific genes also marks this process; expression of remodelling enzymes (such as matrix metalloproteinases) decreases, and there is an increase in expression of constituents of valvular ECM such as the proteoglycans aggrecan and versican [Shelton and Yutzey, 2007]. The molecular mechanisms regulating valve morphogenesis and remodelling are not well understood. Correct positioning of valves is critical, and BMP2 and TBX2 play roles in regulating this process [Harrelson et al., 2004; Ma et al., 2005]. TBX20 expression antagonises the transition from endocardial cushions to remodelled valves [Shelton and Yutzey, 2007]. Notch signalling is important in development of the endocardial cushions that give rise to cardiac valves [Timmerman et al., 2004], and mutations in the human *NOTCH1* gene can result in abnormal aortic / mitral valve development [Garg et al., 2005].

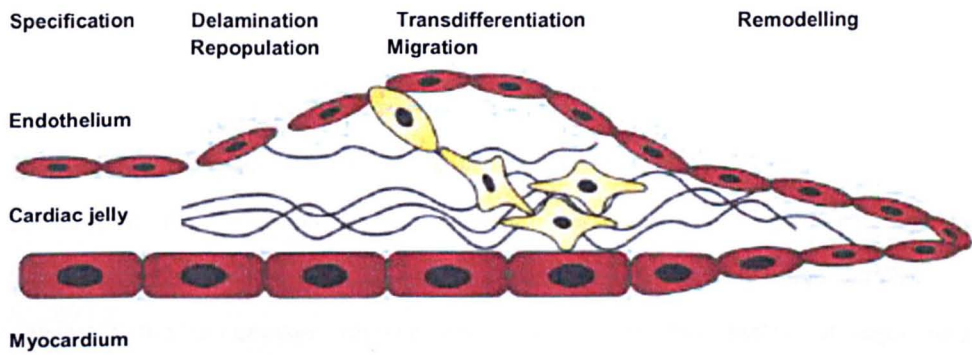


**Figure 1.5 Cardiac valve formation**

The heart tube is composed of an outer myocardial cell layer, and an inner endothelial cell layer, with a layer of extensive extracellular matrix (ECM) in between, termed the cardiac jelly. Specified endothelial cells at the future valve site undergo epithelial-to-mesenchymal transformation (EMT) (they delaminate, differentiate, and migrate into the cardiac jelly layer). Cardiac cushions undergo remodelling to form cardiac valves.

*Adapted from Armstrong and Bischoff et al., 2004*

### **1.1.9 The cardiac conduction system**

The co-ordinated and rhythmic contraction of the heart occurs as a result of precisely timed action potentials generated via the cardiac conduction system (CCS) [Moorman et al., 1997]. The CCS comprises the sino-atrial node (SA node) also known as the pacemaker, the atrioventricular node (AV-node), and the His-Purkinje system [Moorman et al., 1997]. The SA node is found in the wall of the right atrium, and generates the pacemaker impulse which determines the rhythm of myocardial contraction [Moorman et al., 1997]. The AV node is located at the base of the interatrial septum, and serves to slow transmission of the impulse to the ventricles, causing a delay which allows blood to exit the atria prior to ventricular contraction [Moorman et al., 1997]. Signals from the AV node are transmitted via the AV bundle and bundle branches, activating contraction of the ventricles via the Purkinje fibre network system [Moorman et al., 1997]. As the atrial septum is important in this pathway, defects in atrial septation can lead to altered atrial conduction routes [James, 1970].

## **1.2 CONGENITAL HEART DEFECTS**

Congenital heart defects (CHD) are a leading cause of infant mortality, with an incidence of around 7.5 cases per 1000 live births [Samson and Kumar, 2004]. Development of the heart is a complex process and defects can occur at a number of stages leading to a variety of heart malformations, some of which are represented in Figure 1.6. Selected CHDs are described below.

### **1.2.1 Cardiac septation defects**

Defects in cardiac septation account for approximately 50% of CHD cases [Hoffman and Kaplan, 2002]. Atrial septal defects (ASDs), where the atria are not fully septated, can be divided into two categories. Ostium secundum defects are the most common form of ASD, and this type of defect occurs due to excessive degeneration of the septum primum, or inadequate development of the septum secundum [Blom et al., 2005]. This condition is associated with mitral valve prolapse in 10 – 20% of sufferers [Leachman et al., 1976]. Ostium primum defects occur less frequently than ostium secundum defects, usually in association with Trisomy21 [Kaur et al., 2008]. The ostium primum is usually sealed by fusion of superior and inferior endocardial cushions, and ostium primum defects usually occur as a result of failure of ostium primum closure due to defects in the AV endocardial cushions. As these endocardial cushions are also required for mitral and tricuspid valve formation, ostium primum defects are usually accompanied with valve abnormalities [Balchum et al., 1956].

Atrioventricular septal defects (AVSDs), where both the atria and ventricles are not fully septated, arise due to malformation of the atrioventricular canal cushions, which lead to inadequate fusion with the atrial or ventricular septum [Sadler, 2006]. Two types of ventricular septal defects (VSDs) may occur. Muscular ventricular septal defects arise as a result of incomplete proliferation of cardiomyocytes in the muscular portion of the interventricular septum [Soto et al., 1980]. Perimembranous ventricular septal defects arise due to defects in the membranous portion of the septum, occurring as a result of endocardial cushion defects [Soto et al., 1980].

### 1.2.2 Conotruncal and aortic arch artery defects

Cardiac outflow tract and aortic arch defects account for 20 – 30% of CHD cases [Hoffman and Kaplan, 2002]. Since cardiac neural crest cells contribute to this region, many conotruncal defects arise due to defects in their differentiation or migration. Double outlet right ventricle (DORV) is where both great arteries align with the right ventricle, and occurs as a result of defects in neural crest cell migration, or incomplete rotation of the outflow tract [Oblor et al., 2008]. Persistent truncus arteriosus (PTA) occurs due to a failure of conus ridge fusion and truncus septation, resulting in the pulmonary artery arising from the common truncus [Sadler, 2006]. This is always accompanied by a ventricular septal defect as the conus ridges also play a part in interventricular septation. This condition can arise through defects in neural crest cell migration [Kirby, 1987]. Transposition of the great arteries (TGA) occurs when the conotruncal septum does not follow its normal course, leading to connection of the aorta to the right ventricle, and the pulmonary artery to the left ventricle [Sadler, 2006]. This can be due to defects in looping, or in the migration of neural crest cells, which are important in forming the truncal cushions [Kirby et al., 1983]. Anterior displacement of the conotruncal septum and unequal division of the conus region leads to tetralogy of Fallot (TOF), a heart disorder comprising four anatomical defects; narrow right ventricular outflow region, a ventricular septal defect, overriding aorta, and right ventricular hypertrophy [Sadler, 2006]. The ductus arteriosus is the arterial connection between the pulmonary artery and aorta, and serves to shunt blood from the right ventricle away from the lungs, allowing them to be bypassed during foetal development. The ductus normally constricts and closes shortly after birth, and failure to do so results in patent ductus arteriosus (PDA) [Sadler, 2006]. There is evidence that this disorder may arise as a result of defects in cardiac neural crest cell differentiation or migration [Char, 1978], or altered smooth muscle cell contractility in the aorta [Guo et al., 2007; Zhu et al., 2006].

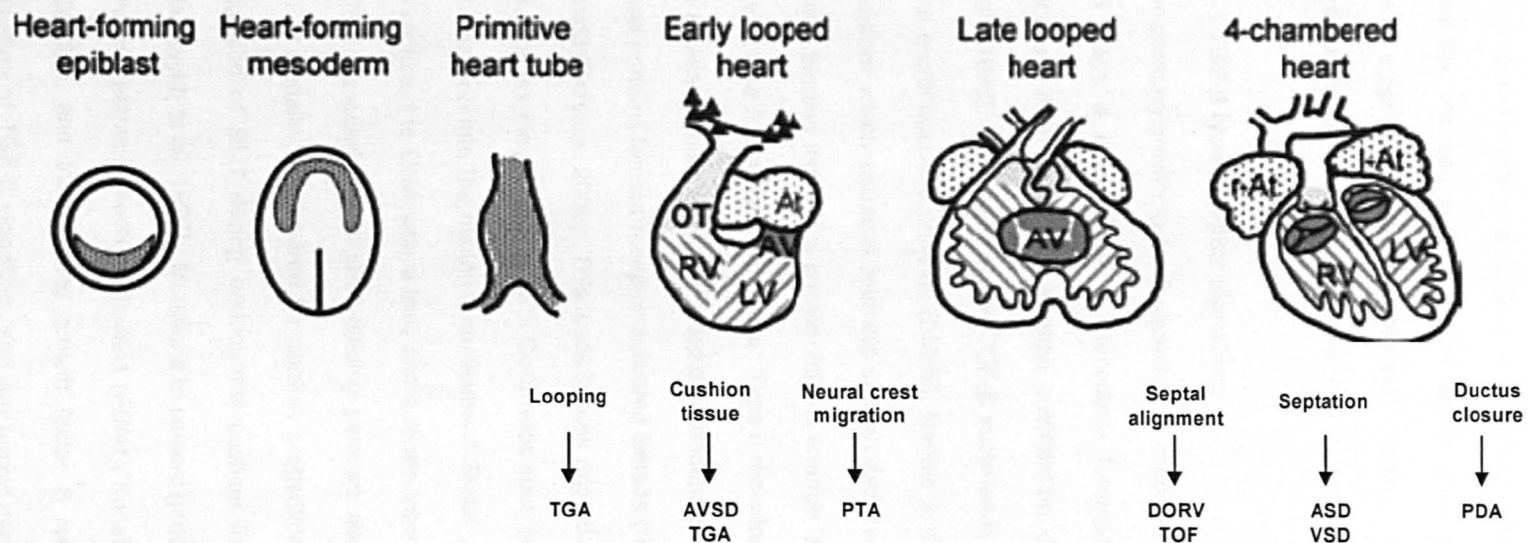


**Figure 1.6 Stages of heart development and associated defects**

Development of the heart is a complex process and defects can occur at a number of stages leading to a variety of heart malformations, some of which are represented. AVSD – atrioventricular septal defect, TGA - transposition of the great arteries, PTA – persistent truncus arteriosus, DORV – double outlet right ventricle, TOF – tetralogy of Fallot, ASD – atrial septal defect, VSD – ventricular septal defect, PDA – patent ductus arteriosus. OT – outflow tract, RV – right ventricle, LV – left ventricle, AV- atrioventricular canal, At – atrium. *Adapted from Sakabe et al., 2005*

### 1.3 GROWTH FACTOR SIGNALLING IN CARDIAC DEVELOPMENT

Patterning of the developing embryo is governed by a group of signalling pathways that co-operate with one another to provide positional information and allow complex cross-talk between tissues for the development of specific organs and structures. This is a tightly regulated process and involves a vast array of signalling molecules. Some of the signalling pathways involved in development of the heart are discussed.

#### 1.3.1 TGF- $\beta$ type receptor signalling

Transforming growth factor- $\beta$  signalling is important in early developmental pathways, and plays a crucial role in mesoderm formation and cardiogenesis, mediating processes such as cell specification, proliferation, differentiation, and apoptosis [Ladd et al., 1998]. Members of the TGF- $\beta$  superfamily of signalling molecules (such as bone morphogenetic proteins (BMPs), Nodals and Activins) bind to type I or type II receptors which possess intrinsic serine/threonine kinase activity [Derynck, 2008]. Ligand binding induces a conformational change leading to cell surface assembly of type I / type II receptor complexes. Type II receptors then phosphorylate and activate the kinase domain of type I receptors, leading to phosphorylation of a subgroup of Smad proteins termed receptor-activated Smads (R-Smads), for example Smad2 and Smad3 [Derynck, 2008]. This leads to their migration towards the nucleus, and during this process they associate with Co-Smads such as Smad4 and Smad4 $\beta$ . Following translocation into the nucleus, multisubunit Smad complexes (Smad4/Smad2/Smad3) are recruited to DNA where they can activate transcription of target genes [Derynck, 2008]. Association with DNA-binding partners allows selective activation of genes. TGF- $\beta$  signalling is required for cardiac progenitor differentiation, and has a role in regulation of EMT during endocardial cushion formation [Yamagishi et al., 2009; Yatskievych et al., 1997]. Mutations in several genes which are involved in the TGF- $\beta$  signalling pathway, such as fibrillin1 (*FBN1*), transforming growth factor  $\beta$  receptor 1 (*TGF $\beta$ R1*), and transforming growth factor  $\beta$  receptor 2 (*TGF $\beta$ R2*), lead to up-regulation of TGF- $\beta$  signalling, and are associated with aortic aneurysms [ten Dijke and Arthur, 2007]. Deletion of the type I receptor Alk3 (BMPRIa) in mouse embryonic

hearts results in impaired EMT in the AV canal with drastically reduced numbers of mesenchymal cells here, demonstrating that BMP signalling via this receptor is essential for endocardial cushion morphogenesis in this region [Song et al., 2007]. Deletion of Smad4 in embryonic cardiomyocytes during mouse development results in severe heart defects, and expression of the cardiac transcription factors Nkx2.5, GATA-4 and MEF2C is disrupted [Qi et al., 2007]. Targeted disruption of Smad6 (an inhibitory Smad) results in cardiac valve hyperplasia and defects in outflow tract septation, indicating a role for Smad6 in endocardial cushion development [Galvin et al., 2000].

#### **1.3.1.1 BMPs**

BMPs are multifunctional signalling proteins belonging to the TGF $\beta$  family. During development, BMPs such as BMP2 and BMP4 secreted by the endoderm cause commitment of mesodermal cells lateral to the Hensen's node to the cardiac cell lineage following gastrulation [Barron et al., 2000; Lough and Sugi, 2000; Yamada et al., 2000]. BMP2 is involved in correct positioning of heart valves [Harrelson et al., 2004; Ma et al., 2005]. BMP2 induces expression of the cardiac transcription factors Nkx2.5 and GATA-4 in the developing chick [Andree et al., 1998], and also acts upstream of the cardiac transcription factor MEF2A, activating its expression in neonatal cardiomyocytes [Wang et al., 2007]. BMP2 null mice do not express Nkx2.5 and display severe defects in heart formation including a failure to undergo looping [Zhang and Bradley, 1996]. BMP4 is expressed asymmetrically in the heart tube, and is important in cardiac looping [Breckenridge et al., 2001]. BMP4 null mice display a reduction or total lack of mesodermal differentiation, and Brachyury (a mesodermal marker) is not expressed [Winnier et al., 1995]. GATA-4 is a downstream transcriptional mediator of BMP4 signalling in the lateral mesoderm in mice [Rojas et al., 2005]. BMP4 activates Smad1, 5 and 8 when added to the outflow tract of the developing chick (E4.5), inducing expression of Sox9 and aggrecan in the semilunar valves, a transcription factor and proteoglycan characteristic of cartilage cell types [Zhao et al., 2007].

### **1.3.2 Receptor tyrosine kinase signalling**

Receptor tyrosine kinases (RTKs) mediate growth factor signalling and are important in processes such as embryogenesis, cell proliferation, and apoptosis [Schlessinger, 2000]. Ligand binding causes receptor dimerisation, activation of tyrosine kinase activity and autophosphorylation of the intracellular domain. Phosphorylated tyrosines in this region serve as binding sites for the Src homology 2 / phosphotyrosine binding domains of signalling proteins, which are phosphorylated upon binding to become activated [Schlessinger, 2000]. This can activate several pathways including the Ras / MAPK pathway, which leads to phosphorylation and activation of transcription factors in the nucleus, regulating expression of target genes. Some examples of growth factors that signal via receptor tyrosine kinases during heart development are discussed below.

#### **1.3.2.1 Fibroblast growth factors**

Fibroblast growth factors (FGFs) are a large family of polypeptide growth factors involved in a range of cellular processes including apoptosis, cell-cell adhesion, cell migration, differentiation, and proliferation [Bottcher and Niehrs, 2005]. FGF signalling during early embryonic development is important in induction, gastrulation, and patterning of the embryo [Bottcher and Niehrs, 2005], and is required for cardiomyocyte differentiation [Zhu et al., 1996]. FGFs signal via binding to fibroblast growth factor receptors (FGFRs), a subfamily of receptor tyrosine kinases. This can lead to activation of three possible FGF signal transduction pathways – the Ras / MAPK pathway (which leads to phosphorylation and activation of target transcription factors), the PLC $\gamma$  / Ca $^{2+}$  pathway (activating protein kinase C and also stimulating intracellular Ca $^{2+}$  release), and the PI3 kinase / Akt pathway (involved in mesoderm induction) [Bottcher and Niehrs, 2005]. FGF2 signalling plays a role in commitment of mesodermal cells to a cardiac lineage during development [Sugi et al., 1993]. FGF2 is expressed early in cardiac development in the trabeculated region of the ventricular myocardium, and is involved in the regulation of myocyte proliferation and differentiation [Consigli and Joseph-Silverstein, 1991]. FGF4 increases MAPK

phosphorylation and signalling, resulting in increased expression of genes that characterise tendon cell types in avian semilunar valves [Zhao et al., 2007]. Inhibition of the FGF signalling pathway in *Xenopus* prevents mesoderm induction. The *Xenopus* genes *sprouty2* and *spred1* have been identified as targets and mediators of FGF signalling, with roles in mesodermal specification [Sivak et al., 2005]. FGF8 is expressed in the mesoderm and participates in directing mesodermal cells to the cardiogenic cell lineage, co-operating with BMP2 in this role [Alsan and Schultheiss, 2002; Lopez-Sanchez et al., 2002; Lough et al., 1996; Zhu et al., 1996]. Cardiogenic induction is thought to be via activation of expression of cardiac transcription factors such as members of the Tbox, GATA and NK families. Both FGF8 and BMP2 are required for expression of Nkx2.5 and MEF2C [Alsan and Schultheiss, 2002]. FGF8 can also direct limb development and induces expression of Wnt2b and Wnt8c (at the forelimb and hindlimb levels respectively) in the intermediate mesoderm of the chicken embryo [Crossley et al., 1996; Kawakami et al., 2001]. FGF10 plays a crucial role in limb development, with TBX5 as an upstream regulator, and there is reciprocal regulation of TBX5 expression by FGF signalling [Ohuchi et al., 1997]. In zebrafish, FGF24 has been shown to act downstream of TBX5 to regulate FGF10 expression [Fischer et al., 2003].

### **1.3.2.2 Vascular Endothelial Growth Factor**

Vascular Endothelial Growth Factor (VEGF) is important in vascular development and heart morphogenesis [Tomanek et al., 2006], and plays an important role in heart valve formation [Lee et al., 2006]. VEGF signalling occurs via VEGFR1 / Flt1 and VEGFR2 / Flk1 receptors. The downstream targets of VEGF signalling are not fully characterised. The gene Down syndrome candidate region 1 (DSCR1) has been identified as one downstream mediator of VEGF signalling, with a role in endothelial cell migration and angiogenesis [Iizuka et al., 2004]. VEGF has also been shown to up-regulate Nkx2.5 in differentiated embryonic stem cells [Chen et al., 2006]. Single allelic loss of VEGF in mice results in defects in endocardial cushion formation, septation, and chamber formation [Stalmans et al., 2003]. Overexpression of VEGF

results in altered expression of eHand (an important cardiac transcription factor) and consequent defects in heart looping [Nagao et al., 2007].

### **1.3.2.3 Epidermal Growth Factors**

Epidermal Growth Factors (EGFs) signal via the four tyrosine kinase receptors of the ErbB family, ErbB1 – ErbB4. EGF signalling is important in embryonic development, in processes such as cell proliferation and differentiation. In the heart, EGF signalling via ErbB2 and ErbB4 is important in trabeculae development [Gassmann et al., 1995; Lee et al., 1995], whilst signalling via ErbB3 is important in endocardial cushion and cardiac valve formation [Erickson et al., 1997]. Mouse knockout of heparin-binding EGF-like growth factor (HB-EGF) results in enlarged heart valves and postnatal lethality in around 50% of cases, demonstrating a role for this type of signalling in correct valve development and function [Nanba et al., 2006].

### **1.3.2.4 Cytokine signalling**

Janus kinases (JAKs) are a family of cytosolic tyrosine kinases associated with membrane receptors that do not possess intrinsic kinase activity. Cytokine binding to these transmembrane receptors leads to receptor-kinase complex dimerisation, kinase activation and receptor phosphorylation [Heinrich et al., 1998]. This allows binding of the SH2 domain of signal transducer and activators of transcription (STATs), a family of transcription factors that become phosphorylated upon binding and translocate into the nucleus to activate transcription of target genes [Heinrich et al., 1998]. The cytokine family members Interleukin-6 (IL-6) and Leukaemia Inhibitory Factor (LIF) are important in the heart, and function through activation of the JAK / STAT pathway which leads to phosphorylation of STAT3 [Heinrich et al., 1998]. STAT3 phosphorylation (mediated by JAK1 or JAK2) results in dimerisation, nuclear translocation, DNA binding, and transcriptional activation [Heinrich et al., 1998]. MAPK also phosphorylates STAT3 at a separate site to influence its transcriptional activity [Jain et al., 1998]. STAT3 directly regulates expression of the cardiac transcription factors TBX5, GATA-4 and Nkx2.5, and is required for differentiation of

P19 cells into cardiomyocytes [Snyder et al.]. In addition, the JAK/STAT pathway is important in ischemic preconditioning [Xuan et al., 2001], with STAT3 mediating cardioprotection against ischemia/reperfusion injury [Oshima et al., 2005]. LIF promotes cardiac cell commitment to the endothelial cell lineage for neovascularisation during tissue remodelling [Mohri et al., 2006]. In the heart, IL-6 is important in cardioprotection, formation of blood vessels, and cell-cell adhesion [Fuji et al., 2004; Oshima et al., 2005; Osugi et al., 2002].

### 1.3.3 Wnt signalling

Wnt genes, defined by their homology to the *Drosophila wingless* gene, encode secreted lipid-modified glycoproteins that are involved in the activation of different intracellular signalling pathways via interaction with seven-transmembrane frizzled receptors [Brade et al., 2006]. There are three known Wnt signalling pathways - the canonical Wnt/ $\beta$ -catenin pathway, and non-canonical Wnt/PCP and Wnt/ $\text{Ca}^{2+}$  pathways [Brade et al., 2006]. The best characterised is the Wnt/ $\beta$ -catenin pathway, in which ligand binding stabilises cytoplasmic  $\beta$ -catenin, allowing it to enter the nucleus for regulation of gene expression through interaction with HMG-box transcription factors [Logan and Nusse, 2004]. This pathway plays a dual role in myocardial specification, promoting cardiac differentiation in early development, and inhibiting this process at later stages [Ueno et al., 2007]. Non-canonical Wnt signalling pathways, which are also important during cardiac development, act via G-protein mediated intracellular calcium influx for activation of calcium sensitive enzymes such as protein kinase C (PKC) or calcineurin, rho family GTPases, and jun N-terminal kinase (JNK) [Veeman et al., 2003]. Wnt11, via non-canonical signalling, promotes differentiation of mesodermal cells to a cardiac lineage in early development [Eisenberg and Eisenberg, 1999]. Loss of this gene is associated with abnormal heart tube formation [Pandur et al., 2002]. In addition, this type of signalling also regulates morphogenetic movements during development through regulation of cadherin-mediated cell adhesion and polarity [Torres et al., 1996; Toyofuku et al., 2000; Ulrich et al., 2005]. A large number of Wnt ligands (Wnt2, Wnt2b, Wnt3a, Wnt5a, Wnt5b,

Wnt7a, Wnt8c, Wnt9, Wnt11) and frizzled receptors (Fz2, Fz4, Fz9) have been identified during murine and/or avian cardiac development, suggestive of distinct but potentially overlapping roles [Dealy et al., 1993; DeRossi et al., 2000; Eisenberg and Eisenberg, 1999; Hume and Dodd, 1993; Jaspard et al., 2000; Liu et al., 1999; Takada et al., 1994; van Gijn et al., 2001; Wang et al., 1999].

#### 1.4 TRANSCRIPTIONAL REGULATION OF CARIOGENESIS AND GENE REGULATORY NETWORKS

Cardiac transcription factors play a key role in regulating expression of the many regulatory and structural genes involved in growth and patterning of the heart, and mutations in a number of important cardiac transcription factors are associated with CHDs. Members of the NK2, Tbox, GATA, MEF2, and HAND gene families form a core cardiac regulatory network which transcriptionally regulates downstream cardiac genes, and additionally, these transcription factors can also regulate expression of one another. Key members of these gene families are described in this section. The target genes of these transcription factors are largely unknown and this area is being widely researched. Figure 1.7 represents this core network and known upstream activators. Nkx2.5, GATA-4, Isl1 and Foxh1 are targets of inductive signals. Nkx2.5 and GATA-4 are upstream activators in the primary heart field, and Isl1 and Foxh1 are upstream activators in the secondary heart field [Cai et al., 2003; Dodou et al., 2004; Lin et al., 1997; von Both et al., 2004]. Cardiac transcription factors function within complex gene regulatory networks, as previously described with respect to GATA-4, -5 and -6, GATA-4 and Nkx2.5 [Peterkin et al., 2005], and overall during various developmental stages of mesendoderm formation in *Xenopus* [Loose and Patient, 2004].

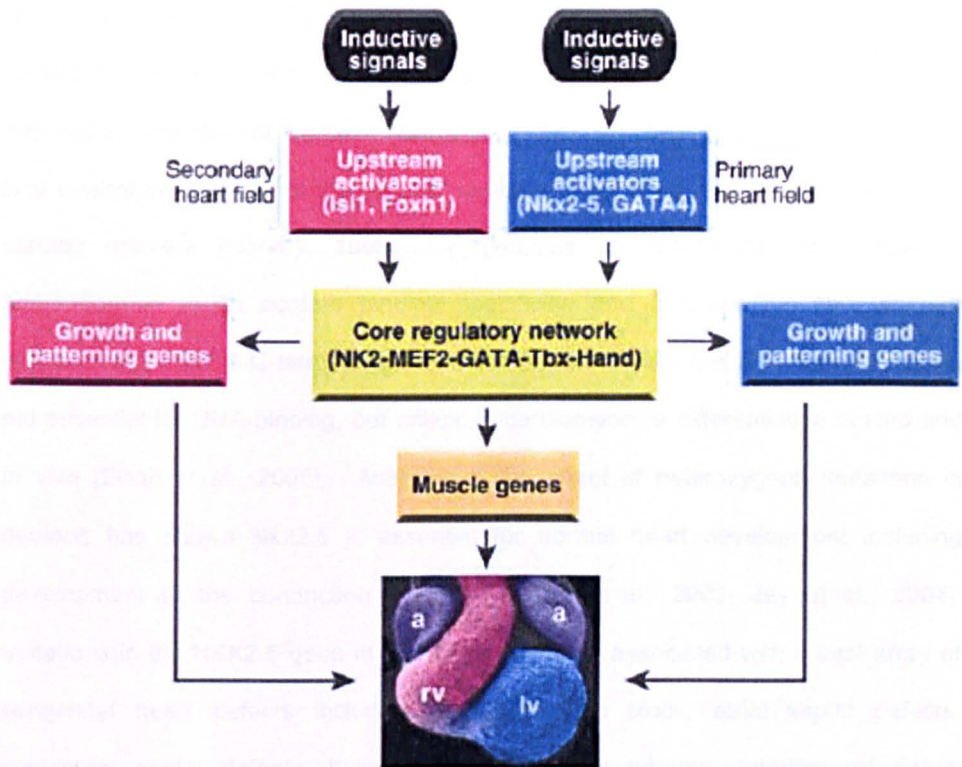


**Figure 1.7 Transcriptional networks involved in heart development**

The core cardiac regulatory network comprising members of the NK2, MEF2, GATA, Tbx and Hand gene families is represented with upstream activators, which are activated by inductive signals. Members of these gene families transcriptionally regulate important downstream genes (structural and regulatory), and can also regulate expression of one another. Nkx2.5 and GATA-4 are upstream activators of primary heart field formation, and Isl1 and Foxh1 are upstream activators of the secondary heart field. The scanning electromicrograph image is of a mouse heart at E14.5, and regions arising from the primary and secondary heart fields are displayed in blue and pink respectively. Regions arising from both i.e. the atria, are shown in purple. a - atrium, rv – right ventricle, lv – left ventricle. *Adapted from Olson, 2006*

### 1.4.1 Nkx2.5

Nkx2.5 is an evolutionarily conserved member of the NK2 class of homeodomain transcription factors. It is a homologue of the *Drosophila tinman* gene, which is required for formation of the heart [Azpiazu and Frasch, 1993; Bodmer, 1993]. Nkx2.5 is a central component of the cardiac regulatory hierarchy and one of the earliest cardiac markers [Harvey, 1996]. It contains an N-terminal TN domain, a homeodomain which confers binding specificity, and a C-terminal NK2 specific domain (NK2-SD). A C-terminal tyrosine rich domain (YRD) has also been identified, not essential for DNA-binding, but critical in cardiomyocyte differentiation *in vitro* and *in vivo* [Elliott et al., 2006]. Analysis of the effect of heterozygous mutations in humans has shown Nkx2.5 is essential for normal heart development including development of the conduction system [Harvey et al., 2002; Jay et al., 2004]. Mutations in the NKX2.5 gene in humans have been associated with a vast array of congenital heart defects including AV conduction block, atrial septal defects, ventricular septal defects, hypoplastic left heart syndrome, tetralogy of Fallot, persistent truncus arteriosus, double outlet right ventricle, and transposition of the great arteries [Benson et al., 1999; Elliott et al., 2003; McElhinney et al., 2003; Pashmforoush et al., 2004; Schott et al., 1998].

Nkx2.5 is expressed in heart precursor cells in the primary and secondary heart fields during mouse development [Komuro and Izumo, 1993], and is highly expressed in the adult heart, with the protein detectable in myocytes of the atria and ventricles [Kasahara et al., 1998]. Mouse knockout of Nkx2.5 results in an arrest in cardiac looping, leading to embryonic lethality at E9/10 [Lyons et al., 1995; Tanaka et al., 1999]. Ventricular restricted knockout has demonstrated a crucial role for Nkx2.5 in development and function of the cardiac conduction system [Pashmforoush et al., 2004], and in line with this, a transient increase in Nkx2.5 expression is seen in developing myocardial conduction cells during development of the conduction system [Thomas et al., 2001].

Nkx2.5 transcriptionally regulates expression of an array of cardiac genes including myosin light chain 2v (MLC2v),  $\alpha$ -cardiac actin, connexin 40, myocardin, ANF, MEF2C, and eHAND [Biben and Harvey, 1997; Bruneau et al., 2001; Chen and Schwartz, 1996; Lyons et al., 1995; Tanaka et al., 1999; Ueyama et al., 2003], Nkx2.5 interacts with several important cardiac transcription factors including some members of the GATA and T-box families, SRF, and others (section 1.5).

#### **1.4.2 The T-box family of transcription factors**

The T-box gene family encodes a group of transcription factors important in the patterning of the vertebrate embryo, and is characterised by a conserved 180 amino acid DNA-binding motif, the T-box. They regulate critical developmental processes such as cell type specification and morphogenesis, and mutations in several T-box genes lead to developmental defects.

*TBX1* – *TBX5*, *TBX18* and *TBX20* are all expressed in the developing heart [Bussen et al., 2004; Chapman et al., 1996; de Lange et al., 2004; Stennard et al., 2003]. Mouse knockout studies have been carried out on each of these genes, and all result in perinatal or embryonic lethality [Bussen et al., 2004; Davenport et al., 2003; Harrelson et al., 2004; Jerome and Papaioannou, 2001; Lindsay, 2001; Lindsay et al., 2001; Stennard et al., 2005; Takeuchi et al., 2003]. *TBX1* heterozygotes display abnormal development of the aorta, pulmonary artery, and fourth pharyngeal artery [Jerome and Papaioannou, 2001; Lindsay et al., 2001], whilst heterozygotes of the other T-box genes are viable and fertile / apparently normal [Bussen et al., 2004; Davenport et al., 2003; Harrelson et al., 2004; Naiche and Papaioannou, 2003; Stennard et al., 2005]. *TBX1* is important in proliferation of cells forming the secondary heart field (which contributes to OFT formation) [Xu et al., 2004; Zhang et al., 2006]. In humans, *TBX1* haploinsufficiency results in DiGeorge syndrome [Merscher et al., 2001], a disorder whose symptoms include outflow tract defects. Mutations in *TBX3* have been associated with Ulnar Mammary syndrome [Bamshad et al., 1997], a rare disorder characterised by upper limb malformation and abnormal

development of the mammary glands, nipples, teeth, genitalia, and apocrine glands [Schinzel, 1987]. Ventricular septal defects have also been observed, therefore this gene is sometimes considered a 'heart-hand' gene [Linden et al., 2009]. *TBX4*, together with *wnt8c* and *fgf10*, is involved in development of the lower limbs [Takeuchi et al., 2003], and *TBX4* mutations are associated with small patella syndrome [Bongers et al., 2004]. There is evidence of a role for *TBX20* in promotion of cell proliferation in valve precursor cells in endocardial cushions during development [Shelton and Yutzey, 2007]. *TBX20* heterozygotes display mild dilated left ventricular cardiomyopathy [Stennard et al., 2005], and mutations in humans have been associated with cardiomyopathy and defects in septation and valve development [Kirk et al., 2007]. *TBX22* mutations are associated with cleft palate [Packham and Brook, 2003].

#### 1.4.2.1 *TBX5*

*TBX5* is a member of the T-box family of transcription factors, and plays an important role in heart development and specifying forelimb identity [Isaac et al., 1998]. Mutations in *TBX5* are associated with Holt-Oram syndrome (HOS) [Basson et al., 1997; Fan et al., 2003; Li et al., 1997], a congenital disorder characterised by upper limb and heart abnormalities. These are usually atrial septal defects (ostium primum or ostium secundum) or ventricular muscular septal defects, but other abnormalities may also occur including mitral valve defects, electrophysiological defects such as AV conduction block, tetralogy of Fallot, and left-sided abnormalities including hypoplastic left heart syndrome, defective trabeculation, and endocardial cushion defects [Basson et al., 1994; Bruneau et al., 1999; Newbury-Ecob et al., 1996; Sletten and Pierpont, 1996]. The majority of HOS associated *TBX5* mutations are found in the T-box [Mori and Bruneau, 2004].

*TBX5* displays expression in the heart and upper limbs during embryogenesis [Chapman et al., 1996]. Expression is initiated early in development, where it is observed throughout the cardiac crescent and in the forelimb field [Begemann and

Ingham, 2000]. Analysis of the cardiac expression pattern of TBX5 in the developing mouse and chick has correlated its expression with the sites of defects observed in HOS; TBX5 is expressed throughout the early heart tube, later becoming restricted to the posterior regions which give rise to the sinus venosus, atria, and left ventricle [Bruneau et al., 1999]. TBX5 is subsequently expressed in the left ventricle, left side of the ventricular septum, trabeculae, and also in the atrial walls, atrial septa, and atrial side of the AV valves, consistent with the ASDs, VSDs, and left-sided malformations seen in HOS [Bruneau et al., 1999].

Studies involving TBX5 knockout / overexpression have allowed elucidation of its function in cardiogenesis. Overexpression of wild type TBX5 transcripts both *in vitro* and *in vivo* (in the embryonic chick) results in an inhibitory effect on cardiomyocyte proliferation, with a resulting decrease in heart size [Hatcher et al., 2001]. Conversely, TBX5 heterozygous null mice, in addition to ventricular and atrial septal defects, display an overall enlargement of the heart, with dilation of the right atrium and ventricle [Bruneau et al., 2001]. Complete knockout of mouse TBX5 results in embryonic lethality by E10.5; heart fails to undergo looping, and hypoplasia (underdevelopment) of the sinuatria and left ventricle occurs [Bruneau et al., 2001]. These findings indicate a regulatory role for TBX5 in chamber morphogenesis. TBX5 can interact with other transcription factors including Nkx2.5 and GATA-4, for synergistic regulation of cardiac genes (section 1.5).

#### **1.4.3 The GATA family of transcription factors**

GATA transcription factors contain two conserved zinc fingers (Cys-X<sub>2</sub>-Cys-X<sub>17</sub>-Cys-X<sub>2</sub>-Cys) that bind to the consensus DNA sequence (A/T) GATA (A/G), a regulatory sequence first identified during studies into the tissue specific expression of erythroid-specific nuclear protein factors [Plumb et al., 1989]. Six members of the GATA family of transcription factors have been identified to date, GATA 1 – 6. Each is expressed in a lineage restricted pattern, regulating expression of genes within specific tissues and playing a major role during development. The GATA factors have been

subdivided into two groups based on their protein structure and expression pattern; GATA-1, -2 and -3 which are important in haematopoiesis and ectodermal patterning [Leonard et al., 1993], and GATA-4, -5 and -6, which are expressed in mesoderm and endoderm derived organs and are important in cardiac development [Peterkin et al., 2005]. Conservation of particular factors between species is higher than conservation of different GATA factors within the same species [Jiang and Evans, 1996] i.e. individuality of the GATA genes has been conserved through evolution implying a unique function for each.

#### **1.4.3.1 GATA-4**

Mutations in the human GATA-4 gene have been associated with atrial and ventricular septal defects [Garg et al., 2003], and tetralogy of Fallot [Nemer et al., 2006]. GATA-4 contains two zinc finger domains, a C-terminal nuclear localisation sequence (for DNA-binding and protein-protein interactions), and two N-terminal transcriptional activation domains (TAD), that are conserved within the GATA-4/5/6 subfamily [Morrissey et al., 1997b]. Expression of GATA-4 is seen in the cardiac ventral mesoderm at the time of linear heart tube formation, and subsequently in the developing atria and ventricles, and in the endocardium but not myocardium [Kelley et al., 1993].

A number of knockdown / knockout studies have been performed to assess the specific functions of GATA-4 in cardiogenesis. The P19 mouse embryonal carcinoma cell line can be induced to differentiate into beating cardiac muscle cells and is thus a widely used *in vitro* model system of cardiac cell differentiation. The effect of a reduction in GATA-4 protein has been investigated in this cell line through stable transfection with GATA-4 antisense expression vectors [Grepin et al., 1995]. Presence of antisense transcripts results in a marked reduction in active GATA-4 protein, but has no effect on the morphology of the cells. However, antisense clones displayed very poor differentiation in comparison to the wild type and control clones, indicating GATA-4 is required for differentiation of cardiac cells. In addition, clones

also failed to express important cardiac muscle markers such as BNP, TpC,  $\alpha$ -MHC,  $\beta$ -MHC, and MLC-1A, consistent with the theory that GATA-4 is essential for activation of cardiac cell differentiation.

GATA-4 null mouse embryos do not survive past early embryonic development, arresting at E7.0 – E9.5 due to defects in ventral morphogenesis and linear heart tube formation [Molkentin and Olson, 1997]. This means they cannot be used to study GATA-4 function later in development or in the adult heart. This has been overcome through the use of Cre/LoxP technology to conditionally inactivate GATA-4 expression in the mouse myocardium at selected time points in order to study its role in cardiac development [Zeisberg et al., 2005]. *GATA-4-loxP*-targeted mice were crossed with mice containing either an *Nkx2-5* locus or an  $\alpha$ -MHC promoter that drives Cre recombinase expression early or late in development respectively. Early myocyte restricted deletion of GATA-4 by *Nkx2-5<sup>Cre</sup>* showed no effect on overall development at E9.5. Whole mount examination of embryos at E9.5 showed cardiac malformations, most commonly a single predominant ventricular chamber. Histological sections showed myocardial hypoplasia, and small atrioventricular and OFT endocardial cushions, suggesting a defect in the EMT of endocardial cells. This was confirmed by selective inactivation of GATA-4 in endothelial derived cells which resulted in failure of endothelium to undergo EMT resulting in hypocellular cushions i.e. GATA-4 is required to form AV cushion mesenchyme which is essential in valve development [Rivera-Feliciano et al., 2006]. GATA-4 is also required subsequently in the remodelling of AV endocardial cushions for ventricular septation. At E10.0, embryos displayed a mild delay in development and pericardial effusions which signify heart failure. Embryonic lethality occurred by E11.5. *GATA-4-loxP*-targeted mice (*Gata4<sup>fl/fl</sup>*) have also been crossed with mice containing an  $\alpha$ -MHC or  $\beta$ -MHC promoter driven Cre transgene to study the function of GATA-4 in the adult heart [Oka et al., 2006]. The resulting mice survived into adulthood despite a 70–95% reduction in GATA-4 protein. Cardiac function was compromised as a result of GATA-4 deletion from the heart; the cardiac hypertrophic response was attenuated, cardiac cell death

increased, and basal gene expression significantly altered. It was concluded that GATA-4 transcriptionally regulates gene expression, hypertrophy, stress compensation, and myocyte viability in the heart.

#### 1.4.3.2 GATA-5

GATA-5 is expressed in the precardiac mesoderm from E7.0 / E8.0, in the atrial and ventricular chambers of the heart at E9.5, and is restricted to the atrial endocardium by E12.5 [Morrissey et al., 1997a]. It is also expressed in the developing lung, urogenital ridge, bladder and gut. The expression pattern of GATA-5 shows marked differences to that of GATA-4 and GATA-6, and unlike GATA-4 and GATA-6 null mice which do not survive into adulthood, GATA-5 null mice are viable and fertile [Molkentin et al., 2000]. Females display defects in the genitourinary system (males are unaffected) suggesting a unique role for GATA-5 in development of this region. One explanation for the mild phenotype is that GATA-4/6 may compensate for the loss of GATA-5.

#### 1.4.3.3 GATA-6

Like *GATA4*<sup>-/-</sup> mice, *GATA6*<sup>-/-</sup> mice also fail to develop beyond gastrulation due to its necessity in the visceral endoderm [Koutsourakis et al., 1999; Morrissey et al., 1998]. This has similarly been overcome through the use of Cre / LoxP technology to create a conditional loss of function allele [Sodhi et al., 2006]. Conditional inactivation of GATA-6 *in vivo* in VSMCs and in the cardiac neural crest results in cardiovascular abnormalities including aortic arch and outflow tract defects, indicating a role for GATA-6 in patterning of these regions [Lepore et al., 2006].

As mice heterozygous for GATA-4 or GATA-6 null mutations appear to be normal, and GATA-4 and GATA-6 have a similar protein structure and expression pattern, it was hypothesised that they may act co-operatively during cardiac development. This was tested by crossing *GATA-4*<sup>+/-</sup> and *GATA-6*<sup>+/-</sup> heterozygotes to produce compound heterozygotes [Xin et al., 2006]. Lethality with complete penetrance occurred at

E13.5. E10.0 embryos displayed enlargement and disorganisation of cranial and intersomitic vasculature suggesting defects in vessel development. Furthermore, mutants displayed failure of septation of the cardiac outflow tract, thinning of the myocardium, and vascular defects. Expression of some cardiac genes was altered, for example  $\beta$ -MHC and MEF2C were down-regulated. This demonstrates that a certain level of GATA-4 and GATA-6 expression is required for cardiovascular development.

#### **1.4.4 The MADS family of transcription factors**

The MADS family of transcription factors contain a 57 amino acid 'MADS box' which is important in homodimerisation and DNA-binding [Shore and Sharrocks, 1995]. Members of the MADS family can recruit other transcription factors to form regulatory complexes, which are important in regulation of target genes [Shore and Sharrocks, 1995; Sprague, 1990]. Relevant members of this family are described below.

##### **1.4.4.1 Serum Response Factor (SRF)**

Serum response factor (SRF) is a member of the MADS family that was initially discovered as an activator of growth factor and cell cycle genes, now known to be highly expressed in differentiating cardiac, skeletal and smooth muscle cells [Belaguli et al., 1997]. SRF is a key regulator of the expression of number of contractile genes, acting through binding to the CArG box (CC(A/T)<sub>6</sub>GG) [Belaguli et al., 1997]. The role of SRF in cardiovascular development has been studied by cardiac and smooth muscle cell-restricted inactivation in Cre recombinase mice [Miano et al., 2004]. Inactivation of the transgene at E8.5 in mice leads to progressively decreasing levels of SRF expression in cardiomyocytes and aortic smooth muscle cells, and poorly developed trabeculations and sarcomeric disorganisation at E10.5. Studies of SRF null mice also show that it is required for cardiac mesoderm formation [Arsenian et al., 1998]. Myocardin is a member of the SAP (SAF-A/B, Acinus, PIAS) domain family of nuclear proteins which have broad regulatory functions relating to transcription and chromatin organisation [Aravind and Koonin, 2000; Kipp et al., 2000]. Myocardin

associates with SRF to act as a highly potent transcriptional co-activator, and has an important function in cardiomyocyte differentiation [Wang et al., 2001]. Myocardin is expressed in cardiac and smooth muscle cells throughout the heart both during development (beginning at the same time as Nkx2.5) and postnatally [Wang et al., 2001], contributing to the muscle specificity of SRF [Wang et al., 2003b]. Mouse knockout of myocardin leads to embryonic lethality by E10.5, with mice displaying developmental delay and severe vascular defects [Li et al., 2003]. Interestingly, abnormalities are smooth muscle cell specific and cardiac morphogenesis is normal, possibly due to functional redundancy with additional myogenic regulators in cardiac muscle cells.

#### **1.4.4.2 The myocyte enhancer factor (MEF) family of transcription factors**

Myocyte enhancer factors 2 (MEF2s) belong to the MADS family of transcription factors and contain a conserved N-terminal MADS box and MEF2 domain, and C-terminal transactivation domain. Vertebrates possess four MEF2 genes, MEF2A – MEF2D, thought to have arisen from a common ancestral gene. They act as homo- or heterodimers and bind to the sequence CAT(A/T)<sub>4</sub>TAG/A [Black and Olson, 1998; McKinsey et al., 2002], which has been identified in the regulatory region of a number of muscle genes for transcriptional control of muscle development. Targets include  $\alpha$ -MHC [Molkentin and Markham, 1993], MLC1/3 [McGrew et al., 1996; Rao et al., 1996], MLC2v [Lee et al., 1994],  $\alpha$ -skeletal actin [Muscat et al., 1992], tropomyosin I [Lin et al., 1996], cardiac troponin T [Wang et al., 1994], cardiac troponin C [Gahlmann and Kedes, 1993; Parmacek et al., 1994], cardiac troponin I [Nakayama et al., 1996], desmin [Kuisk et al., 1996; Li and Capetanaki, 1994], and dystrophin [Klamut et al., 1997; Nishio et al., 1994].

##### **1.4.4.2.1 MEF2C**

MEF2C is expressed early in cardiac development, detectable in the cardiac mesoderm (from which the heart tube originates) at E7.5, and in the myocardium at E8.5 [Edmondson et al., 1994]. MEF2C knockout mice die by E9.5 as a result of

cardiac and vascular defects [Lin et al., 1997]. Conditional *mef2c*<sup>loxP/loxP</sup> knockout in mice results in failure of hearts to undergo looping, absence of right ventricle formation, and lack of expression of a subset of cardiac muscle genes, highlighting its importance in early heart development [Lin et al., 1997]. *Nkx2.5* and *MEF2C* have an up-regulatory effect on the expression of one another and induce cardiomyocyte differentiation on P19 cells [Skerjanc et al., 1998]. *MEF2C* is involved in a physical interaction with *TBX5* which is essential in cardiogenesis [Ghosh et al., 2009].

#### **1.4.4.2.2 MEF2A**

*MEF2A* is expressed in the myocardium during mouse embryogenesis from E8.5 [Edmondson et al., 1994]. It is involved in cardiac development, and mouse knockout of this gene results in right ventricular dilation and an increased likelihood of sudden perinatal death due to conduction defects, thought to result from a mitochondrial deficiency in cardiac muscle [Naya et al., 2002]. A deletion in exon 11 of the human *MEF2A* gene was found to be associated with coronary artery disease (CAD) in a large family of sufferers [Wang et al., 2003a], and a number of missense mutations in this gene were subsequently identified in sporadic CAD patients [Bhagavatula et al., 2004; Gonzalez et al., 2006; Weng et al., 2005].

#### **1.4.5 The HAND family of transcription factors**

The *HAND* gene family are a group of basic helix-loop-helix cardiac transcription factors. *dHand* and *eHand* are co-expressed in the precardiac mesoderm at E7.75, and later display regionally restricted expression in the ventricle forming regions of the heart tube; *dHand* is expressed in the right ventricle forming regions, and *eHand* in the left ventricle forming regions [Srivastava et al., 1997].

Gene deletion of *dHand* results in embryonic lethality by E10.5, and a wide spectrum of abnormalities are observed in cardiac looping, septation, and ventricular formation [Srivastava et al., 1997]. Transgenic mice expressing *dHand* under control of the  $\beta$ -MHC promoter show it is essential for interventricular septum formation and

trabeculation during heart development [Togi et al., 2006]. dHand upregulates ANF, BNP and connexin 40 expression in H9c2 cells and also in transgenic embryos overexpressing dHand. Targeted deletion of dHand in CNC derived cells causes misalignment of the aortic arch arteries and outflow tract, resulting in DORV and VSDs [Holler et al.].

Mice homozygous for an eHand allele die at E8.5 – E9.5 with defects in heart looping, hypoplasia of the left ventricle, and outflow tract abnormalities, demonstrating the importance of this gene in cardiac development [Firulli et al., 1998]. In humans, mutations in the eHand gene are associated with septal defects, outflow tract abnormalities, and hypoplasia [Reamon-Buettner et al., 2008; Reamon-Buettner et al., 2009]. This left-sidedness in expression of eHand is abolished in mouse embryos lacking Nkx2.5, showing Nkx2.5 plays a role in control of this asymmetric expression [Biben and Harvey, 1997].

## 1.5 CO-OPERATIVE ACTIVITY OF CARDIAC TRANSCRIPTION FACTORS

A number of important cardiac transcription factors physically interact to direct and synergistically regulate important pathways and key genes.

TBX5 and GATA-4 form a complex, and the *TBX5* mutations G80R and R237W, which are associated with cardiac septal defects in HOS patients [Basson et al., 1999], disrupt this interaction [Garg et al., 2003]. Functional analysis of a number of other *TBX5* mutations found in HOS has shown diminished binding of TBX5 to both GATA-4 and Nkx2.5, and a resulting decrease in transcriptional activation of ANF and FGF10 [Boogerd et al.]. The *GATA-4* mutation G296S has been linked to ASDs in humans, and also disrupts the TBX5 / GATA-4 interaction [Garg et al., 2003]. These findings together account for the fact that similar heart defects are seen as a result of both GATA-4 and TBX5 mutations, and indicate that these transcription factors direct and synergistically regulate common pathways important in septation. *Gata4*<sup>+/-</sup> *Tbx5*<sup>+/-</sup> compound heterozygous mice were generated during the time of this research (2009) and displayed embryonic lethality with almost full penetrance [Maitra et al., 2009]. Mice displayed defects in AV septation and myocardial thinning. *MYH6*, encoding  $\alpha$ -myosin heavy chain, is a joint target of TBX5 and GATA-4 [Ching et al., 2005; Huang et al., 1995; Molkenstein et al., 1994], and is down-regulated in *Gata4*<sup>+/-</sup> *Tbx5*<sup>+/-</sup> compound heterozygote mice [Maitra et al., 2009]. Brahma-associated factor (BAF) complexes belong to the SWI/SNF family of multi-subunit chromatin remodelling complexes which are important developmentally and can act both as activators and repressors of transcription [Ho and Crabtree]. BAF complexes can interact with a variety of transcription factors in different cell or tissue types, and show context-specific functions depending on their interaction partners [Ho and Crabtree]. Baf60c, a cardiac-specific subunit of BAF chromatin-remodelling complexes, acts by physically linking transcription factors to these complexes during cardiogenesis and is necessary for their function here [Lickert et al., 2004]. TBX5 and GATA-4, in combination with Baf60c (which is essential), can induce a full cardiac transcriptional programme and direct ectopic differentiation of the non-cardiogenic posterior mesoderm and

extraembryonic mesoderm of the amnion (of mouse) into beating cardiomyocytes [Takeuchi and Bruneau, 2009]. Interestingly, TBX5, GATA-4 and MEF2C in combination are able to reprogramme mouse postnatal fibroblasts into functional cardiomyocytes [Ieda et al.].

Tbx5 and Nkx2.5 specifically associate with one another via the N-terminal domain and N-terminal portion of the T-box of TBX5, and the homeodomain of Nkx2.5 [Hiroi et al., 2001]. This interaction is crucial for cardiomyocyte differentiation. TBX5 and Nkx2.5 directly bind to the ANF promoter for synergistic activation [Bruneau et al., 2001; Ghosh et al., 2001; Hiroi et al., 2001]. The *TBX5* mutations G80R and R237Q are both associated with HOS, and both disrupt the interaction with GATA-4 [Garg et al., 2003]. The former mutation results in a severe cardiac phenotype, whilst the latter results primarily in upper limb abnormalities with little effect on the heart [Basson et al., 1999]. The G80R mutation has an inhibitory effect on cardiomyocyte differentiation, and results in significantly diminished activation of the ANF promoter (with Nkx2.5), whilst the R237Q mutation has little or no effect on these, in line with the vast difference in severity of cardiac malformations these mutations underlie [Hiroi et al., 2001]. In a separate study, both mutations have been reported to eliminate target site binding [Ghosh et al., 2001].

TBX5 and MEF2C associate via their DNA binding domains to synergistically activate the MYH6 promoter [Ghosh et al., 2009]. TBX5 and Nkx2.5 act co-operatively to activate expression of connexin 40 [Bruneau et al., 2001], a gap junction protein crucial in conduction in the heart [Kirchhoff et al., 1998; Simon and Goodenough, 1998], suggesting one possible explanation for the conduction abnormalities seen in HOS. Purkinje fibres of the cardiac conduction system express high levels of Nkx2.5 and GATA-4 [Bruneau, 2002; Thomas et al., 2001]. Nkx2.5, GATA-4, and TBX5 act together with the nuclear factor Sp1 to regulate expression of connexin 40 via elements in its minimal promoter region [Linhares et al., 2004]. Nkx2.5 and GATA-4 are able to synergistically activate the promoter, whilst TBX5 counteracts this effect.

TBX20 directly associates with Nkx2.5 and GATA-4 [Stennard et al., 2003] and is also able to interact with the connexin 40 promoter. It represses activation by Nkx2.5 and GATA-4, whilst acting as an activator when the same reporter is stimulated with Nkx2.5 and GATA-5. This demonstrates that Tbx20 can function as a transcriptional activator or repressor depending on its binding partner. TBX20 also associates with TBX5, activating or repressing ANF promoter activity in a concentration dependent manner [Brown et al., 2005].

Mutations in both GATA-4 and Nkx2.5 are associated with familial ASD [Hirayama-Yamada et al., 2005]. Nkx2.5 and GATA-4 associate via helix III of the homeodomain of Nkx2.5 and the C-terminal zinc finger of GATA-4 [Lee et al., 1998]. These transcription factors can activate ANF individually, and in combination for synergistic activation in a manner which requires full transcriptional activity of both (including co-factor activity). The ANF promoter contains binding sites for TBX5, Nkx2.5, GATA (proximal and distal), and SRF [Small and Krieg, 2003]. Mutation of the TBX5, SRF or distal GATA site results in a strong reduction in ANF promoter activity. Mutation of the Nkx2.5 and proximal GATA site singly and together results in persistent expression in the ventricles and outflow tract. This suggests a repressor complex may bind to these sites for atrial specific ANF expression.

Nkx2.5 and SRF together stimulate promoter activity of  $\alpha$ -cardiac actin, and the presence of serum response elements (SREs) is crucial [Chen et al., 1996]. The C-terminal and MADS box of SRF are required for activation with Nkx2.5, and Nkx2.5 alone has no effect. Nkx2.5 and SRF, with GATA-4, also synergistically activates the  $\alpha$ -cardiac actin promoter [Sepulveda et al., 2002]. SRF and GATA-4, in combination with mutant Nkx2.5 which lacks binding capability, are able to activate this promoter. However, Nkx2.5, GATA-4 and mutant SRF (which lacks binding capability) are unable to activate the promoter, and sequential deletion of the four SRE sites in this region results in corresponding decreases in promoter activity. These findings

together demonstrate that SRF binding is necessary for recruitment of Nkx2.5 and GATA-4 to the  $\alpha$ -cardiac actin promoter via a physical interaction. In addition, DNA recruitment assays have demonstrated that Nkx2.5 and GATA-4 together strongly enhance the formation of SRF dependent promoter binding complexes, possibly through conformational changes that increase SRF DNA binding efficiency [Sepulveda et al., 2002]. Combinatorial expression of these three transcription factors also synergistically activates the ANF gene in a co-operative manner [Nishida et al., 2002].

## 1.6 THE EXTRACELLULAR MATRIX

The extracellular matrix (ECM) consists of cells such as fibroblasts, collagens, glycoproteins, proteoglycans, growth factors, and proteases that form a dynamic macromolecular complex which plays an important role in cardiac development and growth by providing structural support for cells and facilitating intercellular communication. Throughout formation of the heart, the processes of cell differentiation, adhesion, migration, and apoptosis are crucial for tissue remodelling and occur in a precisely timed and spatially regulated manner, mediated extensively through signalling that occurs via the ECM. Additionally, ECM composition has an impact on the process of EMT, which is important in cardiac remodelling at various developmental stages including gastrulation, endocardial cushion formation, valvulogenesis, and neural crest cell differentiation (and also in chronic disease states such as hypertension and heart failure). Defects in the remodelling process can lead to loss of organisation and abnormalities such as valve dysfunction and abnormal septation. Components of the ECM and their specific functions are discussed below.

Non-myocyte cells make up approximately 70% of the heart cell population [Nag, 1980; Zak, 1974] and include cardiac fibroblasts, the proportion of which varies depending on species, developmental age and physiological condition [Banerjee et al., 2007]. Fibroblasts are connective tissue cells that synthesise and deposit various ECM components including collagens and fibronectin [Fries et al., 1994] in addition to secreting cytokines, growth factors, and matrix metalloproteinases [Powell et al., 1999]. Cardiac fibroblasts are interconnected to form a network of cells within a collagen matrix, which serves to provide structural integrity through cell-cell and cell-ECM interactions [Baxter et al., 2008].

Collagens are a family of fibrous proteins that are important in maintaining tissue structure. Collagens I, III, IV, V, and VI have been identified in the heart where they each have specific functions [Schaper and Speiser, 1992; Speiser et al., 1991; Speiser et al., 1992]. Collagens I and III account for over 90% of total collagens and

are important in maintaining tissue and blood vessel structure, whilst collagens IV and VI form part of the basal lamina, and allow interaction with receptors such as integrins [Weber, 1989].

Integrins are large transmembrane ECM receptors consisting of  $\alpha$  and  $\beta$  subunits, a large extracellular domain, and a small cytoplasmic signalling domain [Hynes, 1992]. They are essential in interaction with cardiac fibroblasts and myocytes, and mediate cell-cell and cell-ECM communication bidirectionally to regulate cell migration and survival during development and in pathological hypertrophy [Bowers et al.]. Integrins act as receptors for a broad range of ligands which include collagen, laminin and fibronectin [Humphries et al., 2006].

Laminins are glycoproteins that are synthesised by cardiac myocytes, vascular smooth muscle cells (VSMCs), and endothelial cells, and are located in the basement membrane of cardiomyocytes [Corda et al., 2000; Jane-Lise et al., 2000]. Laminins contain binding domains for ECM components, and mouse knockout of laminin subunits results in cardiac abnormalities [Jane-Lise et al., 2000].

Fibronectin is an adhesive extracellular matrix glycoprotein involved in cytoskeletal organisation, cell adhesion, cell migration, and cell spreading [Smith et al., 1990]. Fibronectin associates with multiple ECM components and is crucial during development, with loss of this gene in mice resulting in severe developmental defects to the entire body including the heart [George et al., 1993].

Periostin is an ECM protein most often secreted by fibroblast or fibroblast-like cells, which can bind to several integrin receptors and also interact with ECM proteins such as collagens and fibronectin. During development, the expression pattern of periostin follows that of endocardial cushion and cardiac valve formation [Lindsley et al., 2005], and loss of this gene in mice results in valve defects [Norris et al., 2008]. Periostin is also involved in cardiac hypertrophy and remodelling [Borg and Caulfield, 1980].

Matrix metalloproteinases (MMPs) are a family of secreted zinc-dependent enzymes which are capable of ECM degradation and are therefore important developmentally and during pathologic remodelling in cardiovascular disease [Nagase and Woessner, 1999]. MMPs can be classified into four groups according to their substrate specificity; collagenases (MMP-1 and MMP-13), gelatinases (MMP-2 and MMP-9), stromelysins (MMP-3), and membrane-type MMPs (MT1-MMP) [Fedak et al., 2005]. MMPs also have regulatory functions during normal ECM protein processing [Mann and Spinale, 1998].

## 1.7 THE CONTRACTILE APPARATUS

Contraction of the heart is dependent upon expression of a set of sarcomeric and Z-disc proteins that form the contractile apparatus, represented in Figure 1.8. The sarcomeric thick filament is composed of myosin heavy chains, myosin light chains, myosin binding protein C, and titin. Actins and troponins make up the thin filament. In addition to sarcomeric proteins having an important role in the structure and contractility of the heart, they are now also known to be important in developmental processes such as cardiac septation. Mutations in sarcomeric proteins have been linked to various cardiomyopathies and congenital cardiovascular malformations such as ASDs, VSDs, PDA, and Ebstein anomaly. The mechanism by which mutations in sarcomeric genes can lead to CHDs such as atrial septal defects is unknown. Genes that are mutated in human cardiovascular conditions are represented in Figure 1.8, and relevant muscle genes are described in this section.

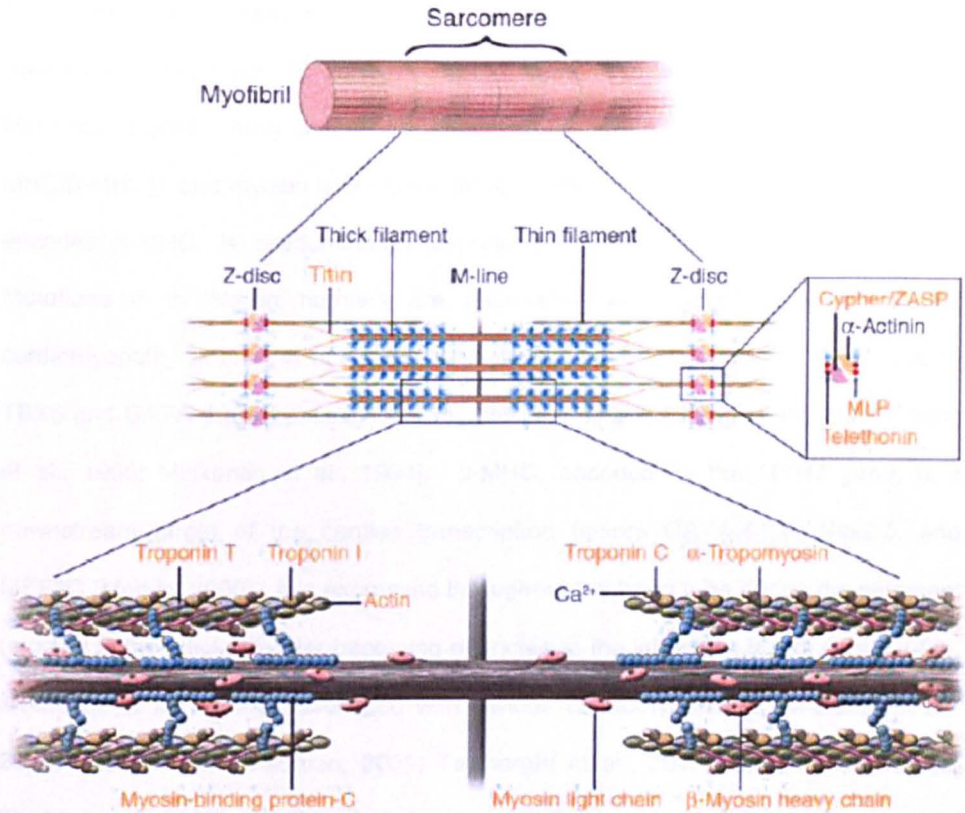


**Figure 1.8 Sarcomeric and Z-disc proteins**

The sarcomeric thick filament is composed of myosin heavy chains, myosin light chains, myosin binding protein C, and titin. Actins and troponins make up the sarcomeric thin filament. Genes that are mutated in human cardiovascular conditions are shown in orange. *Adapted from Morita, 2005*

### 1.7.1 Myosin heavy chains

Sarcomeric complexes in cardiac muscle contain myosin thick and actin thin filaments. Myosin heavy chains (comprising alpha- and beta-myosin heavy chain ( $\alpha$ -MHC/ $\beta$ -MHC)), and myosin light chains (MLC) form the thick filaments. *MYH6*, which encodes  $\alpha$ -MHC, is predominantly expressed in the atria [Somi et al., 2006]. Mutations in *MYH6* in humans are associated with hypertrophic and dilated cardiomyopathy [Morita et al., 2005], and atrial septal defects [Ching et al., 2005]. TBX5 and GATA-4 are transcriptional regulators of *MYH6* [Ching et al., 2005; Huang et al., 1995; Molkentin et al., 1994].  $\beta$ -MHC, encoded by the *MYH7* gene, is a downstream target of the cardiac transcription factors GATA-4/5/6, Nkx2.5, and MEF2C [Morkin, 2000]. It is expressed throughout the heart tube during development (studied in the chicken), later becoming restricted to the ventricles [Somi et al., 2006]. Mutations in *MYH7* are associated with various cardiomyopathies [Meredith et al., 2004; Seidman and Seidman, 2001; Tajsharghi et al., 2003], atrial septal defects [Budde et al., 2007] and Ebstein anomaly (a CHD characterised by displacement of the tricuspid valve leaflets) [Kaneda et al., 2008].

### 1.7.2 Myosin light chains

Myosin light chains are a component of the sarcomeric thick filament and can be classified as either essential or regulatory [Franco et al., 1998]. Regulatory myosin light chains are subject to phosphorylation which influences their sensitivity to calcium during muscle contraction, thereby modulating this process [Szczesna et al., 2002]. These categories can be subdivided into fast and slow isoforms, and multiple isoforms also exist. Three essential isoforms are expressed in the heart; MLC3f (a fast isoform), MLC1V (expressed in the ventricular myocardium), and MLC1a (expressed in the atrial myocardium) [Hailstones and Gunning, 1990; Kelly et al., 1995; Lyons et al., 1990; McGrew et al., 1996]. Three regulatory isoforms are expressed in the heart during cardiac development; MLC2a (expressed in the atrial myocardium), MLC2v (expressed in the ventricular myocardium), and MLC2f (a fast isoform that is transiently expressed in the heart during embryonic development) [Faerman and

Shani, 1993]. Mutations in essential myosin light chain (*MYL3*) and regulatory myosin light chain (*MYL2*) result in hypertrophic cardiomyopathy (HCM) [Bos et al., 2007; Burkett and Hershberger, 2005; Morita et al., 2005].

### 1.7.3 Actins

Actins are a major component of the sarcomeric thin filament. There are four isoforms of actin occurring in muscle; the striated  $\alpha$ -skeletal and  $\alpha$ -cardiac actins which are the primary isoforms in skeletal and cardiac muscle respectively, and  $\alpha$ - and  $\gamma$ - smooth muscle actins, primarily expressed in smooth muscle cells. Alpha-smooth muscle ( $\alpha$ -SM) actin is the earliest expressed actin isoform in the developing heart [Ruzicka and Schwartz, 1988]. Mouse knockout of the  $\alpha$ -SM actin gene *ACTA2* results in impaired vascular contractility and blood flow [Schildmeyer et al., 2000; Tomasek et al., 2006]. Mutations in the human *ACTA2* gene are associated with a variety of vascular diseases such as coronary artery disease (CAD), ischemic strokes, Moyamoya disease (MMD), and thoracic aortic aneurysms and dissections (TAAD) [Guo et al., 2009]. PDA has also been reported in patients with *ACTA2* mutation [Guo et al., 2009]. The striated  $\alpha$ -skeletal and  $\alpha$ -cardiac actins become the predominantly expressed actin isoforms in the heart following dextral looping [Ruzicka and Schwartz, 1988]. Missense mutations affecting conserved amino acids in the cardiac actin gene *ACTC* have been identified in two separate families with idiopathic dilated cardiomyopathy (IDC) [Olson et al., 1998], and mutations in this gene are also associated with atrial and ventricular septal defects [Matsson et al., 2008; Monserrat et al., 2007].

### 1.7.4 Tropomyosin

Tropomyosin (TM) is a dimeric  $\alpha$ -helical coiled actin-binding protein, important as a contractile component of the sarcomeric thin filament and necessary for myocardial function [Perry, 2001]. More than twenty isoforms of tropomyosin have been identified in mammalian species, encoded by four genes, *TPM1* – *TPM4* in humans, which give rise to  $\alpha$ -,  $\beta$ -,  $\gamma$ -, and  $\delta$ -tropomyosin respectively [Pittenger et al., 1994]. These are

expressed predominantly in skeletal, smooth, and cardiac muscle, and at lower levels in non-muscle cytoskeletal and actin associated cells [Pittenger et al., 1994]. Familial hypertrophic cardiomyopathy has been linked to missense mutations in TPM1 which encodes alpha-tropomyosin [Thierfelder et al., 1994]. E40K and E54K mutations in  $\alpha$ -tropomyosin cause dilated cardiomyopathy due to decreased sensitivity to  $\text{Ca}^{2+}$  [Mirza et al., 2007]. Alpha-tropomyosin null mice do not survive past E11.5, whilst heterozygous mice are viable and able to reproduce but display a 50% reduction in cardiac muscle  $\alpha$ -TM mRNA, with no differences in myocardial and myofilament function between these and control mice [Rethinasamy et al., 1998].

### 1.7.5 Troponins

Cardiac troponin is located along the actin thin filament, and the troponin complex comprises three troponin subunits, cardiac troponin C (cTnC), cardiac troponin T (cTnT), and cardiac troponin I (cTnI) which are involved in striated muscle contraction via interaction with  $\text{Ca}^{2+}$  [Farah and Reinach, 1995]. Each of these subunits has a distinct role; cTnC acts as a  $\text{Ca}^{2+}$  sensor, cTnT binds to tropomyosin and transmits the  $\text{Ca}^{2+}$  binding signal from troponin to tropomyosin, and cTnI is inhibitory and prevents actin and myosin association in the absence of  $\text{Ca}^{2+}$  [Farah and Reinach, 1995]. Mutations in cTnI and cTnT are associated with restrictive cardiomyopathy [Knollmann et al., 2003].

## **1.8 CARDIAC MODEL SYSTEMS RELEVANT TO THIS THESIS**

### **1.8.1 The P19 cell line as a model of cardiomyocyte differentiation**

Cardiac cell lines have been used extensively to model cardiomyocyte differentiation and gene regulation. The P19 mouse embryonal carcinoma cell line is pluripotent and can be induced to differentiate by the addition of non-toxic drugs. Retinoic acid induces differentiation to neuroectodermal derived cell types, and dimethyl sulfoxide (DMSO) induces differentiation to endodermal and mesodermal derived cell types such as skeletal and cardiac muscle cells [McBurney, 1993]. Addition of DMSO at 0.5 – 1% (v/v) induces the formation of beating cardiomyocytes at days 6 – 7, thus the P19 cell line provides an excellent *in vitro* model of early development and cardiomyocyte differentiation and is widely used. It has previously been used in a number of functional studies looking at the effect of a reduction or increase in expression of cardiac genes such as TBX5 and GATA-4 [Fijnvandraat et al., 2003; Grepin et al., 1995; Hiroi et al., 2001].

### **1.8.2 The developing chick as a model of cardiogenesis**

The chicken embryo is one of the most widely used non-mammalian vertebrate models of development. Chickens have a short gestational period of 21 days, and development occurs *in ovo* rather than *in utero*, which means ease of manipulation with particular advantages for temporal studies. Complete sequencing of the chicken genome [2004] and the availability of expressed sequence tag (EST) libraries mean sequences are readily available and can be utilised for technologies such as morpholino antisense knockdown in order to study gene function. Additionally, avian cardiac development is very similar to human cardiac development. The primary difference occurs during atrial septation, where a septum secundum forms in the human but not the chicken. This means that ostium primum defects that arise from defects in the septum secundum cannot be modelled. Since this study will be focusing on defects of the septum primum, this is not a major concern.

## 1.9 BACKGROUND TO THIS THESIS

Holt-Oram syndrome (HOS) is a human genetic disorder associated with mutations in the *TBX5* gene [Li et al., 1997], characterised by upper limb deformities and heart defects, usually in atrial or ventricular septation [Lehner et al., 2003]. The *TBX5* mutations G80R and R237W, which are associated with cardiac septal defects in HOS patients [Basson et al., 1999], disrupt the physical interaction between *TBX5* and *GATA-4* [Garg et al., 2003]. The *GATA-4* mutation G296S has been linked to ASDs in humans, and also disrupts the *GATA-4* / *TBX5* interaction [Garg et al., 2003]. These findings together account for the fact that similar heart defects are seen as a result of both *GATA-4* and *TBX5* mutations, and highlight the potential importance of this complex in synergistic regulation of genes involved in septation of the heart. Identification of these downstream targets is crucial in gaining an understanding of the mechanism via which mutations in these transcription factors lead to heart defects. *TBX5* and *GATA-4*, and their combined downstream targets are the focus of this thesis.

This study is based on the work of Jonathan Ronksley (a former PhD student in Prof J David Brook's group) who aimed to identify genes co-ordinately regulated by *TBX5* and *GATA-4* using the P19CL6 mouse embryonal carcinoma cell line as a model of cardiac development [Ronksley, 2007]. The full length human *GATA-4* gene was cloned into a pcDNA3.1/Zeo vector and used to create cell lines overexpressing *GATA-4*. The full length human *TBX5* gene was then additionally cloned in to create double overexpression cell lines. Overexpression of *TBX5* and *GATA-4* was confirmed by western blot analysis and ANF luciferase reporter assays. Two P19 *TBX5* / *GATA-4* overexpression cell lines were selected for further analysis, named G10 and G22. Microarray expression analyses were then performed using the Ocumum Biosolutions Mouse 1400 pmol 30K V2 Oligo set (A/B/C), which contains 50-base pair oligonucleotide probes (1 per gene) for detection of 27 530 targets. A dye swap method (Cy3 and Cy5) was employed in order to eliminate dye bias.

For identification of downstream targets of TBX5 and GATA-4, microarray expression analysis of TBX5 / GATA-4 overexpression cell line RNA in comparison to wild type RNA (at day 0) was carried out. This revealed 80 up-regulated, and 154 down-regulated genes (by >2 fold on 3 out of 4 replicate arrays). Surprisingly, ANF and connexin 40 (which are known targets of TBX5 and GATA-4) could not be detected in any of the wild type or overexpression arrays. However, cardiac troponin I, which is synergistically regulated by TBX5 and GATA-4 (Dr Tushar Ghosh, unpublished data), and alpha cardiac actin (a predicted target of TBX5) [Ghosh et al., 2001] were up-regulated post-differentiation in response to overexpression of TBX5 and GATA-4.

For additional expression profiling of wild type P19 cell differentiation, cells were induced to differentiate by addition of DMSO, and RNA extracted at days 0, 2, 5, 7 and 10. This provided a means to study expression of genes of interest during normal differentiation into cardiomyocytes. QPCR analysis of TBX5 and GATA-4 expression was also carried out during wild type P19 cell differentiation, and revealed significant up-regulation of GATA-4 on days 2, 5 and 7. TBX5 expression was not detectable at day 2, and displayed significant up-regulation on days 5 and 7.

A subset of genes was chosen for further study based on expression changes and current literature. Six down-regulated genes are shown in Table 1.1, and sixteen up-regulated genes in Table 1.2, with average fold changes in expression.

**Table 1.1 Genes down-regulated in microarray expression analysis of TBX5 / GATA-4 overexpression cell lines**

<b>Gene</b>	<b>NCBI Accession ID</b>	<b>Fold change</b>
Annexin A2	AK012563	2.91
VEGF-b	BC046303	2.57
RBBP6	NM_011247	2.22
Annexin A4	AK032703	3.01
Galanin R2	AF042784	2.41
A2-macroglobulin	NM_175628	9.87

Average expression of double overexpression cell lines G10 and G22 at day 0, measured against wild type P19 cells at day 0.

**Table 1.2 Genes up-regulated in microarray expression analysis of TBX5 / GATA-4 overexpression cell lines**

Gene	NCBI Accession ID	Fold change
Gamma Filamin	BC060276	2.24
Tropomyosin	M22479	2.23
Glutaredoxin	AB013137	2.97
S100A10	NM_009112	3.84
Fibronectin	X93167	2.45
Calreticulin	AK075605	2.77
ERp57	AK088721	2.18
Mest / Peg1	AF482999	2.34
HNRPDL	NM_016690	2.50
RBMS1	BC057866	2.51
PMM2	XM_354942	2.65
PA2.26	AJ250246	3.36
PETA-3	AF033620	2.65
Neurofilament 3	AK051696	2.19
AP4e1	BC042530	3.17
Alpha-l-fucosidase	AK002230	2.22

Average expression of double overexpression cell lines G10 and G22 at day 0, measured against wild type P19 cells at day 0.

### **1.10 AIMS AND OBJECTIVES**

This P19 overexpression study was the first study of its kind to attempt identification of the combined targets of TBX5 and GATA-4. Microarray expression profiling resulted in identification of a large number of potential targets. This thesis aimed to build on this research as follows:

- 1) Use of the P19 overexpression study as a starting point for identification of a subset of genes likely to be important in cardiogenesis, taking into account expression, bioinformatic, and functional information
- 2) Development of a novel model system of combined knockdown of TBX5 and GATA-4 allowing phenotypic characterisation, and independent assessment of the responsiveness of candidate genes to these transcription factors
- 3) Investigation of the role of one or more selected genes in cardiogenesis, with the aim to validate and characterise function in a developmental system for evidenced presentation of new cardiac genes
- 4) Use of the model system for identification of new synergistic targets of TBX5 and GATA-4

## CHAPTER 2

### MATERIALS AND METHODS

#### 2.1 MATERIALS

##### 2.1.1 Molecular methods

50x TAE buffer (1 litre)	242 g Tris, 100 ml 0.5M EDTA pH 8.0, 57.1 ml glacial acetic acid
DNA size markers	Hyperladder IV (Bioline) and 1 Kb <sup>+</sup> DNA ladder (Invitrogen)
<i>PfuUltra</i> II Fusion HS DNA polymerase	2.5 U / $\mu$ l (Stratagene)
HotStar Taq	5 U / $\mu$ l (Qiagen)
DNase I	Lyophilised DNase I (1500 kunitz units) dissolved in 550 $\mu$ l RNase free water (Qiagen)
RNaseOUT	40 U / $\mu$ l (Invitrogen)
SuperScript III	200 U / $\mu$ l (Invitrogen)

**2.1.2 Microbial techniques**

LB media (1 litre)	10 g tryptone, 5 g yeast extract, 10 g NaCl
SOC media (1 litre)	20 g tryptone, 5 g yeast extract, 0.5 g NaCl, 10 ml 250 mM KCl, 20 mM glucose, 5 ml 2 M MgCl <sub>2</sub> , 20 ml 1 M glucose. pH adjusted to 7.0 with NaOH
MacConkey agar plates	52 g MacConkey agar per litre, ampicillin added to a final concentration of 50 µg / ml
Ampicillin stock	50 mg / ml in H <sub>2</sub> O
T4 DNA ligase	3 U / µl (Promega)
<i>Taq</i> DNA polymerase	5 U / µl (NEB)

**2.1.3 DNA purification techniques**

Shrimp Alkaline Phosphatase	1 U / µl (Promega)
Exonuclease I	20 U / µl (NEB)

**2.1.4 Whole mount *in situ* hybridisation (WISH)**

Chick saline solution (1 litre)	71.9 g NaCl
---------------------------------	-------------

PBST	PBS (Sigma) containing 0.1% Triton X-100
4% paraformaldehyde (1 litre)	40 g PFA, 100 ml 10x PBS, pH adjusted to 9.1-9.3 using NaOH
Proteinase K	10 mg / ml in DEPC treated H <sub>2</sub> O
Pre-hybridisation solution	50% deionized formamide, 5x SSC, 2% blocking powder, 0.1% Triton X-100, 0.1% CHAPS, 50 µg / ml yeast RNA, 5 mM EDTA, 50 µg / ml heparin
DEPC treated H <sub>2</sub> O	0.5 ml DEPC per litre H <sub>2</sub> O
20x SSC (1 litre)	175 g NaCl, 88 g sodium citrate, pH adjusted to 7.0 with HCl
2.0x SSC with 0.1% Tween20 (1 litre)	100 ml 20x SSC, 10 ml 10% Tween20
0.2x SSC with 0.1% Tween20 (1 litre)	10 ml 20x SSC, 10 ml 10% Tween20
KTBT	50 mM Tris-HCl (pH 7.5), 150 mM NaCl, 10 mM KCl, 1% Triton X-100
NTMT	100 mM NaCl, 100 mM Tris (pH 9.5), 50 mM MgCl <sub>2</sub> , 0.1% Triton X-100
Levamisole	50 mg / ml in DEPC treated H <sub>2</sub> O

Colour reagent (1 ml)	3 $\mu$ l 75 mg / ml NBT in 70% DMF, 2.3 $\mu$ l 50 mg / ml in DMF BCIP, 1 ml NTMT
SacII	20 U / $\mu$ l (NEB)
SpeI	10 U / $\mu$ l (NEB)
T7 RNA polymerase	20 U / $\mu$ l (Roche)
SP6 RNA polymerase	20 U / $\mu$ l (Roche)

### 2.1.5 Western blotting

RIPA buffer (100 ml)	50 mM Tris-HCl, 150 mM NaCl, 1mM EDTA, 1% Triton X-100, 1% sodium deoxycholate, 0.1% SDS, 100 $\mu$ l 0.1 M PMSF, one complete mini inhibitor cocktail tablet (Roche)
PMSF (0.1 M)	0.17 g PMSF, made up to 10 ml in isopropanol
5x sample loading buffer (50 ml)	1.25 g SDS, 24.02 g urea, 5 ml $\beta$ -mercaptoethanol, 10 ml glycerol, 20 ml 0.5 M Tris-HCl, 0.05 g bromophenol blue
Electrophoresis buffer (1 litre)	3 g Tris, 14 g glycine, 1 g SDS
Transfer buffer (1 litre)	9 g Tris, 42 g glycine, 600 ml methanol

TBS (1 litre) 1.2 g Tris, 8.75 g NaCl, pH adjusted to 7.5 with HCl

TBST 1x TBS containing 0.1% Tween20

### 2.1.6 Morpholino knockdown

F127 pluronic gel (100 ml) 15 g F127 pluronic gel made up to 100 ml with HBSS (Sigma)

**Table 2.1 Primers used for PCR amplification of mouse genomic regions of RBMS1**

Primer name	Primer sequence (5' – 3')
RBMS1 mouse intron 1 F1	CACCTCTCTCTACCTGAAAAGATGG
RBMS1 mouse intron 1 F2	ATGGCTAATTATGTTAGGGCCTTGT
RBMS1 mouse intron 1 R1	AAAGCTTTGCATCACAGCATCTTAT
RBMS1 mouse intron 1 R2	GAGATCATGAAGTCACTCACGGTAA
RBMS1 mouse 3' UTR F1	TAAGACAAAAGATGACGAAGCACTG
RBMS1 mouse 3' UTR F2	TGTTCCCCTGAACAGGTTTATTTTA
RBMS1 mouse 3' UTR R1	AAAAACCGACAGGAAGAAGAAAGTT
RBMS1 mouse 3' UTR R2	AATGTCGCTGACATCTATCATCAAA
RBMS1 mouse 5' UTR F1	CTCCTCCAAAGACACTTTCCAAATA
RBMS1 mouse 5' UTR F2	CCCAAGTTTGTAGCTCCTACTGAAA
RBMS1 mouse 5' UTR F3	GTGGGACAATTTGAGCATCTACAAA
RBMS1 mouse 5' UTR R1	TGCAGATACTGGGGGTAGTAATAGG
RBMS1 mouse 5' UTR R2	GGGTAGTAATAGGTGGCGTACTGAG
RBMS1 mouse 5' UTR R3	CTATAGTTAGCAACCCCAGCACTTG

**Table 2.2 Primers used for introduction of SacI restriction sites**

Primer name	Primer sequence (5' – 3')
RBMS1 Int1 SacI primer F	GATCGAGCTCCACCTCTCTCTACCTGAAAAGATGG
RBMS1 Int1 SacI primer R	GATCGAGCTCAAAGCTTTGCATCACAGCATCTTAT

**Table 2.3 QPCR assays designed to candidate genes in the chick**

Gene	Accession ID	Primer name	Primer sequence (5' - 3')	Position	Probe *
PA2.26	XM_001231272.1	PA2.26 F1	CAGAGTTTGAGGAATTACCGACA	368 - 390	44
		PA2.26 R1	CTTCCAAACTGCAAGAGATTTGT	418 - 440	
PA2.26	XM_001231272.1	PA2.26 F2	TTGGAATCATAGTAGCTGTTGGAA	602 - 625	151
		PA2.26 R2	CGAGTACCTGCCTGACATCTT	658 - 678	
PETA-3	NM_001006472.1	PETA-3 F	CGTCGGAATTTGCTAAGAGTGT	510 - 531	2
		PETA-3 R	GCCAGGATTCCAGCAATG	569 - 586	
FUCA1	XM_417835.2	FUCA1 F	AACTGGAATTCITTTGGACACG	409 - 429	33
		FUCA1 R	CAGTCCGTAGCGTATGTTGTTC	476 - 498	
TPM1	NM_205401.1	TPM1 F	GTGGCTCGTAAGCTCGTGAT	668 - 687	1
		TPM1 R	TAGTTCAGCACGCTCCTCAG	711 - 730	
Fibronectin	XM_421868.2	Fibronectin F	GAGGGTGATGAGCCACAGTAT	2287 - 2307	76
		Fibronectin R	CAGGAAGCAAGTCAGGGATG	2340 - 2359	
Desmin	XM_427965.2	Desmin F	CTGCTTTCAGAGCTGACGTG	684 - 703	80
		Desmin R	TCTCCTCCTGCAGGGACTC	746 - 764	
RBMS1	NM_205024.1	RBMS1 F	CTGTGAGATGCCCGGTGT	1228 - 1245	80
		RBMS1 R	ACACCGGCATCTCACAG	1266 - 1287	
GAPDH	NM_204305.1	GAPDH F	GGTCTTATGACCACTGTCCA	568 - 587	76
		GAPDH R	TCCACAGCTCCCAGAGG	622 - 640	
TBP	NM_205103.1	TBP F	GATGTCTCCGGATGTTTTCA	98 - 118	151
		TBP R	CGAAAAGGTTTTTGACCCTCT	153 - 173	
RPLPO	NM_204987.1	RPLPO F	ATGGGGAAGAACACGATGAT	186 - 205	80
		RPLPO R	GCAGCAGCTTCTCCAAGG	244 - 261	
EEF1A1	NM_204157.2	EEF1A1 F	GTTGGAACGGGACAACAT	584 - 602	37
		EEF1A1 R	CTTCCGGGTAACCTTCCAT	639 - 658	
α-MHC	NM_001001302.1	α-MHC F	GACCTGGAGAATGACAAGCAG	190 - 210	65
		α-MHC R	CGAGCATTGAGTGTGTGAGTT	245 - 266	

\*Probe identifiers refer to pre-designed Universal ProbeLibrary probes (Roche). Each probe binds to a specific nucleotide sequence. Probe sequence information can be found online at <https://www.roche-applied-science.com>).

**Table 2.4 Primers designed to the chicken RBMS1 gene**

Primer name	Primer sequence (5' – 3')
RBMS1 exon1F	CCAGTATCTGCAGGCGAAC
RBMS1 exon2F	ACCCAATGGCTCCTCCTAGT
RBMS1 exon5F	TTGCCACTTTCAATGGATGA
RBMS1 exon8F	CCAACCACAGCTGCTTTACA
RBMS1 exon3R	TGCACTTGTTTGTGTCTTATCC
RBMS1 exon5R	TCTTGTTGCTTTGCCATTTG
RBMS1 exon9R	TATGTGGAAACCGGAGAAGC
RBMS1 exon10R	GCTGCATCCAAGAAGGACTC
RBMS1 intron2F	GCACTCAGGTTAGGGCAGAG
RBMS1 intron2R	CCTCACCAGAAACGGACAAT

**Table 2.5 QPCR assays designed to the  $\alpha$ -actin genes in the chick**

Gene	Ensembl ID	Primer name	Primer sequence (5' – 3')	Position	Probe *
$\alpha$ -sma	ENSGALT00000039927	$\alpha$ -sma F	GCACCTGAGGACATTGACATAG	3 – 24	56
		$\alpha$ -sma R	TTACAGAGCCCTGAGCCATT	67 – 86	
$\alpha$ -ske a	ENSGALT00000018064	$\alpha$ -ske a F	GCTCTGGACTTTGAGAACGAG	439 - 459	65
		$\alpha$ -ske a R	CCCATCAGGCAGCTCATAG	498 - 516	
$\alpha$ -ca	ENSGALT00000016005	$\alpha$ -ca F	TGAGAATGAAATGGCCACAG	625 - 644	80
		$\alpha$ -ca R	ACCATCAGGCAATTCGTAGC	672 – 691	

\*Probe identifiers refer to pre-designed Universal ProbeLibrary probes (Roche). Each probe binds to a specific nucleotide sequence. Probe sequence information can be found online at <https://www.roche-applied-science.com>).

**Table 2.6 Primers used in RT-PCR expression analysis of genes identified in microarray analysis of TBX5 / GATA-4 double knockdown embryos**

Gene	Accession ID	Primer name	Primer sequence
TFAP2B	NM_204895.1	TFAP2B F	GGCCGTTTGTCTTTGCTTAG
		TFAP2B R	CCACCAGGGAGGTGAGTAAA
PTPRZ1	XM_001231942.1	PTPRZ1 F	CCTTCTGGTTACGTGGGAAA
		PTPRZ1 R	CGTGCAGACCATTAGAGCAA
FIGF	NM_204568.1	FIGF F	ACCAGATTTGCTGCTGCTTT
		FIGF R	TGCAGCTCAGACTCTCCTCA
NR2E1	NM_205170.1	NR2E1 F	CCAGGCTTTACAGGAGTTG
		NR2E1 R	GATTGGTACATTCCCGATGG
LOC420770	XM_429784.2	LOC420770 F	TGCTTGAGGAAACGAGTGTG
		LOC420770 R	TTTGCTGCAGGCACTATTTG
SUZ12	XM_415658.2	SUZ12 F	ATGAAGCACGGGTTTATTGC
		SUZ12 R	GGGAGGTTCGATTCTCCTTTC
CRABP1	NM_001030539.1	CRABP1 F	AGGACGGGGACCAGTTCTAC
		CRABP1 R	CCTCATCCCAGGTGACAAGT
GOLGA4	XM_418856.2	GOLGA4 F	GAAAGAGGCACTGCAGGAAC
		GOLGA4 R	TGCATTTGTCGCTTTGTCTC
GPC3	XM_001232891.1	GPC3 F	GGAGAGGTACAGTCCCCACA
		GPC3 R	AGCCTCTGCCACAGTCATCT

**Table 2.7 Morpholinos used in the TBX5 / GATA-4 knockdown study**

Morpholino	Sequence (5' – 3')	3' tag
Standard control	CCTCTTACCTCAGTTACAATTTATA	Fluorescein
TBX5 AUG	GGCTCCTTCCTCCCGGTGCAAAGC	Fluorescein
TBX5 AUG 5-mismatch	GG <u>ATC</u> ATTCCTG <u>CCCGT</u> ACAAA <u>AC</u>	Fluorescein
TBX5 AUG 7-mismatch*	G <u>CCT</u> GCTT <u>GCT</u> G <u>CCCGT</u> C(G)CAA <u>CC</u>	Fluorescein
GATA-4 AUG	CATGGCTAAGCTCTGGTACATCTCG	Lissamine
GATA-4 AUG 5-mismatch	CAT <u>CGCT</u> AA <u>CTCT</u> CGTAGAT <u>GTCG</u>	Lissamine
GATA-4 AUG 7-mismatch	CAT <u>CCCT</u> AA <u>CTGT</u> CGTAGAT <u>GTCG</u>	Lissamine

Bases altered in mismatch control morpholinos are underlined and shown in bold. All morpholinos were synthesised by Gene-Tools USA.

\*An error was made by Gene-Tools during the design of this morpholino and an extra base (guanine, shown in brackets) inserted at position 19

**Table 2.8 Morpholinos used in the RBMS1 knockdown study**

Morpholino	Sequence (5' – 3')	3' tag
RBMS1 E2I2	AAGTATCGTACTTACGGTTGGCATA	Fluorescein
RBMS1 E2I2 5-mismatch	AA <u>CTAT</u> C <u>CTAG</u> TTAC <u>CGTTG</u> CATA	Fluorescein
RBMS1 E8I8	GTGTACCAGCACTTAACATACCCAT	Lissamine

Bases altered in mismatch control morpholinos are underlined. All morpholinos were synthesised by Gene-Tools (USA).

## **2.2 METHODS**

### **2.2.1 Molecular methods**

#### **2.2.1.1 Genomic DNA extraction**

Genomic DNA extractions were performed using the Wizard SV Genomic DNA Purification system (Promega), following manufacturer's instructions. A 275  $\mu$ l volume of digestion solution mastermix was added to the tissue sample (maximum 20 mg). Samples were incubated overnight at 55 °C in a heat block, and centrifuged at 2000 x *g*. Supernatant was transferred to a new microcentrifuge tube and 250  $\mu$ l lysis buffer added followed by vortexing. This was transferred to a minicolumn assembly and centrifuged at 13000 x *g* for 3 minutes. Following removal of eluate, 650  $\mu$ l wash solution was added to the column followed by centrifugation at 13000 x *g* for 1 minute. This wash step was repeated 3 times followed by an additional centrifugation step without addition of wash solution in order to remove any traces of ethanol. The column was placed in a new microcentrifuge tube and 250  $\mu$ l H<sub>2</sub>O pipetted directly onto the membrane followed by incubation for 2 minutes at room temperature. DNA was eluted by centrifugation at 13000 x *g* for 1 minute. This elution step was repeated to obtain a final elution volume of 500  $\mu$ l, and DNA concentration assessed by spectrophotometry (section 2.2.1.3).

#### **2.2.1.2 RNA extraction**

RNA extractions were performed using the Qiagen RNeasy minikit or microkit as appropriate, following manufacturer's instructions. RNA*later* stabilised tissue was placed in 600  $\mu$ l buffer RLT containing 1%  $\beta$ -mercaptoethanol and homogenised using a sterile needle (BD Microlance 25G 5/8) and syringe. The resulting lysate was centrifuged at maximum speed for 3 minutes, and supernatant transferred to a new microcentrifuge tube for addition of 1 volume of 70% ethanol. This was transferred to an RNeasy spin column placed in a 2 ml collection tube, centrifuged for 15 seconds at maximum speed, and the flow-through discarded. On-column DNase digestion was

carried out in all cases using the RNase-free DNase set (Qiagen). Buffer RW1 (350  $\mu$ l) was added to the column and centrifugation carried out at maximum speed for 15 seconds. A 10  $\mu$ l volume of DNase I stock solution was added to 70  $\mu$ l buffer RDD and pipetted into the membrane for a 15 minute incubation at room temperature. A 350  $\mu$ l volume of buffer RW1 was added to the column and centrifugation carried out at maximum speed for 15 seconds. A 500  $\mu$ l volume of wash buffer RPE was added to the column followed by centrifugation for 15 seconds at maximum speed to wash the column-bound RNA. The flow-through was discarded, and a further 500  $\mu$ l of buffer RPE added to the column for centrifugation for 2 minutes at maximum speed. The column was placed in a new collection tube and centrifuged at full speed for 1 minute to remove any traces of ethanol. The column was placed in a new microcentrifuge tube, and 30  $\mu$ l RNase-free H<sub>2</sub>O pipetted directly onto the centre of the membrane followed by centrifugation at full speed for 1 minute for RNA elution. RNA purity and concentration was assessed by spectrophotometry (section 2.2.1.3), and RNA stored at -80 °C.

#### **2.2.1.3 Nucleic acid quantification**

Quantifications were performed using the NanoDrop® ND-1000 spectrophotometer. A 1  $\mu$ l volume of sample was pipetted onto the lower measurement pedestal, followed by lowering of the sampling arm, drawing the sample between the two measurement pedestals for spectral analysis.

#### **2.2.1.4 Reverse Transcription**

Reverse transcription reactions were carried out in 20  $\mu$ l reaction volumes. Total RNA (1  $\mu$ g) was combined with 2  $\mu$ l 50 ng /  $\mu$ l random hexamers and 1  $\mu$ l 10 mM dNTPs, and made up to 12  $\mu$ l with H<sub>2</sub>O. Samples were heated at 65 °C for 5 minutes then placed on ice before addition of 4  $\mu$ l 5x first strand buffer, 2  $\mu$ l 0.1 M DTT and 1  $\mu$ l 40 U /  $\mu$ l RNaseOUT (Invitrogen). Samples were incubated at 37 °C for 2 minutes prior to addition of 1  $\mu$ l SuperScript III (Invitrogen), excluding -RT controls. Samples were

incubated at 25 °C for 10 minutes, 37 °C for 50 minutes, 70 °C for 10 minutes before storage at -80 °C.

#### **2.2.1.5 Primer design**

Primers were most frequently designed using online Primer3 software (<http://frodo.wi.mit.edu/primer3/>), or manually when a very specific primer location was required (such as in cases of high homology with other genes or transcripts). Primers were generally 18 – 25 bp in length, with melting temperatures of 55 – 65 °C. Blast searches were carried out for all primers in *Ensembl* (<http://www.ensembl.org/Multi/blastview>).

#### **2.2.1.6 Polymerase chain reaction (PCR)**

##### **2.2.1.6.1 HotStar Taq**

PCR reactions were carried out in 25 µl reaction volumes using 2 µl 10 µM forward and reverse primers, 2.5 µl 10x buffer (Qiagen), 1 µl 10 mM dNTPs, 0.25 µl 5U / µl HotStar Taq (Qiagen), 16.25 µl H<sub>2</sub>O, and 1 µl DNA template. Thermal cycling conditions were based on the following: 95 °C for 15 mins, 35 cycles of 94 °C for 30 secs, 60 °C for 30 secs and 72 °C for 30 secs, and 72 °C for 10 mins.

##### **2.2.1.6.2 PfuUltra 11 Fusion HS DNA Polymerase**

PCR reactions were carried out in 50 µl reaction volumes using 1.0 µl 10 µM forward and reverse primers, 5.0 µl 10x *PfuUltra* II reaction buffer (Stratagene), 5.0 µl 10 mM dNTPs, 1.0 µl *PfuUltra* II Fusion HS DNA polymerase (Stratagene), 36.0 µl H<sub>2</sub>O, and 1 µl 100 ng / µl genomic or plasmid DNA template. Thermal cycling conditions were based on the following: 95 °C for 5 mins, 35 cycles of 94 °C for 30 secs, 60 °C for 30 secs and 72 °C for 30 secs, and 72 °C for 5 mins.

##### **2.2.1.7 Agarose Gel Electrophoresis**

Agarose gels were made up and electrophoresed in TAE buffer. Ethidium bromide was added to a final concentration of 0.1 µg / ml. DNA samples were combined with

5x loading buffer (BioLine) and loaded alongside 10  $\mu$ l 1 Kb<sup>+</sup> DNA ladder (Invitrogen) or 5  $\mu$ l Hyperladder IV (BioLine). Gels were run at 100 - 150 V.

#### **2.2.1.8 DNA sequencing**

Sequencing reactions were carried out using 0.5  $\mu$ l BigDye Terminator v3.1 (Applied Biosystems), 2  $\mu$ l 5x sequencing buffer (Applied Biosystems), 0.4  $\mu$ l 10  $\mu$ M primer, and 3 – 20 ng PCR product / 150 – 300 ng plasmid DNA, made up to a total volume of 10  $\mu$ l with water. Reactions were performed under the following conditions: 96 °C for 16 min, followed by 28 cycles of 96 °C for 10 seconds, 50 °C for 5 seconds, 60 °C degrees for 4 minutes. Samples were ethanol precipitated (section 2.2.3.4) and run on an ABI prism™ 3130xl Genetic Analyser (Applied Biosystems) at the Biopolymer Synthesis and Analysis Unit (University of Nottingham, UK). Sequences were analysed using Chromas software (Technelysium Pty Ltd).

#### **2.2.1.9 Quantitative PCR (QPCR) for validation of mouse targets**

##### **2.2.1.9.1 Methodology**

There are two main methodologies for QPCR analysis of gene expression, the Relative Standard Curve method and the Comparative C<sub>T</sub> ( $\Delta\Delta C_T$ ) method, described here. The Relative Standard Curve method involves the construction of standard curves from known quantities of DNA for both the target and endogenous control on each reaction plate, with sample DNA amplified simultaneously under identical conditions. This allows interpolation of sample target and endogenous reference quantities from the standard curves, and assay efficiency data is generated in parallel, producing highly accurate data. Due to the requirement of standard curves and all samples on each reaction plate, this method uses a large quantity of reagents and is suitable when sample numbers are low. The Comparative C<sub>T</sub> method uses arithmetic formulae for relative quantification calculations. It requires the construction of standard curves for all target and control genes for assessment of amplification efficiencies prior to quantification experiments, and these values are incorporated into

relative quantification calculations. The use of standard curves on each plate is not required, which means this method has economical advantages over the Relative Standard Curve method. It is ideal for high throughput studies where there are a large number of targets and / or samples, such as in the validation of microarray data, and will be used for this purpose here.

#### **2.2.1.9.2 Assay design and experimental conditions**

Assays were designed by Jonathan Ronksley using the online Roche Universal ProbeLibrary assay design centre (<https://www.roche-applied-science.com>). QPCR analyses of gene expression in the mouse P19 cell line were performed using the Comparative  $C_T$  method [Livak and Schmittgen, 2001]. Quantitative PCR was performed in a total volume of 25  $\mu$ l using 12.5  $\mu$ l SensiMix (Quantace), 0.25  $\mu$ l 10  $\mu$ M probe (5' FAM labelled and 3' labelled with a dark quencher dye, Universal ProbeLibrary, Roche), 1.0  $\mu$ l 10  $\mu$ M forward primer, 1.0  $\mu$ l 10  $\mu$ M reverse primer, 1.0  $\mu$ l 50mM  $Mg^{2+}$ , 4.0  $\mu$ l cDNA and 5.25  $\mu$ l dH<sub>2</sub>O. Reactions were performed using the Applied Biosystems 7500 Fast Real-time PCR system under the following thermal cycling conditions: 95 °C for 15 mins, and 40 cycles of 94 °C for 15 secs and 60 °C for 1 min. Negative RT and water controls were included. Primer sequences and probe numbers are shown in Table 2.1. Real-time PCR efficiencies for each assay were calculated from the exponential phase of the slope in the SDS v1.3.1 software, using the equation  $E = 10^{-1/\text{slope}}$ . Reactions were performed in duplicate at five serial dilutions of HH19 wild type cDNA (1, 0.1, 0.01, 0.001, and 0.0001). Quantitative PCR reactions were performed in triplicate on cDNA reverse transcribed from RNA used in the initial microarray analysis. Expression quantifications were corrected for PCR efficiency, with the equation  $R = 2^{-\Delta\Delta C_t}$  modified to the equation  $R = (E_{\text{target}})^{\Delta C_t \text{ target (control - sample)}} / (E_{\text{ref}})^{\Delta C_t \text{ ref (control - sample)}}$ .

### **2.2.1.10 QPCR for expression analysis in the chick**

#### **2.2.1.10.1 Assay design**

QPCR assays were designed using the online Roche Universal ProbeLibrary assay design centre (<https://www.roche-applied-science.com>). For genes with high similarity to other sequences, regions of lowest homology were input and only specific assays selected. Blast searches were carried out for all primers to ensure specificity.

#### **2.2.1.10.2 Amplification conditions**

Quantitative PCR was performed in a total volume of 28  $\mu$ l using 12.5  $\mu$ l TaqMan Universal PCR Master Mix (Applied Biosystems), 0.5  $\mu$ l 10  $\mu$ M probe (5' FAM labelled, Universal ProbeLibrary, Roche), 0.75  $\mu$ l 10  $\mu$ M forward primer, 0.75  $\mu$ l 10  $\mu$ M reverse primer, 5.0  $\mu$ l cDNA, and 5.5  $\mu$ l dH<sub>2</sub>O. Reactions were performed using the Applied Biosystems 7500 Fast Real-time PCR system under the following thermal cycling conditions: 95 °C for 15 mins, and 40 cycles of 94 °C for 15 secs and 60 °C for 1 min. Negative RT and water controls were included in each plate. Primer sequences and probe numbers are shown in Tables 2.4 and 2.5. Data was analysed using Applied Biosystems 7500 v2.0.1 software.

#### **2.2.1.10.3 Comparative C<sub>T</sub> method vs Relative Standard Curve method**

QPCR analyses of gene expression in the chick were carried out using the Relative Standard Curve method. This method is ideal for the detection of small changes in expression as would be expected in an *in ovo* system, and also when sample numbers are low in order that both standard curves and all samples can be run simultaneously in one reaction plate. Reliable quantification depends on accurately constructed standard curves; therefore data generated in this study has only been used when both standard curves meet a stringent set of parameters. These are discussed further in the next section.

#### **2.2.1.10.4 Specification of experimental parameters**

For generation of accurate and reproducible data, a strict set of experimental parameters was set out. Data was used only if both standard curve slopes were in the range -3.2 to -3.6 (a linearity of -3.33 corresponds to an assay efficiency of 100%). Standard curve linearity was a minimum of 0.99 for both genes on the reaction plate.

#### **2.2.1.10.5 Preparation of standard curves**

The preparation of a standard curve requires a cDNA standard which expresses the target and endogenous control genes. This can be obtained from a source independent to the study samples, which has advantages when working with material in low supply. It also allows cDNA standard production on a large scale for comparison of data across all experiments. HH24 whole embryo cDNA was the chosen standard for this study. Dilutions were carried out immediately after cDNA synthesis for storage in single use aliquots to prevent repeated freeze / thaw cycles, and for consistency across reaction plates. RNA preparations often contain inhibitors (such as proteins) which can affect subsequent QPCR reactions. To minimise this, all cDNA was diluted prior to use. cDNA for standards was used at a starting dilution of 1 in 16, and subsequent dilutions were made from this. Sample cDNA dilutions were carried out such that following amplification they would fall within the mid-range of the standard curve. The fold-dilution of standards was selected according to the expected magnitude of expression change. A 4-fold dilution series was chosen as relatively small expression changes were expected due to the fact this experiment was performed *in ovo*.

#### **2.2.1.11 Microarray expression analysis**

Microarray technology allows gene expression profiling of different sample groups on a genome-wide scale. It involves the use of individual spotted probes immobilised on a support in a known arrangement for detection of hybridisation. Sample RNA is reverse transcribed to produce cDNA which is then labelled with fluorescent dyes, most commonly Cy3 / Cy5. Samples are then hybridised onto arrays and scanned

using a confocal laser to produce images from which the relative fluorescent intensity of spots can be assessed for calculation of relative gene expression. Microarray studies were carried out using the Affymetrix service provided by the Nottingham Arabidopsis Stock Centre (NASC), using the Affymetrix GeneChip® Chicken Genome Array (900590). Microarray expression data was analysed using GeneSpring version 11 software (Agilent).

## 2.2.2 Microbial techniques

### 2.2.2.1 A-tailing procedure for cloning into the pGEM-T Vector

PCR products amplified using the *PfuUltra* 11 Fusion HS DNA polymerase are blunt ended and need to be modified using an A-tailing procedure for cloning into the pGEM-T Vector. Reactions were set up as follows: 1 - 7  $\mu$ l gel purified PCR product, 1  $\mu$ l 10x *Taq* standard PCR buffer containing  $MgCl_2$  (NEB), 0.4  $\mu$ l 5 mM dATP, 1  $\mu$ l 5U /  $\mu$ l *Taq* DNA polymerase (NEB), and  $dH_2O$  to a final volume of 10  $\mu$ l. Samples were incubated at 70 °C for 30 minutes, and 1 - 2  $\mu$ l used per ligation reaction.

### 2.2.2.2 Ligation of vector – insert

Ligations were carried out using the TOPO cloning kit (Promega). Reactions were set up with 5  $\mu$ l 2x rapid ligation buffer, 1  $\mu$ l vector (50 ng /  $\mu$ l), 1  $\mu$ l T4 DNA ligase, and insert at an approximate insert:vector molar ratio of 3:1, made up to a total volume of 10  $\mu$ l with  $dH_2O$ . Samples were incubated at room temperature for 1 hour, or at 4 °C overnight. Positive controls (containing vector and control insert) and background controls (containing vector and no insert) were included in each set of ligations / transformations.

### 2.2.2.3 Transformation

The *Escherichia coli* (*E.coli*) DH5 $\alpha$  strain was used in all bacterial work. DH5 $\alpha$  cells were thawed on ice (30  $\mu$ l aliquots) and 2  $\mu$ l ligation reaction added, mixed by flicking, then placed on ice for 25 – 30 minutes. Cells were subjected to heat-shocking at 42 °C for 45 seconds, placed on ice for 2 minutes, and 950  $\mu$ l SOC media added for incubation at 37 °C shaking for 1 hour. Cells were pelleted by centrifugation at 1000 g for 10 minutes, resuspended in 300  $\mu$ l SOC media, and spread onto MacConkey agar plates containing 50  $\mu$ g / ml ampicillin for overnight incubation at 37 °C. MacConkey agar is selective for gram negative bacteria (due to the fact it contains crystal violet and bile salts). It also differentiates between lactose fermenting bacteria (which do not contain an insert) and appear pink, and non lactose fermenting bacteria

(containing an insert) which appear colourless. Colour screening can therefore be used to accurately detect transformed colonies.

#### **2.2.2.4 Colony PCR**

Colony PCR reactions were performed for detection of the presence / absence of insert. PCR reactions were carried out in 25 µl reaction volumes using 2 µl 10 µM forward and reverse primers, 2.5 µl 10x buffer (Qiagen), 1 µl 10 mM dNTPs, 0.25 µl 5U / µl HotStar Taq (Qiagen), and 16.25 µl H<sub>2</sub>O. Reactions were inoculated using individual colonies picked from agar plates. Colonies picked from the positive control plate were used as negative insert controls, in addition to a standard negative PCR control. Thermal cycling conditions were based on the following: 95 °C for 15 mins, 35 cycles of 94 °C for 30 secs, 60 °C for 30 secs and 72 °C for 30 secs, and 72 °C for 10 mins.

#### **2.2.2.5 Overnight cultures**

Single colonies were used to inoculate 5 ml LB media containing ampicillin (50 µg / ml), and a negative control was included with each set of overnight cultures to verify sterility. Cultures were incubated at 37 °C shaking overnight.

#### **2.2.2.6 Preparation of glycerol stocks**

A 200 µl volume of glycerol was added to 800 µl fresh overnight culture (final concentration 20%). Samples were mixed and stored at -80 °C.

#### **2.2.2.7 Plasmid DNA isolation (Miniprep)**

For plasmid minipreps, DNA was extracted from 3 ml of bacterial culture. This was divided into two 1.5 ml aliquots which were sequentially centrifuged at maximum speed for 1 minute to pellet the cells. DNA was extracted using the GenElute Plasmid Miniprep Kit (Sigma) according to manufacturer's instructions. The bacterial pellet was resuspended by addition of 200 µl resuspension solution and vortexing. Cells were lysed by addition of 200 µl lysis solution and gentle inversion. Cell debris was

precipitated by addition of 350 µl of neutralisation/binding solution and gentle mixing, followed by centrifugation at maximum speed for 10 minutes. Following column preparation, the cleared lysate was transferred to the column and centrifuged at maximum speed for 1 minute. A 750 µl volume of wash solution was added to the column, a 1 minute centrifugation performed, and the flow-through discarded prior to a second centrifugation for 2 minutes to remove any traces of ethanol. The column was transferred to a clean microcentrifuge tube and 100 µl H<sub>2</sub>O pipetted directly onto the membrane followed by centrifugation for 1 minute at maximum speed to elute DNA. DNA was quantified using the NanoDrop® ND-1000 spectrophotometer (section 2.2.1.3).

#### **2.2.2.8 Plasmid DNA isolation (Maxiprep)**

A single colony was picked from a plate and used to inoculate a 3 ml starter culture in LB media which was incubated for 8 hours at 37 °C shaking. A volume of 200 µl starting culture was made up to 100 ml (1 / 500 dilution) with LB media and grown at 37 °C shaking overnight. DNA was extracted from 100 ml bacterial culture using the Plasmid Maxi kit (Qiagen). Cells were harvested by centrifugation at 6000 x g for 15 minutes at 4 °C. The bacterial pellet was resuspended in 4 ml buffer P1, followed by addition of 4 ml of lysis buffer P2 and incubation at room temperature for 5 minutes. Chilled buffer P3 was then added at a volume of 4 ml, mixed, and incubated on ice for 15 minutes. This was followed by centrifugation at maximum speed at 4 °C for 30 minutes. The supernatant was removed and re-centrifuged under identical conditions for 15 minutes. The supernatant was then applied to an equilibrated QIAGEN-tip and allowed to enter the resin. The tip was then washed twice with 10 ml buffer QC, and DNA eluted in 5 ml buffer QF. DNA was precipitated by addition of 3.5 ml isopropanol, mixing, and centrifugation at maximum speed for 30 minutes at 4 °C. The supernatant was carefully removed and the DNA pellet washed with 2 ml 70% ethanol followed by centrifugation at maximum speed for 10 minutes. The supernatant was carefully decanted and the DNA pellet allowed to air-dry prior to

being re-dissolved in an appropriate volume of H<sub>2</sub>O. DNA was quantified using the NanoDrop® ND-1000 spectrophotometer (section 2.2.1.3).

#### **2.2.2.9 Plasmid linearization by restriction digestion**

Digests were performed using restriction enzymes, buffers, and BSA (if required) from NEB. Reactions were set up as follows: 1 - 2 µg plasmid DNA, 1 µl restriction enzyme, 2 µl 10x buffer, 1 µl 20x BSA if necessary, made up to 20 µl with H<sub>2</sub>O. Samples were incubated at 37 °C for 3 - 4 hours, or overnight. Agarose gel electrophoresis was performed using 100 ng to confirm digestion was complete.

#### **2.2.2.10 Introduction of restriction sites by PCR amplification for subcloning into the pGL3-Basic and pGL3-Promoter vectors**

Primers incorporating restriction sites (in this case SacI) were designed and used for PCR amplification of insert (as described in section 2.1.1.5.2) using plasmid DNA as template, for subcloning into a second vector. Products were subjected to agarose gel electrophoresis, and purified by gel extraction (section 2.1.3.3).

#### **2.2.2.11 Restriction digestion and vector dephosphorylation**

For subcloning into a second vector, the destination vector and modified insert were cut using the same restriction enzyme to produce complementary ends. Linearised vector DNA was dephosphorylated using Shrimp Alkaline Phosphatase (SAP) to prevent recircularisation by removal of 5' phosphate groups from both termini.

### **2.2.3 DNA purification techniques**

#### **2.2.3.1 Shrimp Alkaline Phosphatase / Exonuclease I treatment**

This is a simple enzymatic procedure for preparing PCR products for sequencing. SAP catalyses the dephosphorylation of 5' phosphates from DNA, removing excess dNTPs. Exonuclease I (ExoI) digests single stranded DNA in the 3' to 5' direction, removing unincorporated primers. PCR products were purified for sequencing in 7  $\mu$ l reaction volumes using 1.5  $\mu$ l 1 U /  $\mu$ l SAP (Promega) and 0.5  $\mu$ l 20 U /  $\mu$ l ExoI (NEB) with 5  $\mu$ l PCR product. Samples were incubated at 37 °C for 1 hour, followed by an enzyme inactivation step of 80 °C for 20 mins.

#### **2.2.3.2 Column purification of PCR products**

PCR products > 100 bp were purified using the Sigma GenElute PCR clean up kit according to manufacturer's instructions. Briefly, following column preparation, 5 volumes of binding solution was combined with PCR product. This was applied to the column for centrifugation at maximum speed for 1 minute, and the eluate discarded. Column-bound DNA was then washed by addition of 0.5 ml wash solution and centrifugation at maximum speed for 1 minute. Following eluate disposal, the column was centrifuged for a further 2 minutes at maximum speed to remove any traces of ethanol. The column was transferred to a fresh collection tube and 50  $\mu$ l water pipetted directly onto the centre of the membrane followed by incubation at room temperature for 1 minute. DNA was eluted by centrifugation at maximum speed for 1 minute, and stored at -20 °C.

#### **2.2.3.3 DNA extraction from agarose gels**

DNA was purified using the QIAquick Gel Extraction Kit (Qiagen) according to manufacturer's instructions. Briefly, the DNA fragment was visualised under UV light and excised from the agarose gel using a scalpel blade. The gel slice was then weighed and 3 volumes of buffer QG added followed by incubation at 50 °C for 10 minutes with vortexing every 2 - 3 minutes, allowing the gel to dissolve. Isopropanol

was added to the sample at 1 gel volume, mixed, and applied to the column for centrifugation for 1 minute at maximum speed. The eluate was discarded and column-bound DNA washed by addition of 0.75 ml buffer PE and centrifugation for 1 minute at maximum speed. The column was re-centrifuged for an additional minute to remove all traces of ethanol. The column was placed in a clean microcentrifuge tube and 50  $\mu$ l water pipetted directly onto the centre of the membrane for DNA elution by centrifugation at maximum speed for 1 minute. DNA was stored at -20 °C.

#### **2.2.3.4 Ethanol precipitation of DNA**

Ethanol was added at 2.5 volumes, and 1 / 10 volume of 3 M NaOAc pH 5.5 added to each sample, mixed by inversion, and incubated at room temperature for 15 minutes. Samples were centrifuged at 13000 rpm for 30 minutes and the supernatant carefully removed. The DNA pellet was washed with 70% ethanol, and centrifuged at 13000 rpm for 10 minutes. The supernatant was carefully removed and the pellet air-dried before resuspension in an appropriate volume of H<sub>2</sub>O.

## **2.2.4 Chick embryo techniques**

### **2.2.4.1 General care and conditions**

Fertile white Leghorn eggs (Henry Stewart & Co Ltd) were stored at 12 °C prior to use. Eggs were incubated at 37 °C gently rotating in a humidified incubator for the appropriate time.

### **2.2.4.2 Embryo staging**

A small opening was created at the top of each egg and 4 ml albumen removed. Individual embryos were staged visually whilst in the egg according to Hamburger & Hamilton (HH) chicken developmental stages [Hamburger and Hamilton, 1992]. Chick developmental stages are further described in Appendix A.

## **2.2.5 Chick expression studies**

### **2.2.5.1 Collection of chick embryonic tissue for RT-PCR, QPCR, and microarray expression analysis**

Embryos were excised and placed in sterile ice cold PBS (Sigma). Membranes were removed and the relevant tissue was isolated at the required stage of development and immediately placed in RNAlater (Ambion) for storage at -20 °C. In the case of morpholino treated embryos (section 2.1.4.5), embryos were excised from the egg and placed in sterile ice cold PBS. The outer and inner membranes were quickly removed, and the embryo placed in RNAlater for assessment of morpholino uptake under fluorescent light using a Zeiss Stemi SV11 microscope. Embryos were photographed where necessary and morpholino positive hearts isolated and stored in RNAlater at -20 °C prior to extraction of RNA.

### **2.2.5.2 Whole mount in situ hybridisation (WISH)**

#### **2.2.5.2.1 Embryo collection and preparation**

Embryos were placed in ice-cold sterile chick saline solution for membrane removal followed by overnight fixation in 4% paraformaldehyde (PFA). Embryos were subjected to 3x 5 minute washes in PBS with 0.5% Tween (PBST), bleached for 1 hour in 3% H<sub>2</sub>O<sub>2</sub> (Sigma) in PBS, followed by 5 minute washes in a graded methanol series of PBST, 25% methanol (in PBST), 50% methanol (in PBS), 75% methanol (in DEPC treated water), and 100% methanol, then stored in 10 ml of methanol for a minimum overnight at -20 °C (maximum 1 week). Embryos were subjected to 5 minute washes in the methanol series ending in PBST, then digested with proteinase K in PBS (HH16: 10 µg / ml, HH19 and HH24: 20 µg / ml) for 20 minutes. Samples were washed for 10 minutes in PBST, fixed for 20 minutes in 4% PFA with 0.2% glutaraldehyde, and subjected to two 10 minute washes in PSBT. PBST was removed and samples incubated in pre-hybridisation solution at 65 °C for 2 hours.

The pre-hybridisation solution was replaced with fresh pre-hybridisation solution and embryos stored at -20 °C for up to 10 days prior to use.

#### **2.2.5.2.2 Probe synthesis and digoxigenin (DIG) labelling**

Single stranded DIG-labelled RNA probes were synthesised using the DIG RNA Labelling Mix (Roche) by *in vitro* transcription with SP6 or T7 RNA polymerases, which incorporate DIG-11-UTP at approximately every 20 – 25 bases. Reactions were set up on ice as follows: 500 ng - 1 µg linearised plasmid DNA, 2 µl 10x DIG RNA labelling mix, 2 µl 10x transcription buffer, 2 µl 20 U / µl SP6 or T7 RNA polymerase, sterile RNase free water to a final volume of 20 µl. Reactions were incubated at 37 °C for 3 hours, then template DNA was removed by addition of 2 µl DNase I (RNase free) and further incubation at 37 °C for 30 minutes. Reactions were stopped by addition of 1 µl 0.5 M EDTA pH 8.0, and 9 µl DEPC treated H<sub>2</sub>O added.

#### **2.2.5.2.3 Probe purification and quantification**

Probes were purified using Microspin G-50 columns (Illustra) according to manufacturer's instructions. Briefly, column preparation involved resuspension of the resin by vortexing, the cap was then loosened by one quarter of a turn, and the bottom closure snapped off prior to placement in the collection tube. The column was pre-spun for 1 minute at low speed (735 x *g*). The column was placed in a new microcentrifuge tube. DIG labelling reactions were made up to a volume of 50 µl with Probe Elution and Storage Buffer, carefully applied to the top centre of the resin, and centrifuged at 735 x *g* for 2 minutes for elution. Probes were quantified using the NanoDrop® ND-1000 spectrophotometer and stored at -80 °C.

#### **2.2.5.2.4 *In situ* hybridisation**

Prepared embryos were warmed in a hybridisation oven (Biometra OV3) at 65 °C for 2 hours. Pre-hybridisation solution was replaced with fresh pre-warmed pre-hybridisation solution containing probe at 150 ng / µl, and samples incubated at 65 °C for 22 hours. Embryos were subjected to 10 minute wash steps at 65 °C in each of

the following: 100% pre-hybridisation solution, 75% pre-hybridisation solution / 25% 2x SSC, 50% pre-hybridisation solution / 50% 2x SSC, 25% pre-hybridisation solution / 75% 2x SSC, 100% 2x SSC, then 4x 15 minute washes at 65 °C in 0.2 x SSC. Embryos were then subjected to 5 minute washes at room temperature in the following: 75% 0.2x SSC / 25% KTBT, 50% 0.2x SSC / 50% KTBT, 25% 0.2x SSC / 75% KTBT, 100% KTBT. Embryos were blocked in KTBT containing 10% sheep serum (Invitrogen) and 2 mg / ml BSA (Fisher Scientific) for 3 hours at room temperature (sheep serum was inactivated by incubation at 65 °C for 30 minutes prior to use). This was followed by incubation with anti-DIG-AP Fab fragment (Roche) at 1 / 5000 in blocking solution at 4 °C overnight. Embryos were subjected to 5x 1 hour washes in KTBT gently rotating at room temperature, and then 2x 15 minute washes in fresh NTMT (containing levamisole at 25 µg / ml). Colour reagent was made immediately before use and 2 ml added to each sample for initial incubation in the dark at room temperature for 20 minutes, then longer as necessary. The colour reaction was stopped by 2x 15 minute rinses in KTBT and one 15 minute wash in PBS. Embryos were taken through in a graded methanol series ending in 100% methanol, where they were incubated until sufficient background was removed. Embryos were then rehydrated through the methanol series ending in PBS, and transferred to 70% glycerol for photography. Embryos were washed in PBS and stored in pH 5.5 PBS containing 1 mM EDTA at 4 °C in the dark.

### **2.2.5.3 Western blotting**

#### **2.2.5.3.1 Collection of tissue**

HH24 wild type embryonic tissue was isolated as sample material for initial technique development. Embryos were excised from the egg and placed in sterile ice cold PBS. The outer and inner membranes were quickly removed, and if necessary, assessment of morpholino uptake carried out under fluorescent light using a Zeiss Stemi SV11

microscope. Embryos were photographed where necessary and morpholino positive hearts isolated and snap frozen in liquid nitrogen prior to extraction of protein.

#### **2.2.5.3.2 Preparation of tissue lysates**

Embryonic tissue was isolated and placed in approximately 5x volume of chilled RIPA buffer (containing 1 mM PMSF and protease inhibitor cocktail (Roche)). Samples were immediately homogenised using a sterile needle (BD Microlance 25G 5/8) and syringe, and placed on ice for 30 minutes. Samples were centrifuged at maximum speed for 10 minutes and the supernatant removed and stored at -80 °C prior to use.

#### **2.2.5.3.3 HeLa cell growth and isolation**

Cells were grown and isolated by Sukrat Arya. Passage 8 HeLa cells were grown in 20 ml complete media (Dulbecco's minimal essential media (DMEM) with 10% v/v foetal bovine serum and peninstrep). Media was discarded and dead cells removed by washing with PBS. A 2 ml volume of trypsin was spread gently around the flask and incubated at 37 °C for 4 minutes to detach and round the cells. A volume of 18 ml complete media was added to the cells, mixed, and centrifuged at 1500 rpm for 3 minutes. The supernatant was discarded and cells were resuspended in 10 ml PBS prior to centrifugation at 1500 rpm for 3 minutes. The supernatant was discarded and the pellet stored on ice prior to immediate extraction of protein.

#### **2.2.5.3.4 Preparation of HeLa cell lysates**

HeLa cell pellets were dissolved in 300 µl chilled RIPA buffer and placed on ice for 30 minutes. Samples were mixed by flicking then subjected to two 5 – 10 minute freeze / thaw cycles at -80 °C. Samples were centrifuged at 12000 rpm for 15 minutes, and the supernatant removed and stored at -80 °C.

#### **2.2.5.3.5 Protein quantification**

Protein content was measured by Bradford assay using the Biorad protein assay kit, using a 50 µg / ml – 1 mg / ml BSA standard curve. Absorbances were measured at 750 nm on a Biorad SmartSpec™ 3000 spectrophotometer.

#### **2.2.5.3.6 SDS PAGE and western blotting**

Samples were combined with 5x sample buffer and boiled for 10 minutes at 100 °C prior to loading onto 5 - 20% SDS PAGE gradient gels (20 - 30 µg total protein loaded per lane). Samples were electrophoresed using Atto apparatus alongside the Precision Plus Protein Standard (BioRad) at 100 V for approximately 90 minutes in electrophoresis buffer. Protein was transferred onto a Hybond C Extra nitrocellulose membrane (Amersham Biosciences) by a semi-dry blotting technique, using a transfer sandwich comprising gel and membrane, sandwiched between 2 layers of absorbent paper (Atto) soaked in transfer buffer on either side. Electroblothing was performed with Atto apparatus at 20 V for 2 hours. Following transfer, membranes were washed in deionised water and blocked in the appropriate agent overnight at 4 °C with gentle shaking. Membranes were subjected to three 10 minute washes in TBST, then incubated with primary antibody at the appropriate dilution for 1 hour at room temperature with gentle shaking. Membranes were again subjected to three 10 minute washes in TBST, and then incubated with secondary antibody for 1 hour at room temperature with gentle shaking. Membranes were again subjected to three washes in TBST. ECL reactions were then performed using the Western Lightning Chemiluminescence Reagent Plus kit (PerkinElmer) for protein detection.

#### **2.2.5.3.7 Conditions tested for antibody optimisation**

For GAPDH detection, membranes were blocked with 5% milk powder in TBS and incubated with a mouse monoclonal antibody (ab8245, Abcam) at a dilution of 1 / 1000. Rabbit anti-mouse HRP conjugated secondary antibody (P0260, Dako) was used at 1 / 1500, and a 36 kDa band successfully detected.

For TBX5 detection, a rabbit polyclonal antibody to TBX5 (ab49308, Abcam) was tested in 5% milk powder / PBS. Swine anti-rabbit HRP conjugated secondary antibody (P0217, Dako) was used at 1 / 5000. A band of unexpected size (~ 75 kDa, expected size 50 – 53 kDa) was detected.

For detection of GATA-4, a rabbit polyclonal antibody to GATA-4 (ab25992, Abcam) was tested in two blocking agents - 5% milk powder / TBS, and 5% BSA / TBS. Swine anti-rabbit HRP conjugated secondary antibody (P0217, Dako) was tested at 1 / 1500. A very high level of background resulted in both cases and it was not possible to accurately distinguish any bands.

For RBMS1 detection, membranes were blocked with 5% milk powder in TBS and incubated with a rabbit polyclonal antibody (ARP40428\_T100, Aviva Systems Biology) at a dilution of 1 / 100. Swine anti-rabbit HRP conjugated secondary antibody (P0217, Dako) was used at 1 / 1500. Antibodies were tested on HeLa cell lysate and chick tissue lysate. A band of unexpected size (~ 120 kDa, expected size 46 kDa) was detected.

## **2.2.6 Morpholino knockdown**

### **2.2.6.1 Morpholino knockdown technology**

Morpholino knockdown is an antisense loss-of-function technology used widely in developmental studies. A morpholino oligomer is a synthetic DNA analogue usually consisting of around 25 subunits, with a morpholine moiety replacing the riboside moiety and phosphorodiamidate intersubunit linkages instead of phosphodiester linkages [Summerton and Weller, 1997]. These modifications confer stability to the oligomer, and cellular enzymatic degradation does not occur [Hudziak et al., 1996]. Morpholinos have high affinity for RNA and do not elicit an immune response. They can be end-labelled with 3' carboxyfluorescein or lissamine (sulforhodamine B) for confirmation of uptake.

Morpholinos function by two major gene targeting strategies. They can be designed to bind to the initiating AUG sequence (or in close proximity) in order to sterically blocking ribosomal binding and inhibit translation [Summerton and Weller, 1997]. Translational blocking morpholinos are most effective when designed within a 100 bp region between the 75 bp upstream and 25 bp downstream region of the initiating AUG. Morpholinos can also be designed to target nuclear processing and modify pre-mRNA splicing through complementary binding to splice sites [Morcos, 2007].

Morpholinos have been utilised to study the effect of gene knockdown in cultured cells, and in the developing embryos of a number of organisms such as *Xenopus* [Falk et al., 2007], zebrafish [Draper et al., 2001], and chick [Voiculescu et al., 2008]. They are particularly useful for temporal gene knockdown studies, where the role of a particular gene at specific stages of development can be elucidated.

### **2.2.6.2 Identification of target regions for morpholino design**

Human homologues of genes of interest were identified on the NCBI database (<http://www.ncbi.nlm.nih.gov/>) and their genomic location noted. Protein sequences

were blasted in the BBSRC ChickEST database (<http://www.chick.manchester.ac.uk/>). ESTs were then blasted in Ensembl (<http://www.ensembl.org>) against the chick genome in order to locate the corresponding chick gene, and viewed in a chromosomal contig view. Synteny of the chick genomic location against the expected human genomic region was confirmed. Translation software (<http://expasy.org/tools/>) was used to aid identification of the initiating ATG. ESTs around this region were aligned with the theoretical mRNA sequence for sequence confirmation using sequence alignment software (<http://align.genome.jp/>). The region 75 base pairs upstream and 25 base pairs downstream of the initiating ATG was identified for morpholino design. Where it was not possible to design a morpholino to this region, morpholinos were designed to modify pre-mRNA splicing by targeting exon / intron boundaries (splice sites). These were predicted to result either in deletion of an exon and cause a frameshift and premature termination, or retention of an intron causing insertion of incorrect amino acids followed by a premature stop.

#### **2.2.6.3 Morpholino design and preparation**

Morpholino antisense oligonucleotides were designed to a 25 base pair region using the following guidelines: 40% - 60% GC content, maximum 36% G, maximum run of 3 Gs, avoidance of G or A on 3' end where possible (<http://www.genetools.com>). Morpholinos had either 3' carboxyfluorescein or 3' lissamine end modifications for confirmation of uptake. Morpholinos were resuspended at 2  $\mu$ M in HBSS and stored at -20 °C.

#### **2.2.6.4 Morpholino delivery**

Morpholinos are most commonly introduced into embryos by microinjection, and in the case of the chick, by electroporation [Kos et al., 2003]. However, this method is not always effective for knockdown outside the central nervous system, particularly mesenchymal tissues [Kos et al., 2003]. In recent years the use of F127 pluronic gel has been employed as an alternative method of morpholino delivery into the chick embryo [Ching et al., 2005; Rutland et al., 2009].

F127 pluronic gel is a non-ionic co-polymer of polyethylene oxide and polypropylene oxide with thermosensitive properties. Upon reaching physiological temperatures it undergoes a liquid to gel phase transition, and in terms of *in vivo* application, this means it is injectable and will polymerise locally *in situ* i.e. it has potential uses as a vehicle for drug delivery. It has been tested in a number of biomedical applications such as the local delivery of an anti-tumour agent into mice [Yang et al., 2009], ocular delivery of ophthalmic agents [El-Kamel, 2002; Miyazaki et al., 2001], and in vaccine delivery systems [Coeshott et al., 2004]. It has also been used for local application of antisense phosphorothioate oligodeoxynucleotides into major blood vessels *in vivo* for loss of function studies [Abe et al., 1994; Castier et al., 1998; Herbert et al., 1997]. For gene knockdown in the developing chick, pluronic gel can be combined with morpholino antisense oligonucleotides and applied directly onto the embryo where it undergoes gelation, facilitating morpholino entry into the embryo. This is the method of choice for this study.

#### **2.2.6.5 Application of morpholino via F127 pluronic gel to embryos in ovo**

Eggs were opened as described previously and embryo ages assessed. Prior to use, morpholinos were heated to 65 °C for 5 minutes, incubated on ice, and combined with HBSS and F127 pluronic gel (BASF) at a final concentration of 15%, for a final morpholino concentration of 250 µM or 500 µM. In the case of double knockdown, morpholinos were combined at this stage, each at a final concentration of 250 µM. A 7 µl volume of morpholino / F127 pluronic gel mix was pipetted directly onto the chick (usually at HH12 – HH16). Eggs were sealed using tape and incubated at 37 °C until the required stage of development was reached.

## **2.2.7 Phenotypic analysis of embryos**

### **2.2.7.1 Embryo isolation and processing**

Chick embryos were excised from the egg, placed in PBS, and the outer and inner membranes carefully removed to avoid damage to the embryo. Morpholino uptake was assessed under fluorescent light, and embryos photographed where appropriate at 1.6x and 4.0x zoom using a Zeiss Stemi SV11 microscope. Embryos were incubated in 4% PFA at room temperature for 90 mins, and stored at 4 °C in PBS for up to 1 week. Embryos were dehydrated by 2x 15 minute incubations in each of the following; dH<sub>2</sub>O, 75% ethanol, 95% ethanol, 100% ethanol, and xylene (room temperature). A final 50% xylene / 50% wax incubation was carried out at 65 °C before transfer into wax at 65 °C overnight.

### **2.2.7.2 Embedding and sectioning**

Embryos were correctly positioned and left to set at room temperature overnight. Embryos were sectioned in a coronal orientation at 10 microns using a Leica DSC1 microtome. Sections were floated in a heated water bath (40 °C) and mounted onto glass slides. Slides were air-dried overnight at room temperature.

### **2.2.7.3 Haemulum staining and mounting of slides**

Sections were de-waxed and rehydrated by 5 minute incubations in the following: 100% xylene x 2, 100% ethanol x 2, 95% ethanol, 75% ethanol, 50% ethanol, dH<sub>2</sub>O. Excess water was blotted away before incubation in Mayer's Haemulum (Raymond A Lamb) for 3 minutes. Slides were washed then dehydrated by 5 minute incubations in the following: dH<sub>2</sub>O, H<sub>2</sub>O, dH<sub>2</sub>O, 50% ethanol, 75% ethanol, 95% ethanol, 100% ethanol, 100% xylene. Slides were removed from xylene, mounted with DPX (Bios Europe) and allowed to dry overnight before photography.

#### **2.2.7.4 Photography and analysis**

Sections were photographed at 2.5x and 5.0x magnification under a Zeiss Axioscope 40 microscope connected to a Macintosh computer and OpenLab software (PerkinElmer, UK).

## **CHAPTER 3**

### **IDENTIFICATION OF DOWNSTREAM TARGETS OF TBX5 and GATA-4 IN THE MOUSE P19 CELL LINE**

#### **3.1 AIMS**

This chapter aims to use the P19 study as a basis for further research into the combined targets of TBX5 and GATA-4 as follows:

- a) Validation of previous microarray data by QPCR
- b) Selection of genes for further study based on expression data and review of current literature
- c) Bioinformatic analysis of candidate gene promoter regions for identification of evolutionarily conserved TBX5 and GATA-4 binding sites
- d) Luciferase reporter assays to test promoter activation of one or more genes by TBX5 and GATA-4

## **3.2 RESULTS**

### **3.2.1 QPCR validation of microarray data**

Genome-wide microarray expression analyses allow identification of a large number of targets which display differential regulation. These results are often variable, and validation by an independent method with greater sensitivity is necessary. QPCR is one of the most precise methods of expression quantification available, and was used to confirm and more accurately quantify previous microarray gene expression data. QPCR validation experiments were performed in collaboration with Jonathan Ronksley.

#### **3.2.1.1 Assay design**

QPCR assays were designed by Jonathan Ronksley using the online Roche Universal ProbeLibrary assay design centre (<https://www.roche-applied-science.com>). Assays spanned a 60 – 100 bp region including an exon-exon boundary where possible, and were used with an annealing temperature of 60 °C. Primer sequences and assay information are given in Appendix B. These primers were used for RT-PCR amplification to confirm products sizes and single product amplification prior to QPCR, using cDNA from wild type (day 0 and 7) and overexpression cell lines (day 0) (not shown).

#### **3.2.1.2 Selection of endogenous controls**

Selection of an appropriate endogenous control gene for normalisation is crucial and allows correction of any skewing of data arising from small differences in starting quantity of total nucleic acid. The endogenous control must be expressed at the same time as the target gene, and display uniform expression across all samples i.e. expression should not be affected by sample treatments. A total of six genes were selected for assessment of their suitability as controls, based on stable expression in the original microarray study -  $\beta$ -tubulin, non-POU-domain containing / nono,

ribosomal protein L13a / rpl13a, bolA-like 2 / bola2, dynactin, and transmembrane protein 131 / tmem131.

### 3.2.1.2.1 Analysis of endogenous control variation across study samples

In order to determine suitability of the above genes as endogenous controls, their expression across all study samples was measured for assessment of variability. Real time reactions were performed in triplicate, and relative expression was measured against undifferentiated P19 wild type cells. Baseline and threshold values were set manually. Fold change in expression was calculated using the following equation:

$$\begin{aligned} R &= 2^{-[\Delta Ct \text{ sample} - \Delta Ct \text{ control}]} \\ &= 2^{-\Delta \Delta Ct} \end{aligned}$$

R = relative expression,  $\Delta Ct$ : Ct difference between samples, control = wild type day 0 sample, sample = overexpression cell line day 0 or wild type sample at day 2, 5 or 7.

Expression results are shown in Table 3.1. Variation between samples was assessed by calculation of the range of variation (maximum value – minimum value), and the coefficient of variation was also calculated. Tmem131 displayed the smallest range of variation between samples (0.36), and also the smallest coefficient of variation across experimental samples (0.18).

**Table 3.1 Relative expression of six candidate endogenous control genes in study samples**

	Relative expression					
	$\beta$ -tubulin	nono	rpl13a	bola2	dynactin	tmem131
G10	0.79	1.01	1.05	0.75	0.82	0.71
G22	0.95	1.19	1.03	1.21	1.30	1.07
WT Day 2	0.98	1.32	0.96	0.94	1.09	0.86
WT Day 5	0.67	0.83	0.84	0.64	0.81	0.74
WT Day 7	0.59	0.84	0.64	0.61	0.76	0.77
<b>Range of variation</b>	<b>0.39</b>	<b>0.49</b>	<b>0.41</b>	<b>0.6</b>	<b>0.54</b>	<b>0.36</b>
<b>Coefficient of variation</b>	<b>0.21</b>	<b>0.22</b>	<b>0.19</b>	<b>0.30</b>	<b>0.24</b>	<b>0.18</b>

Expression of six candidate endogenous control genes was measured in G10 and G22 overexpression cell lines, and wild type differentiating P19 cells at days 2, 5 and 7, measured against undifferentiated P19 cells (day 0).

**3.2.1.2.2 Test normalisation using short-listed endogenous control genes**

Tmem131 and dynactin were used for test normalisation of  $\alpha$ -l-fucosidase, which was up-regulated in microarray analysis of the two overexpression cell lines. Relative expression values are shown in Table 3.2. The two controls gave almost identical results and confirmed up-regulation of alpha-l-fucosidase. Tmem131 was selected for use as the endogenous control as this gene previously displayed the lowest range of variation and coefficient of variation across experimental samples (Table 3.1).

**Table 3.2 Relative expression of FUCA1 when normalised against candidate endogenous control genes tmem131 and dynactin**

Sample	Relative expression of FUCA1	
	Normalisation with tmem131	Normalisation with dynactin
G10 day 0	1.627	1.625
G22 day 0	1.131	1.094

Expression of alpha-l-fucosidase (up-regulated in the microarray study) was measured in G10 and G22 overexpression cell lines against undifferentiated P19 cells (day 0), normalised to both tmem131 and dynactin. The two controls gave highly similar results.

**3.2.1.3 Analysis of target and control gene amplification efficiency**

The maximum PCR efficiency of a reaction ( $E$ ) is 2, if every single template is replicated in each cycle [Pfaffl, 2001]. Target and control genes should ideally show similar amplification efficiency, but data can be corrected for differences in assay efficiency by prior calculation of these values. Real-time PCR efficiencies for each gene were calculated from the exponential phase of the slope in the SDS v1.3.1 software, using the equation  $E = 10^{-1/\text{slope}}$ . Reactions were performed in duplicate

using a 5-point 10-fold dilution series of P19 wild type day 0 cDNA (1, 0.1, 0.01, 0.001, and 0.0001). Assay properties are shown in Table 3.3. A value of -3.33 corresponds to an assay efficiency of 100%, and generally -3.2 to -3.6 is considered acceptable. However, as expression quantifications will be corrected for PCR efficiency (see section 3.2.1.4), assays with efficiency outside this range are also usable. Linearity values  $\geq 0.99$  are desirable, and assays to all genes with the exception of RBMS1 met this.

**Table 3.3 Target and endogenous control real time assay linearity and efficiency**

Gene	Linearity ( $R^2$ )	Slope	Efficiency ( $E$ )
PETA-3	0.995	- 4.01	1.78
RBMS1	0.986	- 3.03	1.89
VegfB	0.992	- 3.62	1.89
Annexin A4	0.994	- 3.37	1.98
Tropomyosin	0.998	- 3.29	2.01
Gamma-filamin	0.997	- 3.62	1.89
mRbap46	0.998	- 3.53	1.92
PMM2	0.997	- 3.42	1.96
Neurofilament 3	0.998	- 5	1.58
Glutaredoxin	0.997	- 3.27	2.02
HNRPDL	0.991	- 3.27	2.02
Erp57	0.994	- 3.42	1.97
PA2.26	0.998	- 3.42	1.90
$\alpha$ -l-fucosidase	0.995	- 4.22	1.72
Fibronectin	0.997	- 3.51	1.93
$\alpha$ -2-macroglobulin	0.997	- 3.78	1.84
Calreticulin	0.998	- 3.72	1.85
Ap4e1	0.996	- 3.34	2
S100A10	0.996	- 3.74	1.85
Tmem131	0.992	- 3.83	1.82

Standard curves were constructed for all target and control genes using cDNA from P19 wild type undifferentiated cells. Reactions were performed in duplicate at five serial dilutions of P19 wild type day 0 cDNA (1, 0.1, 0.01, 0.001, and 0.0001).

### 3.2.1.4 Expression analysis

Quantitative PCR reactions were performed in triplicate on cDNA reverse transcribed from RNA used in the initial microarray analysis. For correction of expression quantifications to take into account PCR efficiency (E), the equation  $R = 2^{-\Delta\Delta Ct}$  was modified to the equation below:

$$R = \frac{(E_{\text{target}})^{\Delta Ct_{\text{target}}(\text{control} - \text{sample})}}{(E_{\text{reference}})^{\Delta Ct_{\text{ref}}(\text{control} - \text{sample})}}$$

R = relative expression, E = efficiency of QPCR assay,  $\Delta Ct$ : Ct difference between samples, target = gene of interest, reference = endogenous control gene, control = wild type day 0 sample, sample = overexpression cell line at day 0 / wild type sample at day 2, 5 or 7.

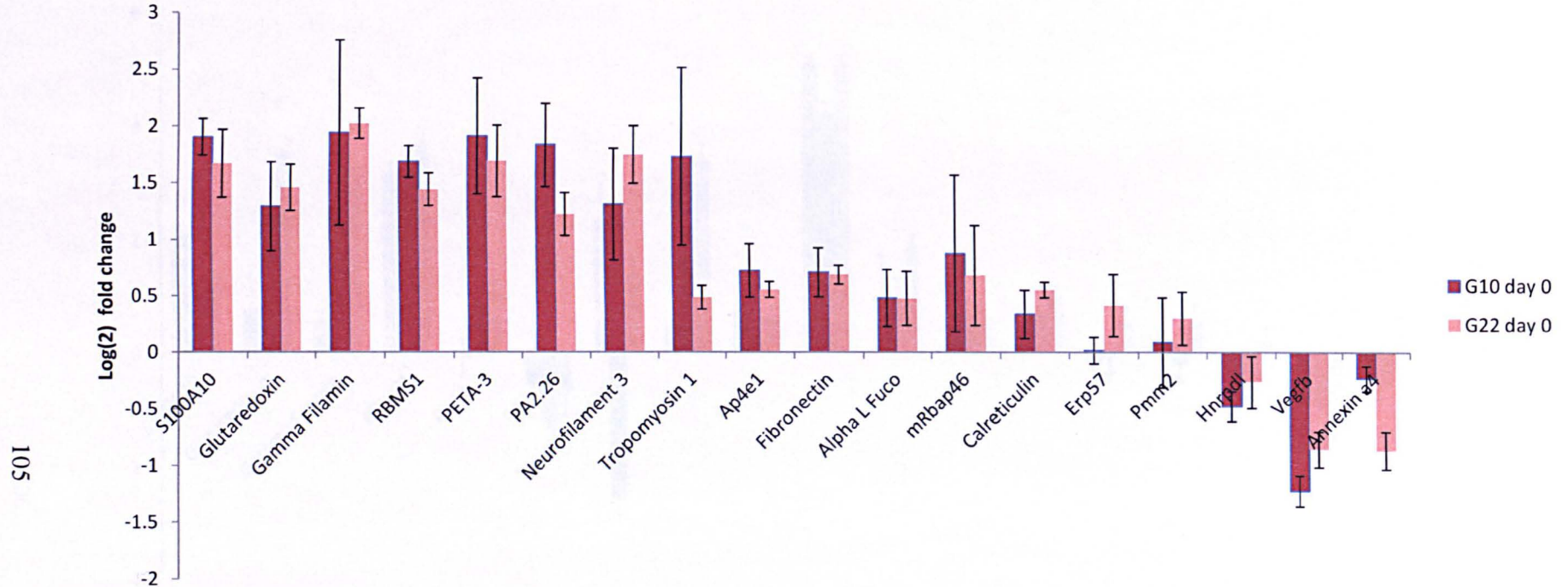
Expression data is represented in Table 3.4 and Figures 3.1 and 3.2. Figure 3.1 shows relative expression of 18 genes of interest in the two TBX5 / GATA-4 overexpression cell lines at day 0 of differentiation, displayed as  $\log_2$  fold change. A number of genes displayed average up-regulation of 2-fold or greater including S100A10, glutaredoxin,  $\gamma$ -filamin, RBMS1, PETA-3, PA2.26, neurofilament 3, and  $\alpha$ -tropomyosin.

Figure 3.2 displays expression profiles of the 18 genes of interest in wild type differentiating P19 cells, represented as  $\log_2$  fold change. As mentioned previously, wild type TBX5 and GATA-4 expression in differentiating P19 cells is switched on at day 2 and day 0 of differentiation respectively, and shows a massive increase over days 5 and 7. A number of genes followed the same pattern of expression including glutaredoxin,  $\gamma$ -filamin, RBMS1, PETA-3,  $\alpha$ -tropomyosin, calreticulin, erp57, and annexin A4.

**Table 3.4 Relative expression of candidate genes in TBX5 / GATA4 overexpression cell lines and wild type differentiating wild type cells, measured by QPCR**

Gene	Fold change					
	Overexpression cell lines			Wild type		
	G10 day 0	G22 day 0	G10/G22 average	WT day 2	WT day 5	WT day 7
S100A10	3.74	3.18	3.46	4.40	1.87	2.75
Glutaredoxin	2.45	2.75	2.60	1.75	5.94	11.6
Gamma filamin	3.85	4.06	3.96	1.50	6.11	9.89
RBMS1	3.22	2.71	2.97	9.29	9.66	13.2
PETA-3	3.76	3.23	3.50	0.94	1.84	2.25
PA2.26	3.57	2.34	2.96	0.68	0.43	0.58
Neurofilament	2.48	3.37	2.93	5.19	0.17	2.60
Tropomyosin 1	3.32	1.40	2.36	1.37	3.11	10.5
AP4e1	1.65	1.47	1.56	1.65	1.12	1.57
Fibronectin	1.64	1.61	1.63	34.7	18.9	34.2
$\alpha$ -l-fucosidase	1.40	1.39	1.40	1.97	1.92	3.64
Mrbpa46	1.84	1.61	1.73	1.39	1.60	1.49
Calreticulin	1.26	1.47	1.37	1.08	1.59	1.99
Erp57	1.01	1.33	1.17	0.85	0.92	1.42
Pmm2	1.06	1.23	1.15	1.20	0.85	1.44
Hnrpd1	0.72	0.83	0.78	0.63	0.54	1.13
Vegfb	0.43	0.55	0.49	0.53	0.50	0.42
Annexin A4	0.85	0.55	0.70	0.51	0.74	1.23

QPCR analysis of candidate genes was carried out in TBX5 / GATA-4 overexpression cell lines G10 and G22, and P19 wild type cells at days 2, 5 and 7, measured against undifferentiated wild type P19 cells. Data was normalised against *tmem131* and corrected for real time assay efficiencies.



**Figure 3.1 Relative expression of candidate genes in TBX5 / GATA4 overexpression cell lines G10 and G20**

QPCR analysis of candidate genes was carried out in overexpression cell line G10 and G22 at day 0, measured against wild type P19 cells on day 0. Expression is represented as log<sub>2</sub> fold change, and error bars represent standard deviation. Data was corrected for real time assay efficiencies and normalised against tmem131.

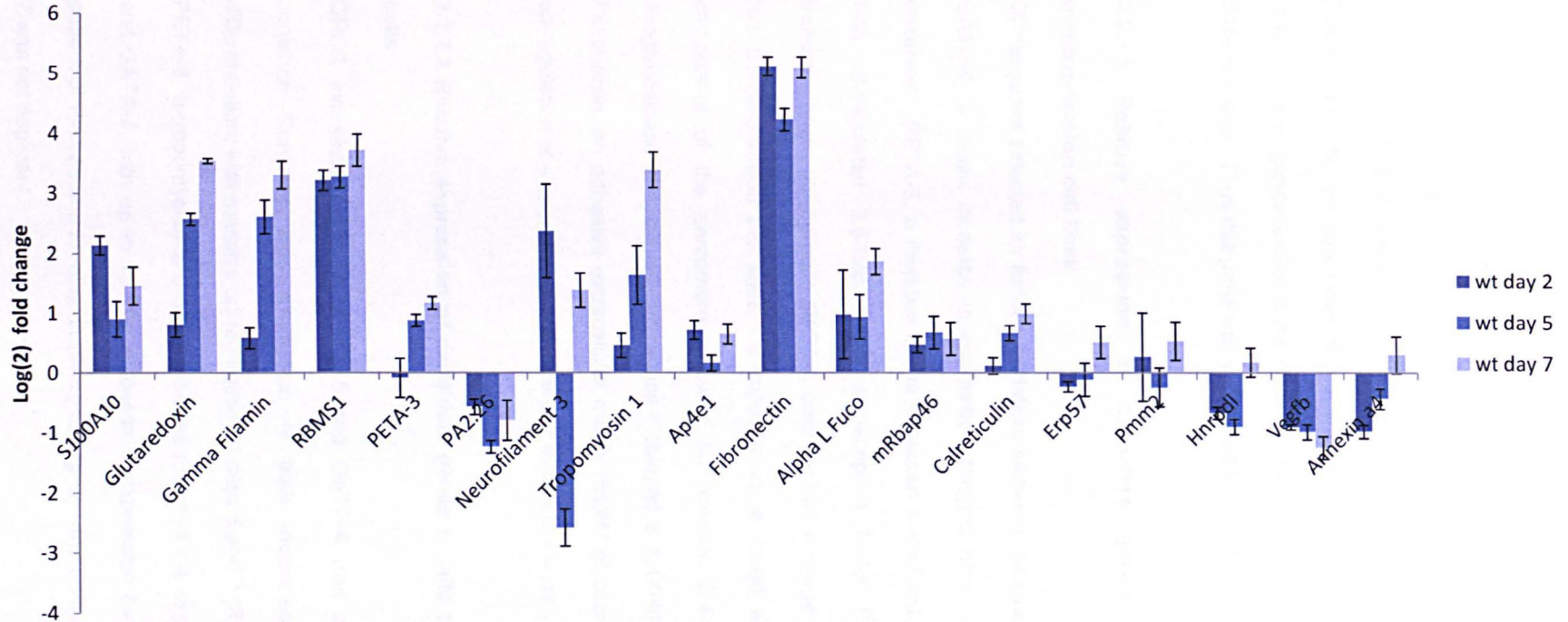


**Figure 3.2 Relative expression of candidate genes in wild type differentiating wild type cells**

QPCR analysis of candidate genes was carried out in P19 wild type cells at days 2, 5 and 7, measured against wild type P19 cells on day 0. Expression is represented as log<sub>2</sub> fold change, and error bars represent standard deviation. Data was corrected for real time assay efficiencies and normalised against tmem131.

### **3.2.2 Selection of genes for further study**

Genes displaying the highest fold increases in expression in the overexpression cell lines, and following the same pattern of expression as TBX5 and GATA-4, were selected for further analysis. These included TPM1, PETA-3, PA2.26, RBMS1, FUCA1, and FN.  $\gamma$ -Filamin was also of interest, but a future aim of this research was to study these genes further in the chick embryo, and a chick homologue of this gene does not exist. Thus this gene was eliminated from further study.

#### **3.2.2.1 Relative expression of candidate genes in TBX5 / GATA-4 overexpression cell lines**

Of the genes selected for further validation, following the overexpression of TBX5 and GATA-4, a mean increase in expression ranging from 1.4-fold to 3.5 fold was observed. PETA-3, a member of the tetraspan superfamily of membrane proteins, was up-regulated 3.5-fold. The transcription factor RBMS1, and the small transmembrane glycoprotein PA2.26, displayed an average increase of 3-fold in the two overexpression cell lines.  $\alpha$ -tropomyosin, a coiled actin-binding protein and component of the sarcomere, showed an average 2.4-fold increase, and the exoglycosidase enzyme  $\alpha$ -L-fucosidase displayed a 1.4-fold increase in expression. Fibronectin, an adhesive extracellular matrix (ECM) glycoprotein, displayed 1.6-fold up-regulation of expression in both overexpression cell lines.

#### **3.2.2.2 Relative expression of candidate genes in wild type differentiating P19 cells**

QPCR expression analysis of TBX5 and GATA-4 was performed previously by Jonathan Ronksley, and expression of both increased during cardiomyocyte differentiation, with massive up-regulation on days 5 and 7 [Ronksley, 2007]. RBMS1, PETA-3,  $\alpha$ -tropomyosin and  $\alpha$ -L-fucosidase mirrored the expression pattern of TBX5 and GATA-4, with up to 13-fold increases in expression by day 7. The expression pattern of PA2.26 and fibronectin diverged slightly, and an increase from day 2 to day 7 was not apparent.

### 3.2.3 Candidate genes

The candidate genes *TPM1*, *PETA-3*, *PA2.26*, *RBMS1*, *FUCA1*, and *FN* were chosen for further study of their function during cardiac development. An additional gene (*DES*), encoding the sarcomeric filament protein desmin, was added to the study. This was based on a similar microarray study carried out by Dr Lynn Amy (a former Post-Doctoral researcher in the lab), where *TBX5* and *GATA-4* were transiently overexpressed in the P19 cell line and desmin was identified as a potential target.

#### 3.2.3.1 TPM1

*TPM1* belongs to the tropomyosin gene family and encodes  $\alpha$ -tropomyosin, a dimeric  $\alpha$ -helical coiled actin-binding protein. It is a contractile component of the sarcomeric thin filament, crucial for myocardial function [Perry, 2001]. The tropomyosins are expressed predominantly in skeletal, smooth, and cardiac muscle, and at lower levels in non-muscle cytoskeletal and actin associated cells [Pittenger et al., 1994]. Familial dilated and hypertrophic cardiomyopathy have been linked to mutations in *TPM1* [Lakdawala et al., ; Thierfelder et al., 1994]. E40K and E54K mutations in *TPM1* cause dilated cardiomyopathy due to decreased sensitivity to  $Ca^{2+}$  [Mirza et al., 2007]. *TPM1* null mice do not survive past E11.5, whilst heterozygous mice are viable and fertile [Rethinasamy et al., 1998].

#### 3.2.3.2 Fibronectin

Fibronectin (discussed in section 1.6.5) is an ECM glycoprotein expressed in the myocardium, endocardium, and foregut [Waterman and Balian, 1980], and also in the cardiac jelly, with expression highest in regions adjacent to the myocardium where endocardial cushion cell migration occurs [Ffrench-Constant and Hynes, 1988]. There is evidence of a role for fibronectin in endocardial cell migration [Icardo et al., 1992]. Fibronectin null homozygous embryos display abnormalities such as a shortened anterior-posterior axes, and defects in the neural tube, heart, embryonic vessels and mesoderm derived tissues become apparent at E7.5 - E8.0, worsening as development proceeds and eventually leading to embryonic lethality [George et al.,

1993]. Heart development defects occur, with heart primordia remaining unfused. Less severely affected embryos have fused primordia with abnormal morphology. Myocardial tissue thickening, a deficiency in cardiac jelly, and abnormal endocardium morphology has also been observed.

### **3.2.3.3 Desmin**

Desmin is a sarcomeric type III intermediate filament protein which associates with Z-discs and connects myofibrils to one another and to the plasma membrane. It has an important contractile role in cardiac, skeletal and smooth muscle. Mouse knockout of desmin results in cardiomyopathy, and heart tissue from these animals displays abnormally shaped and distributed mitochondria [Thornell et al., 1997]. Disturbances in cardiac conduction in desmin null mice have also been observed [Schrickel et al.]. A range of mutations in the desmin gene have been associated with familial cardiac and skeletal myopathy [Bergman et al., 2007; Fidzianska et al., 2005; Goldfarb et al., 1998; Goudeau et al., 2001; Olive et al., 2007; Sung et al., ; Taylor et al., 2007; Vernengo et al., ; Vrabie et al., 2005]. Features of this disease include atrial dilation, cardiac arrhythmia, conduction block, and sudden death due to conduction defects [Vernengo et al.].

### **3.2.3.4 PETA-3**

Platelet endothelial tetraspan antigen-3 or PETA-3 is a member of the transmembrane 4 or tetraspan superfamily of membrane proteins, which strongly associate with laminin binding integrins such as  $\alpha 3\beta 1$ , and other tetraspans (e.g. CD9 or CD63). PETA-3 is thought to have a role in cell-cell adhesion, cell migration, platelet adhesion, and angiogenesis [Wright et al., 2004]. PETA-3 expression is observed in the endothelium and epithelium, Schwann and dendritic cells, megakaryocytes, platelets, and in skeletal, smooth and cardiac muscle [Sincock et al., 1997]. In cardiac muscle, PETA-3 expression is seen (at high levels) in the sarcolemma of muscle cells and capillary endothelium [Sincock et al., 1997]. The phenotype of PETA-3 null mice has been characterised in three separate studies. The first study described PETA-3

null mice as viable, healthy and fertile, but displaying defects in haemostasis with extended bleeding times and greater blood loss [Wright et al., 2004]. A separate study examining the role of PETA-3 in angiogenesis additionally revealed PETA-3 null mice do not display defects in vasculature during normal development [Takeda et al., 2007]. However, alternative *in vivo* and *in vitro* assays did show an effect as a result of mouse gene knockout, with changes in adhesion, spreading and invasion, all of which are important processes in angiogenesis [Takeda et al., 2007]. Nonsense mutations in the human PETA-3 gene have been associated with kidney failure, and a third study of PETA-3 knockout mice revealed that with age, these mice developed a similar pathological state to that seen in human patients; knockout mice displayed proteinuria due to focal glomerulosclerosis, glomerular basement membrane disorganisation, and tubular cystic dilation [Sachs et al., 2006].

#### **3.2.3.5 PA2.26**

PA2.26 is a small 172 amino acid transmembrane glycoprotein originally identified as a cell surface antigen, that is expressed in skeletal muscle, heart, lung and placental tissue [Martin-Villar et al., 2005]. Its function has been studied by transfection of PA2.26 into immortalised keratinocytes that do not express the protein [Scholl et al., 1999]. These cells displayed differences in cell-cell adhesion, and actin cytoskeletal reorganisation, altering the cell morphology from epithelial to fibroblastoid, indicating PA2.26 plays a role in cell migration. A specific role for PA2.26 in the heart has not yet been demonstrated. As a protein involved in the extracellular matrix, it may be involved in cardiac remodelling.

#### **3.2.3.6 FUCA1**

Alpha-L-fucosidases are exoglycosidases that are involved in fucosylated glycoconjugate processing (they catalyse terminal L-fucose residue removal), and also possess transglycosylation properties [Intra et al., 2006]. These enzymes are involved in inflammation, cancer development, cystic fibrosis, and lysosomal storage disease [Intra et al., 2006].

### 3.2.3.7 RBMS1

RBMS1 is a multifunctional gene involved in transcriptional regulation, activation of DNA replication, cell cycle regulation, and apoptosis. The human RBMS1 gene gives rise to multiple splice variants encoding proteins of approximately 400 amino acids [Takai et al., 1994]. RBMS1 contains two ribonucleoprotein consensus sequences, each containing an RNA-binding protein consensus motif (RNP1-A and RNP1-B), which are essential to its function [Dreyfuss et al., 1988]. RBMS1, via its RNP domains, interacts with the N-terminal region of a catalytic subunit of DNA polymerase  $\alpha$ , stimulating its polymerase activity [Niki et al., 2000a]. RBMS1, via these domains, also binds to the c-myc protein which has important functions in cell cycle regulation, cell transformation, and apoptosis [Niki et al., 2000b]. RBMS1 transcriptionally regulates a number of genes including  $\alpha$ -smooth muscle actin [Kimura et al., 1998] (discussed in Chapter 5), MHC Class I and II genes [Balducci-Silano et al., 1998], and the thyrotropin receptor [Shimura et al., 1995]. RBMS1 expression has been studied by northern blot analysis in the adult mouse, where expression was detected in all tissues examined except testis [Fujimoto et al., 2000]. A more detailed spatial analysis of expression has not been performed. Expression of RBMS1 is induced by mitogens such as serum [Fujimoto et al., 2001]. *Rbms1*<sup>-/-</sup> mice once born appear healthy but display an atypical Mendelian ratio i.e. disruption of this gene results in embryonic lethality in some homozygous mice [Fujimoto et al., 2001]. RBMS1 knockout embryos display growth and developmental abnormalities at E2.5 when cultured *in vitro* for 5 days, and female adult mice show a reduced progesterone concentration. These findings together account for the embryonic lethality observed. It is not clear whether cardiac defects occur in these mice. RBMS1 suppresses transcription of  $\alpha$ -smooth muscle actin, which is important in myofibrillogenesis, via *cis*-elements in its promoter region [Kimura et al., 1998]. This could indicate a potential regulatory role for RBMS1 in the heart.

### 3.2.4 Bioinformatic identification of conserved TBX5 and GATA-4 binding sites within putative targets

In order to identify evolutionarily conserved transcription factor binding sites in genes of interest, multi-species sequence alignments were performed using online Mulan software (<http://mulan.dcode.org/>). This software allows detection of evolutionarily conserved regions (ECRs) and specific consensus sequences within them [Ovcharenko et al., 2005]. Full genomic sequences of candidate genes plus 10 kb upstream from the first exon and 10 kb downstream from the last exon, were manually exported from the *Ensembl* database ([www.ensembl.org](http://www.ensembl.org)) and input into Mulan. TBX5 binds to the consensus sequence [A/G/T]GGTG[T/C][C/T/G][A/G] [Ghosh et al., 2001] and GATA-4 to the consensus sequence [A/T]GATA[A/G] [Plumb et al., 1989]. The search input sequences DGGTGYBR and WGATAR were used in accordance with IUPAC-IUB codes for nucleic acid bases (Appendix C).

Jonathan Ronksley previously performed similar analyses between human and mouse and found multiple binding sites for both TBX5 and GATA-4 in all of the genes examined, with *RBMS1* displaying the highest number of conserved consensus binding sites for TBX5 and GATA-4 [Ronksley, 2007]. In the next chapter of this thesis, candidate genes will be studied in the developing chick embryo, including assessment of their responsiveness to TBX5 and GATA4. In light of this, alignments have been performed between chicken and human sequences in addition to mouse and human sequences, for identification of regions conserved between all three species.

Figure 3.3i-vii displays Mulan analysis results for the seven genes of interest. No multi-species conserved consensus binding sites for either TBX5 or GATA-4 were identified upon analysis of the *PA2.26*, *PETA-3* and *FUCA1* genes (Figures 3.3i, 3.3ii and 3.3iii). Analysis of the *TPM1* gene revealed two conserved binding sites for TBX5, and one for GATA4, all within the coding region (Figure 3.3iv). Figure 3.3v shows Mulan analysis of the *DES* gene. Two conserved TBX5 consensus binding

sites were identified the coding region, and no GATA-4 sites were found. Figure 3.4vi shows analysis of the *FN* gene. Three conserved sites for both GATA-4 and TBX5 were identified, all within the coding region. *RBMS1* analysis resulted in identification of three putative binding sites for TBX5 (all within the coding region), and four GATA-4 sites were identified, two in the coding region, and two in the 3' UTR (Figure 3.3vii). Of the genes studied, *RBMS1* displayed the highest number of multi-species conserved putative binding sites for both TBX5 and GATA-4.

Figure 3.3i Mulan analysis of the PA2.26 gene in human, mouse and chicken

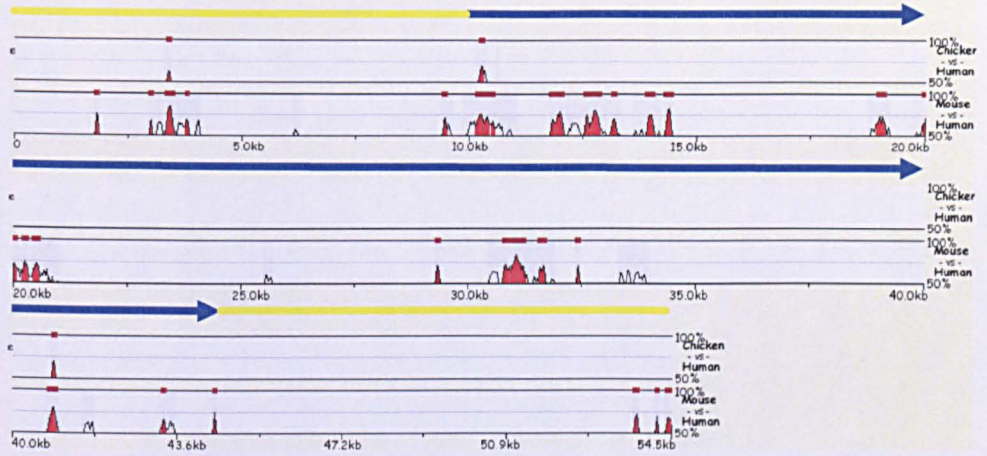


Figure 3.3ii Mulan analysis of the PETA-3 gene in human, mouse and chicken

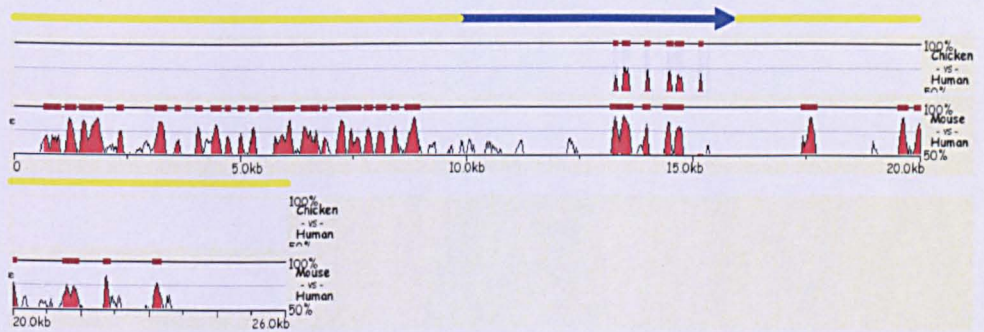


Figure 3.3iii Mulan analysis of the FUCA-1 gene in human, mouse and chicken

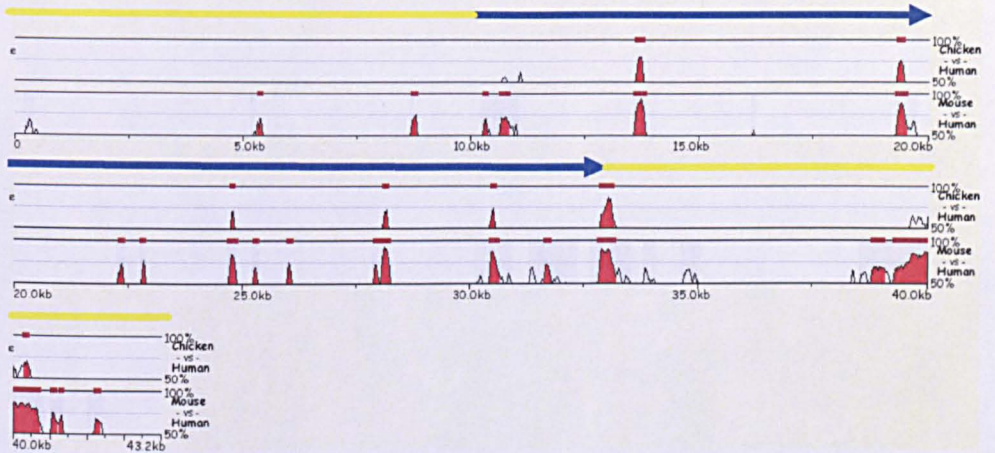


Figure 3.3iv Mulan analysis of the TPM1 gene in human, mouse and chicken

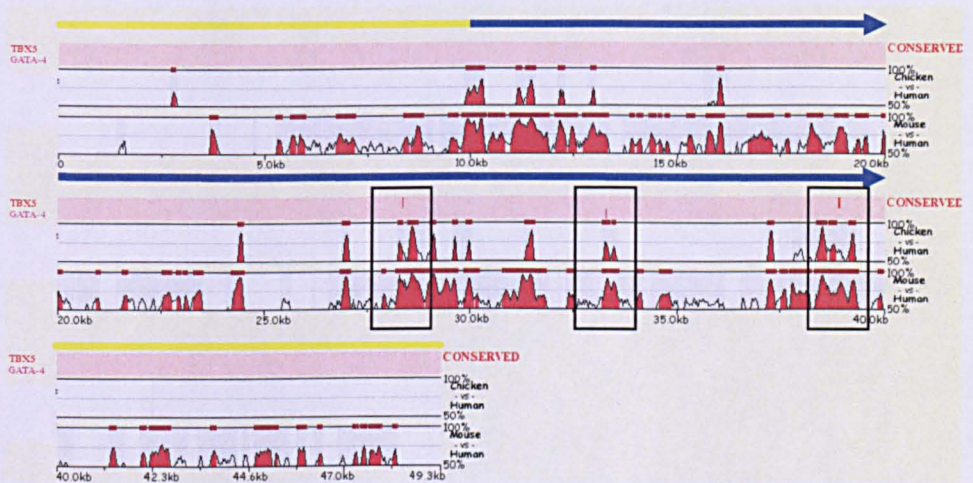


Figure 3.3v Mulan analysis of the desmin gene in human, mouse and chicken

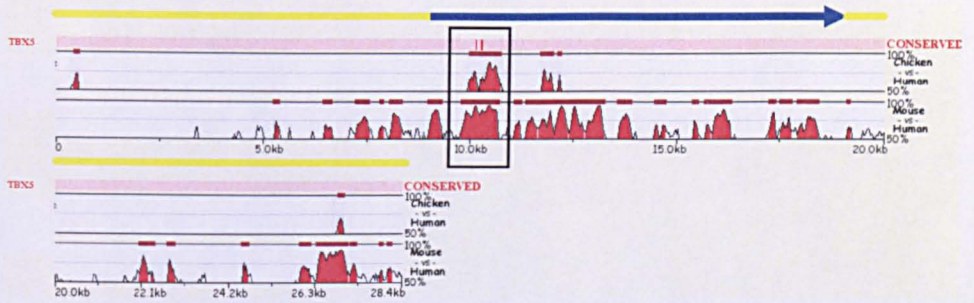


Figure 3.3vi Mulan analysis of the fibronectin gene in human, mouse and chicken

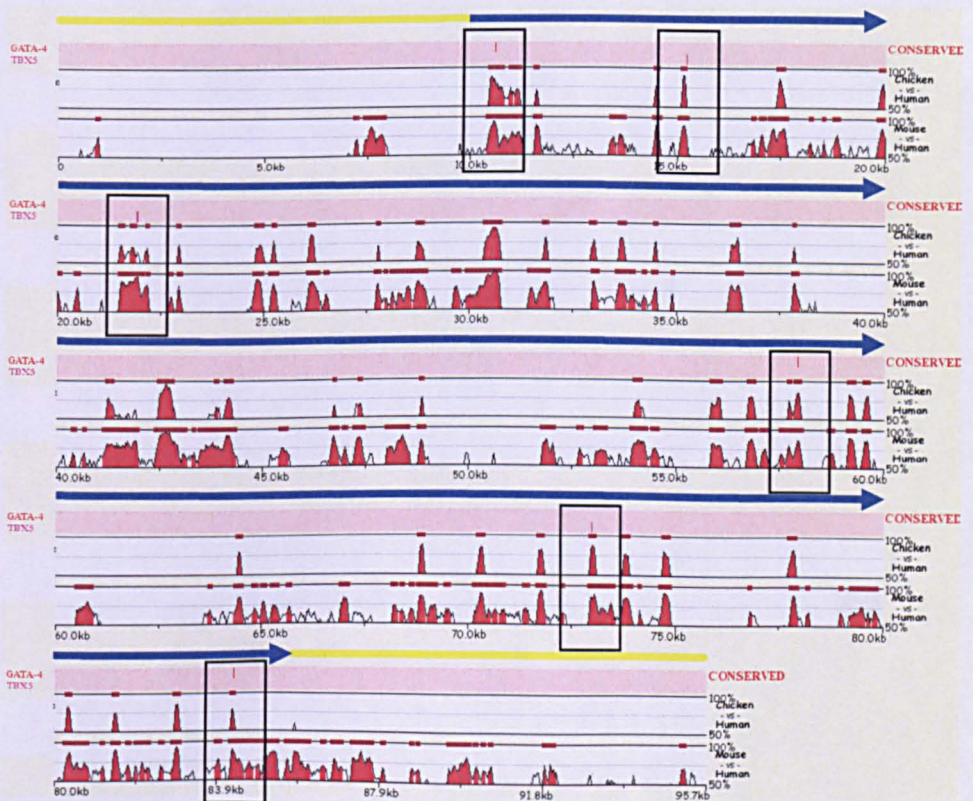
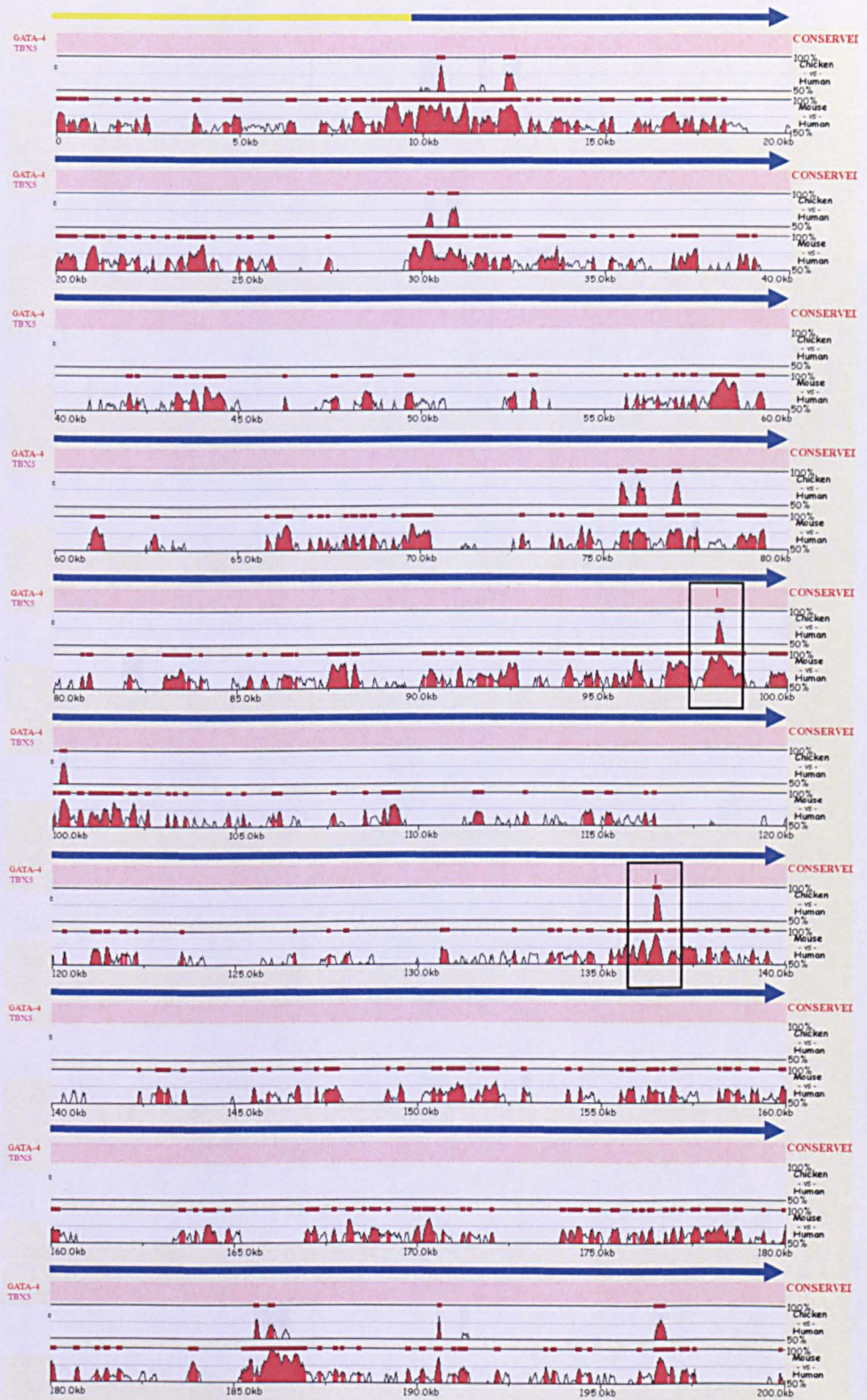
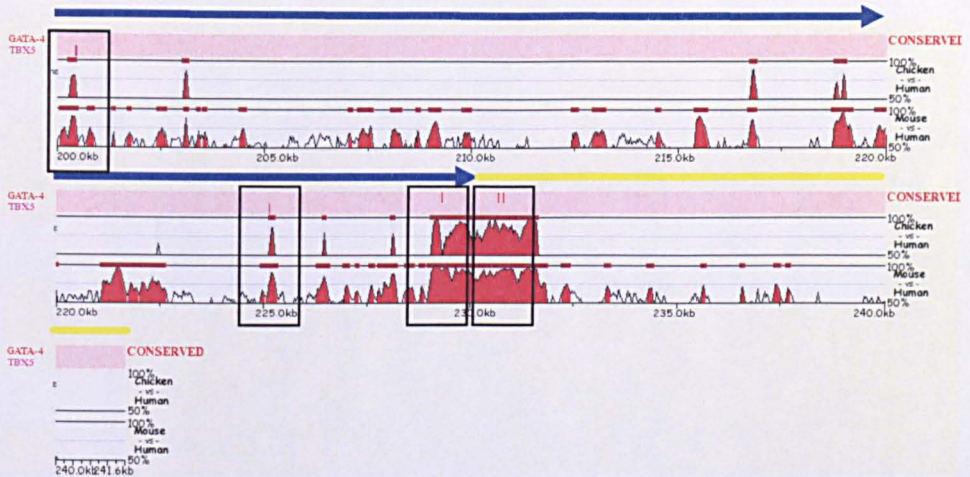


Figure 3.3vii Mulan analysis of the RBMS1 gene in human, mouse and chicken





**Figure 3.3i-vii** Mulan analysis of candidate genes in human, mouse and chicken

Alignment of full length genes (marked by blue arrows) plus 10 kb upstream and downstream (marked by yellow lines) in human, mouse and chicken was performed for identification of consensus TBX5 and GATA-4 binding sites using the transcription factor binding site identification tool in Mulan software (<http://mulan.dcode.org/>). Evolutionarily conserved regions with  $\geq 50\%$  homology between species are plotted, and regions meeting the input criteria (100 nucleotide run, minimum 70% identity) are indicated by the red rectangles on top of each plot. The lower scales represent mouse / human sequence alignment, and the upper scales represent chicken / human sequence alignment. Consensus sites conserved between all three species are represented by vertical red or purple dashes for TBX5 or GATA-4 respectively, and have been boxed. Genes analysed are PA2.26 (i), PETA-3 (ii), FUCA1 (iii), TPM1 (iv), DES (v), FN (vi), and RBMS1 (vii). No conserved consensus binding sites were identified for either TBX5 or GATA-4 in PA2.26, PETA-3 or FUCA1. Two conserved binding sites for TBX5 and one for GATA-4 were identified within the coding region of TPM1. Two conserved TBX5 consensus binding sites were identified the coding region, and no GATA-4 sites were found in the DES gene. In the FN gene, three conserved sites for both GATA4 and TBX5 were identified, all within the coding region. RBMS1 analysis resulted in identification of three putative binding sites for TBX5 (all within the coding region), and four GATA-4 sites were identified, two in the coding region, and two in the 3' UTR.

### **3.2.5 Cloning of RBMS1 fragments for functional analysis of evolutionarily conserved regions (ECRs) in RBMS1**

Whilst bioinformatic analysis is a useful tool for identifying conserved consensus transcription factor binding sites, the functional significance of these regions needs to be confirmed experimentally. Luciferase reporter studies are useful for measuring promoter response in cells. RBMS1 was selected for further study based on its high number of conserved putative binding sites and the fact that this is a novel gene in terms of a cardiac function.

#### **3.2.5.1 Identification of regions of the RBMS1 gene for further study**

In order to assess transcriptional activation of RBMS1 by TBX5 and GATA-4, luciferase reporter studies were carried out on regions of interest in the mouse promoter. For this purpose Mulan alignment between human and mouse sequences only was performed and is displayed in Figure 3.4. Conserved regions containing putative binding sites for both TBX5 and GATA-4 were identified across the gene. Three regions of particular interest are boxed. The first region of interest is the main promoter region of the 5' UTR, containing single conserved TBX5 and GATA-4 sites 4 kb – 5kb upstream from the ATG translational start site. The transcriptional start site of this gene has not been determined (this was attempted in the next section, see 3.3.5.2). Another conserved region of approximately 1 kb was identified within intron 1, found to contain single putative sites for both TBX5 and GATA-4 within 100 bp of one another. Both sites are conserved between the human and mouse, and the TBX5 site is also conserved with the chick. The high degree of conservation of this non-coding region indicates this may serve as an enhancer or repressor element. A third 3 kb region was identified within the 3' UTR, containing one putative binding site for TBX5 and multiple conserved GATA-4 sites, three of which are also present in the chicken sequence.

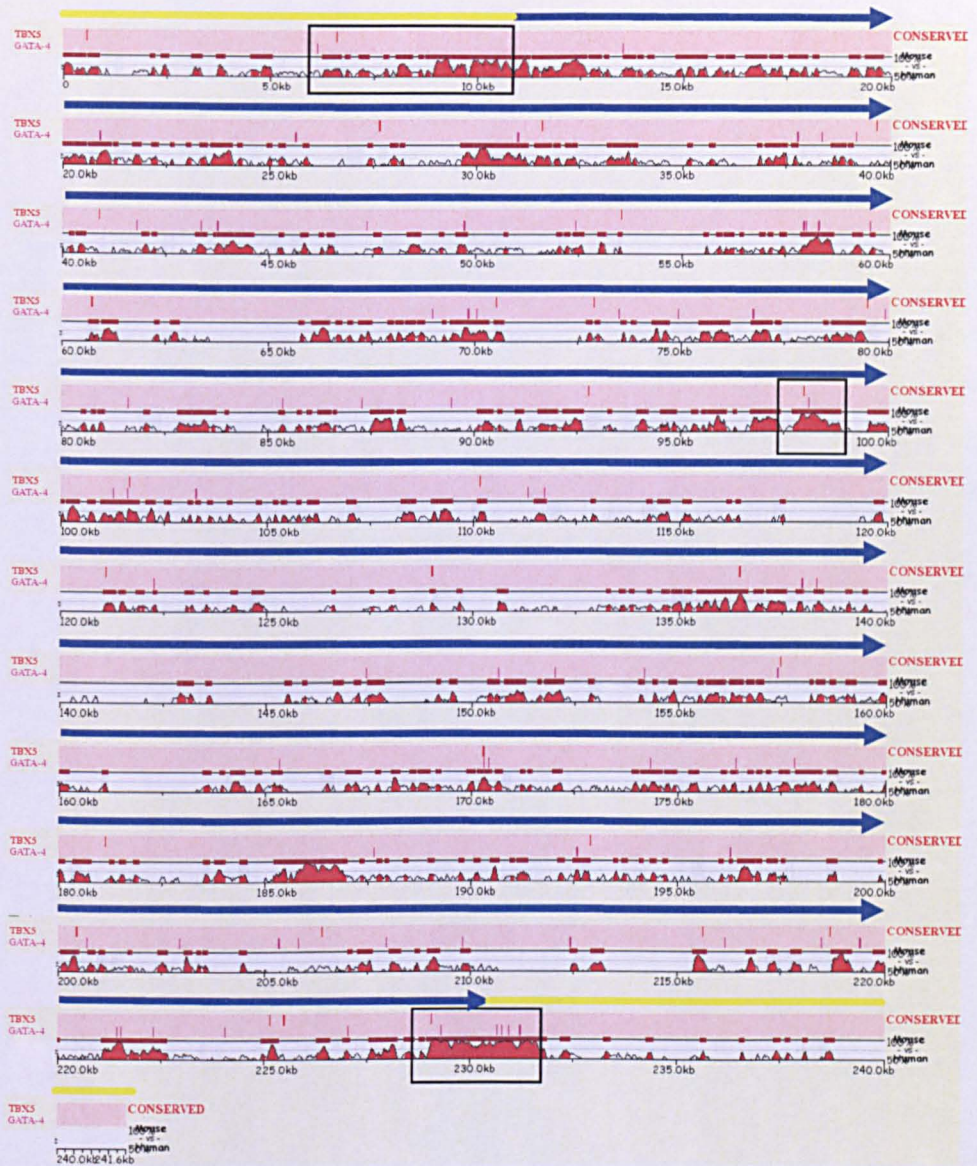


**Figure 3.4** Mulan analysis of the RBMS1 gene in human and mouse

Alignment of the full RBMS1 gene plus 10 kb upstream and downstream in human and mouse was performed for identification of consensus TBX5 and GATA-4 binding sites using the online Mulan transcription factor binding site identification tool (<http://mulan.dcode.org/>). Evolutionarily conserved regions with  $\geq 50\%$  homology between species are plotted. Conserved consensus sites are represented by vertical red or purple dashes for TBX5 or GATA-4 respectively. Multiple conserved GATA-4 and TBX5 sites were identified throughout the gene. Regions of interest in the 5' UTR, intron 1, and in the 3' UTR are boxed.

### 3.2.5.2 Primer design and PCR amplification

In order to assess the regulatory activity of regions of interest, they needed to be PCR amplified and cloned into suitable reporter vectors. PCR reactions were carried out using *PfuUltra* II Fusion HS DNA polymerase, a proof-reading enzyme that requires dramatically shortened extension times and is therefore ideal for accurate amplification of long targets. Initially, two primer pairs were designed to each region (sequences in Table 2.2), and PCR amplification attempted with all four primer combinations. The intron 1 region was successfully amplified with all primer combinations, and the fragment selected for cloning is displayed in Figure 3.5. PCR of the 5' and 3' UTR regions resulted either in no amplification, or amplification of multiple bands.

The large size of the 5' UTR region (4.6 kb from the GATA-4 site to the initiating ATG) may have contributed to the difficulties in its amplification, and could also pose problems in subsequent cloning. For study of this region as a promoter the transcriptional start site (but not the translational start site) needs to be included. Two strategies were employed in order to minimise the size of this region; mouse EST searches were carried out to identify the transcribed region, and determination of the transcriptional start site was attempted using a number of online prediction tools. One matching EST was found extending 690 bp 5' of the ATG translational start site (GenBank Accession ID: BP765823). Transcription start site identification tools all gave differing results, so this data was not taken into account. An additional two primer pairs were designed to the shortened region (4 kb) and multiple combinations tested for PCR amplification under various conditions. This again resulted either in no amplification, or amplification of multiple bands.

The 3' UTR region contains long runs of adenine nucleotides which can cause DNA polymerase slippage, resulting in difficulties in PCR amplification. An additional two primer pairs were designed and multiple combinations tested for PCR amplification, again without success.

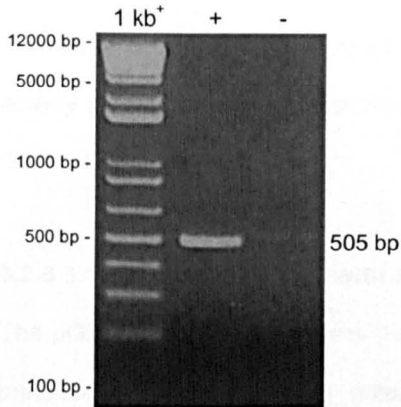


**Figure 3.5 PCR amplification of the conserved region within intron 1 of RBMS1**

PCR reactions were electrophoresed on 2% agarose gels using 1 kb<sup>+</sup> DNA ladder (Invitrogen) as a size marker. Negative PCR controls (where water was added in place of template) were included.

### **3.2.5.3 Destination vectors**

The intron 1 fragment was cloned into two destination vectors for assessment of its activity as a regulatory element and the individual and combined effects of TBX5 and GATA-4.

#### **3.2.5.3.1 pGL3-Basic vector with ANF minimal promoter**

The pGL3-Basic vector contains the luciferase gene but lacks upstream promoter or enhancer sequences, which means that luciferase expression depends on the insertion of a functional promoter. The human ANF minimal promoter (70 bp) was previously cloned into the KpnI site of this vector by Dr Tushar Ghosh, who kindly provided this for use as a destination vector in this study. The ANF promoter displays basal promoter activity which means this is a sensitive system and allows detection of discrete changes in activation. The intron 1 fragment was cloned into the SacI site of the multiple cloning region of this vector, and is represented in Figure 3.6.

#### **3.2.5.3.2 pGL3-Promoter vector**

The pGL3-Promoter vector contains an SV40 promoter upstream of the luciferase gene, and regions of DNA containing putative enhancer elements can be inserted upstream or downstream of this unit. The SV40 promoter displays strong activity and has advantages when quantifying large changes in activation. The intronic fragment was cloned into the SacI site of the multiple cloning region of this vector, and is displayed in Figure 3.7.

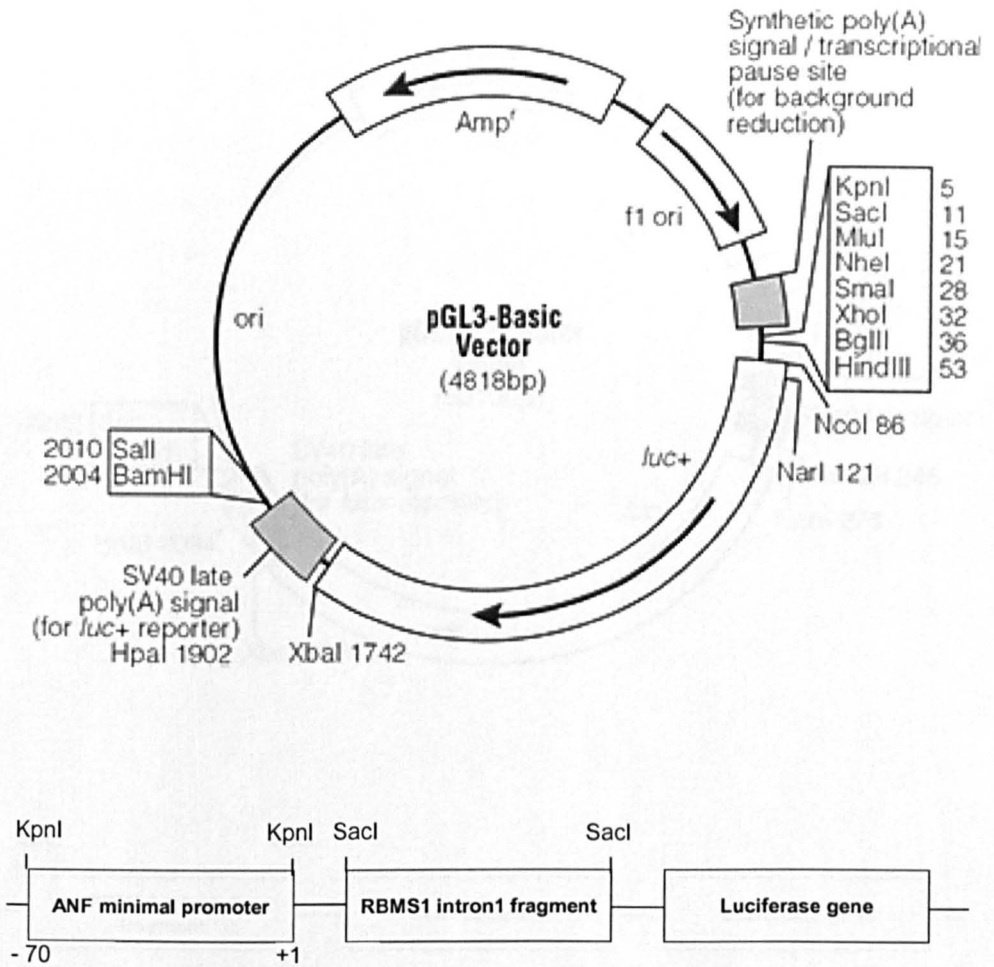


**Figure 3.6 pGL3-Basic Vector circle map and schematic displaying position of inserts**

The pGL3-Basic vector contains the luciferase gene but lacks upstream promoter or enhancer sequences, which means that luciferase expression depends on the insertion of a functional promoter. The human ANF minimal promoter (70 bp) was previously cloned into the KpnI site of this vector by Dr Tushar Ghosh, and this was kindly provided for use as a destination vector in this study. The intron 1 fragment was cloned into the SacI site of the multiple cloning region of this vector.

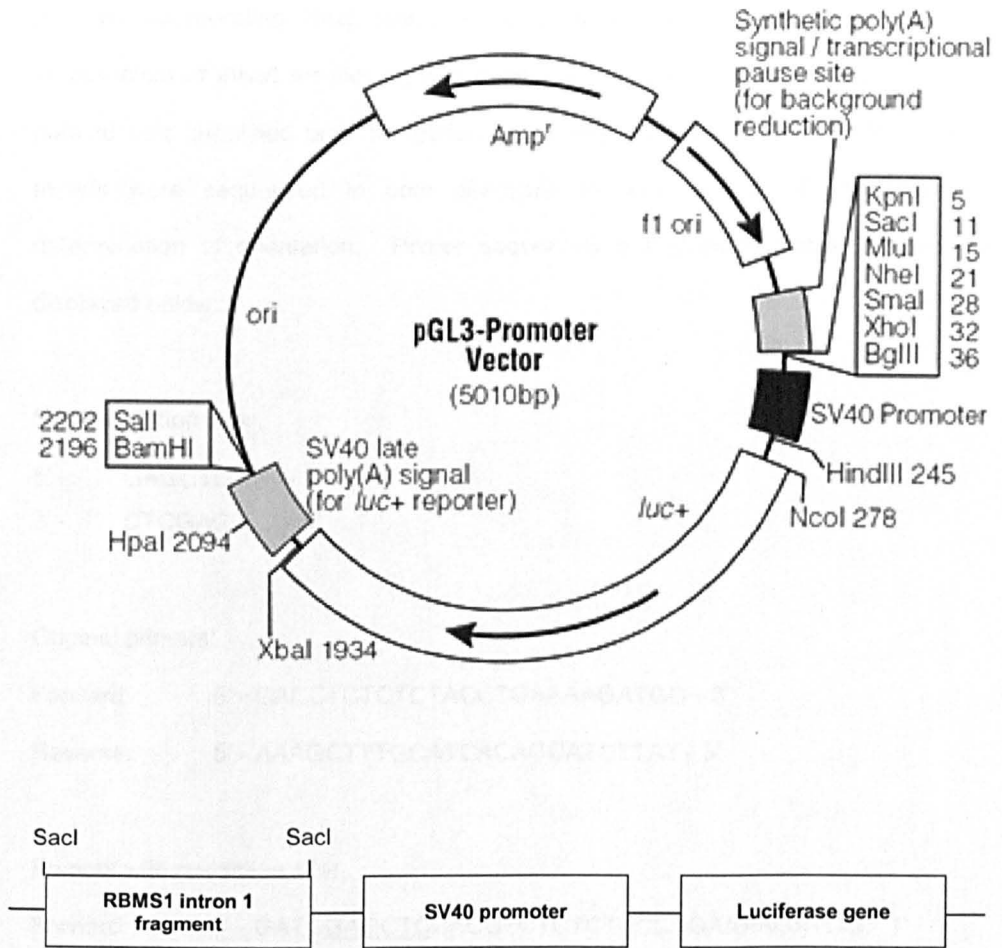


**Figure 3.7 pGL3-Promoter Vector circle map and schematic displaying position of insert**

The pGL3-Promoter vector contains an SV40 promoter upstream of the luciferase gene, and regions of DNA containing putative enhancer elements can be inserted upstream or downstream of this unit. The intronic fragment was cloned into the SacI site of the multiple cloning region of this vector.

### 3.2.5.4 Cloning of the RBMS1 intron 1 fragment

Primers incorporating *SacI* restriction sites were designed and used for PCR amplification of insert for cloning into destination vectors. PCR products were gel-purified and quantified prior to ligation and initial cloning into the pGEM-T vector. Inserts were sequenced in both directions for confirmation of sequence and determination of orientation. Primer sequences are given in Table 2.3 and are displayed below:

*SacI* restriction site:

```

5' -   GAGCTC   - 3'
      ▼
3' -   CTCGAG   - 5'
      ▲

```

Original primers:

Forward: 5' - CACCTCTCTCTACCTGAAAAGATGG - 3'

Reverse: 5' - AAAGCTTTGCATCACAGCATCTTAT - 3'

Primers with restriction site:

Forward: 5' - GATCGAGCTCCACCTCTCTCTACCTGAAAAGATGG - 3'

Reverse: 5' - GATCGAGCTCAAAGCTTTGCATCACAGCATCTTAT - 3'

Luciferase reporter assays were performed by Dr Tushar Ghosh, and results are displayed in Appendix D. GATA-4 had a repressive effect on promoter activity via this region, whilst TBX5 had no effect.

## CHAPTER 4

### STUDY OF CANDIDATE GENES IN THE EMBRYONIC CHICK

#### 4.1 AIMS

This chapter aims to investigate the expression and responsiveness of candidate genes to TBX5 and GATA-4 in the developing chick as follows:

- a) Confirmation of expression of candidate genes in the developing chick heart including investigation of temporal expression
- b) Development of an *in ovo* model of TBX5 and GATA-4 knockdown with appropriate controls
- c) Model validation by phenotypic analysis of embryos subjected to single and double knockdown of TBX5 and GATA-4 during key stages of cardiac development
- d) Development of a robust QPCR method for cardiac expression analysis, and study of candidate gene expression in TBX5 / GATA-4 double knockdown embryonic hearts

## 4.2 RESULTS

### 4.2.1 Investigation of candidate gene temporal expression profiles by RT-PCR

Expression of the candidate genes (*PA2.26*, *PETA-3*, *FUCA1*, *FN*, *TPM1*, *DES*, and *RBMS1*) in the developing chick heart was examined at seven stages of development (HH12, HH14, HH16, HH19, HH22, HH24 and HH26). These developmental stages encompass the early stages of heart looping, chamber formation, atrial septation, and the start of ventricular septation. Wild type embryonic age was assessed visually according to Hamburger and Hamilton stages [Hamburger and Hamilton, 1992], and hearts removed under sterile conditions before immediate storage in RNA $\text{later}$ . Hearts were pooled prior to RNA extraction and cDNA synthesis. PCR amplification was performed using HotStar Taq. Primers were designed using the online Roche Universal ProbeLibrary assay design centre (<https://www.roche-applied-science.com>) as these primers would subsequently be used for QPCR expression analysis (section 4.3.4). Consequently, all products are 60 – 90 bp. Assays spanning exons were selected wherever possible. In the case of  $\alpha$ -tropomyosin, alignments with other members of this gene family were performed during assay design to ensure specificity, and the RT-PCR product generated was cloned into the pGEM-T Easy vector for sequencing to confirm amplification of the correct product. Primer sequences and positional information is given in Table 2.4. Expression of all candidate genes was detected in the developing heart at all stages examined (Figure 4.1). Negative RT controls were included and did not display amplification (Appendix E). In addition, amplicons were electrophoresed on the same gel in order to confirm relative sizes (Appendix F).

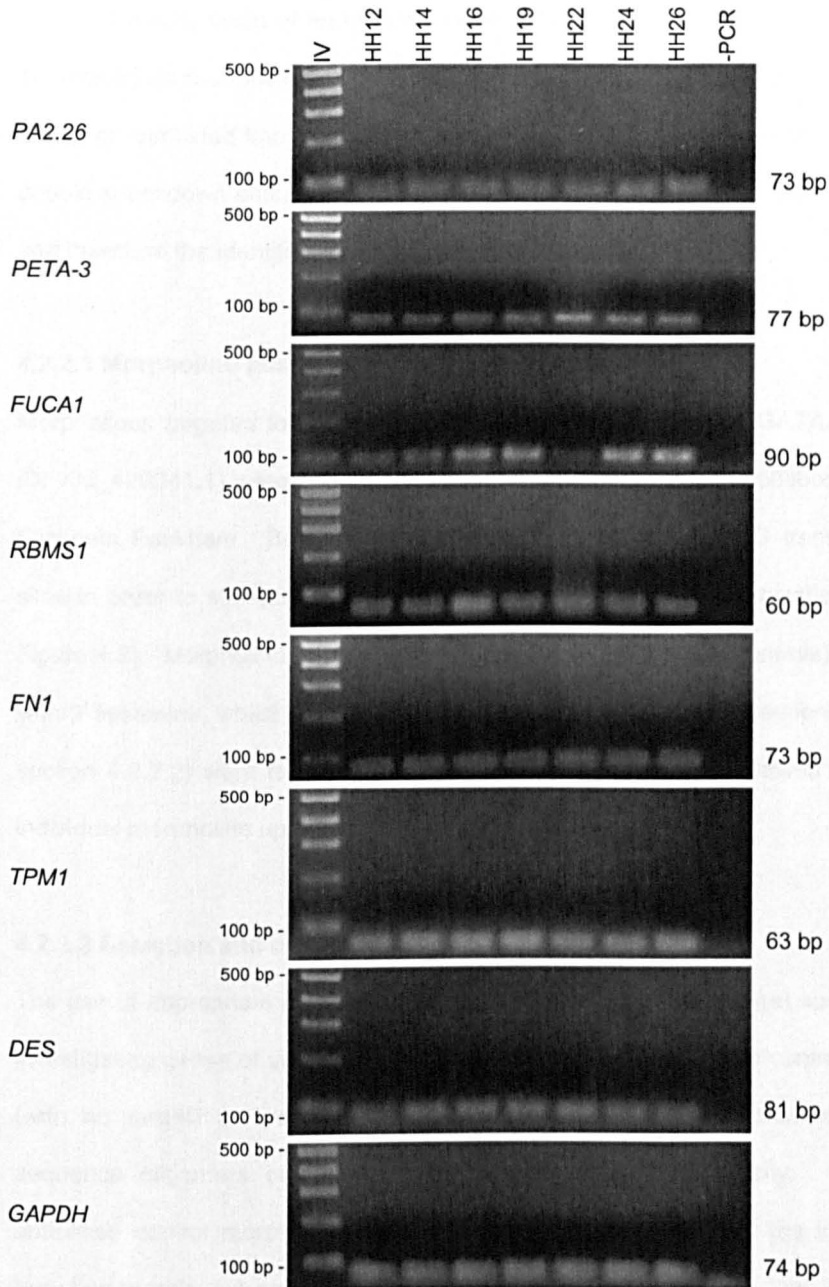


**Figure 4.1 RT-PCR expression profiles of candidate genes in the chick heart**

RT-PCR products were electrophoresed on 2% agarose gels using Hyperladder IV as a size marker (500 bp and 100 bp bands are indicated along with product sizes). Expression was studied at HH12, HH14, HH16, HH19, HH22, HH24 and HH26. GAPDH was included as a housekeeper gene. Negative PCR controls (where water was added in place of template) are shown (-PCR). Negative RT controls (where reverse transcriptase enzyme was not added) were also included and did not display amplification (Appendix E).

## **4.2.2 Development of an *in ovo* model of TBX5 and GATA-4 knockdown**

To investigate the functional significance of the TBX5 / GATA-4 interaction, an *in ovo* model of combined knockdown was generated. This enabled phenotypic analysis of double knockdown embryos, and expression analysis of candidate downstream genes and therefore the identification of new genes for analysis.

### **4.2.2.1 Morpholino position and design**

Morpholinos targeted to TBX5 (Accession ID: AF033671.1) and GATA-4 (Accession ID: XM\_420041.1) were previously designed by Gene-Tools in collaboration with Dr Elizabeth Packham. Both morpholinos are designed to the AUG translational start sites in order to sterically block ribosomal binding and protein translation (Table 2.7, Figure 4.2). Morpholinos targeted to TBX5 (and corresponding controls) were tagged with 3' lissamine, whilst morpholinos targeted to GATA-4 (and corresponding controls, section 4.2.2.2) were tagged with 3' carboxyfluorescein. This allowed evaluation of individual morpholino uptake during combinatorial use.

### **4.2.2.2 Selection and design of specificity controls**

The use of appropriate controls is essential for confirmation of target specificity when investigating genes of unknown function. A pre-designed standard control morpholino (with no target) is available from Gene-Tools (USA), and a number of custom sequence oligomers can also be used as controls of specificity. The inverse-antisense control morpholino is an oligomer whose sequence is the inverse of the targeting morpholino sequence. The advantage of this control is that its length and base composition are identical to that of the antisense morpholino. This is not however widely used as a control of specificity. The sense control morpholino is an oligomer with the reverse complement sequence of the targeting morpholino (identical to the target region). In some cases these have been reported to have an up-regulatory effect on target expression, and are not strongly recommended. The 5-base mismatch control incorporates five mismatched bases into the sequence of the targeting morpholino, most effective when three of out five of these are cytosine-

guanine substitutions or vice versa. At the time this research was carried out (2008), this was considered the most rigorous control of specificity, and was used in addition to the standard control morpholino. Sequences are given in Table 2.7, and Figures 4.2 and 4.3 additionally display morpholino target regions. Actual bases to be mis-paired were selected by Gene-Tools. 5-base mismatch control morpholinos were subsequently replaced with 7-base mismatch morpholinos (section 4.2.2.5), and sequences of these are also shown in Table 2.7 and Figures 4.2 and 4.3.

**Chicken TBX5 AUG morpholino**

Actual AUG '7-mismatch' MO\*  
Planned AUG 7-mismatch MO\*  
AUG 5-mismatch MO  
AUG MO

3'- CCAAACGCTGCCCTCGTTCGTCCG - 5'  
3'- CGAAAGCTGCCCTCGTTCGTCCG - 5'  
3'- CAAAACATGGCCTCCTTACTAGG - 5'  
3'- CGAAACGTGGCCTCCTTCCTCCG - 5'

mRNA

5'- CUCUCCGCUUUGCACCCGGGAGGAAGGAGCCGGAAUGCUCCGCGCCCGCGGACCAGUGGGGGAUUCGGCGAAGGAAGCUCGUAAACAUGGCGGACACCGAGG - 3'

Protein

M L R A R G P V G D S A K E A R N M A D T E

132

**Figure 4.2 TBX5 targeting morpholino sequence and target region**

Morpholino sequences are shown in the 3' – 5' direction, and target binding regions are boxed, with AUG start sites shaded in grey. Bases altered in mismatch control morpholinos are underlined. \*An error was made during the design of this morpholino and an extra base (guanine) inserted at position 19 in the 5' – 3' direction.

**Chicken GATA-4 AUG morpholino**

AUG 7-mismatch MO

AUG 5-mismatch MO

AUG MO

mRNA

Protein

3' - GCTGTAGATGCTGTCCAATCCCTAC - 5'3' - GCTGTAGATGCTTCCAATCGCTAC - 5'

3' - GCTCTACATGGTCTCGAATCGGTAC - 5'

5' - AUUGCGCUCGGAGACCCAUCUGGGGUUUGGGGGCCCCGUGCGAGAUGUACCAGAGCUUAGCCAUGGCGGCGAACCCCGGCCCCCGUCCUACGAAGGG - 3'

M Y Q S L A M A A N P G P P S Y E G

**Figure 4.3 GATA-4 targeting morpholino sequence and target region**

Morpholino sequences are shown in the 3' – 5' direction, and target binding regions are boxed, with the AUG start site shaded in grey. Bases altered in mismatch control morpholinos are underlined.

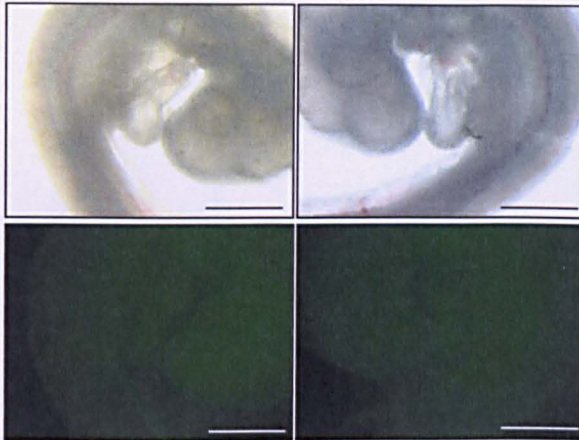
#### **4.2.2.3 Selection of a developmental window for morpholino application**

One of the practical considerations in selecting a timeframe for morpholino application is the ease with which embryonic age can be assessed. Based on initial experiments, it was possible to accurately assess the developmental stage of embryos *in ovo* from HH10 onwards, and this is also the stage at which the heart starts to beat. Prior to this a dye such as India ink (commonly used to view vasculature in chicken embryos [Latker et al., 1986]), would be required for visualisation, rendering the embryo unusable for a knockdown study. Also, at any selected time-point, there is a large degree of variation in embryonic age. This means it would be extremely laborious to attempt knockdowns at one focused stage of development, particularly on the scale intended in this study. In light of these considerations, morpholinos were applied at HH10 – HH16, and embryos harvested for analysis at HH19. These are key developmental stages which encompass looping of the heart (dextral looping occurs at HH10 – HH12, post dextral-looping at HH12 – HH17/18), and initiation of atrial septation (HH14). Since TBX5 and GATA-4 mutations have been associated with atrial septal defects, knockdown of these transcription factors in the early stages of atrial septation is ideal for elucidation of their individual and joint functions, and analysis of the effect on postulated downstream targets.

#### **4.2.2.4 Morpholino application and assessment of uptake**

Embryos were staged visually prior to morpholino application, as described in section 2.1.6.5. In cases of dual morpholino treatment, two morpholinos each at a concentration of 250  $\mu\text{M}$  were combined (resulting in a final concentration of 500  $\mu\text{M}$ ). Standard control morpholino was applied singly at 500  $\mu\text{M}$  in order to match the total concentration of experimental morpholino. Wild type embryos were simultaneously opened and staged. Following incubation, extra-embryonic membranes were removed for assessment of morpholino uptake and photography. Fluorescence levels of two embryos classed as positive for morpholino uptake are shown in Figure 4.4 and indicate typical levels for all embryos used in the study.

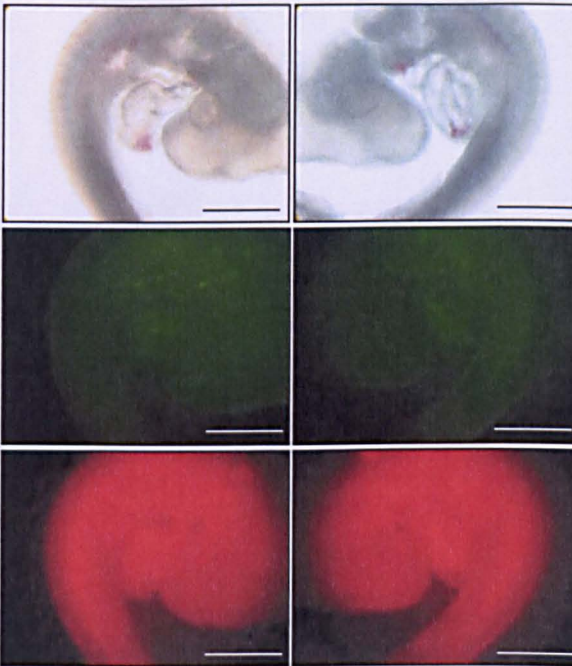
**A**



Single morpholino treatment:

Standard control 500  $\mu$ M  
(fluorescein tag)

**B**



Dual morpholino treatment:

TBX5 5-base mismatch  
250  $\mu$ M (fluorescein tag)

+

GATA-4 5-base mismatch  
250  $\mu$ M (lissamine tag)

**Figure 4.4 Assessment of morpholino uptake**

Bright field and fluorescent views of embryos classed as positive for morpholino uptake are displayed and indicate typical fluorescence levels for all embryos used in the study. (A) Single embryo treated with a single fluorescein tagged standard control morpholino at 500  $\mu$ M (displayed from the left and right). (B) Single embryo treated with two morpholinos, TBX5 5-base mismatch at 250  $\mu$ M, and GATA-4 5-base mismatch at 250  $\mu$ M (displayed from the left and right). Scale bars represent 1000  $\mu$ m.

#### 4.2.2.5 Preliminary testing of targeting and control morpholinos *in ovo*

Initial phenotypic analysis of embryos was carried out externally and is displayed in Figure 4.5. Outflow tract and ventricular regions are labelled. Figure 4.5 A1-A2 and B1-B2 depict wild type and standard control treated embryonic hearts, which display normal curvature and shape. C1 and C2 represent examples of TBX5 / GATA-4 double 5-base mismatch treated embryos, which respectively display a constricted outflow tract and dilated ventricle. Of the double mismatch control embryos, 3 / 10 externally harboured a cardiac defect. Since these were similar to, but less severe than, the abnormalities observed in knockdown embryos (discussed later in section 4.2.7), it was hypothesised that one or both of the control morpholinos was still able to bind to the target region, but with lower affinity than the targeting morpholinos. In order to overcome this problem, and upon recommendation by Gene-Tools, both 5-base mismatch morpholinos were replaced with 7-base mismatch controls. Where possible, different bases were altered to those originally modified (Table 2.7, Figures 4.2 and 4.3). The new controls were again tested prior to use to rule out low affinity binding or mis-targeting effects.

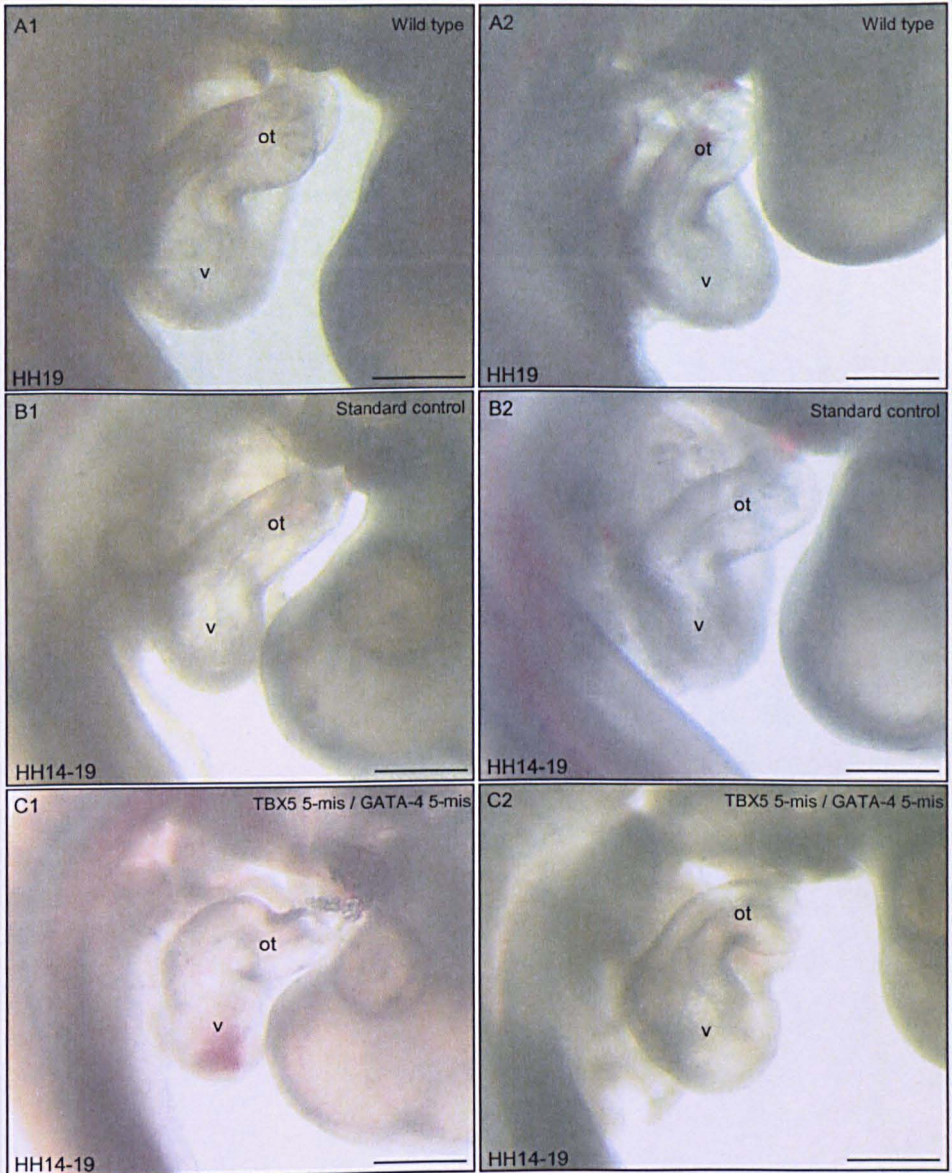


**Figure 4.5 External phenotypic analysis of embryos treated with 5-mismatch morpholinos in comparison to standard control-treated and wild type embryos**

Bright field lateral embryonic views are displayed with developmental stages of morpholino application and embryo harvest. Standard control morpholino was applied at a concentration of 500  $\mu$ M (B1 and B2), and 5-mismatch control morpholinos each applied at 250  $\mu$ M for a final morpholino concentration of 500  $\mu$ M (C1 and C2). Scale bars represent 500  $\mu$ m. ot – outflow tract, v - ventricle

#### **4.2.2.6 External phenotypic analysis of single and double knockdown embryos**

##### **4.2.2.6.1 Whole body analysis**

Figure 4.6 shows whole embryonic views of animals subjected to various morpholino treatments. Wild type, standard control and double mismatch control embryos display a normal body shape and 'c' shaped curvature (Figure 4.6 A1, B1 and C1 respectively). Embryos subjected to individual knockdown of TBX5 and GATA-4 (Figure 4.6 D1 and E1) diverted only slightly from this. In contrast, double knockdown embryos (Figure 4.6 F1 – F5) displayed a variety of defects including growth retardation (F3), body kinking and/or twisting (F1, F3, F4), and severe defects in heart looping (F2 and F5).

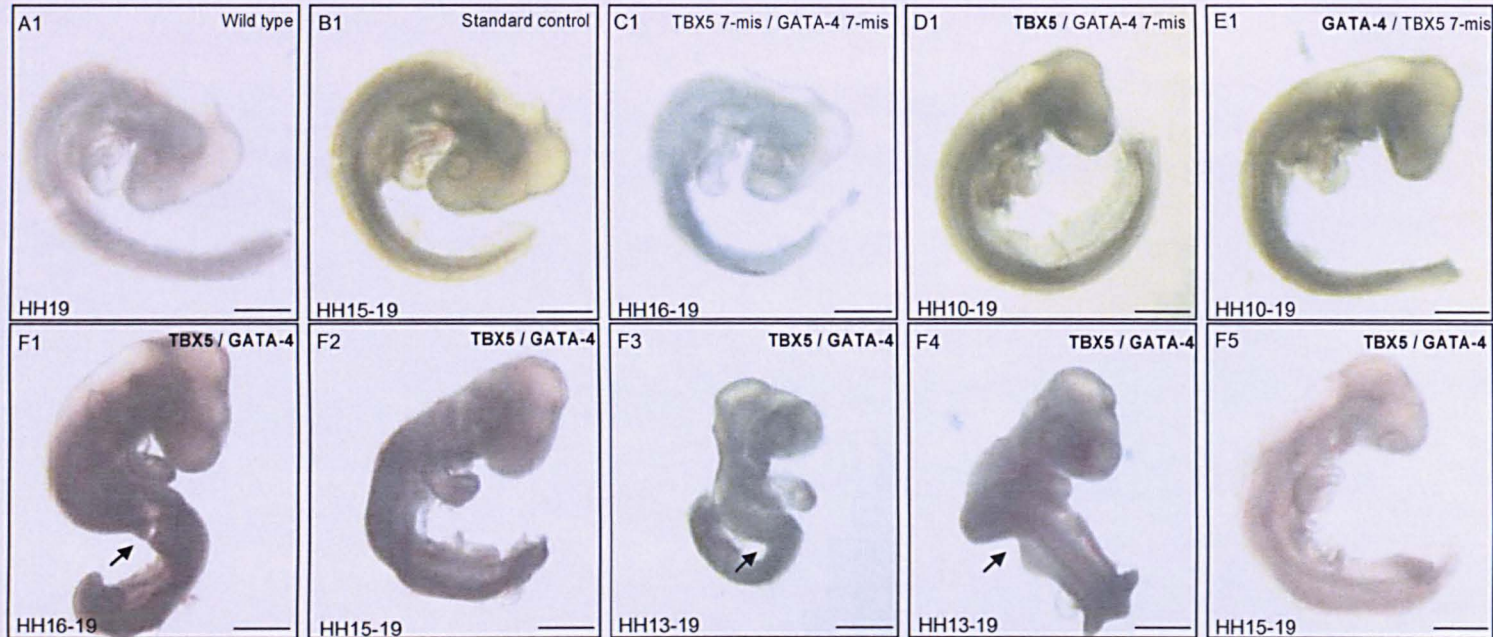


**Figure 4.6 External whole body analysis of TBX5 / GATA-4 single and double knockdown embryos**

Bright field lateral embryonic views are displayed with developmental stages of morpholino application and embryo harvest. Embryos were treated with a final morpholino concentration of 500  $\mu\text{M}$ . A1, B1 and C1 show a wild type, standard control and double mismatch control embryo respectively. D1 and E1 are examples of TBX5 single knockdown and GATA-4 single knockdown embryos respectively. F1 – F5 are examples of double knockdown embryos. Arrows indicate abnormalities in body shape. Scale bars represent 1000  $\mu\text{m}$ .

#### 4.2.2.6.2 Cardiac analysis

External analysis focusing on embryonic hearts was also performed and is displayed in Figure 4.7. Outflow tract and ventricular regions are marked where identifiable. Embryos in the three control groups showed no outward abnormalities (Figure 4.7 A1 – C1). TBX5 knockdown resulted in heart malformations, primarily ventricular (Figure 4.7 D1) in 2 / 3 embryos. GATA-4 single knockdown embryos displayed a similar phenotype (Figure 4.7 E1), and 3 / 4 embryos were affected. A variety of heart defects were observed in double knockdown animals and five examples are shown (Figure 4.7 F1 – F5). These included severe heart-restricted growth retardation (F3), ventricular constriction (F4), and overall malformations with abnormal heart looping in all embryos shown (F1 – F5). Cardiac defects were present in 9 / 12 double knockdown embryos. External phenotypic analysis data is summarised in Table 4.2 (with additional internal analysis data, see next section). These findings are consistent with the phenotype of *Gata4*<sup>+/-</sup> *Tbx5*<sup>+/-</sup> mice [Maitra et al., 2009], published during the time of this study.

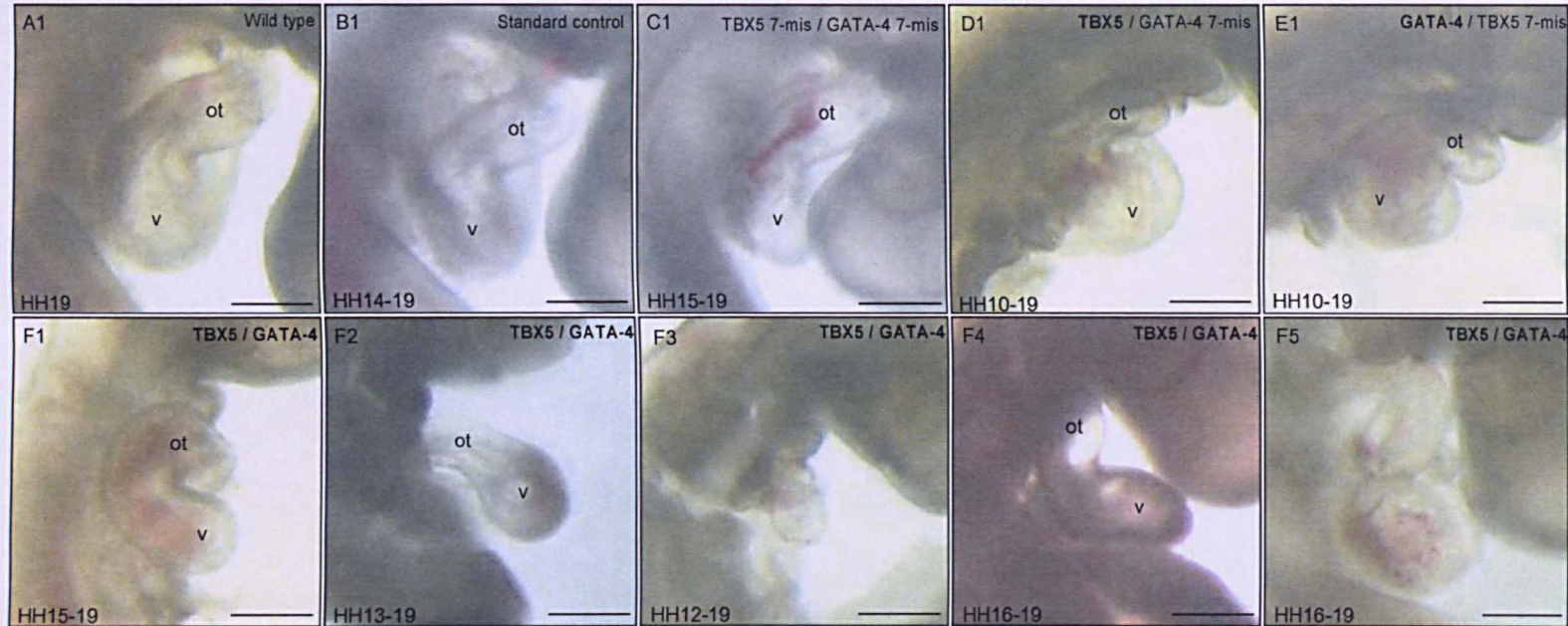


**Figure 4.7 External cardiac analysis of TBX5 / GATA-4 single and double knockdown embryos**

Bright field lateral embryonic views are displayed with developmental stages of morpholino application and embryo harvest. Embryos were treated with a final morpholino concentration of 500  $\mu$ M. A1, B1 and C1 show a wild type, standard control and double mismatch control embryo respectively. D1 and E1 are examples of TBX5 single knockdown and GATA-4 single knockdown embryos respectively. F1 – F5 are examples of double knockdown embryos. Scale bars represent 500  $\mu$ m. ot – outflow tract, v - ventricle

#### 4.2.2.7 Histological analysis of embryos

Following photography, embryos were fixed in 4% PFA then dehydrated in a graded ethanol series prior to being embedded in wax. Embryos were sectioned coronally at 10 microns and sections were transferred onto slides for haemulium staining and mounting with DPX. Due to the high proportion of knockdown embryos with gross cardiac malformations (particularly in cardiac looping), consistent orientation of hearts for sectioning in the same plane was not possible in all cases, with resulting difficulties in comparative phenotypic analysis.

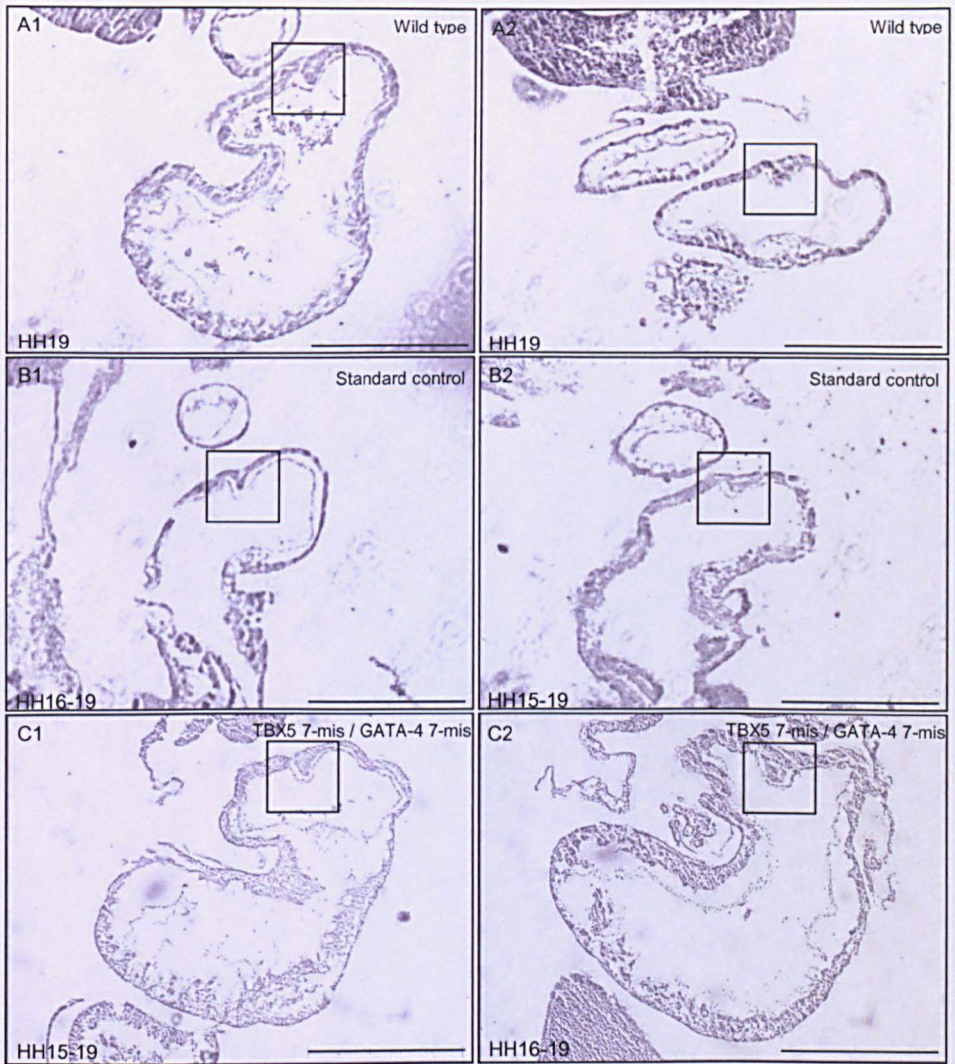
Figure 4.8 shows haemulium stained sections through embryos in the three control groups; (A) wild type, (B) standard control, and (C) TBX5 7-base mis / GATA-4 7-base mis, and two example embryos from each group are displayed. Regions of atrial septum formation are shown at their maximum point upon viewing serial sections throughout the embryo, and are boxed. All embryos displayed normal sized atrial septa.

Figure 4.9 shows haemulium stained sections through TBX5 and GATA-4 single and double knockdown embryos. Again, regions of atrial septum formation are shown at their maximum size. TBX5 knockdown embryos, in addition to the external cardiac defects seen, displayed a slight reduction in atrial septum size (Figure 4.9 A1 and A2). GATA-4 knockdown also resulted in a less pronounced atrial septum size in one embryo (Figure 4.9 B1). Unfortunately the orientation of other sectioned GATA-4 knockdown embryos did not allow analysis of septa size (e.g. B2).

Double knockdown of TBX5 and GATA-4 resulted in a number of internal cardiac defects (Figure 4.9 C1 and C2). C1 displayed an abnormal shape, and upon viewing sections throughout the heart, a complete lack of trabeculation was also observed. The beginnings of an atrial septum were visible. The second double knockdown embryo shown (C2) displayed a localised thickening of the cardiac jelly at the point of atrial septum formation, but no septum, despite the large overall size of the heart.

Phenotypic analysis data is summarised in Table 4.2. Approximately 75% of double knockdown embryos displayed a cardiac defect.

These findings are consistent with the phenotype of *Gata4*<sup>+/-</sup> *Tbx5*<sup>+/-</sup> compound heterozygote mice [Maitra et al., 2009], published at the time of this study (2008/9). Due to the phenotypic characterisation of compound heterozygote embryos performed in this publication, analysis of phenotype was not carried out on as large a scale as originally planned, and was used primarily for the purposes of technique validation and confirmation of knockdown.



**Figure 4.8 Histological analysis of the three control groups**

Haemalum stained coronal embryonic sections through two embryos in each group are displayed. Three control groups were studied; (A) wild type, (B) standard control, and (C) TBX5 7-base mis / GATA-4 7-base mis. Developmental stages of morpholino application (where applicable) and embryo harvest are indicated. A final morpholino concentration of  $500 \mu\text{M}$  was used in cases of morpholino treatment. Regions of atrial septa formation are boxed, shown at their maximum size upon viewing serial sections throughout the embryo. Scale bars represent  $500 \mu\text{m}$ .

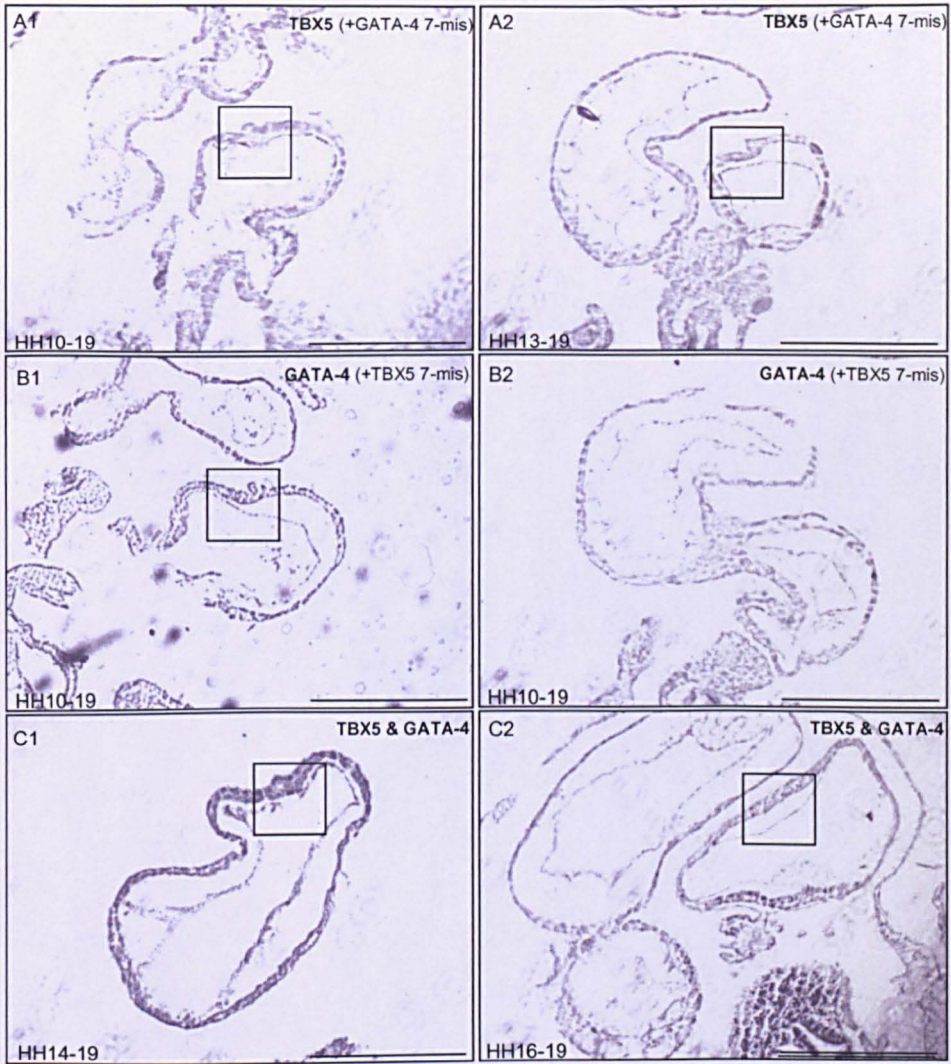


**Figure 4.9 Histological analysis of TBX5 and GATA-4 knockdown embryos**

Haemulium stained coronal embryonic sections through two embryos in each group are displayed. Three knockdown groups are represented; (A) TBX5 single knockdown (+ GATA-4 7-base mis), (B) GATA-4 single knockdown (+TBX5 7-base mis), and (C) TBX5 / GATA-4 double knockdown. Developmental stages of morpholino application (where applicable) and embryo harvest are indicated. Each morpholino was applied at a concentration of 250  $\mu\text{M}$ , resulting in a final morpholino concentration of 500  $\mu\text{M}$ . Regions of atrial septa formation are boxed, shown at their maximum size upon viewing serial sections throughout the embryo. Scale bars represent 500  $\mu\text{m}$ .

**Table 4.1 Summary of abnormalities seen in TBX5 / GATA-4 single and double knockdown embryos and controls**

Nature/region of heart abnormality		Wild type	Standard control	Double mismatch control	TBX5 knockdown / GATA-4 mismatch	GATA-4 knockdown / TBX5 mismatch	TBX5 / GATA-4 double knockdown
External analysis	Body size / shape	0 / 3	0 / 3	0 / 3	0 / 3	1 / 4	7 / 12
	Heart size / shape	0 / 3	0 / 3	0 / 3	2 / 3	2 / 4	8 / 12
	Heart looping	0 / 3	0 / 3	0 / 3	2 / 3	1 / 4	8 / 12
	Other	0 / 3	0 / 3	0 / 3	1 / 3	1 / 4	2 / 12
	<b>Total</b>	<b>0 / 3</b>	<b>0 / 3</b>	<b>0 / 3</b>	<b>2 / 3</b>	<b>3 / 4</b>	<b>9 / 12</b>
Internal analysis	Atrial septum	0 / 3	0 / 3	0 / 3	2 / 2	1 / 1	1 / 3
	Trabeculae	0 / 3	0 / 3	0 / 3	0 / 3	-	2 / 3
	Cardiac jelly	0 / 3	0 / 3	0 / 3	1 / 3	0 / 3	2 / 3
	<b>Total</b>	<b>0 / 3</b>	<b>0 / 3</b>	<b>0 / 3</b>	<b>2 / 3</b>	<b>1 / 3</b>	<b>3 / 3</b>

Groups represented are wild type, standard control, TBX5 / GATA-4 double mismatch control, TBX5 single knockdown (with GATA-4 mismatch control), GATA-4 single knockdown (with TBX5 mismatch control), and TBX5 / GATA-4 double knockdown.

### **4.2.3 QPCR expression analysis of candidate genes in TBX5 / GATA-4 double knockdown embryos**

For assessment of the responsiveness of candidate genes to TBX5 and GATA-4 in the developing chick heart, expression was analysed by QPCR in double knockdown embryos and controls.

#### **4.2.3.1 Sample collection and preparation**

Approximately 600 eggs were opened in total for this study. Morpholino was applied to around half following exclusion of embryos which were no longer viable or not within the desired range of development (HH12 – HH16). Morpholino uptake was confirmed in HH19 stage embryos prior to tissue isolation. Eight hearts were pooled per sample, and three biological replicates collected per group (3 groups: wild type (calibrator), double 7-base mismatch control, and double knockdown). Exactly 1 µg RNA was used per 20 µl reverse transcription reaction for identical loading in subsequent reactions. cDNA for all samples was prepared simultaneously, appropriately diluted (section 2.2.1.10.5), aliquoted, and stored at -80 °C prior to use. HH24 whole embryo cDNA was used for generation of standard curves.

#### **4.2.3.2 QPCR assay design**

QPCR assays were designed as set out in section 2.2.1.10.1, generally spanning a 60 – 100 bp region including an exon-exon boundary, and were suitable for use with an annealing temperature of 60 °C. Primer sequences and assay information are given in Table 2.4. These primers were also used for RT-PCR expression profiling (Figure 4.1) which additionally served to confirm products sizes and single product amplification prior to QPCR. Assays were designed to all seven candidate genes (*PA2.26*, *PETA-3*, *FUCA1*, *FN*, *TPM1*, *DES*, and *RBMS1*), and four potential endogenous control genes - *GAPDH*, *TBP*, *EEF1A1*, and *RPLPO*. The gene *MYH6*, a known target of TBX5 and GATA-4 [Ching et al., 2005; Huang et al., 1995; Molkenin et al., 1994], was also included as a positive control. During the time of this study,

MYH6 was additionally shown to be down-regulated in *Gata4*<sup>+/-</sup> *Tbx5*<sup>+/-</sup> compound heterozygote mice at E11.5 and E13.5 [Maitra et al., 2009].

#### 4.2.3.3 Comparative C<sub>T</sub> method ( $\Delta\Delta C_T$ ) versus Relative Standard Curve method

In Chapter 3, the Comparative C<sub>T</sub> method was used for QPCR expression analysis in the P19 cell line using transmembrane protein 131 (*tmem131*) as an endogenous control, generating a data set that was both accurate and reproducible. This method was attempted here using GAPDH as an endogenous control, but it was not possible to obtain reproducible results (not shown). The Comparative C<sub>T</sub> method does not require the use of standard curves on each reaction plate, and whilst this has economical and time-savings advantages (particularly for high-throughput screening) it also means that it is not possible to assess the efficiency or reliability of each individual run. An alternative method, the Relative Standard Curve method, overcomes this limitation and was tested and optimised for quantification of gene expression in the chick. This method involves the construction of standard curves from known quantities of DNA for both the target and endogenous control, with sample DNA amplified simultaneously under identical conditions. Sample target and endogenous reference quantities are determined using this information, and assay efficiency data is generated in parallel, producing highly accurate data.

#### 4.2.3.4 Selection of an endogenous control for relative quantification

Selection of an appropriate endogenous control gene is a crucial step in relative quantification experiments. Normalisation to an endogenous control allows correction of any skewing of data arising from small differences in starting quantity of template. The endogenous control must be expressed at the same time as the target gene, and display uniform expression across all samples i.e. expression should not be affected by sample treatments. Four genes were selected as potential candidates – *TBP* (TATA box binding protein), *GAPDH* (glyceraldehyde-3-phosphate dehydrogenase), *EEF1A1* (eukaryotic translation elongation factor 1 alpha 1) and *RPLPO* (large ribosomal protein). These are commonly used as endogenous controls in QPCR.

Primer sequences and assay information are given in Table 2.4. RT-PCR products generated using these primers were checked for size and specificity prior to QPCR (data not shown).

#### **4.2.3.4.1 Preparation of standard curves**

In order to assess QPCR assay efficiency and suitability of these four genes for use as endogenous controls, standard curves were constructed for each gene (using a 10 point dilution series of 4-fold). These are shown in Figures 4.10 – 4.13, and standard curve linearity and assay efficiency values are summarised in Table 4.2. As mentioned, a linearity of  $\geq 0.99$  and slope in the range -3.2 to -3.6 is desirable. All assays generated standard curves that met the linearity criteria. The slope (and therefore efficiency) of the GAPDH assay was outside the acceptable range so this gene was excluded. TBP, whilst meeting the criteria set out, generated a poor amplification plot (Figure 4.11a) with amplification starting at the high cycle number of 26 (EEF1A1 and RPLPO expression was observed from 18 and 16 cycles respectively). On this basis, TBP was also excluded, and EEF1A1 and RPLPO were short-listed for normalisation of data.

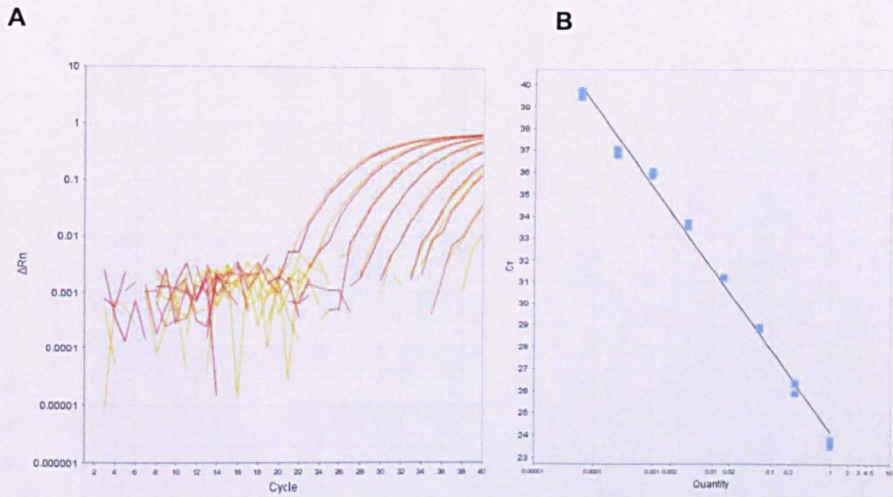


**Figure 4.10 GAPDH amplification plot (A) and resulting standard curve (B)**

Two replicate reactions were performed at ten concentrations of cDNA, based on a 4-fold dilution series. Amplification efficiency was calculated from the slope of the standard curve using the equation  $E = 10^{-1/\text{slope}}$ . Slope: -3.738,  $R^2$ : 0.992, Efficiency (%): 85.132

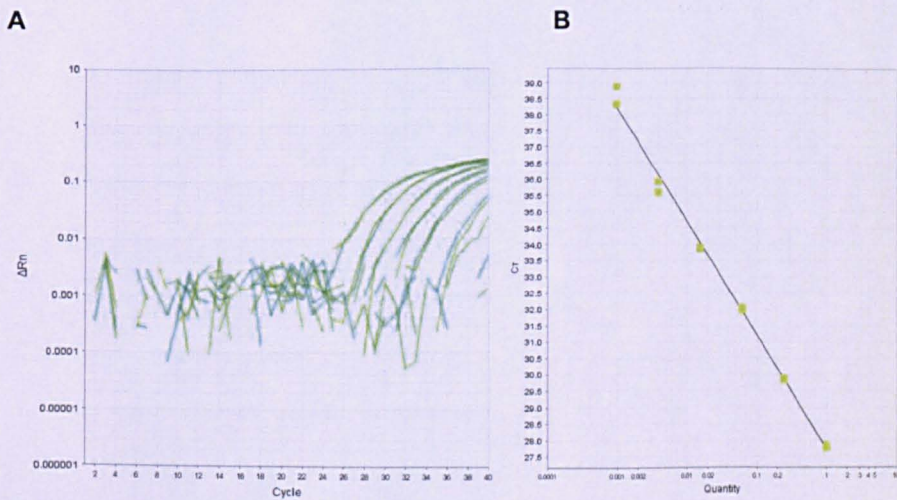


**Figure 4.11 TBP amplification plot (A) and resulting standard curve (B)**

Two replicate reactions were performed at ten concentrations of cDNA, based on a 4-fold dilution series. Amplification efficiency was calculated from the slope of the standard curve using the equation  $E = 10^{-1/\text{slope}}$ . Slope: -3.49,  $R^2$ : 0.994, Efficiency (%): 93.427

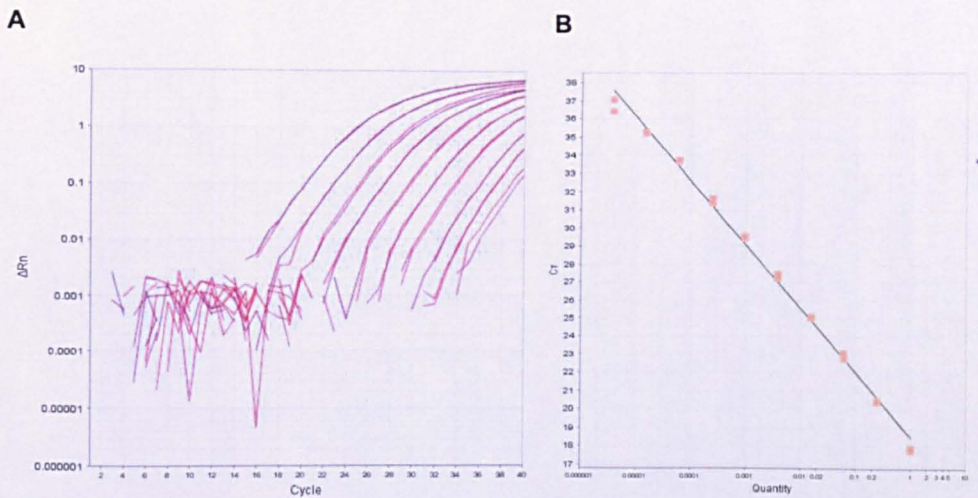


**Figure 4.12 EEF1A1 amplification plot (A) and resulting standard curve (B)**

Two replicate reactions were performed at ten concentrations of cDNA, based on a 4-fold dilution series. Amplification efficiency was calculated from the slope of the standard curve using the equation  $E = 10^{-1/\text{slope}}$ . Slope: -3.513,  $R^2$ : 0.995, Efficiency (%): 92.611

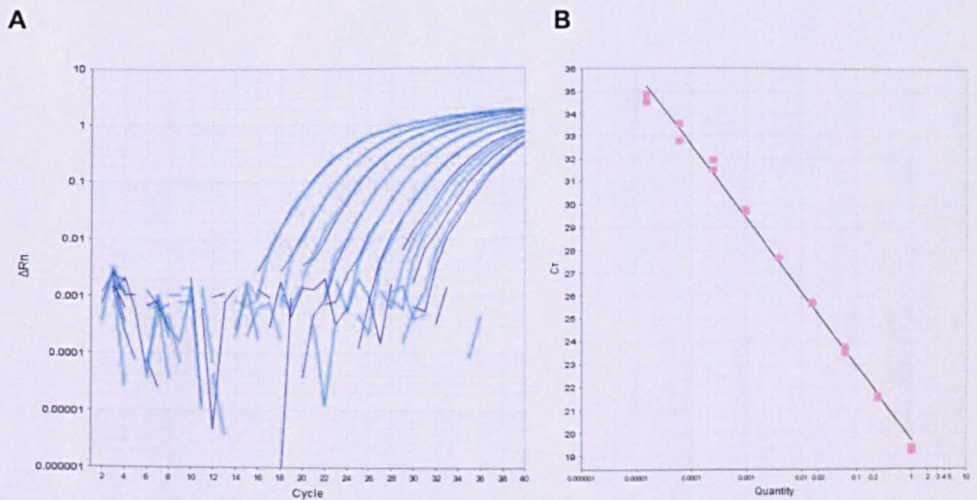


**Figure 4.13 RPLPO amplification plot (A) and resulting standard curve (B)**

Two replicate reactions were performed at ten concentrations of cDNA, based on a 4-fold dilution series. Amplification efficiency was calculated from the slope of the standard curve using the equation  $E = 10^{-1/\text{slope}}$ . Slope: -3.226,  $R^2$ : 0.995, Efficiency (%): 104.142

**Table 4.2 Summary of endogenous control gene assay properties**

Gene	Linearity (R <sup>2</sup> )	Slope	Efficiency (%)	Starting cycle
GAPDH	0.992	-3.738	85.1	22
TBP	0.994	-3.490	93.4	26
EEF1A1	0.995	-3.513	92.6	18
RPLPO	0.995	-3.226	104.1	16

Values are based on standard curves prepared from a 10-point 4-fold dilution series using HH24 whole embryo cDNA (Figures 4.10 – 4.13).

#### 4.2.3.4.2 Analysis of variation of endogenous control expression levels in study samples

Expression of an endogenous control genes used for normalisation of data must not be affected by experimental treatments, so should display uniform expression levels across all sample groups (3 groups: wild type (calibrator), double 7-base mismatch control, and double knockdown). To investigate this, C<sub>T</sub> values of EEF1A1 and RPLPO were measured in triplicate for each sample following their identical preparation and dilution.  $\Delta C_T$  values were calculated for each group (Table 4.3) from mean C<sub>T</sub> values of biological and experimental replicates using the equation:

$$\Delta C_{T(\text{sample})} = \text{Average } C_{T(\text{calibrator})} - \text{Average } C_{T(\text{sample})}$$

Samples with higher template concentrations than the calibrator result in lower C<sub>T</sub> values and positive  $\Delta C_T$  values, and vice-versa. A  $\Delta C_T$  value of 1 equates to a two-fold difference in expression, and the  $\Delta C_T$  value of an ideal endogenous control will vary only slightly from zero indicating stable expression. Both RPLPO and EEF1A1 displayed relatively constant expression across samples (maximum  $\Delta C_T$  values of 0.36 and 0.44 respectively) and were suitable for use.

RPLPO was selected for use as the endogenous control since the range of  $\Delta C_T$  values observed across samples was narrowest, and assay linearity (0.995) and efficiency (104%) were closest to ideal.

**Table 4.3 Mean  $C_T$  and  $\Delta C_T$  values of *EEF1A1* and *RPLPO* in study samples**

Sample	RPLPO		EEF1A1	
	Mean $C_T$	$\Delta C_T$	Mean $C_T$	$\Delta C_T$
Wild type (calibrator)	27.17389	0	26.54730	0
7-mismatch control	26.85162	0.322276	26.71622	-0.16892
Double knockdown	26.81002	0.363879	26.99526	-0.44797

Three biological samples were analysed per group, each assayed in triplicate. Standard curves for both genes were run in parallel on the same reaction plate for confirmation of assay quality.

#### 4.2.3.5 QPCR expression analysis of candidate genes

The calibrator sample (in this case untreated or wild type) serves as a baseline for comparison of target and endogenous control levels, and also allows comparison across reaction plates. Baseline and threshold values were set manually, and absolute quantities of each gene generated from the standard curves in Applied Biosystems 7500 v2.0.1 software. Standard curves for target and endogenous control genes were included on each plate, with each point measured in duplicate. All samples were run simultaneously on the same plate, each assayed in triplicate. Reaction plates were run twice. Biological and experimental replicates were grouped for data normalisation and standard deviation calculations.

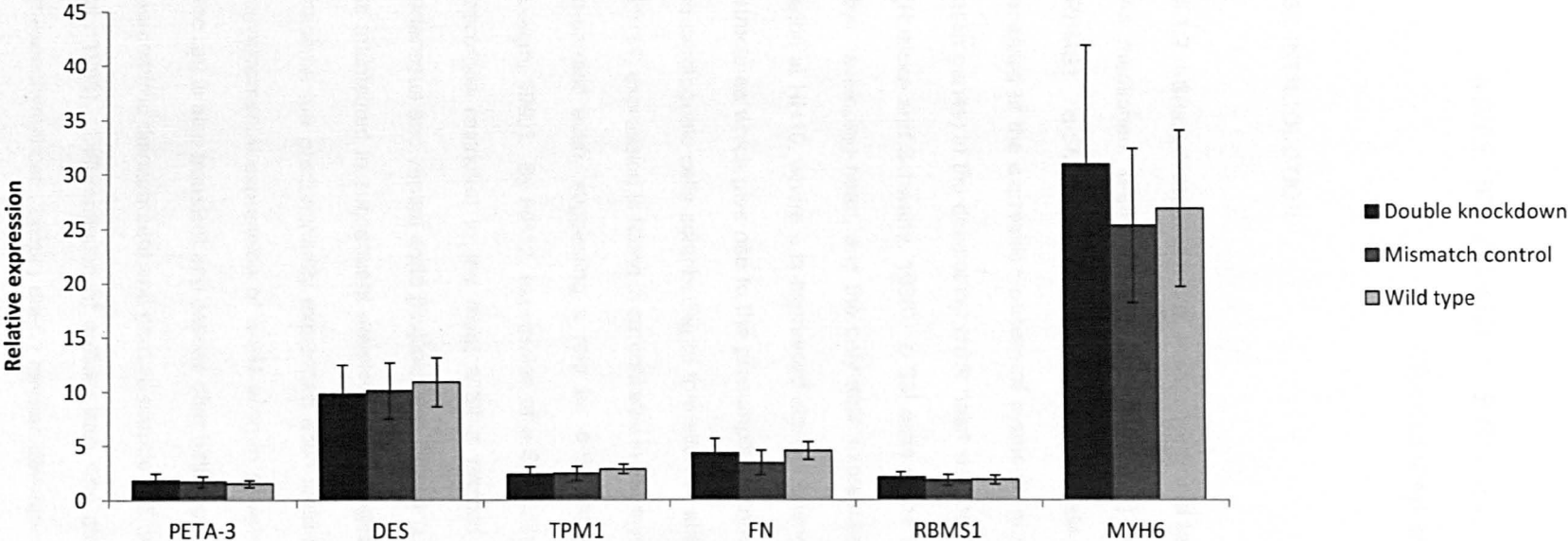
Results of QPCR expression analysis are displayed in Table 4.4 and Figure 4.14. Expression is displayed relative to expression of the endogenous control RPLPO. PA2.26 and FUCA1 displayed very low expression levels which were not accurately

quantifiable, and it was therefore necessary to exclude these from the QPCR study. Expression of the other five candidate genes (PETA-3, DES, TPM1, FN, and RBMS1) was accurately quantified but no significant differences were observed between the double knockdown and control groups (measured by the student's t test using  $p < 0.05$  as the threshold value). MYH6 was used as a positive control in this study as it known to be regulated by TBX5 and GATA-4 [Ching et al., 2005; Huang et al., 1995; Molkenin et al., 1994]. This gene did not however display any change in expression.

**Table 4.4 QPCR expression analysis of candidate genes in TBX5 / GATA-4 knockdown animals and controls**

Gene	Relative expression		
	Double knockdown	Double mismatch control	Wild type (untreated control)
PETA-3	1.80 ± 0.64	1.69 ± 0.47	1.50 ± 0.31
Desmin	9.79 ± 2.66	10.1 ± 2.58	10.9 ± 2.26
α-tropomyosin	2.34 ± 0.75	2.45 ± 0.67	2.86 ± 0.44
Fibronectin	4.31 ± 1.38	3.43 ± 1.14	4.53 ± 0.81
RBMS1	2.10 ± 0.49	1.81 ± 0.49	1.84 ± 0.41
MYH6	31.0 ± 10.9	25.3 ± 7.1	26.9 ± 7.2

QPCR expression analysis was performed on cardiac tissues from TBX5 / GATA-4 double knockdown embryos, TBX5 7-mis / GATA-4 7-mis control embryos, and wild type embryos (3 biological replicates per group). Each reaction plate was run in duplicate. Data was normalised to RPLPO. No significant differences in expression were observed for any gene (measured between the knockdown group and both control groups by the student's t test using  $p < 0.05$  as the threshold value).



156

**Figure 4.14 Relative expression of candidate genes in TBX5 / GATA-4 knockdown animals and controls**

QPCR expression analysis was performed on TBX5 / GATA-4 double knockdown embryos, TBX5 7-mis / GATA-4 7-mis controls, and wild type embryos (3 biological replicates per group). Each reaction plate was run in duplicate. Data was normalised to RPLPO. Error bars represent standard deviation. No significant differences in expression were observed for any gene (measured between the knockdown group and both control groups by the student's t test, using  $p < 0.05$  as the threshold value).

## CHAPTER 5

# INVESTIGATION OF THE ROLE OF RBMS1 IN CARDIAC DEVELOPMENT

### 5.1 INTRODUCTION

#### 5.1.2 $\alpha$ -Smooth muscle actin, a transcriptional target of RBMS1

As mentioned,  $\alpha$ -smooth muscle actin ( $\alpha$ -SM) is a known downstream target of RBMS1.  $\alpha$ -SM is the major actin isoform present in vascular tissue. A detailed analysis of the expression pattern of  $\alpha$ -smooth muscle actin (and the two striated  $\alpha$ -actin genes) in the developing chick heart was performed by Ruzicka and co-workers [Ruzicka and Schwartz, 1988].  $\alpha$ -SM actin is the earliest expressed actin isoform in the developing heart, and the only actin expressed at HH8/9. It is the predominant actin at HH10, where it is expressed along the length of the tubular heart, in anterior structures which give rise to the presumptive conus arteriosus and ventral aorta, and in cardiogenic cells contributing to formation of atrial and sinus venosus regions. At HH11, expression is found in sarcomeres in the myocardium, alongside  $\alpha$ -skeletal and  $\alpha$ -cardiac actin, suggesting a role for  $\alpha$ -SM actin in myofibrillogenesis [Sugi and Lough, 1992]. By HH12, expression of  $\alpha$ -SM actin is selectively down-regulated and becomes restricted to the most anterior regions of the heart, namely the conus arteriosus and ventral aorta [Ruzicka and Schwartz, 1988]. This pattern of expression is maintained in subsequent developmental stages. The two striated  $\alpha$ -actin genes become the predominantly expressed actin isoforms from HH12 in the heart. The developmental expression of  $\alpha$ -SM actin in skeletal and myocardial cells (studied in the rat) is also transient and ceases after birth, again indicating a role for  $\alpha$ -SM actin in sarcomeric development and cardiac muscle cell differentiation [Woodcock-Mitchell et al., 1988]. Differentiation of outflow tract and atrioventricular endothelial cells into mesenchymal cells occurs during cardiac development, forming endocardial cushions

which are essential for heart valve and septa formation.  $\alpha$ -SM actin plays an important role in this crucial process of endothelial-mesenchymal transformation [Nakajima et al., 1997], indicating an additional role in cardiogenesis.

Mouse knockout of the  $\alpha$ -SM actin gene (*ACTA2*) results in impaired vascular contractility and blood flow, with no reported effects on development of the heart [Schildmeyer et al., 2000; Tomasek et al., 2006]. However, these findings were based upon gross examination of embryos and cross-sectional analysis of cardiac muscle. Internal heart structures were not examined for abnormalities. Mutations in *ACTA2* in humans are associated with a variety of vascular diseases such as coronary artery disease (CAD), ischemic strokes, Moyamoya disease (MMD), and thoracic aortic aneurysms and dissections (TAAD) [Guo et al., 2009]. In addition, *ACTA2* mutations are also associated with the CHD patent ductus arteriosus [Guo et al., 2007].

### 5.1.3 Transcriptional regulation of $\alpha$ -smooth muscle actin

Expression of  $\alpha$ -SM actin is mediated by positive and negative cis-elements and their corresponding trans-acting factors. A number of positive regulators have been identified e.g. serum response factor (SRF) which acts via the CArg box [Hautmann et al., 1997; Shimizu et al., 1995; Simonson et al., 1995], and essential transcriptional enhancer factor-1 (TEF-1) which acts via the purine rich motif [Cogan et al., 1995]. Less is known about the negative regulation of this gene. Until recently, only two negative regulators of  $\alpha$ -SM actin, vascular  $\alpha$ -SM actin single-strand binding factors 1 and 2 (VACssBF1 and VACssBF2), were identified, both acting via the TEF-1 binding domain in single stranded DNA [Cogan et al., 1995]. A novel negative regulatory element has since been identified in the  $\alpha$ -SM actin promoter region, ranging from -238 to -219. Mutation and deletion analyses revealed the sequence TATCTTA (-228 to -222) is essential for negative regulation [Kimura et al., 1998]. Gel shift assays (using smooth muscle cell nuclear extracts) were designed to identify protein factors specifically interacting with this sequence, and resulted in identification of the nuclear protein RBMS1. RBMS1 was found to interact with both single and double stranded

DNA containing this sequence. Furthermore, RBMS1 overexpression resulted in suppression of  $\alpha$ -SM actin promoter activity. This provided evidence of a novel role for RBMS1 in the negative transcriptional regulation of  $\alpha$ -SM actin.

#### **5.1.4 $\alpha$ -cardiac and $\alpha$ -skeletal actin**

The striated actins,  $\alpha$ -skeletal and  $\alpha$ -cardiac actin, are the major actin isoforms in skeletal and cardiac muscle respectively. Due to the common ancestry and high level of homology between these and  $\alpha$ -smooth muscle actin, it is possible these genes may have retained some common regulatory elements, and the regulatory effect of RBMS1 on all three actins will be assessed in this chapter. Both  $\alpha$ -cardiac and  $\alpha$ -skeletal actin are expressed in the heart where they each have an important function. Expression of  $\alpha$ -cardiac actin begins at HH9 (at lower levels than  $\alpha$ -smooth muscle actin) in the ventricular myocardium, subsequently spreading in a spatial pattern corresponding with the progression of myofibrillogenesis [Ruzicka and Schwartz, 1988]. Mutations in alpha cardiac actin produce atrial and ventricular septal defects [Matsson et al., 2008]. Expression of  $\alpha$ -skeletal actin is detectable from HH12, with the pattern of expression largely following that of  $\alpha$ -cardiac actin, with greater expression in the conus region [Ruzicka and Schwartz, 1988]

## 5.2 AIMS

This chapter aims to study RBMS1 in the developing chick embryo as follows:

- a) Bioinformatic characterisation of the chicken RBMS1 gene and transcripts
- b) Determination of the expression pattern of RBMS1 in the developing chick
- c) Morpholino knockdown of RBMS1 for phenotypic analysis
- d) Characterisation of the effect of morpholinos on RBMS1 mRNA splicing and / or mRNA levels
- e) Bioinformatic characterisation of  $\alpha$ -smooth muscle actin and related genes, and QPCR expression analysis of these in RBMS1 knockdown embryos versus controls

## 5.3 RESULTS

### 5.3.1 Bioinformatic Identification and characterisation of the chicken RBMS1 gene

The human RBMS1 gene was identified at chromosome 2: 161,101,000–161,378,000 using NCBI. The corresponding chicken gene was identified at chromosome 7: 23,214,270–23,352,271 (method described in section 2.2.6.1). Synteny of the chick genomic location with the known human genomic region of RBMS1 was confirmed, establishing identification of the true orthologue (Figure 5.1). Gene sequence alignments were performed in the online ECR browser (<http://ecrbrowser.dcode.org>) for ten species against the human (base) genome (Figure 5.2), showing this gene is conserved across a multitude of species. Two chicken RBMS1 protein transcripts were identified and multispecies alignment of RBMS1 protein sequences again showed this gene is highly conserved between the chicken, human, chimpanzee, mouse and rat (Figure 5.3). Sequence alignment of the two corresponding chicken mRNA transcripts is shown in Figure 5.4. ESTs matching the RBMS1 transcripts were identified and aligned with the theoretical mRNA sequences for sequence confirmation, represented in Figure 5.5. Transcript ENSGALT00000018146 contains a 9 bp insertion in exon 7, likely to have been introduced through an alternative splicing mechanism. Each transcript has been assigned a different AUG translational start site based on the postulated protein sequences. It is unclear which (if either) is the predominant transcript.

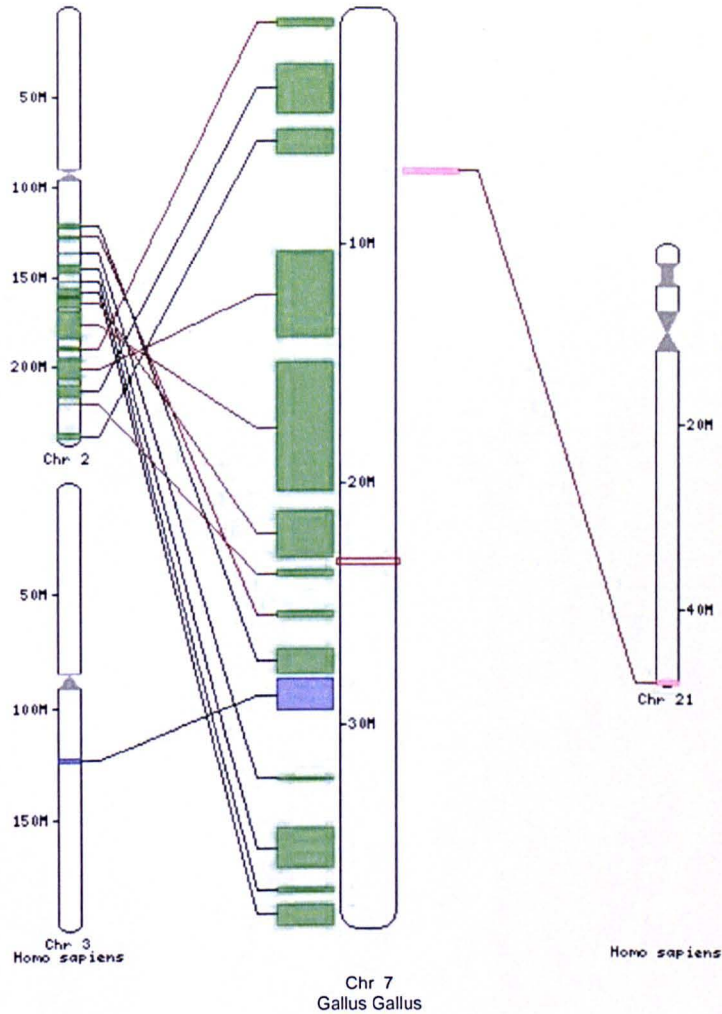


**Figure 5.1 Synteny of the chicken and human RBMS1 genes**

Synteny between the chromosomal location of the chicken RBMS1 gene and the known chromosomal location of the human RBMS1 gene was confirmed in *Ensembl* (<http://www.ensembl.org>). The centre block represents the species and region of interest (chicken, chromosome [7:23214240-23352391](#)), and the smaller chromosomes represent syntenic regions with the second species (human). Chromosome [2:161128662-161350305](#) is of interest. Blocks are coloured according to the chromosome of the second species. Black lines connect syntenic blocks with the same orientation, and brown lines connect syntenic blocks with opposite orientation. The RBMS1 gene is marked with the small red box.

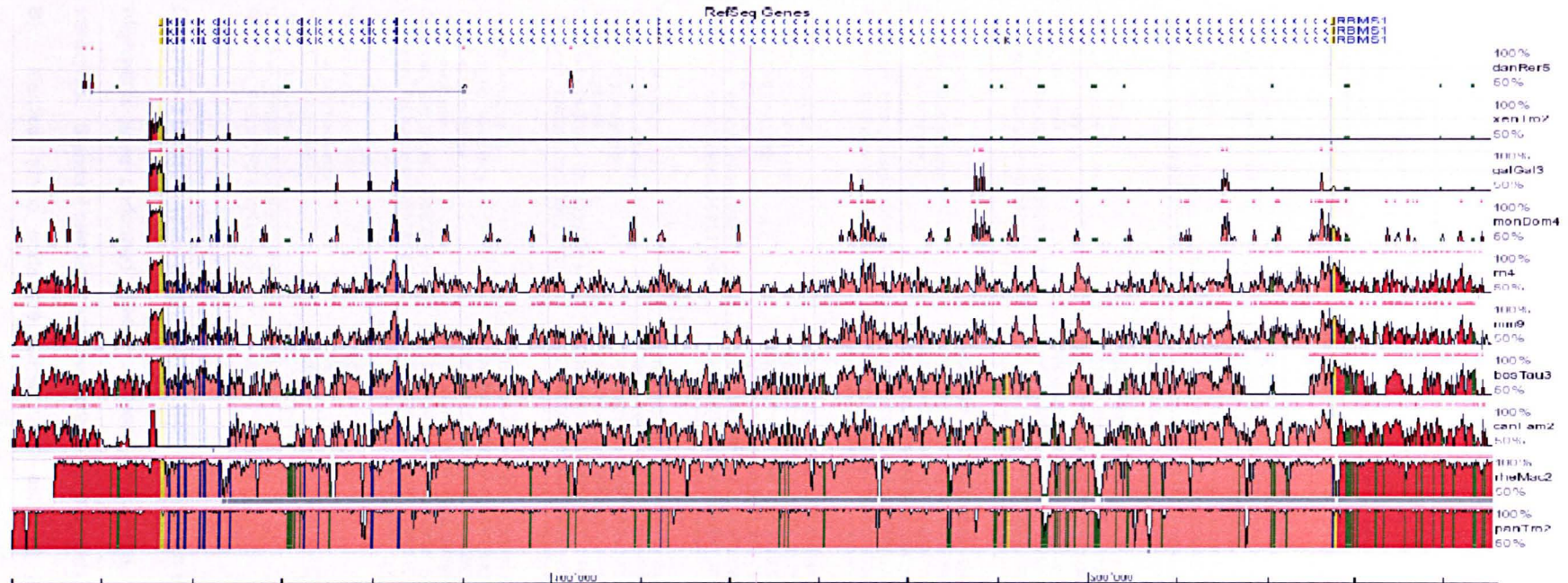


**Figure 5.2 Multispecies conservation of the RBMS1 gene**

Sequence alignments were performed in the online ECR browser (<http://ecrbrowser.dcode.org>) for ten species against the human (base) genome. The y-axis represents the percentage identity between the base and aligned genomes, and regions meeting the input criteria (100 nucleotide run, minimum 70% identity) are indicated by the pink rectangles on top of each plot. Blue lines indicate coding exons and salmon regions indicate intronic regions. Untranslated regions are shown in yellow, and red areas indicate intergenic regions. Green regions represent transposable elements and simple repeats.

```

Mus_musculus -----MAPPSPTSSNNSSS
Rattus_norvegicus MGKVKQMYPOYATYYYPPYLAQKSLVPAHPMAPPSPSTSSNNSSS
Pan_troglodytes --MIFPSSSGNPGSSNCRTPYRKQSLVPAHPMAPPSPSTSSNNSSS
Homo_sapiens MGKVKQMYPOYATYYYPPYLAQKSLVPAHPMAPPSPSTSSNNSSS
Chicken_ENSGALP00000032479 -----MYPQYTTYPPYLLAKQSI VPAHPMAPPSPSTSSNNSSS
Chicken_ENSGALP00000018124 -----MAPPSPTSSNNSSS
*****

Mus_musculus SSNSGWDQLSKTNLYIRGLPPNTTDQDLVKLCQPYGKIVSTKAILDKATN
Rattus_norvegicus SSNSGWDQLSKTNLYIRGLPPNTTDQDLVKLCQPYGKIVSTKAILDKATN
Pan_troglodytes SSNSGWDQLSKTNLYIRGLPPHTTDQDLVKLCQPYGKIVSTKAILDKTTN
Homo_sapiens SSNSGWDQLSKTNLYIRGLPPHTTDQDLVKLCQPYGKIVSTKAILDKTTN
Chicken_ENSGALP00000032479 SSNSGWDQLSKTNLYIRALPPNTTDQDLVKLCQPYGKIVSTKAILDKTTN
Chicken_ENSGALP00000018124 SSNSGWDQLSKTNLYIRALPPNTTDQDLVKLCQPYGKIVSTKAILDKTTN
*****.***:*****.***

Mus_musculus KKGYGFD FDS PAAQKAVSALKANGVQAQMAKQQEQDPTNLYISNLPL
Rattus_norvegicus KKGYGFD FDS PAAQKAVSALKASGVQAQMAKQQEQDPTNLYISNLPL
Pan_troglodytes KKGYGFD FDS PAAQKAVSALKASGVQAQMAKQQEQDPTNLYISNLPL
Homo_sapiens KKGYGFD FDS PAAQKAVSALKASGVQAQMAKQQEQDPTNLYISNLPL
Chicken_ENSGALP00000032479 KKGYGFD FDS PAAQKAVSALKASGVQAQMAKQQEQDPTNLYISNLPL
Chicken_ENSGALP00000018124 KKGYGFD FDS PAAQKAVSALKASGVQAQMAKQQEQDPTNLYISNLPL
*****

Mus_musculus SMDEQELENMLKPFQVIVSTRVLRDSSGAS RGVGFARMESTEKCEAVIGH
Rattus_norvegicus SMDEQELENMLKPFQVIVSTRVLRDSSGAS RGVGFARMESTEKCEAVIGH
Pan_troglodytes SMDEQELENMLKPFQVIVSTRILRDSGTS RGVGFARMESTEKCEAVIGH
Homo_sapiens SMDEQELENMLKPFQVIVSTRILRDSGTS RGVGFARMESTEKCEAVIGH
Chicken_ENSGALP00000032479 SMDEQELENMLKPFQVIVSTRILRDSGTS RGVGFARMESTEKCEAVIAH
Chicken_ENSGALP00000018124 SMDEQELENMLKPFQVIVSTRILRDSGTS RGVGFARMESTEKCEAVIAH
*****.***:*****.***

Mus_musculus FNGKFIKTPPGVSAPTEPLLCKFADGGQKKRQNPNKYIPNGRWPWPRDG--
Rattus_norvegicus FNGKFIKTPPGVSAPTEPLLCKFADGGQKKRQNPNKYIPNGRWPWREG--
Pan_troglodytes FNGKFIKTPPGVSAPTEPLLCKFADGGQKKRQNPNKYIPNGRWPWREG--
Homo_sapiens FNGKFIKTPPGVSAPTEPLLCKFADGGQKKRQNPNKYIPNGRWPWREGEV
Chicken_ENSGALP00000032479 FNGKFIKTPAGVSVPAEPLLCKFADGGQKKRQNPNKYIQNGRAWHREG--
Chicken_ENSGALP00000018124 FNGKFIKTPAGVSVPAEPLLCKFADGGQKKRQNPNKYIQNGRAWHREGV
*****.***.***:*****.***

Mus_musculus -EAGMTLTYDPTTAAALHNGFYSPYSIATNRMITQTSITPYIASPVSAAYQ
Rattus_norvegicus -EAGMTLTYDPTTAAALHNGFYSPYSIATNRMITQTSITPYIASPVSAAYQ
Pan_troglodytes -EAGMTLTYDPTTAAIQNGFYSPYSIATNRMITQTSITPYIASPVSAAYQ
Homo_sapiens -EAGMTLTYDPTTAAIQNGFYSPYSIATNRMITQTSITPYIASPVSAAYQ
Chicken_ENSGALP00000032479 -EAGMTLTYDPTTAAALQNGFYSPYSITANRMITQTSITPYIASPVSTYQ
Chicken_ENSGALP00000018124 -EAGMTLTYDPTTAAALQNGFYSPYSITANRMITQTSITPYIASPVSTYQ
*****.***:*****.***

Mus_musculus VQSPSWMQPPYILQHPGAVLTPSMEHTMSLQPASMISPLAQQMSHLSLG
Rattus_norvegicus VQSPSWMQPPYILQHPGAVLTPSMEHTMSLQPASMISPLAQQMSHLSLG
Pan_troglodytes VQSPSWMQPPYILQHPGAVLTPSMEHTMSLQPASMISPLAQQMSHLSLG
Homo_sapiens VQSPSWMQPPYILQHPGAVLTPSMEHTMSLQPASMISPLAQQMSHLSLG
Chicken_ENSGALP00000032479 VQSPSWMQPPYIMQHHPGAVLTPSMDHTMSLQPASMISPLTQQMSHLSLG
Chicken_ENSGALP00000018124 VQSPSWMQPPYIMQHHPGAVLTPSMDHTMSLQPASMISPLTQQMSHLSLG
*****.***:*****.***

Mus_musculus STGTYPATSAMQGAYLPQYTHMQTAAVPVEEASGQQQVAVETSNDHSPY
Rattus_norvegicus STGTYPATSAMQGAYLPQYTHMQTAVPVEEASGQQQVAVETSNDHSPY
Pan_troglodytes STGTYPATSAMQGAYLPQYAHMQTTAVPVEEASGQQQVAVETSNDHSPY
Homo_sapiens STGTYPATSAMQGAYLPQYAHMQTTAVPVEEASGQQQVAVETSNDHSPY
Chicken_ENSGALP00000032479 STGTYPATTAMQGAYIPQYTHVQTAAPVVEEASGQQQVAVETSNDHSPY
Chicken_ENSGALP00000018124 STGTYPATTAMQGAYIPQYTHVQTAAPVVEEASGQQQVAVETSNDHSPY
*****.***:*****.***

Mus_musculus TFPPNK
Rattus_norvegicus TFPPNK
Pan_troglodytes TFQPNK
Homo_sapiens TFQPNK
Chicken_ENSGALP00000032479 TYQQNK
Chicken_ENSGALP00000018124 TYQQNK
*: **

```

**Figure 5.3 Multispecies alignment of RBMS1 protein sequences**

Alignments were performed between human, chimpanzee, mouse, rat, and both chicken transcripts. Standard one letter abbreviations for amino acids have been used (see Appendix B). Identical amino acids are marked with asterisks, and RNP1 motifs are boxed.



```

ENSGALT00000033119      GTTACAGTAGAGACGTCCAGTGACCATTCTCCGTATACGTATCAACAAAATAAG TAACTG
ENSGALT00000018146      GTTACAGTAGAGACGTCCAGTGACCATTCTCCGTATACGTATCAACAAAATAAG TAACTG
*****

ENSGALT00000033119      TGAGATGCCCGGTGTGACCCGGCCTGGAGAAGGGTGCAAAGGCTGAAACAATCATGGAT
ENSGALT00000018146      TGAGATGCCCGGTGTGACCCGGCCTGGAGAAGGGTGCAAAGGCTGAAACAATCATGGAT
*****

ENSGALT00000033119      TTTACTGATCAATTGTGCTTTAGGAATTATTGACAGTTTGCACAGGTTCTTGAAAATGT
ENSGALT00000018146      TTTACTGATCAATTGTGCTTTAGGAATTATTGACAGTTTGCACAGGTTCTTGAAAATGT
*****

ENSGALT00000033119      TATTTATAATGAAATCAACTAAAAC TATTTTGCTATAAGTTC TATAAGGTGCATAAGAA
ENSGALT00000018146      TATTTATAATGAAATCAAC-----
*****

ENSGALT00000033119      AAACCTTAATTTCATCTAGTAGCTGCCATGAACAGGTTATTTTAGTAAAAAAAAA
ENSGALT00000018146      -----

ENSGALT00000033119      ATTTTATCAAGTGTTACG
ENSGALT00000018146      -----

```

**Figure 5.4 ClustalW alignment of the two chicken RBMS1 mRNA transcripts**

Identical bases are marked with asterisks. ATG translation start sites are shown in green, and stop codons in red. RNP1 motif encoding regions are boxed. Sequences are from *Ensembl* ([www.ensembl.org](http://www.ensembl.org)), April 2010.



**Figure 5.5 Representation of the two chicken RBMS1 mRNA transcripts and EST coverage**

Diagrams are drawn to scale based on the transcripts ENSGALT00000018146 and ENSGALT00000033119 (*Ensembl*, April 2010). Exons that differ between transcripts are shown with dashed lines, and untranslated regions are shown in grey. Regions encoding the two RNP1 motifs are marked. Matching ESTs and regions of sequence identity are indicated.

### **5.3.2 Investigation of RBMS1 expression in the developing chick**

#### **5.3.2.1 RT-PCR**

RBMS1 expression was initially examined by RT-PCR in chick embryonic segments at three stages of development (HH16, HH19 and HH24) as a preliminary means of temporal / spatial characterisation of expression. Primers were designed to bind to both RBMS1 transcripts resulting in amplification of a 488 bp fragment (sequences in Table 2.5, primer positions are represented in Figure 5.7, A). Figure 5.6 shows results of RT-PCR expression analysis. Expression was detected in all segments (head, heart, body / limbs) at all three developmental stages examined (Figure 5.6, A). Negative RT controls were included and did not display amplification (Figure 5.6, B).

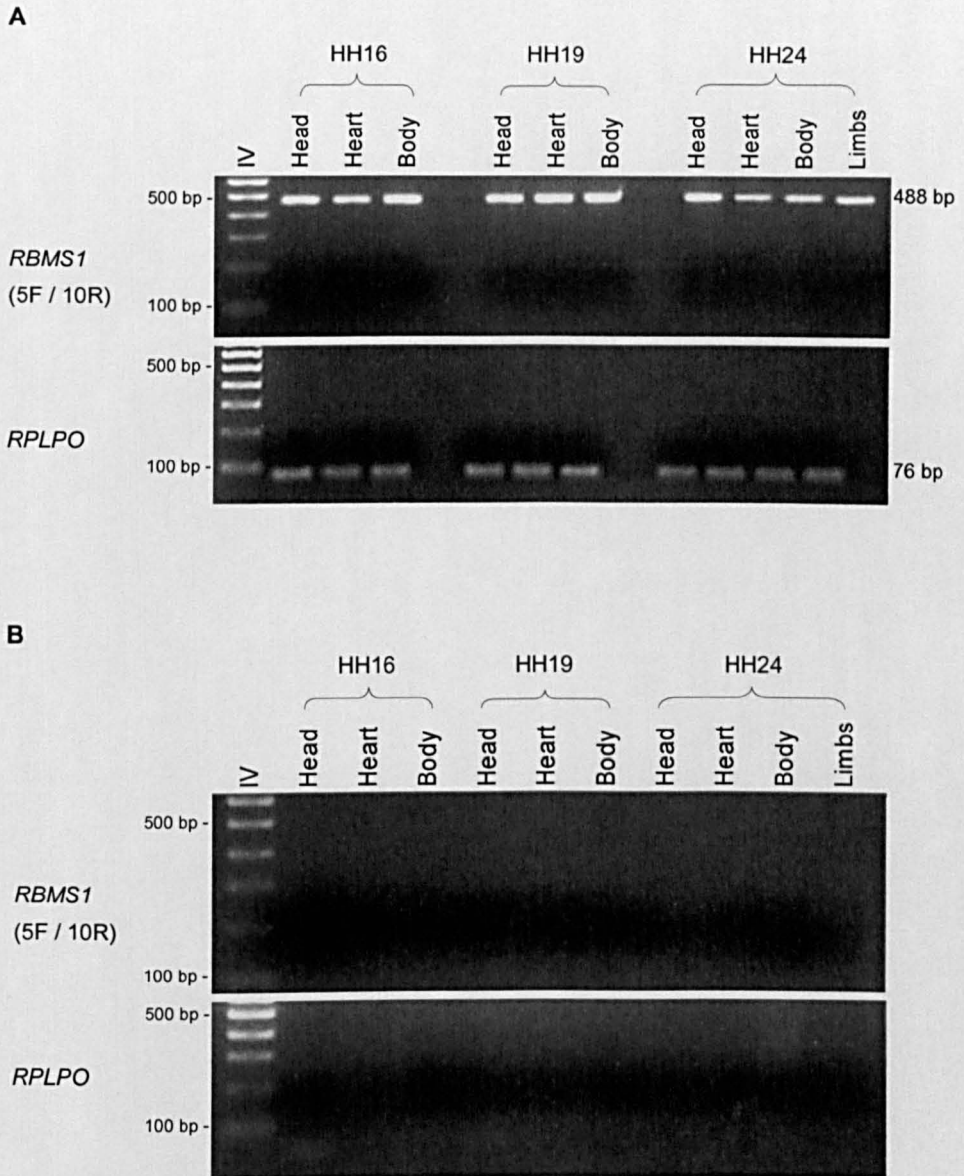


**Figure 5.6 RT-PCR expression analysis of RBMS1**

Products were electrophoresed on 2% agarose gels using Hyperladder IV (Bioline) as a size marker (500 bp and 100 bp bands are indicated along with product sizes). (A) Expression was examined in wild type chick embryonic body segments at HH16, HH19 and HH24. RPLPO was used as a housekeeping gene. (B) Negative RT controls where reverse transcriptase enzyme was not added were included for both genes and did not result in amplification.

### 5.3.2.2 Whole mount *in situ* hybridisation

RT-PCR expression analyses show that RBMS1 is expressed in the developing chick heart at HH12 – HH26 (Chapter 4), and throughout the embryo at HH16, HH19 and HH24 (Figure 5.6). These did not however allow identification of specific regions or structures of the heart giving rise to these signals. In order to obtain a more detailed picture of the localisation of RBMS1 transcripts, whole mount *in situ* hybridisation was performed. Two non-overlapping probes were generated against RBMS1 using the RT-PCR products shown in Figure 5.7, designed to bind to both RBMS1 transcripts. RT-PCR products were gel purified, cloned into the pGEM-T Easy vector, and sequenced in both directions for confirmation of sequence and determination of orientation. Clones selected contained insert in the forward orientation. Plasmid linearisation was carried out using an appropriate enzyme whose restriction site was not present within the insert, in this case *SpeI* for antisense probes, and *SacII* for sense probes (Appendix F). Single stranded DIG-labelled RNA probes were synthesised using a DIG RNA labelling mix by *in vitro* transcription with T7 RNA polymerase (antisense) or SP6 RNA polymerase (sense). Expression was examined at HH16, HH19 and HH24. For colour development, samples were incubated in fresh colour reagent at room temperature for 20 minutes in the dark, and longer as appropriate up to a maximum of 90 minutes due to the high strength of the signal. Background was reduced by washing in KTBT and a graded methanol series. Samples were stored in PBS and photographed in 70% glycerol.

RBMS1 expression was detected in the heart and throughout the embryo at all three stages of development, and represented in Figures 5.8 – 5.10. *In situ* hybridisation results for HH16 and HH19 early stage embryos (using the 5F/10R probe) are displayed in Figure 5.8. At HH16, staining to the heart was very weak, and other regions of the embryo including the somites displayed strong expression. The HH19 embryo displayed general expression, and staining to the heart was stronger at this stage. HH24 stage embryos are displayed in Figure 5.9 (probe 1F/5R) and Figure

5.10 (probe 5F/10R). RBMS1 displays expression in all areas of the heart, and is highly expressed in the developing forelimb and hind limb buds, somites, and brain.

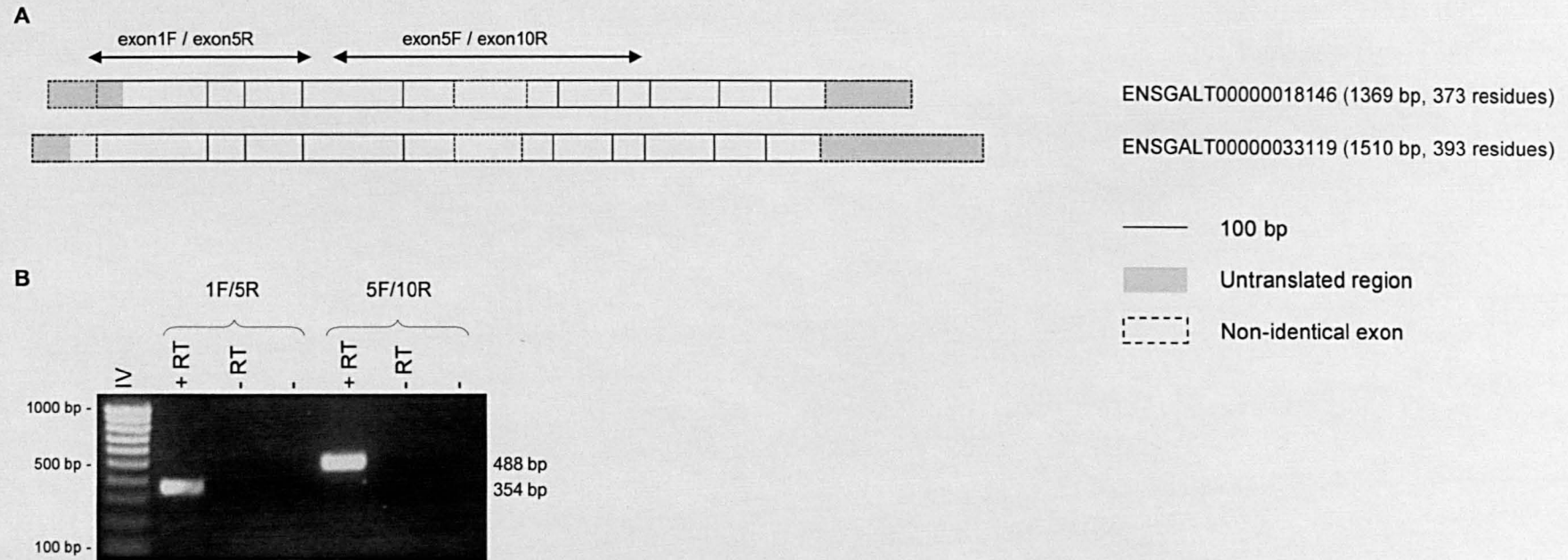


**Figure 5.7 Amplicons used for RNA probe synthesis**

(A) Representation of the two chicken RBMS1 mRNA transcripts, ENSGALT00000018146 and ENSGALT00000033119 are shown, and primer positions are indicated by the arrows. (B) RT-PCR products were amplified from HH19 chick heart cDNA and are displayed in the gel image, and product sizes are indicated

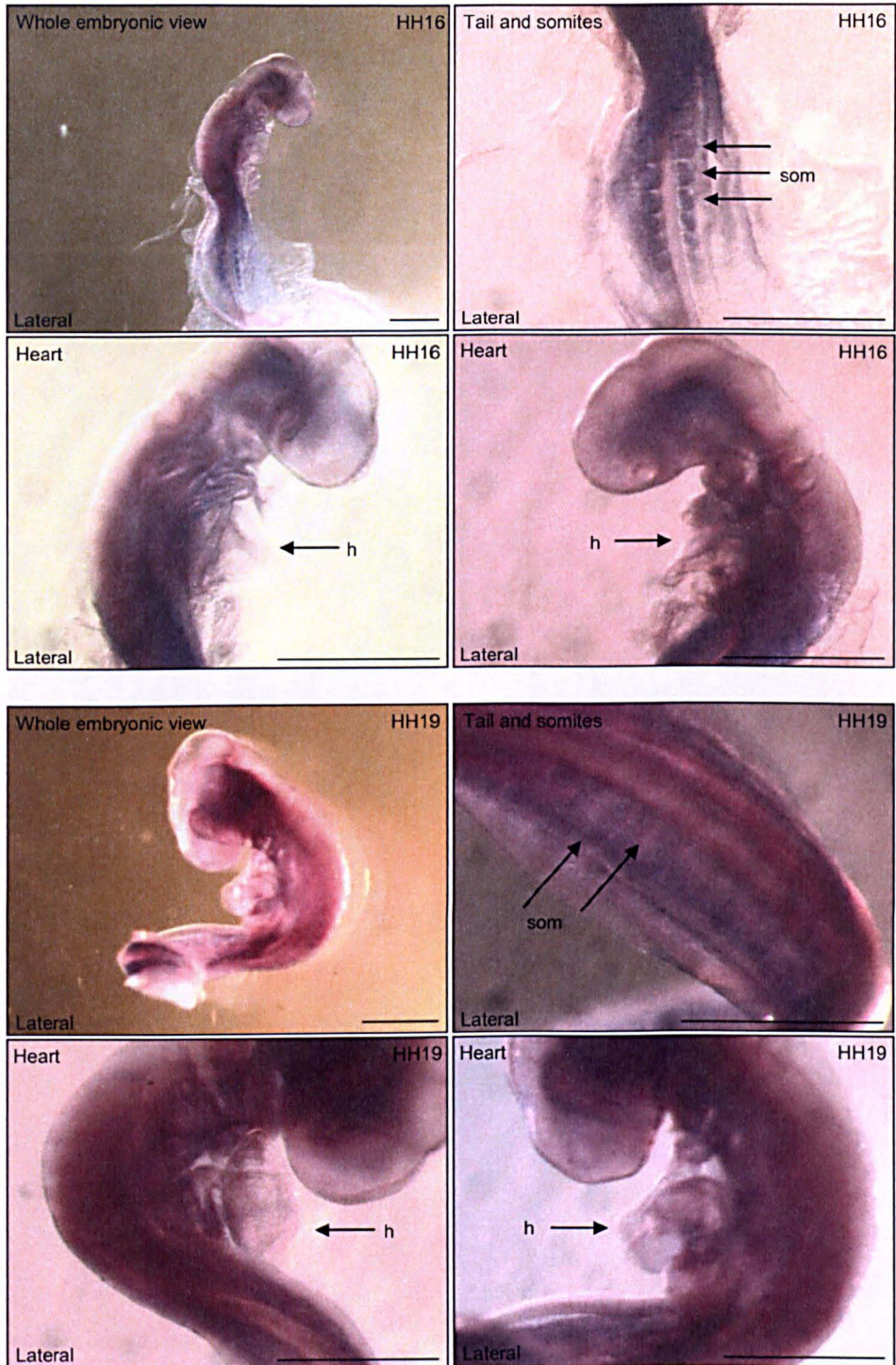


**Figure 5.8** *In situ* hybridisation expression analysis of RBMS1 in the HH16 and HH19 chick embryo using the 5F/10R probe

Lateral embryonic views of embryos are displayed, and embryonic age is indicated. Expression was detected with the 1F/5R antisense probe, using the corresponding sense probe as a control (shown in Figure 5.11). Scales bars represent 500  $\mu\text{m}$ . h – heart, som - somites

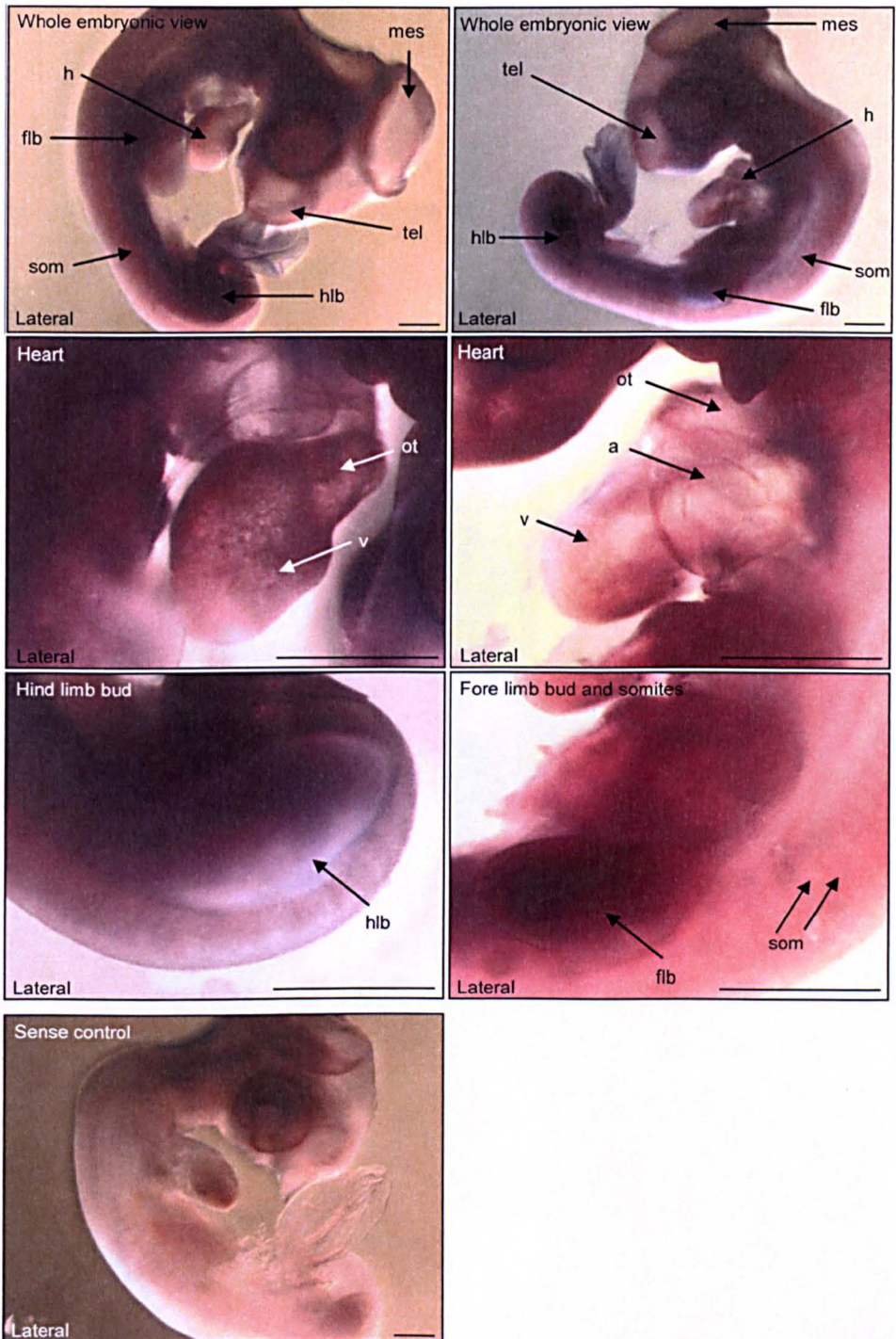


**Figure 5.9** *In situ* hybridisation expression analysis of RBMS1 in the HH24 chick embryo using the 1F/5R probe

Lateral embryonic views of embryos are displayed. Expression was detected with the 1F/5R antisense probe, using the corresponding sense probe as a control. Scales bars represent 500  $\mu$ m. tel – telencephalon, mes – mesencephalon, h – heart, ot – outflow tract, a – atrium, v – ventricle, hlb – hind limb bud, flb – forelimb bud, som - somite

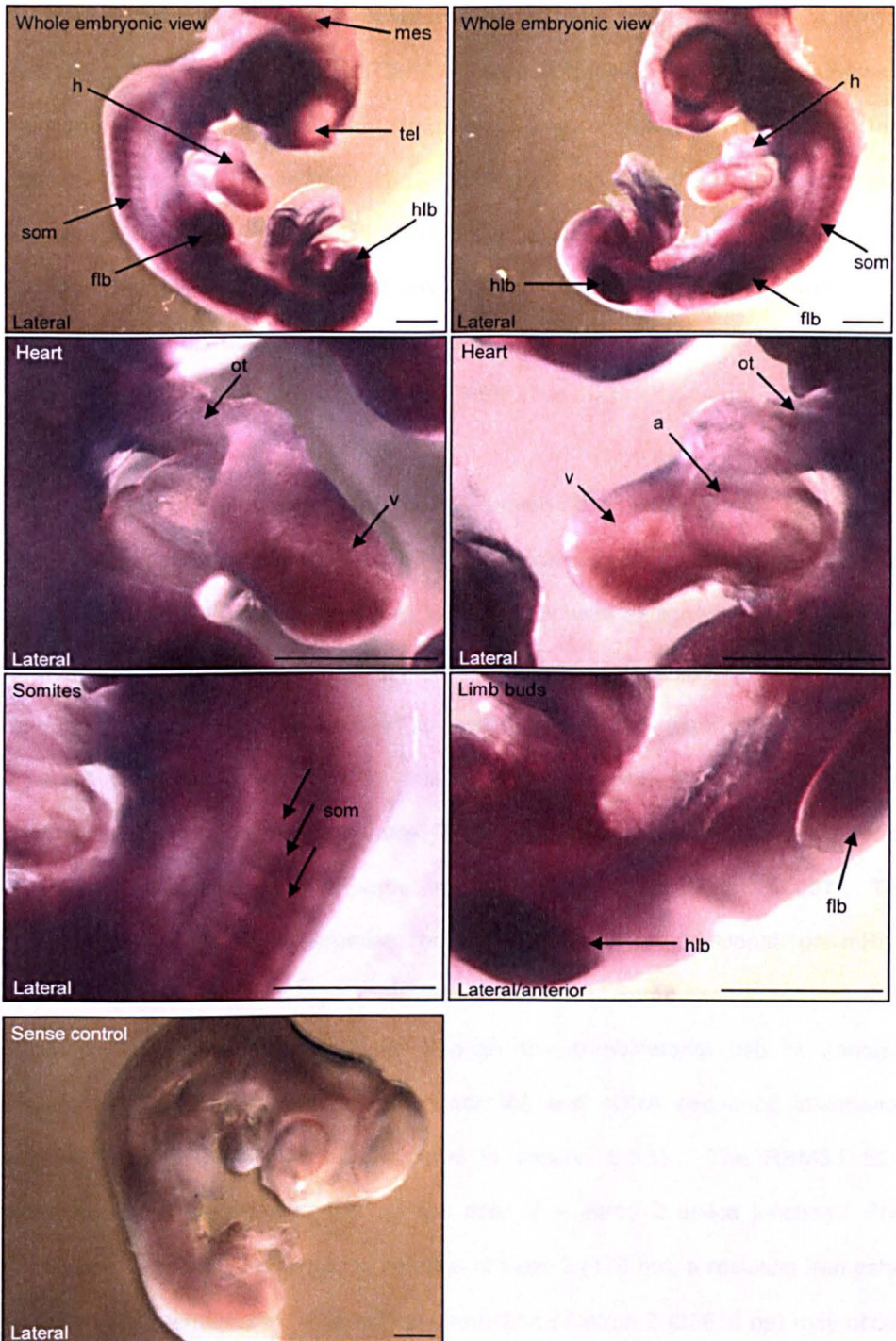


**Figure 5.10** *In situ* hybridisation expression analysis of RBMS1 in the HH24 chick embryo using the 5F/10R probe

Lateral embryonic views of embryos are displayed. Expression was detected with the 5F/10R antisense probe, using the corresponding sense probe as a control. Scales bars represent 500  $\mu\text{m}$ . tel – telencephalon, mes – mesencephalon, h – heart, ot – outflow tract, a – atrium, v – ventricle, hnb – hind limb bud, flb – forelimb bud, som - somite

### 5.3.3 RBMS1 morpholino knockdown studies

In order to investigate the role of RBMS1 in cardiac development, morpholino loss of function studies were carried out. Morpholinos were applied at HH10 – HH16, and embryos harvested for analysis at HH19. At HH10 - HH12, dextral looping of the heart occurs, and looping continues until HH17/HH18. Endocardial cushion formation in the AV canal has begun by HH12, and development of the interatrial septum begins at HH14. These are crucial stages in cardiac development, and gene knockdown at this time will provide information into the role of RBMS1 in these processes.

#### 5.3.3.1 Design of splice-junction targeting morpholinos and controls

Due to the presence of two RBMS1 mRNA transcripts, each potentially with a distinct ATG translational start site (Figure 5.4), morpholinos were designed to common splice junctions in order to modify gene splicing in both transcripts. Splice-blocking morpholinos can either be targeted to splice donor sites (exon-intron) or splice acceptor sites (intron-exon), and most commonly result in exon skipping, or alternatively in intron retention [Morcos, 2007]. Activation of cryptic splice sites may also occur, which can result in partial insertions or deletions [Morcos, 2007]. The design of splice-junction targeting morpholinos requires additional pre-mRNA sequence information, with well defined exon-intron and intron-exon junctions. This sequence information was obtained through the combinatorial use of genomic sequence information (extracted from *Ensembl*) and cDNA sequence information (verified with EST evidence, as outlined in section 5.3.1). The RBMS1 E2I2 morpholino was designed to bind to the exon 2 – intron 2 splice junction. This morpholino was predicted to cause deletion of exon 2 (176 bp), a resulting frameshift and premature termination. Alternatively, retention of intron 2 (25676 bp) may occur, also resulting in a premature termination. Morpholino sequence, target region and possible effects are displayed in Figure 5.11. A corresponding 5-base mismatch morpholino was also designed as a control of specificity and is displayed. Morpholino sequences are displayed in Table 2.8.

**Chicken RBMS1 E2I2 morpholino**

E2I2 5-mismatch morpholino

3' - ATACCGTTGCCATTGATGCTATCAA - 5'

E2I2 morpholino

3' - ATACGGTTGGCATTTCATGCTATGAA - 5'

Pre-mRNA

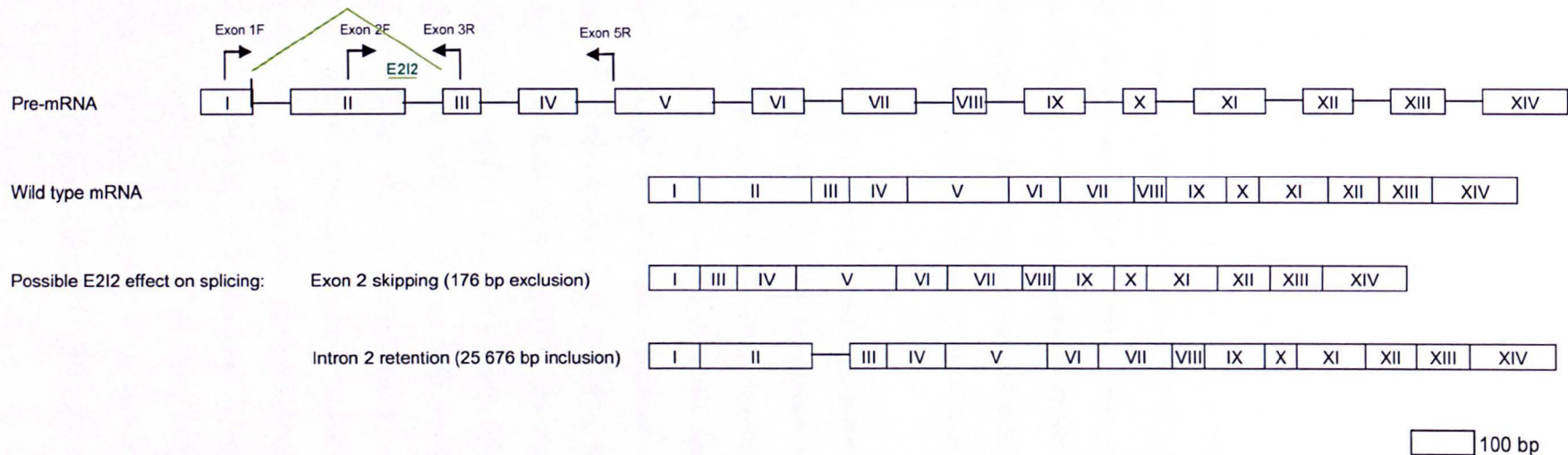
5' - GCACUGCCUCCAAACACCACUGAUCAGGACCU~~GGU~~AAAAUUAUGCCAACCGUAAGUACGAUACUUAAAUACGGAAUACGGAAUCGUACCUUAUAAGUUUG - 3'

mRNA

5' - GCACUGCCUCCAAACACCACUGAUCAGGACCUUAUGCCAACC - 3'

Protein

A L P P N T T D Q D L V K L C Q

**Figure 5.11 RBMS1 E2I2 and control morpholino sequences and predicted effects on mRNA splicing**

The shorter of the two mRNA transcripts (ENSGALT00000018146) is represented for simplicity; all morpholinos, primers etc have been designed to bind to common regions of both transcripts. Exons are drawn to scale, and intron sizes have been standardised. Morpholino sequences are shown in the 3' – 5' direction, and target binding regions are boxed.

Bases altered in mismatch control morpholinos are underlined.

### 5.3.3.2 Preliminary testing of morpholinos *in ovo*

Initial phenotypic analysis of embryos was carried out externally and is displayed in Figure 5.12. The degree of abnormality was determined by gross examination of embryo size and shape, followed by visual assessment of heart shape and structure. Figure 5.12 A1 and B1 depict wild type and standard control treated embryonic hearts, which display normal size, curvature and shape. Figure 5.12 C1 and C2 are examples of embryos treated with the E212 5-mismatch morpholino at 250  $\mu\text{M}$  and 500  $\mu\text{M}$  respectively, both displaying an abnormal heart shape and constriction to the ventricle. In total, 2 / 8 embryos treated with the mismatch control at 250  $\mu\text{M}$ , and 5 / 18 embryos treated at 500  $\mu\text{M}$  harboured a cardiac defect. Since these were similar to the abnormalities observed in knockdown embryos (discussed later in section 5.3.3.4), it was thought that the 5-base mismatch morpholino was still able to bind to the target region (as in Chapter 4), and a new control of specificity was required.

### 5.3.3.3 Selection and design of an alternative control of specificity

At the time of this research, it emerged that the use of mismatch morpholinos was no longer considered the best control of specificity (personal communication with Dr Jon Moulton, Gene-Tools). This was based on the frequency with which mismatch morpholinos were able to generate an effect due to retained binding capability to target sites, or off-target effects, as demonstrated in this thesis. Instead of moving to a 7-base mismatch control (as previously in Chapter 4), the use of a second non-overlapping targeting morpholino to the same gene was recommended in order to look for morpholino specificity upon generation of a common phenotype, since it was deemed unlikely the same off-target effect would be created by separate morpholinos. Morpholino specificity and effect on target mRNA or protein could then be determined by other means. Consequently, a second splice site morpholino was designed; the RBMS1 E818 morpholino was designed to bind to the exon 8 – intron 8 splice junction, and predicted to cause deletion of exon 8 (50 bp) and a resulting frameshift, or retention of intron 8 (92 bp) which would result in a premature stop. This is represented in Figure 5.13, and morpholino sequences are given in Table 2.8.

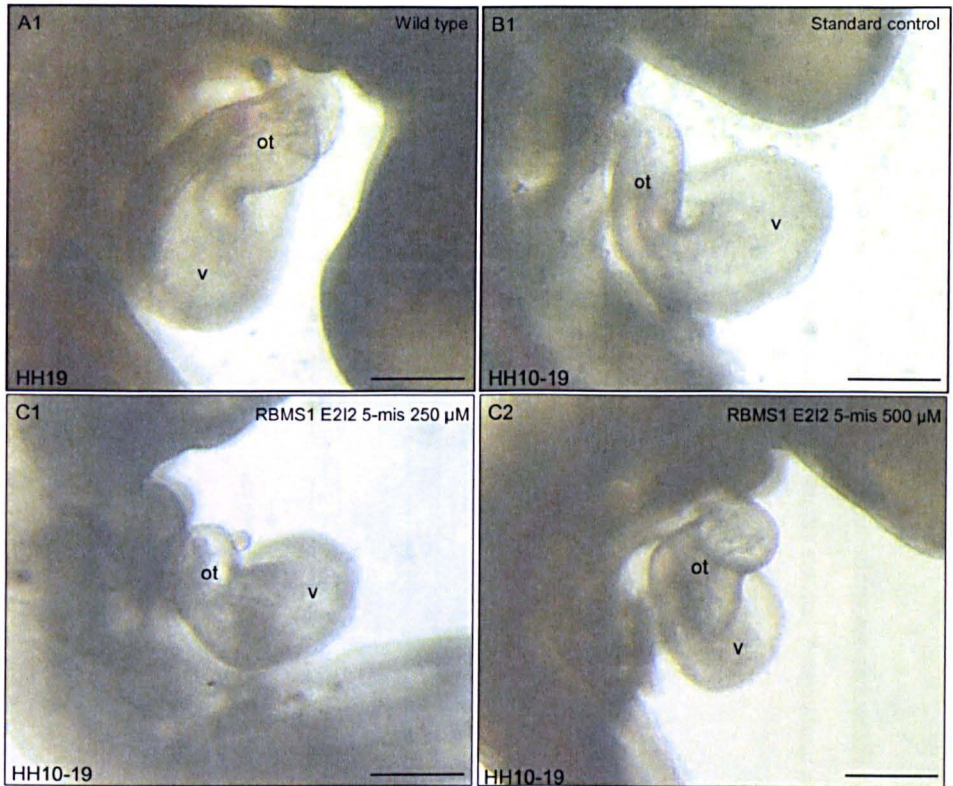


**Figure 5.12 External phenotypic analysis of embryos treated with RBMS1 E2I2 5-base mismatch morpholinos in comparison to standard control-treated and wild type embryos**

Bright field lateral embryonic views of wild type (A1), standard control (B1), and E2I2 5-mismatch control (C1-C2) are displayed with developmental stages of morpholino application and embryo harvest. Standard control morpholino was applied at a concentration of 500  $\mu\text{M}$ , and mismatch control morpholinos applied at both 250  $\mu\text{M}$  and 500  $\mu\text{M}$  as indicated. Scale bars represent 500  $\mu\text{m}$ . ot – outflow tract, v – ventricle

**Chicken RBMS1 E8I8 morpholino**

E8I8 morpholino

3' - TACCCATACAATTCACGACCATGTG - 5'

Pre-mRNA

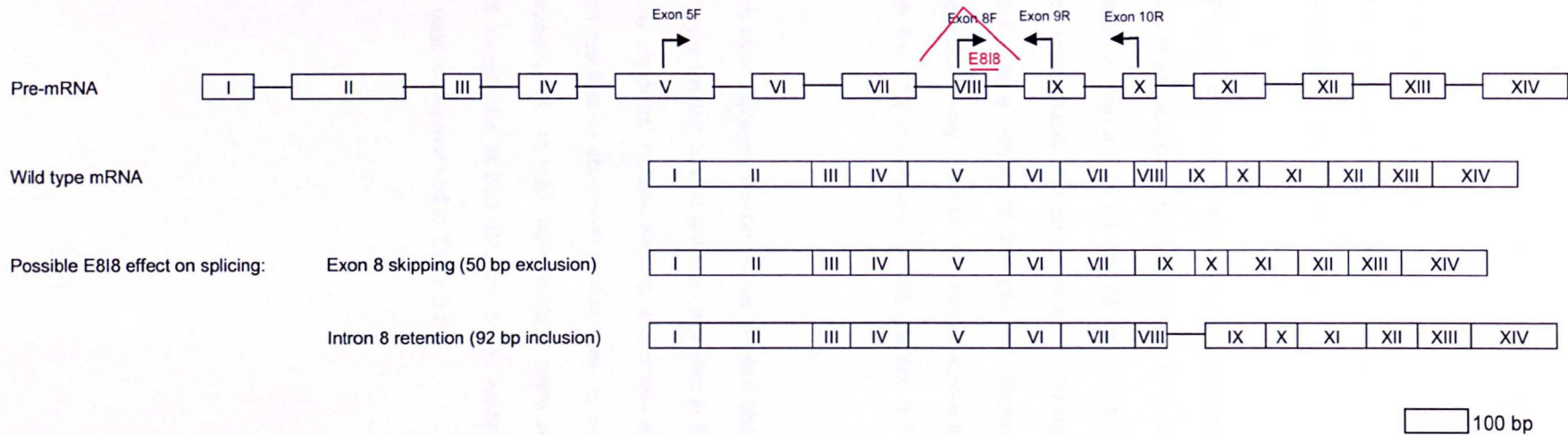
5' - GCUGGAAUGACACUCACUUUUGAUCCAACCACAGCUGCUUUACAAAUGGGUAUGUUUAGUGCUGGUACACUAAGAAAAAAAUGUUUGCAUUAUGAAAGUU - 3'

mRNA

5' - GCUGGAAUGACACUCACUUUUGAUCCAACCACAGCUGCUUUACAAAUGG - 3'

Protein

A G M T L T Y D P T T A A L Q N

**Figure 5.13 RBMS1 E8I8 morpholino sequence and predicted effect on splicing**

The shorter of the two mRNA transcripts (ENSGALT00000018146) is represented for simplicity; all morpholinos, primers etc have been designed to bind to common regions of both transcripts. Exons are drawn to scale, and intron sizes have been standardised. Morpholino sequences are shown in the 3' – 5' direction, and target binding regions are boxed. Bases altered in mismatch control morpholinos are underlined.

#### 5.3.3.4 External phenotypic analysis of RBMS1 knockdown embryos

External analysis focusing on embryonic hearts was performed on animals subjected to various morpholino treatments (Figure 5.14). Wild type and standard control treated embryos displayed no outward abnormalities (Figure 5.14 A1 and B1 respectively) whilst treatment with RBMS1 targeting morpholinos resulted in a range of cardiac abnormalities (Figure 5.14 C1-C4, D1-D4).

Treatment with the RBMS1 E2I2 targeting morpholino resulted in heart malformations at both concentrations of application (Figure 5.14 C1 – C4). Morpholino was applied to the embryos depicted in Figure 5.14 C1 and C2 at 250  $\mu$ M, and these respectively display an abnormal heart shape and defect in heart looping. Embryos shown in Figure 5.14 C3 and C4 were treated at 500  $\mu$ M and display a bulbous heart and irregular heart shape respectively. In total, cardiac abnormalities were seen in 2 / 11 embryos treated with the E2I2 morpholino at 250  $\mu$ M and 5 / 16 embryos treated at 500  $\mu$ M.

E8I8 treated embryos also displayed abnormalities in heart shape and looping (Figure 5.14 D1 – D4). Embryos treated at 250  $\mu$ M are displayed in Figure 5.14 D1 and D2, and respectively show abnormal cardiac looping and a thin almost tubular ventricle. Treatment at 500  $\mu$ M resulted in abnormal cardiac looping and heart shape (Figure 5.14 D3 and D4 respectively). In total, abnormalities were seen in 2 / 15 embryos treated with the E8I8 morpholino at 250  $\mu$ M, and 8 / 17 embryos treated at 500  $\mu$ M. Phenotypic analysis data is summarised in Table 5.2.

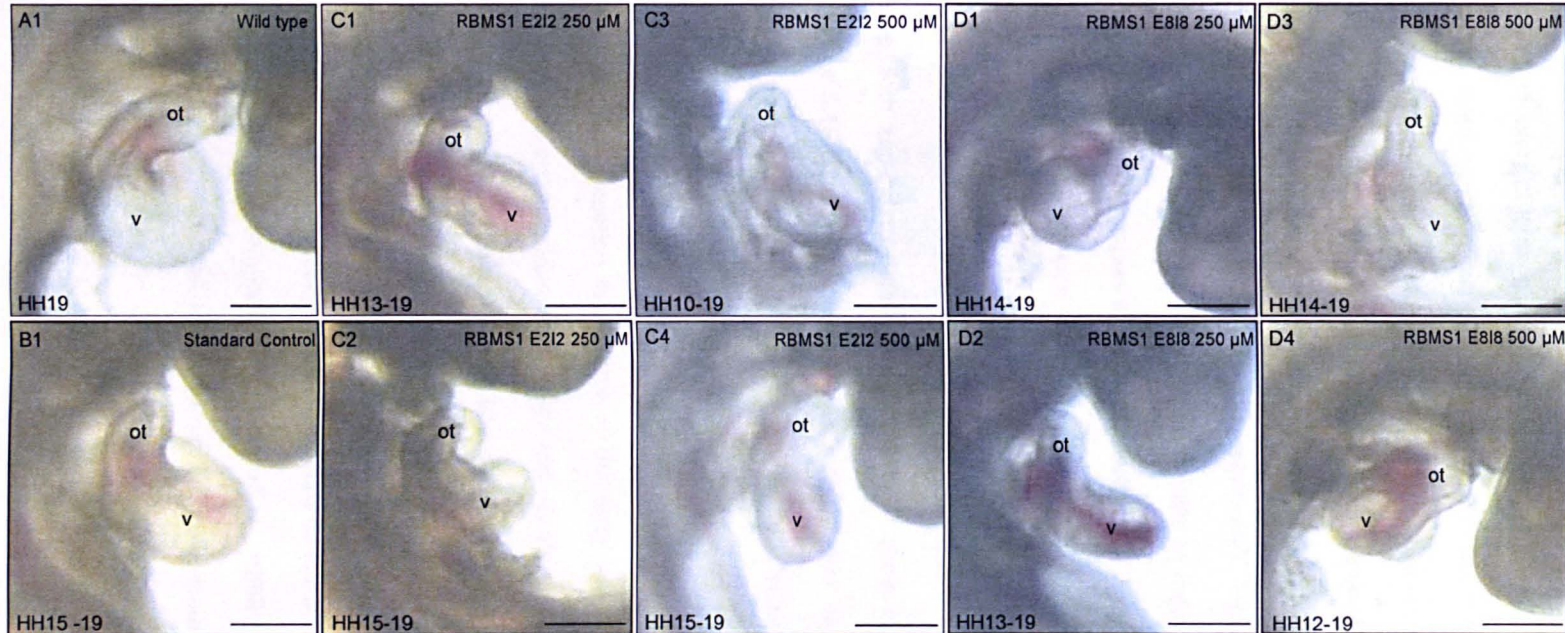


**Figure 5.14 Altered cardiac morphology of RBMS1 knockdown embryos**

Bright field lateral embryonic views of wild type (A1), standard control (B1), RBMS1 E2I2 applied at 250  $\mu\text{M}$  (C1-C2) and 500  $\mu\text{M}$  (C3 and C4), and RBMS1 E8I8 applied at 250  $\mu\text{M}$  (D1-D2) and 500  $\mu\text{M}$  (D3-D4) are displayed. Developmental stages of morpholino application and embryo harvest are indicated. Two examples of embryos subjected to each treatment are displayed. Scale bars represent 500  $\mu\text{m}$ . ot – outflow tract, v - ventricle

### 5.3.3.5 Histological analysis of RBMS1 knockdown embryos

Embryos were fixed in 4% PFA and dehydrated in a graded ethanol series prior to wax embedding. Embryos were sectioned coronally at a thickness of 10 microns, and sections transferred onto slides for haemalum staining and mounting with DPX. The high frequency of looping abnormalities did not always allow sectioning in the correct plane, resulting in difficulties in assessment of septum size in some cases. Figure 5.15 shows haemalum stained sections through control and knockdown embryos at points where the atrial septum is visible at its maximal size. Wild type and standard control embryos displayed a normal overall heart shape and structure including atrial septum size (Figure 5.15 A1 and B1 respectively). Treatment with the splice targeting morpholinos resulted in a reduction in the size of the atrial septum. Figure 5.15 C1 and C2 are two examples of embryos treated with the E212 morpholino at 250  $\mu$ M; C1 displayed a complete lack of septum, and C2 was normal. In total, 1 / 7 embryos in this treatment group displayed an internal cardiac defect. A larger proportion of embryos treated at 500  $\mu$ M displayed cardiac abnormalities (5 / 11), primarily in septal size, with secondary defects also present in some cases. Both examples shown (Figure 5.15 C3 and C4) are abnormal, with an atrial septum absent in C3. C4 shows septal growth but the heart is under-developed. Treatment with the E818 morpholino at 250  $\mu$ M (Figure 5.15 D1 and D2) did not have an effect on the internal structure of the heart (based on 8 embryos). However, treatment with this morpholino at 500  $\mu$ M resulted in a reduction in the size of the atrial septum in 6 / 13 cases. The two morpholinos produced overlapping but distinct abnormalities, which may be explained by the fact that each was targeted to a different region of the RBMS1 gene, resulting in different functional domains being affected in surviving proteins. This is observed with genes such as *TBX5* in HOS, where mutations in the 5' end of the T-box most significantly affect the heart, whilst mutations in the 3' end of the T-box have a more predominant effect on the limbs [Basson et al., 1999] (although there are exceptions [Boogerd et al.]). Overall, knockdown of RBMS1 resulted in refinement of the original phenotype observed in *TBX5* / *GATA-4* double knockdown embryos, with abnormalities restricted to the heart. This was surprising in view of the widespread

expression pattern of RBMS1, particularly when compared to the more restricted expression patterns of both TBX5 and GATA-4.

**Figure 5.15 Histological analysis of altered cardiac morphology of RBMS1 knockdown embryos at HH19**

Haemalum stained coronal embryonic sections through two embryos in each group are displayed. Groups represented are; (A) wild type, (B) standard control (500  $\mu$ M), (C) RBMS1 E212 (250  $\mu$ M and 500  $\mu$ M), and (D) RBMS1 E818 (250  $\mu$ M and 500  $\mu$ M). Developmental stages of morpholino application (where applicable) and embryo harvest are indicated. Regions of atrial septa formation (or expected septation) are boxed, shown at their maximum size upon viewing serial sections throughout embryo. Scale bars represent 500  $\mu$ m.

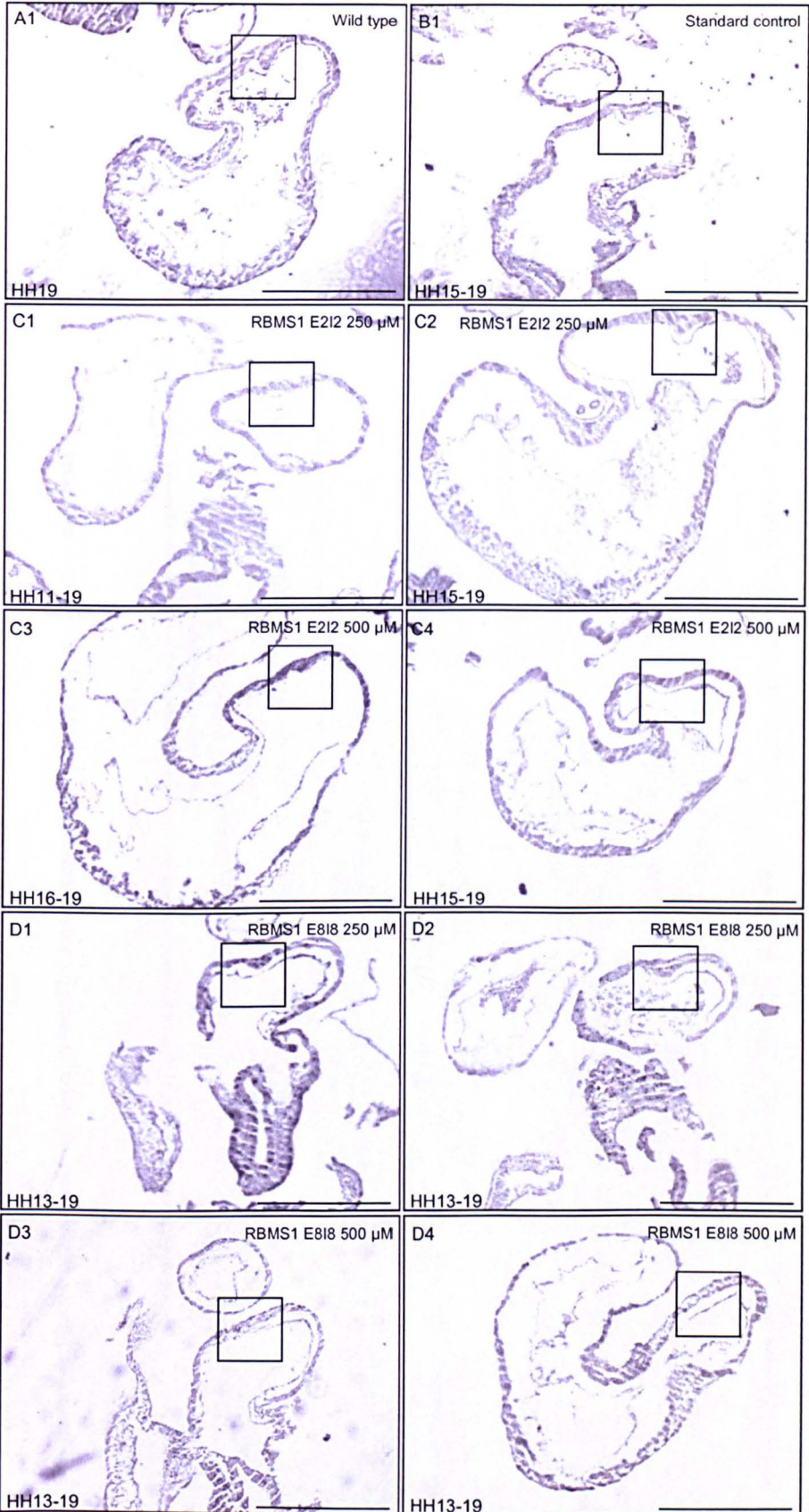


Table 5.1 Summary of heart abnormalities seen in RBMS1 knockdown embryos in comparison to controls

Nature/region of heart abnormality		Embryos with heart abnormality							
		Untreated (wild type)	Standard control 500 $\mu$ M	RBMS1 E2I2 5-mis 250 $\mu$ M	RBMS1 E2I2 5-mis 500 $\mu$ M	RBMS1 E2I2 250 $\mu$ M	RBMS1 E2I2 500 $\mu$ M	RBMS1 E8I8 250 $\mu$ M	RBMS1 E8I8 500 $\mu$ M
External analysis	Heart size / shape	1 / 30	0 / 10	2 / 8	2 / 18	1 / 11	3 / 16	2 / 11	6 / 17
	Heart looping	1 / 30	0 / 10	2 / 8	3 / 18	1 / 11	2 / 16	0 / 11	2 / 17
	Ventricle formation	0 / 30	0 / 10	0 / 8	0 / 18	0 / 11	0 / 16	0 / 11	0 / 17
	<b>Total</b>	<b>2 / 30</b>	<b>0 / 10</b>	<b>2 / 8</b>	<b>5 / 18</b>	<b>2 / 11</b>	<b>5 / 16</b>	<b>2 / 15</b>	<b>8 / 17</b>
Internal analysis	Atrial septation	1 / 10	0 / 10	1 / 1	2 / 3	1 / 7	5 / 11	0 / 8	6 / 13
	Trabeculation	0 / 10	0 / 10	1 / 1	1 / 3	1 / 7	3 / 8	0 / 8	0 / 6
	Cardiac jelly	0 / 10	0 / 10	0 / 1	0 / 3	0 / 7	0 / 8	0 / 8	0 / 13
	<b>Total</b>	<b>1 / 10</b>	<b>0 / 10</b>	<b>1 / 1</b>	<b>2 / 3</b>	<b>1 / 7</b>	<b>5 / 11</b>	<b>0 / 8</b>	<b>6 / 13</b>

Groups represented are wild type, standard control (500  $\mu$ M), RBMS1 E2I2 (250  $\mu$ M and 500  $\mu$ M), and RBMS1 E8I8 (250  $\mu$ M and 500  $\mu$ M).

### **5.3.4 Characterisation of morpholino effects on splicing**

For characterisation of morpholino effects on splicing, RT-PCR was carried out using strategically placed primers for detection of alternatively spliced products.

#### **5.3.4.1 RBMS1 E2I2 morpholino**

##### **5.3.4.1.1 Sample collection and preparation**

RBMS1 E2I2 morpholino was applied to approximately 100 eggs following exclusion of embryos which were no longer viable or not within the desired range of development (HH12 – HH16). Morpholino-treated embryos were excised from the egg at HH19, placed in sterile chilled PBS, and membranes quickly removed. Morpholino uptake was assessed under fluorescent light and positive hearts isolated and stored in *RNAlater* at -20 °C. Eight hearts were pooled per sample, and three biological replicates collected per group (2 groups: knockdown and wild type). RNA was column-extracted and concentration assessed by spectrophotometry. Exactly 1 µg RNA was used per 20 µl reverse transcription reaction, and samples made up to 100 µl prior to use.

##### **5.3.4.1.2 Primer placement for detection of alternatively spliced transcripts**

As previously mentioned, the E2I2 morpholino would be expected to result either in exon 2 skipping, or intron 2 retention (Figure 5.12). Morpholino binding to splice junctions can also result in activation of cryptic splice sites, leading to partial insertions or deletions. Primers were therefore designed to flank the entire region which may be affected, in order to determine the nature of the morpholino effect through amplification of alternatively spliced transcripts and assessment of their size. Thus, the initial set of primers was placed in exon 1 and exon 5. An additional set of primers was also designed to exon 2 and exon 3; these could amplify any products with partial intronic retention (dependent on the size of the intronic region retained). Due to the large size of intron 2 (25676 bp), it would not be possible to amplify this whole region by PCR in the event of full intronic retention. Instead, a third set of primers was

designed within intron 2 in order to attempt PCR amplification of a small portion of this region (243 bp) for comparison between knockdown animals and untreated controls. Primer sequences are given in Table 2.5. RPLPO was used as an internal control and amplified in parallel.

#### **5.3.4.1.3 RT-PCR amplification and sequencing of mRNA transcripts**

PCR products generated using the above primers are shown in Figure 5.16. PCR using exon 1F and exon 5R primers resulted in sole amplification of the wild type transcript (354 bp) in all samples. Amplification using a second set of primers, exon 2F and exon 3R, also generated a single wild type product (213 bp) in all samples. Amplification using the above primer pairs was performed using extension times ranging from 30 seconds to 5 minutes, all yielding the same result. Products were also sequenced (one knockdown and one wild type from each group) to assess whether alternative splicing events (which may not have altered product sizes) had occurred, and all transcripts detected were normal. A third set of primers designed to detect retention of intron 2 produced an intronic band of the expected size (243 bp) in all samples. This was thought to be a pre-mRNA transcript, as amplification did not occur in negative RT controls (where no reverse transcriptase enzyme was added). RPLPO was also assayed as an internal control.

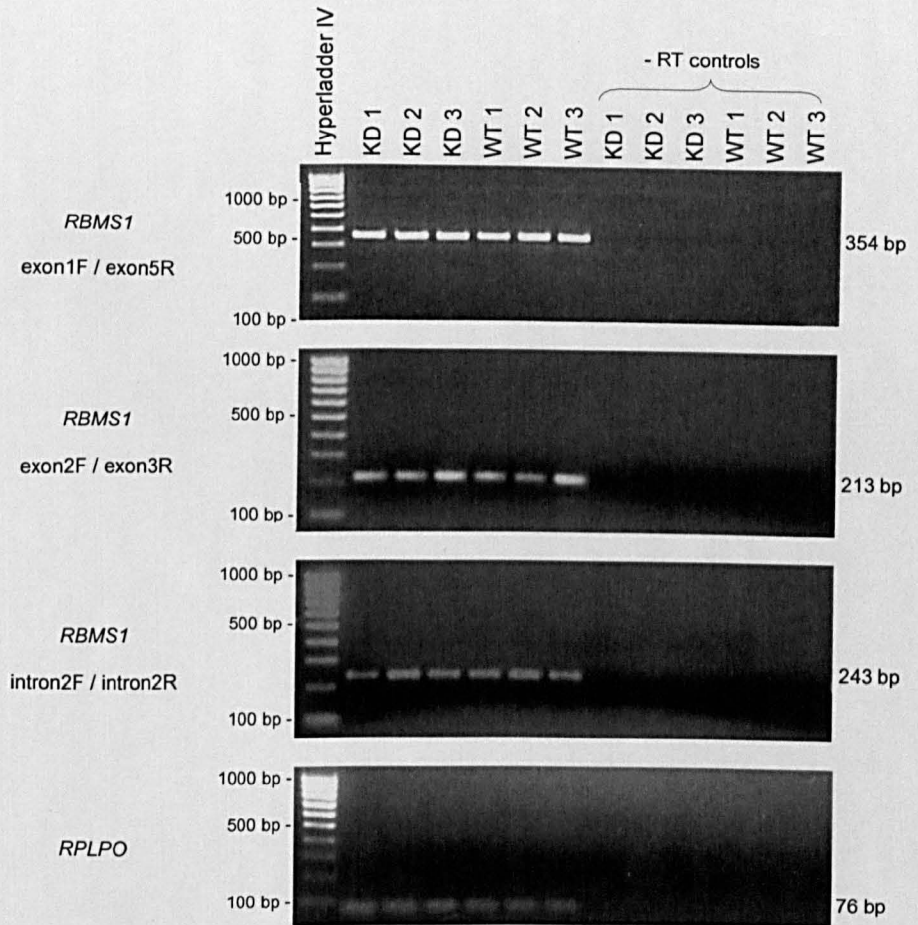


**Figure 5.16 Characterisation of the effect of the RBMS1 E2I2 morpholino on mRNA splicing**

PCR was performed at an annealing temperature of 60 °C with 35 cycles of amplification, and samples electrophoresed on 2% agarose gels. Three biological replicates were assayed for morpholino-treated and wild type groups. Three sets of primers were used for amplification of RBMS1 transcripts, and RPLPO was assayed in parallel as an endogenous control.

### **5.3.4.2 RBMS1 E818 morpholino**

#### **5.3.4.2.1 Sample collection and preparation**

Embryos were treated with morpholino as previously (section 5.3.4.1.1). Three wild type and three morpholino positive whole embryos were harvested at HH19, and RNA column extracted and quantified for cDNA synthesis using 1 µg RNA in a 20 µl volume. Samples were made up to 100 µl prior to use.

#### **5.3.4.2.2 Primer placement for detection of alternatively spliced transcripts**

The E818 morpholino would be expected to result in exon 8 skipping (50 bp), or intron 8 retention (92 bp) (Figure 5.13). Flanking primers were designed to exon 5 and exon 10 for detection of alternatively spliced transcripts. An additional set of primers was also designed to exon 8 / exon 9, which would result in amplification of products harbouring partial/full intron retention. Primer sequences are given in Table 2.5. RPLPO was included as an endogenous control.

#### **5.3.4.2.3 RT-PCR amplification and sequencing of mRNA transcripts**

Figure 5.17 shows results of RT-PCR amplification using the above primers. Both sets of primers resulted in amplification of a single wild type transcript in all samples i.e. alternatively spliced products were not found. The product generated from the KD1 sample appeared to be fainter than the others in both RT-PCR assays, and QPCR was used to quantify any changes (see next section, 5.3.5). RT-PCR products from a single wild type and knockdown sample were also sequenced to assess any changes, but only wild type sequences were detected.

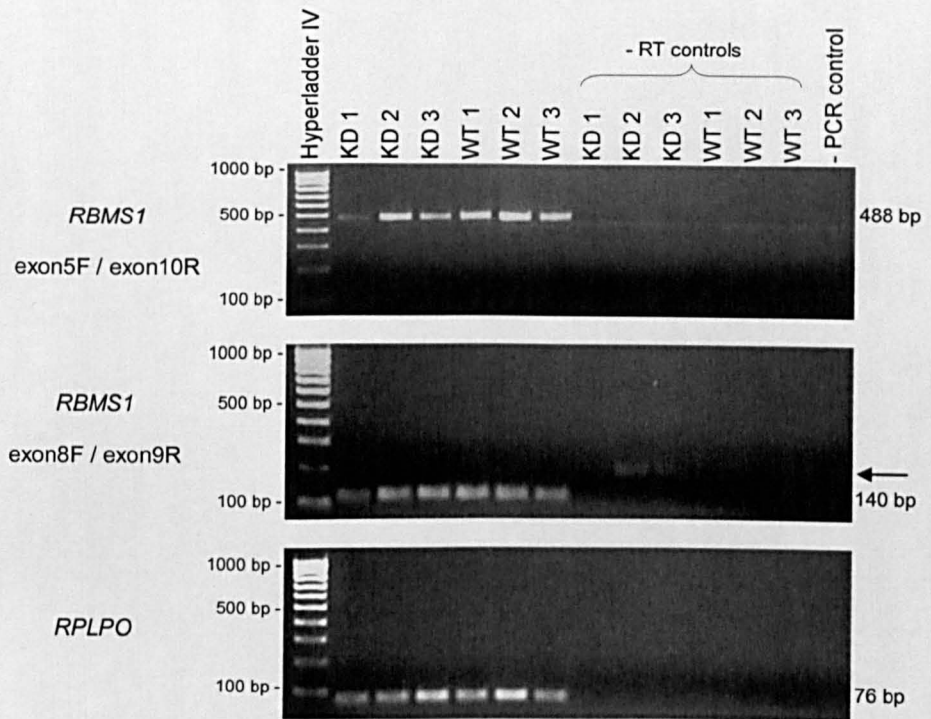


**Figure 5.17 Characterisation of the effect of the RBMS1 E8I8 morpholino on mRNA splicing**

PCR was performed at an annealing temperature of 60 °C with 35 cycles of amplification, and samples electrophoresed on 2% agarose gels. Three biological replicates were assayed per group. Two sets of primers were used for amplification of RBMS1 transcripts, and RPLPO was assayed in parallel as an endogenous control. The arrow indicates bands generated from low level genomic contamination in -RT samples KD2 and KD3 (152 bp product).

### **5.3.5 QPCR analysis of morpholino effects on mRNA levels**

RT-PCR did not result in detection of alternatively spliced products as a result of treatment with either morpholino. Nonsense-mediated decay (NMD) is a cellular mechanism in which aberrant mRNAs are detected (through recognition of premature termination codons (PTCs)), and degraded [Hentze and Kulozik, 1999]. It was possible that NMD was eliminating alternatively spliced transcripts in morpholino-treated embryos, which would result in a corresponding decrease in wild type RBMS1 mRNA transcripts. QPCR expression analysis was performed in order to quantify any morpholino-induced change in RBMS1 mRNA levels. RNA isolated previously for splicing characterisation was used, and new reverse transcriptase reactions were performed. Dilutions of cDNA were carried out immediately upon synthesis, as described in 2.2.1.10.5.

#### **5.3.5.1 Validation of RPLPO as an appropriate endogenous control**

RPLPO was used in Chapter 4 as an endogenous control for normalisation of data, where its suitability was assessed by study of assay properties and analysis of variation of expression levels in study samples. In order to confirm that RPLPO expression was not affected by samples treatments here,  $C_T$  values of RPLPO were measured in triplicate for each sample following their identical preparation and dilution, and are displayed in Table 5.2. RPLPO displayed constant expression across samples for both experimental groups ( $\Delta C_T$  values of -0.24 (E2I2 treatment) and 0.16 (E8I8 treatment)), and was used as an endogenous control gene.

**Table 5.2 Mean  $C_T$  and  $\Delta C_T$  values of RPLPO in study samples**

<b>Morpholino</b>	<b>Sample</b>	<b>Mean <math>C_T</math></b>	<b><math>\Delta C_T</math></b>
RBMS1 E2I2	Wild type (calibrator)	25.42368	0
	Morpholino treated	25.66415	-0.24048
RBMS1 E8I8	Wild type (calibrator)	18.03443	0
	Morpholino treated	17.87218	0.162246

Three biological samples were analysed per group, each assayed in triplicate. A standard curve was run in parallel on the same reaction plate for confirmation of assay quality.

### 5.3.5.2 QPCR analysis of RBMS1 in morpholino treated embryos

Baseline and threshold values were set manually, and absolute quantities of each gene generated from the standard curves in Applied Biosystems 7500 v2.0.1 software. Standard curves for target and endogenous control genes were included on each plate, with each point measured in duplicate. All samples were run simultaneously on the same plate, each assayed in triplicate. Biological and experimental replicates were grouped for data normalisation and standard deviation calculations. Results of QPCR analysis are shown in Table 5.3 and Figures 5.18 and 5.19. No difference in mRNA levels of RBMS1 was observed between morpholino treated and wild type animals (data non-significant by student's t test). It is not clear why these approaches (both RT-PCR and QPCR) did not show any change at the mRNA level, given the identical and specific phenotype generated by the two morpholinos.

**Table 5.3 QPCR expression analysis of RBMS1 in E212 and E818 morpholino treated animals and controls**

Morpholino	RBMS1 relative expression	
	Morpholino treated	Wild type
RBMS1 E212	1.01 ± 0.44	1.04 ± 0.19
RBMS1 E818	0.39 ± 0.11	0.41 ± 0.12

QPCR expression analysis was performed on RBMS1 E212 morpholino treated embryonic hearts (8 per sample), and E818 treated whole embryos (1 per sample), each with corresponding wild type controls. 3 biological replicates were assayed per group. Expression is measured relative to the endogenous control RPLPO. Data was not significant (student's t test,  $p < 0.05$ ).

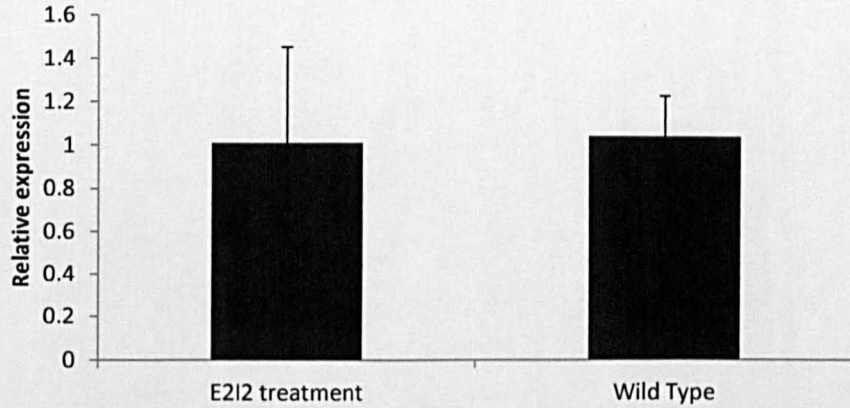


**Figure 5.18 QPCR expression analysis of RBMS1 in E2I2 morpholino treated animals and controls**

QPCR expression analysis was performed on RBMS1 E2I2 morpholino treated embryonic hearts (8 per sample), with corresponding wild type controls. 3 biological replicates were assayed per group. Expression is measured relative to RPLPO. Error bars represent standard deviation. Data was not significant by student's t test.

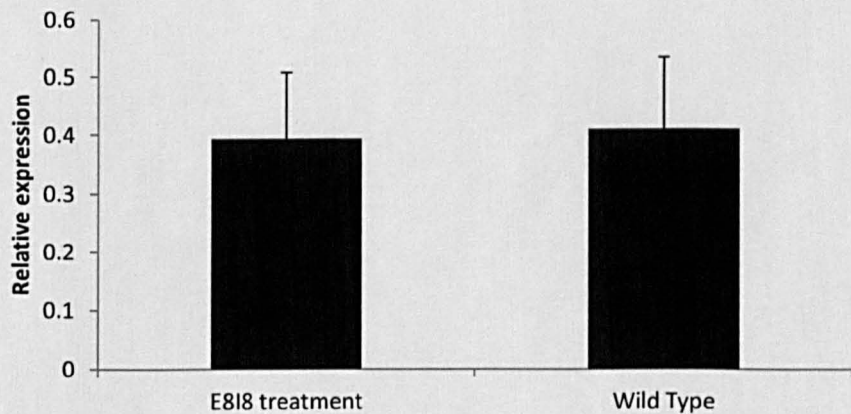


**Figure 5.19 QPCR expression analysis of RBMS1 in E8I8 morpholino treated animals and controls**

QPCR expression analysis was performed on E8I8 morpholino treated whole embryos (1 per sample), with corresponding wild type controls. 3 biological replicates were assayed per group. Expression is measured relative to RPLPO. Error bars represent standard deviation. Data was not significant by student's t test.

### 5.3.6 Bioinformatic promoter analysis of the $\alpha$ -actin genes

The  $\alpha$ -actins are likely to have arisen from a common ancestral gene and show a high level of sequence similarity. Work by others has shown that RBMS1 negatively regulates expression of  $\alpha$ -smooth muscle actin via a TATCTTA sequence found in the promoter region at position -228 to -222 [Kimura et al., 1998]. Due to the high degree of conservation between  $\alpha$ -smooth muscle actin and other  $\alpha$ -actins ( $\alpha$ -skeletal and  $\alpha$ -cardiac actin), it was postulated that RBMS1 may also play a role in the transcriptional regulation of these genes. The TATCTTA motif in  $\alpha$ -smooth muscle actin displays only partial conservation (57%) with other species such as human, rat and mouse [Kimura et al., 1998]. This means that multi-species alignment for promoter analysis (as performed in Chapter 3) would not be an appropriate tool for identification of this motif. Promoter analysis was instead performed to examine the presence of the TATCTTA regulatory sequence solely in chicken striated  $\alpha$ -actin genes, using the 'fuzznuc' search function (<http://emboss.bioinformatics.nl/>) which searches for patterns in nucleotide sequences. The TATCTTA motif was identified in both striated actin genes, located approximately 7 kb and 4.5 kb upstream of the first exon of  $\alpha$ -cardiac and  $\alpha$ -skeletal actin respectively. The position of these in relation to transcriptional start sites has not been determined. Additional motifs were identified within the coding regions and further 3'.

### **5.3.7 QPCR expression analysis of the actin genes in RBMS1 E2I2 morpholino treated animals and controls**

RBMS1 negatively regulates transcription of  $\alpha$ -smooth muscle actin, which means this gene can act as a positive control for knockdown. QPCR expression analysis was performed to assess whether  $\alpha$ -smooth muscle actin and other  $\alpha$ -actin genes were up-regulated in RBMS1 E2I2 morpholino treated embryonic hearts. The effect of the E8I8 morpholino on expression of these genes would also have been performed, but time restrictions did not allow this.

#### **5.3.7.1 QPCR assay design**

As previously, QPCR assays were designed using the online Roche Universal ProbeLibrary assay design centre (<https://www.roche-applied-science.com>) following the same general guidelines. Sequence alignments between the three  $\alpha$ -actins were performed for design of assays to regions of maximal diversity for gene-specificity. The relevant regions including primer and probe binding sequences and RT-PCR products generated are shown in Figure 5.20. Amplicons were cloned into the pGEM-T Easy vector for sequencing to confirm assay specificity. Primer sequences and positional information are given in Table 2.6.

**$\alpha$ -smooth muscle actin**  
 $\alpha$ -skeletal muscle actin  
 $\alpha$ -cardiac muscle actin

GCACCTGAGGACATTGACATAGAAGATGTGTGAGGAGGAGGACAGCACTGCCCTTGTTTGTGACAATGGCTCAGGGCTCTGTAA  
 -----  
 -----ATCAGCCAAGATGTGTGACGACGAGGAGACCACCGCGTGGTGTGCGACAACGGCTCGGGGCTGGTCAA

$\alpha$ -smooth muscle actin  
 **$\alpha$ -skeletal muscle actin**  
 $\alpha$ -cardiac muscle actin

AGCATATTACTGTGAATGTATTCAGGAAAATACATTCTTAAATTTTCATTCCATAAATCTTTCATCGTAATGGCTGGTTAATTGGATACGGTGTA  
TGCCAACCAC-----ACTCAGGATGACA-ATCTTGTAGGTTCCAGGCTGCTGAGGACC---TGCACCAGCCATGCAACTT-----TC  
 TTCCCACTCAG-----GATGACGACAGTATGCTTCTTGGAGTCT--TCTGGCAGCCCTTC--CTGAACTCCTCCGTCATTGTACAGTTGTT

$\alpha$ -smooth muscle actin  
 $\alpha$ -skeletal muscle actin  
 **$\alpha$ -cardiac muscle actin**

TGAAAACGAGATGGCCACTGCTGCCTCTTCCTCCTCTCTGGAAAAAGCTATGAGCTTCTGATGGC  
 TGAGAACGAGATGGCCACCGCTGCCTCCTCCTCCTGGAGAAAGAGCTATGAGCTGCCTGATGGG  
 TGAGAATGAAATGGCCACAGCTGCTTCGTCATCCTCCCTGGAGAAGAGCTACGAATTGCCTGATGGT

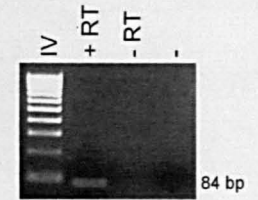


**Figure 5.20** QPCR assays used for expression analysis of the three actin genes

Primer binding sites are underlined, and probe binding sites are boxed. Sequences have been aligned with the corresponding region of the other two  $\alpha$ -actin genes (shown in grey). 2% agarose gel images displaying the RT-PCR products generated are shown on the right. Specificity of each assay was confirmed by sequencing of RT-PCR products following cloning into the pGEM-T Easy vector.

### 5.3.7.2 Expression analysis

QPCR expression analysis was performed using the same samples as previously, on RBMS1 E2I2 morpholino treated embryonic hearts (8 per sample) and corresponding wild type controls. Three biological replicates were assayed per group. Data was normalised to RPLPO. Table 5.5 and Figure 5.21 show results obtained from QPCR analysis of the  $\alpha$ -actins in E2I2 treated embryos and controls. Expression was measured relative to RPLPO. In wild type HH19 embryonic hearts,  $\alpha$ -cardiac actin was the most highly expressed actin, followed by  $\alpha$ -skeletal actin, with  $\alpha$ -smooth muscle actin displaying the lowest level of expression. Expression of  $\alpha$ -smooth muscle actin was found to be greater in the E2I2 treatment group than in wild type embryos (significant by the student t test,  $p < 0.05$ ). No significant differences in expression of the striated actins were observed between the treated and untreated groups.

**Table 5.5 QPCR expression analysis of actin genes in RBMS1 E2I2 morpholino treated animals and controls**

Gene	Relative expression	
	RBMS1 E2I2 treatment	Wild Type
$\alpha$ -smooth muscle actin	$3.87 \pm 1.13^*$	$2.25 \pm 0.95$
$\alpha$ -skeletal muscle actin	$30.3 \pm 8.28$	$23.4 \pm 8.48$
$\alpha$ -cardiac muscle actin	$29.3 \pm 11.6$	$33.1 \pm 4.31$

QPCR expression analysis was performed on RBMS1 E2I2 treated animals and wild type controls (3 biological replicates per group). Expression is measured relative to the endogenous control RPLPO. \*Significant difference between E2I2 treated sample and wild type control ( $p < 0.05$ , student's t test).

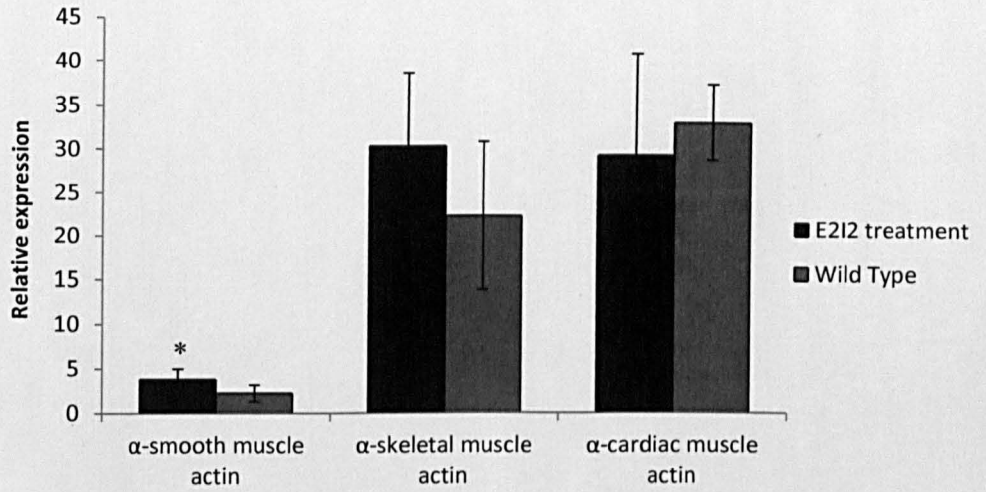


**Figure 5.21 QPCR expression analysis of the three actin genes in RBMS1 E2I2 morpholino treated animals and controls**

QPCR expression analysis was performed on RBMS1 E2I2 treated animals and wild type controls (3 biological replicates per group). Expression is measured relative to the endogenous control RPLPO. Error bars represent standard deviation. \*Significant difference between E2I2 treated sample and wild type control ( $p < 0.05$ , student's t test).

## CHAPTER 6

### MICROARRAY EXPRESSION ANALYSIS OF TBX5 / GATA-4 DOUBLE KNOCKDOWN EMBRYOS

#### 6.1 AIMS

This chapter aims to identify new downstream targets of TBX5 and GATA-4 in the developing chick heart by performing microarray analysis of double knockdown embryos as follows:

- a) Morpholino knockdown and collection of tissue. Extraction of RNA and assessment of concentration and purity
- b) Microarray expression analysis of TBX5 / GATA-4 double and single knockdown embryos and controls
- c) Review of literature and selection of candidate genes for further study
- d) Preliminary expression analyses in the chick embryo

## 6.2 RESULTS

### 6.2.1 Morpholino knockdown and tissue collection

Morpholinos were applied as described previously (Chapter 4) to create five sample groups:

- 1) TBX5 and GATA-4 double knockdown
- 2) TBX5 single knockdown (with GATA-4 7-mismatch control)
- 3) GATA-4 single knockdown (with TBX5 7-mismatch control)
- 4) TBX5 7-mismatch control and GATA-4 7-mismatch control
- 5) Wild type

Approximately 300 eggs were opened in total for this study. Morpholino was applied to around half following exclusion of embryos which were no longer viable or not at the required stage of development. Morpholinos were applied at HH15 for harvest at HH19 at a concentration of 250  $\mu$ M each, and uptake was assessed by fluorescent microscopy. Morpholino positive embryonic hearts were isolated and stored in RNA $\text{later}$  prior to appropriate pooling of samples for column extraction of RNA. One sample was collected per experimental group, each comprising eight hearts (this was found to be the minimum number of HH19 stage hearts required for successful isolation of RNA). It would have been preferable to include three samples per experimental group; however resource did not allow this. As a result, this approach does not provide enough statistical power, and data will require further validation either by subsequent addition of a further two samples per group for microarray analysis, or by QPCR validation using a minimum of three samples per group.

### 6.2.2 Assessment of RNA quality

High RNA purity and quality is of paramount importance in applications such as microarray expression analysis. Impurities can affect RNA labelling efficiency and the stability of the fluorescent label. RNA concentration and purity was initially measured

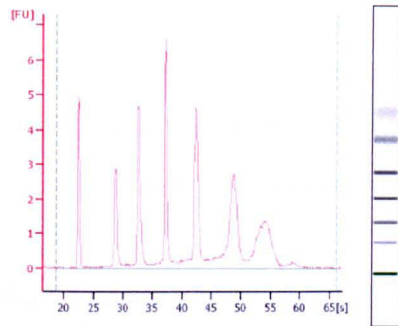
by spectrophotometry, and is displayed in Table 6.1. All samples displayed 260/280 ratios of approximately 2, and 260/230 ratios equal to or greater than 1.8, indicating high RNA purity. Samples were sent to the Nottingham Arabidopsis Stock Centre (NASC) for further QC analysis of RNA using the Agilent bioanalyser, and subsequent microarray expression profiling. Traditionally, RNA integrity is assessed by agarose gel electrophoresis, but this method requires large amounts of sample RNA (0.5 – 2.0 µg) and is not very sensitive in detecting degradation. The bioanalyser allows capillary based electrophoretic sample separation according to molecular weight, and subsequent fluorescent detection to generate electropherogram and in gel-like images. It requires far smaller quantities of RNA (as low as 200 pg) and is a more sensitive and reliable method [Imbeaud et al., 2005]. Figure 6.1 shows bioanalyser RNA profiles and in gel-like images generated using the five samples purified for microarray analysis. The two peaks represent the 18S and 28S ribosomal RNA subunits, and the absence of smaller degradation products indicates high quality RNA. RNA integrity numbers (RIN) are a means of numerically categorising sample integrity from electrophoretic traces, and range from 1 (fully degraded RNA) to 10 (intact RNA) [Schroeder et al., 2006]. RIN values generated are displayed in Table 6.1 and ranged from 9.3 to 10, indicating intact RNA.

**Table 6.1: RNA concentration, purity, and integrity of samples used for microarray expression analysis**

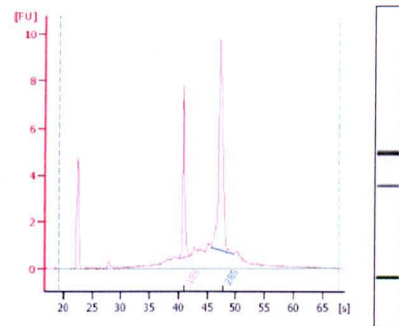
Sample	Spectrophotometry			Bioanalysis
	260 / 280	260 / 230	Concentration (ng / $\mu$ l)	RIN value
TBX5 / GATA-4 double knockdown	2.11	1.79	240.8	9.3
TBX5 knockdown (+ GATA-4 7-mis)	2.09	2.07	157.2	9.4
GATA-4 knockdown (+ TBX5 7-mis)	2.05	2.04	339.3	10
TBX5 7-mis / GATA-4 7-mis	2.09	1.99	315.8	9.9
Wild Type	2.09	2.16	282.0	9.8

RNA concentration and purity was measured by spectrophotometry, and RNA integrity numbers (RIN) assessed using a bioanalyser. All samples displayed 260/280 ratios of approximately 2, and 260/230 ratios greater than or equal to 1.8, indicating high RNA purity. RIN numbers ranged from 9.2 to 10, indicating RNA was intact.

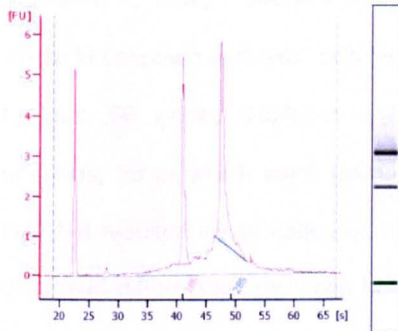
**Ladder**



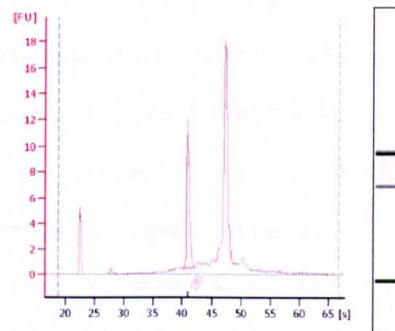
**TBX5 / GATA-4 double knockdown**



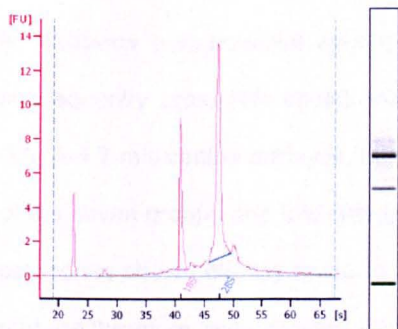
**TBX5 knockdown (+ GATA-4 7-mis)**



**GATA-4 knockdown (+ TBX5 7-mis)**



**TBX5 7-mis / GATA-4 7-mis**



**Wild type**

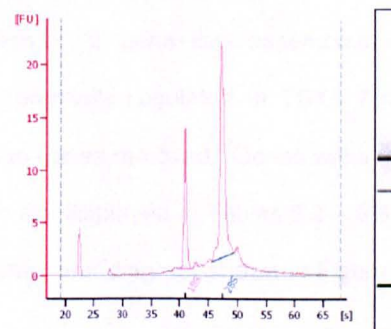


**Figure 6.1 Bioanalyser analysis of RNA samples prior to microarray analysis**

Bioanalyser QC analysis of RNA was performed by NASC. Electropherograms are displayed with in gel-like images to the right. The two peaks represent the 18S and 28S ribosomal RNA subunits, and the absence of smaller degradation products indicates high quality RNA. RIN values ranged from 9.3 - 10 and are displayed in Table 6.1.

### **6.2.3 Microarray expression study**

Microarray expression profiling analysis was performed by the NASC using the Affymetrix GeneChip® Chicken Genome Array. Probe sets on this array are designed with 11 oligonucleotide pairs for specific detection of transcripts. Each array contains coverage of over 28000 chicken genes and 32773 transcripts.

#### **6.2.3.1 Analysis of data**

Data was analysed in GeneSpring software (Agilent). Genes displaying changes of 2-fold or greater in comparison to wild type embryos were selected. Genes differentially regulated in TBX5 / GATA-4 double knockdown, TBX5 single knockdown, GATA-4 single knockdown embryos, and overlapping categories are represented in Figure 6.2. In total, 56 genes displayed altered expression in TBX5 / GATA-4 knockdown embryos, 28 of which were unique to this group. Single knockdown of TBX5 and GATA-4 resulted identification of 109 and 67 genes respectively. A number of genes displayed differential regulation both in response to double knockdown of TBX5 and GATA-4, and in response to single knockdown of one or both of these transcription factors. These genes were also of relevance, particularly those displaying a greater fold change in expression in the double knockdown group compared to single knockdowns (i.e. potential synergistic activation). All gene lists assembled were subsequently cross-referenced with genes differentially regulated in TBX5 7-mis / GATA-4 7-mis control embryos, and any common genes removed. Genes within each of the seven groups and fold changes observed are displayed in Tables 6.2 – 6.8. All categories shown directly relate to sections of the venn diagram shown in Figure 6.2, and are therefore mutually exclusive.

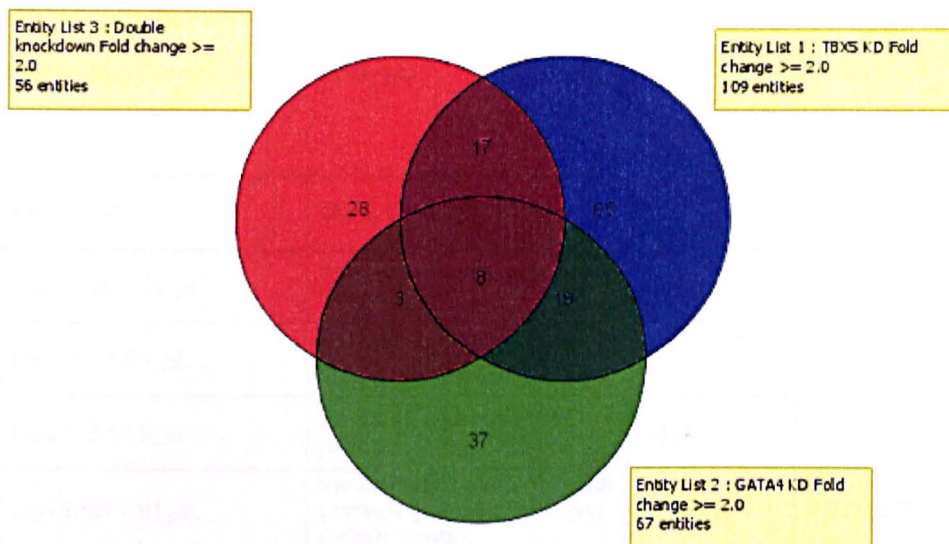


**Figure 6.2 Genes differentially regulated in microarray analysis of TBX5 and GATA-4 single and double knockdown**

Venn diagram displaying genes which show a  $\geq 2.0$  fold change in TBX5 / GATA-4 double knockdown, TBX5 single knockdown and GATA-4 single knockdown embryos in comparison to wild type animals. Gene lists created were subsequently cross-referenced genes differentially regulated in TBX5 7-mis / GATA-4 7-mis control embryos and common genes removed.

**Table 6.2 Genes differentially regulated in microarray analysis of TBX5 / GATA-4 double knockdown chick embryos**

Probe Set ID	Gene Title	Gene Symbol	Fold change
Gga.3795.1.S1_at	SRY (sex determining region Y)-box 3	SOX3	2.0196466 ↑
Gga.153.1.S1_at	Zic family member 1 (odd-paired homolog, Drosophila)	ZIC1	2.5582569 ↑
Gga.153.1.S2_at	Zic family member 1 (odd-paired homolog, Drosophila)	ZIC1	26.636639 ↑
Gga.9289.1.S1_at	transcription factor AP-2 beta (activating enhancer binding protein 2 beta)	TFAP2B	2.2718828 ↑
Gga.2977.1.S1_at	protein tyrosine phosphatase, receptor-type, Z polypeptide 1	PTPRZ1	6.1341915 ↑
Gga.3219.1.S1_at	c-fos induced growth factor (vascular endothelial growth factor D)	FIGF	2.2266912 ↑
Gga.556.1.S1_at	paired box gene 6	PAX6	2.6883574 ↑
Gga.657.1.S1_at	forkhead box G1	FOXG1	2.8416626 ↑
Gga.3535.1.S1_at	nuclear receptor subfamily 2, group E, member 1	NR2E1	2.7937800 ↑
Gga.952.1.S1_at	NK2 homeobox 1	NKX2-1	11.427207 ↑
Gga.10.1.S1_at	orthodenticle homeobox 2	OTX2	16.048748 ↑
GgaAffx.20141.1.S1_at	orthodenticle homeobox 2	OTX2	2.7658422 ↑
GgaAffx.20545.1.S1_s_at	Finished cDNA, clone ChEST1015n20		2.0427935 ↑
Gga.1862.1.S1_at	hypothetical gene supported by CR390114	LOC420770	2.6278262 ↑
Gga.9574.1.S1_at	similar to enhancer of split related protein-7	LOC419390	2.6523864 ↑
Gga.11969.1.S1_at	cytokine-like 1	CYTL1	2.2584643 ↑
Gga.14235.1.S1_at	Finished cDNA, clone ChEST125m3		2.6366910 ↑
Gga.2646.1.S1_at	Phospholipase C, eta 1	PLCH1	2.7627573 ↑
Gga.16236.1.S1_s_at	Finished cDNA, clone ChEST928e1		2.5964615 ↑
Gga.14703.1.S1_at	SP8		2.0750513 ↑

Gga.19600.1.S1_at	Finished cDNA, clone ChEST963k5		3.6129053 ↑
Gga.19626.1.S1_s_at	suppressor of zeste 12 homolog (Drosophila)	SUZ12	2.0030265 ↑
Gga.4546.1.S1_at	cellular retinoic acid binding protein 1	CRABP1	4.9209270 ↑
GgaAffx.23845.1.S1_at	golgi autoantigen, golgin subfamily a, 4	GOLGA4	2.0230920 ↑
GgaAffx.3795.1.S1_at	glypican 3	GPC3	2.3861866 ↑
GgaAffx.24879.4.S1_at			2.2617579 ↓

Genes displaying fold changes of 2-fold or greater in comparison to wild type embryos were selected, and fold changes observed are indicated. Genes displaying up-regulation are displayed in black, and down-regulated genes are displayed in red. Gene lists were cross-referenced with genes differentially regulated in TBX5 7-mis / GATA-4 7-mis control embryos, and common genes removed.

Gga.19600.1.S1_at	Finished cDNA, clone ChEST963k5		3.6129053 ↑
Gga.19626.1.S1_s_at	suppressor of zeste 12 homolog (Drosophila)	SUZ12	2.0030265 ↑
Gga.4546.1.S1_at	cellular retinoic acid binding protein 1	CRABP1	4.9209270 ↑
GgaAffx.23845.1.S1_at	golgi autoantigen, golgin subfamily a, 4	GOLGA4	2.0230920 ↑
GgaAffx.3795.1.S1_at	glypican 3	GPC3	2.3861866 ↑
GgaAffx.24879.4.S1_at			2.2617579 ↓

**Table 6.3 Genes differentially regulated in microarray analysis of TBX5 single knockdown chick embryos**

Probe Set ID	Gene title	Gene symbol	Fold change
Gga.919.1.S1_at	distal-less homeobox 5	DLX5	2.356541 ↑
Gga.5334.1.S1_a_at	regulator of G-protein signaling 4	RGS4	2.195912 ↑
Gga.32.1.S1_at	mab-21-like 1 (C. elegans)	MAB21L1	2.133591 ↑
Gga.8359.1.S1_at	glutathione S-transferase A3	GSTA3	4.219509 ↑
Gga.9334.1.S1_at	serum/glucocorticoid regulated kinase 1	SGK1	2.062817 ↑
Gga.635.1.S1_at	Spindling	SPIN	2.516693 ↑
Gga.827.1.S1_at	erythroid-specific transcription factor eryf1	LOC396450	2.594897 ↑
Gga.580.1.S2_at	growth factor independent 1B transcription repressor	GF11B	2.200138 ↑
GgaAffx.20420.1.S1_at	NEDD4 binding protein 2-like 1	N4BP2L1	2.208199 ↑
GgaAffx.21102.1.S1_s_at	aldolase B, fructose-bisphosphate	ALDOB	3.452897 ↑
GgaAffx.21598.1.S1_s_at	Similar to trans-Golgi protein GMx33	LOC425502	2.764642 ↑
GgaAffx.20558.1.S1_at	Chromodomain helicase DNA binding protein 1	CHD1	3.355640 ↑
Gga.4981.1.S1_s_at	hemoglobin, gamma G /// hemoglobin, gamma A	HBG1 /// HBG2	5.235574 ↑
GgaAffx.20789.1.S1_at	hemoglobin, alpha 1	HBA1	2.144276 ↑
Gga.2909.1.S1_at	hemoglobin, alpha 2	HBA2	2.369730 ↑
Gga.3078.1.S1_at	similar to general transcription factor	LOC430910	2.022142 ↑
Gga.5205.1.S1_at	benzodiazapine receptor (peripheral)-like 1	BZRPL1	2.122973 ↑
Gga.17132.1.S1_at	Finished cDNA, clone ChEST120n19		2.293467 ↑
Gga.7809.1.S1_at	Hypothetical protein LOC771069	LOC771069	3.389699 ↑
Gga.8915.1.S1_s_at	chromosome 20 open reading frame 108	C20orf108	2.639697 ↑

Gga.5139.1.S1_at	fructose-1,6-bisphosphatase 1	FBP1	2.028548 ↑
Gga.9054.1.S1_s_at	adenosine deaminase	ADA	2.316033 ↑
Gga.11474.1.S1_a_at	Rieske (Fe-S) domain containing	RFESD	2.534035 ↑
Gga.20049.1.S1_at	hypothetical gene supported by CR406891	LOC421241	2.146337 ↑
Gga.14585.1.S1_at	Finished cDNA, clone ChEST488o16		3.843172 ↑
Gga.16155.1.S1_at	Finished cDNA, clone ChEST38i14		2.132346 ↑
Gga.10658.1.S1_at	Finished cDNA, clone ChEST1007e10		2.608275 ↑
Gga.8463.1.S1_s_at	chromodomain helicase DNA binding protein 1	CHD1	2.508791 ↑
Gga.10138.1.S1_at	Finished cDNA, clone ChEST126i3		2.291931 ↑
Gga.12484.1.S1_at	Myelin oligodendrocyte glycoprotein	MOG	2.693002 ↑
Gga.16904.1.S1_at	Finished cDNA, clone ChEST749o23		2.043179 ↑
Gga.13093.1.S1_at	Finished cDNA, clone ChEST900p6		2.143198 ↑
Gga.11630.2.S1_a_at	Hypothetical LOC426615	LOC426615	2.957734 ↑
Gga.11630.2.S1_at	Hypothetical LOC426615	LOC426615	2.785122 ↑
Gga.14069.1.S1_s_at	erythrocyte membrane protein band 4.2	EPB42	2.005124 ↑
Gga.20011.1.S1_at	coiled-coil domain containing 84	CCDC84	2.052319 ↑
Gga.9566.2.S1_s_at	solute carrier family 25, member 37	SLC25A37	2.479893 ↑
Gga.11848.1.S1_at	Finished cDNA, clone ChEST394j22		2.073347 ↑
Gga.19575.1.A1_at	Finished cDNA, clone ChEST445p2		2.270295 ↑
Gga.10138.3.S1_at	Finished cDNA, clone ChEST126i3		2.569093 ↑
GgaAffx.11738.1.S1_s_at	early growth response 1	EGR1	2.099442 ↑
GgaAffx.12834.1.S1_at	cyclin D3	CCND3	2.027003 ↑
GgaAffx.23623.2.S1_at	AHNAK nucleoprotein 2	AHNAK2	2.430334 ↑

GgaAffx.23789.1.S1_at	STEAP family member 3	STEAP3	2.233264 ↑
GgaAffx.24779.1.S1_s_at	Finished cDNA, clone ChEST556p11		2.307856 ↑
Gga.6201.1.S1_at	putative ISG12-2 protein	ISG12-2	2.257 ↑
Gga.7505.1.S1_at	Acyl-CoA synthetase short-chain family member 1	ACSS1	2.126091 ↑
Gga.6481.1.S1_at	Transcribed locus		3.182043 ↑
Gga.6758.1.S1_at	Transcribed locus		2.482223 ↑
Gga.6836.1.S1_at	Transcribed locus		2.606474 ↑
Gga.6590.1.S1_at	Transcribed locus, moderately similar to NP_446096.1 cadherin 23 (otocadherin) [Rattus norvegicus]		2.269154 ↑
Gga.6209.1.A1_at			2.011379 ↓
Gga.2087.1.S1_s_at	casein kinase 1, epsilon	CSNK1E	2.123844 ↓
GgaAffx.20789.1.S1_at	Ribosomal protein, large, P1	RPLP1	2.076906 ↓
Gga.13093.1.S1_at	Finished cDNA, clone ChEST430n10		2.134106 ↓
Gga.19320.1.S1_at	hypothetical gene supported by CR406681	LOC426510	2.192061 ↓

Genes displaying fold changes of 2-fold or greater in comparison to wild type embryos were selected, and fold changes observed are indicated. Genes displaying up-regulation are displayed in black, and down-regulated genes are displayed in red. Gene lists were cross-referenced with genes differentially regulated in TBX5 7-mis / GATA-4 7-mis control embryos, and common genes removed.

**Table 6.4 Genes differentially regulated in microarray analysis of GATA-4 single knockdown chick embryos**

Probe set ID	Gene Title	Gene Symbol	Fold change
Gga.2551.2.S1_s_at	lactotransferrin	LTF	2.918124 ↑
Gga.3641.1.S1_at	annexin A2	ANXA2	2.408555 ↑
Gga.3133.1.S1_a_at	collapsin response mediator protein 1	CRMP1	2.367408 ↑
Gga.16863.1.S1_s_at	Gal 10	GAL10	5.975876 ↑
Gga.3381.1.S2_at	homeobox A3	HOXA3	2.480355 ↑
Gga.2648.1.S2_at	homeobox B3	HOXB3	2.833412 ↑
GgaAffx.20083.1.S1_at	homeobox A6	HOXA6	3.819832 ↑
GgaAffx.21240.1.S1_at	Finished cDNA, clone ChEST875h18		2.303639 ↑
Gga.1546.1.S1_at	paired related homeobox 1	PRRX1	2.023035 ↑
Gga.1546.1.S2_a_at	Paired related homeobox 1	PRRX1	2.171399 ↑
Gga.8241.1.S1_at	transcription factor 21	TCF21	3.786901 ↑
Gga.4112.1.S1_at	apolipoprotein B (including Ag(x) antigen)	APOB	3.427132 ↑
Gga.12649.1.S1_at	galanin prepropeptide	GAL	2.365781 ↑
GgaAffx.22999.1.S1_s_at	collagen, type I, alpha 2	COL1A2	2.244431 ↑
Gga.496.1.S1_at	reelin	RELN	2.224683 ↑
Gga.18984.1.S1_at	Finished cDNA, clone ChEST608b15		2.356632 ↑
Gga.3676.1.S1_at	N-acetylgalactosamine 4-sulfate 6-O-sulfotransferase	LOC423952	2.042442 ↑
Gga.18151.1.S1_at	Basonuclin 1	BNC1	3.634063 ↑
Gga.12185.1.S1_at	matrix metalloproteinase 23B	MMP23B	2.182316 ↑
Gga.12849.1.S1_at	SPARC related modular calcium binding 2	SMOC2	2.460695 ↑

Gga.13425.1.S1_at	Finished cDNA, clone ChEST130f3		2.062347 ↑
Gga.14858.1.S1_at	nuclear autoantigenic sperm protein (histone-binding)	NASP	2.072035 ↑
GgaAffx.25098.1.S1_at	propionyl Coenzyme A carboxylase, alpha polypeptide	PCCA	2.053286 ↑
GgaAffx.5758.1.S1_at	carbonic anhydrase X	CA10	2.506326 ↑
GgaAffx.1913.1.S1_at	homeobox B5	HOXB5	2.937861 ↑
Gga.5598.1.S1_at	Transcribed locus		2.189897 ↓
Gga.6873.1.S1_at	Transcribed locus		2.017625 ↓
Gga.17020.1.S1_at	Titin	TTN	2.514681 ↓
Gga.13915.1.S1_at	Titin	TTN	2.158793 ↓
Gga.12775.1.A1_at	titin	TTN	3.282518 ↓
Gga.4777.5.A1_at	Finished cDNA, clone ChEST145d21		2.097747 ↓
Gga.17680.1.S1_at	Clone cDNA3F microsatellite MCW108 sequence		2.054327 ↓

Genes displaying fold changes of 2-fold or greater in comparison to wild type embryos were selected, and fold changes observed are indicated. Genes displaying up-regulation are displayed in black, and down-regulated genes are displayed in red. Gene lists were cross-referenced with genes differentially regulated in TBX5 7-mis / GATA-4 7-mis control embryos, and common genes removed.

**Table 6.5 Genes differentially regulated in microarray analysis of TBX5 / GATA-4 double knockdown, TBX5 single knockdown, and GATA-4 single knockdown chick embryos**

Probe Set ID	Gene Title	Gene Symbol	Fold change		
			TBX5 & GATA4 knockdown	TBX5 knockdown	GATA-4 knockdown
GgaAffx.21116.1.S1_s_at	oxidative stress induced growth inhibitor 1	OSGIN1	2.695851 ↑	4.087098 ↑	2.051297 ↑
Gga.16169.1.S1_at	Finished cDNA, clone ChEST45e16		2.7834854 ↑	4.394274 ↑	2.013999 ↑
Gga.19101.1.S1_at	Finished cDNA, clone ChEST926n8		3.4982224 ↑	5.769498 ↑	2.229745 ↑
Gga.10138.2.S1_a_at	Finished cDNA, clone ChEST126l3		2.3702402 ↑	2.630745 ↑	2.022664 ↑
Gga.5092.1.S1_s_at	annexin A2	ANXA2	2.1296182 ↑	2.098631 ↑	2.408555 ↑
Gga.9032.1.S1_s_at	RNA binding motif protein 35B	RBM35B	2.97302 ↑	4.49394 ↑	2.480706 ↑
GgaAffx.11525.1.S1_s_at	claudin 1	RCJMB04_2c8	3.8028853 ↑	4.62055 ↑	2.624394 ↑
GgaAffx.7796.1.S1_s_at	solute carrier family 39 (zinc transporter), member 8	SLC39A8	3.7550573 ↑	5.402943 ↑	2.87964 ↑

Genes displaying fold changes of 2-fold or greater in comparison to wild type embryos were selected, and fold changes observed are indicated. Gene lists were cross-referenced with genes differentially regulated in TBX5 7-mis / GATA-4 7-mis control embryos, and common genes removed.

**Table 6.6 Genes differentially regulated in microarray analysis of TBX5 / GATA-4 double knockdown and TBX5 single knockdown and chick embryos**

Probe Set ID	Gene Title	Gene Symbol	Fold change	
			TBX5 & GATA-4 knockdown	TBX5 knockdown
Gga.4842.2.S1_a_at	solute carrier family 4, anion exchanger, member 1	SLC4A1	2.0272145 ↑	3.647175 ↑
GgaAffx.21696.1.S1_at	Finished cDNA, clone ChEST747k12		2.0174587 ↑	2.58259 ↑
GgaAffx.20824.1.S1_at	Finished cDNA, clone ChEST722f15		2.6281042 ↑	4.631784 ↑
GgaAffx.21220.1.S1_s_at	Finished cDNA, clone ChEST881h18		2.0515776 ↑	3.366277 ↑
Gga.4156.1.S1_at	Finished cDNA, clone ChEST79b1		2.0187516 ↑	2.235081 ↑
Gga.8098.1.S1_at	Finished cDNA, clone ChEST811h18		3.2116323 ↑	4.168608 ↑
Gga.8089.1.S1_at	Kruppel-like factor 1 (erythroid)	KLF1	2.1141534 ↑	3.243578 ↑
Gga.7581.1.S1_at	Finished cDNA, clone ChEST885i1		18.489647 ↑	2.456972 ↑
Gga.10042.1.S1_a_at	CD200 receptor 1	CD200R1 /// RCJMB04_25i16	2.0964477 ↑	2.639697 ↑
Gga.11763.2.S1_a_at	similar to RIKEN cDNA 1110067D22	LOC423277	2.2741299 ↑	3.876498 ↑
Gga.17183.1.S1_at	Finished cDNA, clone ChEST397p8		2.011654 ↑	3.013425 ↑
Gga.13903.1.S1_at	paired-like homeodomain 1	PITX1	2.1853464 ↑	4.573031 ↑
GgaAffx.2993.1.S1_at	erythrocyte membrane protein band 4.2	EPB42	2.5261283 ↑	2.005124 ↑
GgaAffx.7796.1.S1_at	solute carrier family 39 (zinc transporter), member 8	SLC39A8	2.1189318 ↑	4.271026 ↑
Gga.5243.1.S1_at	Transcribed locus		2.2414985 ↑	2.84958 ↑
Gga.7750.1.S1_at	hypothetical LOC422459	LOC422459	2.2732491 ↑	3.474953 ↑

Gga.8578.1. S1_at	Transcribed locus		2.2378054 ↑	4.381073 ↑
----------------------	----------------------	--	-------------	------------

Genes displaying fold changes of 2-fold or greater in comparison to wild type embryos were selected, and fold changes observed are indicated. Gene lists were cross-referenced with genes differentially regulated in TBX5 7-mis / GATA-4 7-mis control embryos, and common genes removed.

**Table 6.7 Genes differentially regulated in microarray analysis of TBX5 / GATA-4 double knockdown and GATA-4 single knockdown and chick embryos**

Probe Set ID	Gene Title	Gene Symbol	Fold change	
			TBX5 & GATA-4 knockdown	GATA-4 knockdown
Gga.2558.1.S1_a_at	collagen, type XIV, alpha 1 (undulin)	COL14A1	2.3760216 ↑	3.037223 ↑
Gga.2354.1.S1_at	Transcribed locus		2.1046243 ↑	2.661268 ↑
GgaAffx.11659.1.S1_at	sorcin	RCJMB04_3f15	2.0217292 ↓	4.004279 ↓

Genes displaying fold changes of 2-fold or greater in comparison to wild type embryos were selected, and fold changes observed are indicated. Genes displaying up-regulation are displayed in black, and down-regulated genes are displayed in red. Gene lists were cross-referenced with genes differentially regulated in TBX5 7-mis / GATA-4 7-mis control embryos, and common genes removed.

**Table 6.8 Genes differentially regulated in microarray analysis of TBX5 single knockdown and GATA-4 single knockdown chick embryos**

Probe Set ID	Gene Title	Gene Symbol	Fold change	
			TBX5 knockdown	GATA-4 knockdown
Gga.2551.2.S1_a_at	lactotransferrin	LTF	2.283916 ↑	2.918124 ↑
Gga.2620.1.S1_at	transthyretin	TTR	2.76807 ↑	4.394575 ↑
Gga.1165.1.S1_at	fibrinogen gamma chain	FGG	2.900268 ↑	2.899903 ↑
GgaAffx.21581.1.S1_s_at	chemokine (C-X-C motif) ligand 14	CXCL14	2.399975 ↑	2.832924 ↑
Gga.9481.1.S1_s_at	otokeratin	LOC395772	2.136159 ↑	2.031168 ↑
Gga.9087.1.S1_at	succinate-CoA ligase, GDP-forming, beta subunit	SUCLG2	3.021066 ↑	2.887826 ↑
GgaAffx.20374.1.S1_at	cadherin 1, type 1, E-cadherin (epithelial)	CDH1	2.103267 ↑	2.213427 ↑
Gga.4557.1.S1_at	fibrinogen beta chain	FGB	3.862611 ↑	7.627894 ↑
GgaAffx.26441.1.S1_at	hypothetical LOC424460	LOC424460	12.39564 ↑	3.578772 ↑
Gga.6860.1.A1_at			2.082896 ↓	2.786701 ↓
Gga.14594.1.A1_at	Finished cDNA, clone ChEST240e14		2.196702 ↓	2.082312 ↓
Gga.3690.1.A1_at	Zinc finger protein 207	ZNF207	2.009688 ↓	2.287068 ↓
Gga.9087.1.S1_at	transcription factor Crx	LOC395160	2.93964 ↓	2.535343 ↓
Gga.285.1.A1_at	myomesin	LOC395524	2.096654 ↓	2.205535 ↓
GgaAffx.11133.1.A1_s_at	cyclic AMP phosphoprotein, 19 kD	RCJMB04_4f12	2.789666 ↓	2.607948 ↓

Genes displaying fold changes of 2-fold or greater in comparison to wild type embryos were selected, and fold changes observed are indicated. Genes displaying up-regulation are displayed in black, and down-regulated genes are displayed in red. Gene lists were cross-referenced with genes differentially regulated in TBX5 7-mis / GATA-4 7-mis control embryos, and common genes removed.

#### **6.2.4 Genes identified in microarray analysis of TBX5 and GATA-4 knockdown**

The purpose of this genome-wide microarray study was to identify genes co-ordinately regulated by TBX5 and GATA-4. Five sample groups were analysed, generating seven categories of genes differentially regulated in response to TBX5 / GATA-4 double knockdown, TBX5 single knockdown, GATA-4 single knockdown, and overlapping groups (represented in Figure 6.2). Of these seven categories, genes identified in the TBX5 / GATA-4 knockdown group but not other groups were of greatest interest. Secondary to this group, genes appearing in the TBX5 / GATA-4 knockdown group and one or both of the single knockdown groups were also of interest, particularly those genes which showed a greater fold change in expression in the double knockdown group compared to single knockdowns. However, time did not allow study of all of these groups, and the TBX5 / GATA-4 knockdown group were given primary focus. In total, 26 transcribed loci were identified displaying differential regulation in TBX5 / GATA-4 double-knockdown embryos (by  $\geq 2$  fold in comparison to wild type animals) but not in single knockdown embryos or controls. Not all loci identified corresponded to known or hypothesised genes. Eighteen of the genes of interest are 'known' genes and a full description of these is given in Appendix I.

##### **6.2.4.1 Reliability of data and general considerations**

There is always a false-discovery rate (FDR) associated with microarray gene expression profiling, which means it is unlikely that all of the genes identified by this technique are genuine targets. The FDR increases as the number of arrays per group decreases [Pawitan et al., 2005] i.e. biological replicates are very important in microarray expression profiling, exemplified in a number of studies [Kerr et al., 2000; Lee et al., 2000; Manduchi et al., 2000]. In this study one biological replicate was assayed per group which means the likelihood of obtaining false positives is very high. However, as only 18 genes of interest were identified (due to the high threshold set and large number of control groups), post-analysis elimination of false positives is not a lengthy procedure in this case.

It is surprising that knockdown of two cardiac transcription factors seems to result in misexpression of so many neurological genes and so few heart genes, particularly given that this is a heart tissue specific study. A high false positive rate due to limited biological replicates could be one contributing factor (as discussed above). There is also evidence that certain transcripts cannot be accurately detected by any technique (microarray expression analysis or QPCR) due to sequence specific effects [Larkin et al., 2005]. Also, any small levels of contaminating tissue from non-cardiac regions of the embryo may have resulted in anomalous results.

This study has resulted in the identification of a number of strong candidate genes, in particular CRABP1, GPC3, and TFAP2B. TFAP2B is arguably the most interesting as mutations in this gene are already associated with the heart-hand disorder Char syndrome [Satoda et al., 1999; Satoda et al., 2000], whose anomalies include patent ductus arteriosus (PDA), facial dysmorphism, strabismus, hearing abnormalities, and an abnormal fifth digit of the hand [Char, 1978]. The ductus arteriosus is the arterial connection between the pulmonary artery and aorta, and serves to shunt blood from the right ventricle away from the lungs, allowing blood to bypass the lungs during foetal development. The ductus normally constricts and closes shortly after birth, and failure to do so results in PDA. Structures affected in Char syndrome are all contributed to by neural crest cells [Moser et al., 1997] and fate mapping studies have shown that the medial layer of the ductus, but not the pulmonary artery and descending aorta, arises from cardiac neural crest (CNC) cells [Waldo et al., 1999]. It is likely that TFAP2B has a role in the migration or differentiation of neural crest cells, which results in a specific effect on the ductus but not surrounding arterial structures. It is interesting that this heart-hand gene may be transcriptionally regulated by another heart-hand gene, TBX5, in conjunction with GATA-4.

### 6.2.5 Gene expression analysis using GEISHA

Assessment of the anatomical expression pattern of genes is a useful starting point for candidate gene selection. Embryonic expression of genes was initially researched using the online GEISHA (gallus expression in situ hybridisation analysis) resource (<http://geisha.arizona.edu/geisha/index.jsp>). This is a database containing *in situ* hybridisation information for genes expressed at 0.5 - 6 days of development in chicken embryos, input via in house *in situ* hybridisation screening, review of literature, and unpublished expression information from laboratories.

The whole body expression pattern of a number of genes was described in GEISHA including SOX3, ZIC1, FOXG1, NKX2-1, PAX6, and OTX2, and is described in Table 6.9. Developmental stages HH12 – HH19 have been included where possible as these are of interest to this study. All six genes researched in GEISHA did not display obvious expression in the heart so were not considered further.

**Table 6.9 Gene expression data from GEISHA**

Gene	Developmental stage and region of expression
SOX3	HH7 – HH12: Ectoderm, neural plate/tube [Abu-Elmagd et al., 2001] HH13 – HH18: Ectoderm, neural plate/tube, pharyngeal arches and clefts, placcode [Abu-Elmagd et al., 2001]
ZIC1	HH13 – HH18: Dermatome, myotome, neural plate/tube, sclerotome, somites, spinal cord [Sun Rhodes and Merzdorf, 2006] HH19 – HH21: Dermatome, face mesenchyme, myotome, sclerotome, somites [Sun Rhodes and Merzdorf, 2006]
FOXG1	HH7 – HH12: Forebrain, telencephalon [Bell et al., 2001] HH13 – HH15: Ear/otic placcode, forebrain, pharyngeal arches and clefts (Chapman SC, 2008, unpublished) HH13 – HH19: Telencephalon [Bell et al., 2001]
NKX2-1	HH7 – HH12: Diencephalon, neural plate/tube (Chapman SC, 2008, unpublished) HH13 – HH17: Diencephalon, pharyngeal arches and clefts (Chapman SC, 2008, unpublished)
PAX6	HH7 – HH12: Diencephalon, eye, forebrain, neural plate/tube, spinal cord [Ohuchi et al., 2007] HH13 – HH24: Diencephalon, hindbrain, telencephalon [Garcia-Calero et al., 2006]
OTX2	HH7 – HH12: Forebrain, midbrain, neural plate/tube (Chapman SC, 2008, unpublished) HH13 – HH18: Eye, forebrain, midbrain, pharyngeal arches [Plouhinec et al., 2005]

Chicken whole embryo developmental expression profiles of the genes SOX3, ZIC1, FOXG1, NKX2-1, PAX6 and OTX2 have been previously characterised by *in situ* hybridisation and were found in the GEISHA database (<http://geisha.arizona.edu/geisha/index.jsp>). Expression patterns are summarised and include developmental stages HH12 – HH19 (of interest in this study) where possible.

### 6.2.6 RT-PCR expression analysis

In order to assess expression of other identified genes, nine of the twelve remaining genes were selected for RT-PCR expression analysis (TFAP2B, PTPRZ1, FIGF, NR2E1, LOC420770, SUZ12, CRABP1, GOLGA4, and GPC3). CYTL1, PLCH1 and LOC419390 were not studied due to limited resources and time restrictions.

RT-PCR expression analysis was performed once in chick embryonic segments at three stages of development (HH16, HH19 and HH24) as a preliminary means of temporal / spatial characterisation. Primers sequences are given in Table 2.7. Equal amounts of template were used in all reactions. PCR reactions were performed with HotStar Taq using an annealing temperature of 60 °C, extension time of 30 seconds, and 30 PCR cycles. Negative RT controls were included for each gene and did not display amplification (Appendix J). Results of expression analyses are displayed in Figure 6.3 and are described below. RT-PCR was not performed in a quantitative manner and descriptions are subjective.

SUZ12, GOLGA4 and GPC3 were expressed in all embryonic segments (head, heart, body / limbs) at all three stages of development indicating ubiquitous expression. Further studies would have to be performed to determine the exact spatial expression patterns of these genes.

Expression of TFAP2B was detected in all embryonic segments at HH16. Heart expression appeared to be lower at HH19, and was not detectable at HH24. Consistent expression was observed in other regions throughout all three stages. CRABP1 was also expressed in all regions at the stages examined. Heart expression appeared to be strongest at HH16, becoming reduced at HH19 and HH24. PTPRZ1 expression was detected in all embryonic segments at all three stages of development. Heart expression appeared to be fainter at HH24. TFAP2B, CRABP1, and PTPRZ1 follow a similar pattern, displaying expression throughout the embryo with heart expression appearing to be strongest early in development, and decreasing

in later stages. This could be indicative of a specific function in early heart development.

LOC420770 expression was detectable in the heart and body (but not head) at all three stages. Interestingly, expression at HH24 was more prominent in the limbs than body indicating a heart/limb expression profile, potentially similar to that of TBX5.

FIGF was expressed in all embryonic segments, with highest expression in the head and body and fainter expression in the heart. NR2E1 was expressed almost exclusively in the head region, with faint expression in the body (at all three stages). Heart expression could not be detected at any of the stages examined.

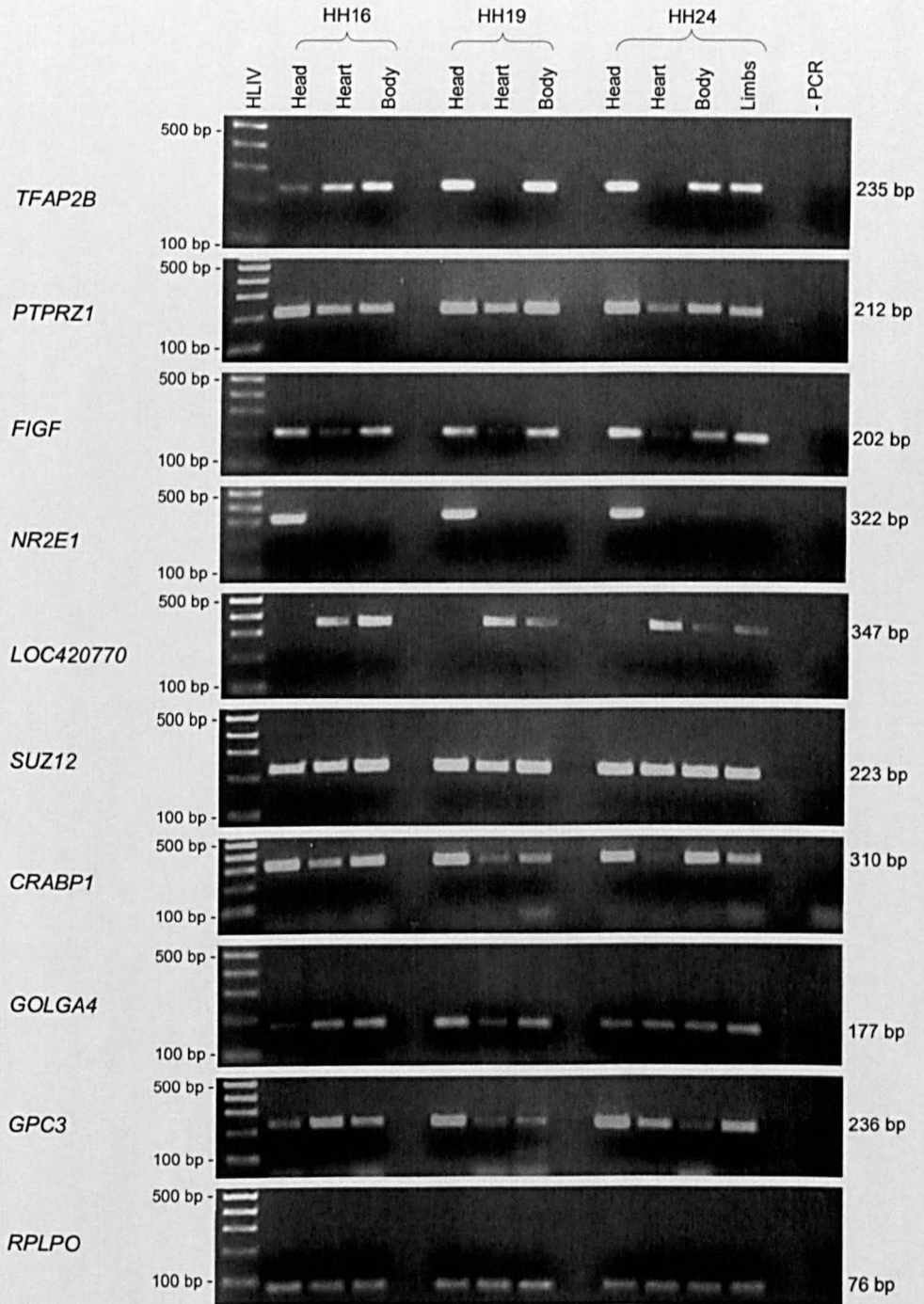


**Figure 6.3 RT-PCR expression analysis of nine candidate genes**

RT-PCR products were electrophoresed on 2% agarose gels using Hyperladder IV as a size marker (500 bp and 100 bp bands are indicated along with product sizes). Expression was studied in chick embryonic segments at HH16, HH19, and HH24. RPLPO was included as a housekeeper gene. Negative PCR controls (-PCR) are shown. Negative RT controls did not show amplification for any of the genes and are displayed in Appendix J.

## CHAPTER 7

### DISCUSSION

#### 7.1 TBX5 and GATA-4 in cardiac development

Development of the heart is a highly complex and dynamic process involving a vast network of genes. These genes are diverse in function, encoding growth factors, signalling molecules, transcription factors and their co-factors and regulators, components of the extracellular matrix, and structural proteins. Defects in cardiac genes can lead to congenital heart defects, and understanding the molecular pathways involved in normal cardiogenesis will allow elucidation of the pathogenesis of disease. This in turn is the first step toward improved diagnoses and potentially novel therapies.

Heart development is a highly regulated process involving complex interplay between numerous transcription factors, which can also regulate transcription of one another. In addition, a number of transcription factors physically interact to co-ordinately regulate key genes and developmental pathways. Members of the NK2, MEF2, GATA, Tbx and Hand gene families make up a core cardiac regulatory network whose expression is initiated by inductive signals and upstream activators [Olson, 2006]. Mutations in a number of key cardiac transcription factors in this core group, including Nkx2.5, TBX5, and GATA-4, have been associated with CHDs [Garg et al., 2003; Li et al., 1997; Schott et al., 1998]. In addition, these transcription factors also interact with one another for joint regulation of targets [Garg et al., 2003; Hiroi et al., 2001; Lee et al., 1998]. TBX5 and GATA-4 are considered master regulators of cardiac development, and these two genes, in combination with Baf60c, can induce a full cardiac transcriptional programme [Takeuchi and Bruneau, 2009]. Additionally, the specific combination of TBX5, GATA-4 and MEF2C has recently been found to be able to reprogramme mouse postnatal fibroblasts into functional cardiomyocytes that

display cardiomyocyte-like global gene expression and beat spontaneously [Ieda et al.]. *TBX5* is a T-box transcription factor and a so called 'heart-hand' gene as it has an important role in heart development and specification of forelimb identity [Isaac et al., 1998]. Mutations in *TBX5* are associated with Holt-Oram syndrome [Basson et al., 1997; Fan et al., 2003; Li et al., 1997], a congenital disorder characterised by upper limb and heart abnormalities. These are usually atrial or ventricular septal defects, but can include mitral valve defects, cardiac conduction defects, tetralogy of Fallot, and hypoplastic left heart syndrome [Basson et al., 1994; Bruneau et al., 1999]. *GATA-4* is a member of the GATA family of transcription factors and has a crucial role in cardiogenesis [Molkentin and Olson, 1997; Rivera-Feliciano et al., 2006; Zeisberg et al., 2005]. Mutations in *GATA-4* are associated with atrial and ventricular septal defects [Garg et al., 2003] and tetralogy of Fallot [Nemer et al., 2006]. *TBX5* and *GATA-4* display distinct but overlapping expression patterns [Bruneau et al., 1999; Kelley et al., 1993] and form a complex that is thought to direct and synergistically regulate common cardiac pathways [Garg et al., 2003]. A number of *TBX5* mutations that are associated with cardiac septal defects abolish this biochemical interaction [Garg et al., 2003], and the *GATA-4* mutation G296S that is linked to ASDs also has this effect [Garg et al., 2003]. These data indicate the *TBX5* / *GATA-4* complex has a critical regulatory role in cardiac septation, and provide insight into why similar phenotypes are so often seen as a result of mutations in these genes. The downstream targets of *TBX5* and *GATA-4* are largely unknown, and a major aim of this thesis has been to identify and analyse these genes. This is crucial in understanding the mechanism via which mutations in these transcription factors lead to congenital heart defects.

## **7.2 Identification of targets of *TBX5* and *GATA-4* in the mouse P19 cell line**

The research carried out in this thesis was based on a previous study that aimed to identify downstream targets of *TBX5* and *GATA-4* using the mouse P19 cell line, which provides an excellent model of cardiomyocyte differentiation [McBurney, 1993]. Microarray expression analysis of two cell lines stably transfected with *TBX5* / *GATA-4*

overexpression vectors was carried out allowing identification of a number of genes which displayed differential regulation. This was supplemented with temporal gene expression data, quantified at selected time-points of wild type cardiomyocyte differentiation. Sixteen up-regulated genes displaying wild type expression profiles mirroring wild type TBX5 and GATA-4 expression, and two down-regulated genes, were selected for further study.

### 7.2.1 Validation of gene expression and preliminary bioinformatic analysis

In Chapter 3 of this thesis, expression of genes of interest was validated by QPCR using the Comparative C<sub>T</sub> method for confirmation and more accurate quantification of expression data. Genes displaying the highest fold increases in expression in the overexpression cell lines, and following the same pattern of expression as TBX5 and GATA-4 (a general increase from day 2 - day 7 of differentiation), were selected for further analysis. These included *TPM1*, *PETA-3*, *PA2.26*, *RBMS1*, *FUCA1*, and *FN*, which displayed 1.4 - 3.5 fold increases in expression in the overexpression cell lines. An additional gene (*DES*) encoding the intermediate filament protein desmin was added to the study based on a similar study where this gene showed up-regulation in response to transient overexpression of TBX5 and GATA-4 in the P19 cell line. Bioinformatic analysis of gene promoter regions was performed in Mulan software by alignment between chicken, mouse and human sequences for identification of evolutionarily conserved regions (ECRs) and consensus transcription factor binding sites within them. Putative binding site analysis revealed *RBMS1* as the best target; three potential consensus binding sites for TBX5 were identified (all within the coding region), and four GATA-4 sites were identified (two in the coding region, and two in the 3' UTR). This gene was selected for further study of its activation by TBX5 and GATA-4. Reporter assays were designed to test activation of an intronic fragment of the mouse *RBMS1* gene containing both a TBX5 and a GATA-4 site. This was thought to be a downstream enhancer or repressor element, and data showed that GATA-4 had a repressive effect on promoter activity via this region, whilst TBX5 had no effect. Attempts to study the effect of TBX5 and GATA-4 on the 5' promoter region

are ongoing. Further in depth study of RBMS1 in the developing chick was carried out and is discussed in 7.4.

### 7.2.2 Candidate genes

The identified genes are diverse in function, encoding muscle proteins, extracellular matrix molecules, a transcription factor and an enzyme, and this is a reflection of the role of TBX5 and GATA-4 as master regulators in the heart. The importance of sarcomeric proteins in muscle contractility is well established, and many of these genes are now also known to be important developmentally in processes such as septation. Thus, mutations in a number of genes encoding sarcomeric proteins are associated with both cardiomyopathies and congenital heart defects. *MYH6* is a well known example of such a gene whose mutations are associated with hypertrophic and dilated cardiomyopathy [Morita et al., 2005], and atrial septal defects [Ching et al., 2005]. This gene is also a known synergistic target of TBX5 and GATA-4 [Huang et al., 1995; Molkentin et al., 1994]. Other sarcomeric protein encoding genes that are associated with ASDs include *MYH7* ( $\beta$ -myosin heavy chain) [Budde et al., 2007] and *ACTC* ( $\alpha$ -cardiac actin) [Matsson et al., 2008; Monserrat et al., 2007]. Mutations in *ACTA2* ( $\alpha$ -smooth muscle actin) and *MYH11* (myosin heavy chain 11) are associated with patent ductus arteriosus [Guo et al., 2007; Zhu et al., 2006]. Initial studies by Dr Lynn Amy and Jonathan Ronksley led respectively to the identification of the muscle proteins desmin and  $\alpha$ -tropomyosin as potential cardiac targets of TBX5 and GATA-4 [Ronksley, 2007]. Desmin is a type III intermediate filament protein with an important contractile role in muscle. In humans, numerous mutations in the desmin gene have been associated with familial cardiac and skeletal myopathy [Bergman et al., 2007; Fidzianska et al., 2005; Goldfarb et al., 1998; Goudeau et al., 2001; Olive et al., 2007; Sung et al., ; Taylor et al., 2007; Vernengo et al., ; Vrabie et al., 2005]. The *TPM1* gene encodes  $\alpha$ -tropomyosin, which is an important contractile component of the sarcomere [Perry, 2001]. Missense mutations in *TPM1* have previously been linked with familial hypertrophic cardiomyopathy and dilated cardiomyopathy [Lakdawala et

al., ; Thierfelder et al., 1994]. To date, neither of these genes has been associated with atrial septal defects.

The extracellular matrix (ECM) consists of collagens, glycoproteins, growth factors, and proteases that form a macromolecular complex which interacts and communicates with various cardiac cell types to undergo changes in composition (remodelling) for determination of its function. The ECM plays an important role in cardiac development and growth. The ECM component fibronectin was identified in Jonathan Ronksley's study [Ronksley, 2007]. Fibronectin is an adhesive ECM glycoprotein involved in cytoskeletal organisation, cell adhesion, cell migration, and cell spreading [Waterman and Balian, 1980], and is thought to play a role in the migration of precardiac cells [Linask and Lash, 1986]. Mouse knockout of fibronectin has a pronounced effect on the heart, with heart primordia often remaining unfused [George et al., 1993]. Embryos that are not as severely affected have fused primordia with abnormal morphology. Cardiac defects such as thickening of the myocardial tissue, cardiac jelly deficiency, and abnormal endocardium morphology also occur, demonstrating the importance of fibronectin in cardiac development [George et al., 1993]. PETA-3 is a tetraspan membrane protein involved in cell-cell adhesion, cell migration, platelet adhesion, and angiogenesis [Wright et al., 2004]. PA2.26 is a small transmembrane glycoprotein and also plays a role in cell-cell adhesion and cell migration [Scholl et al., 1999]. The process of cell migration is important in formation of endocardial cushions in the heart which are essential for septa and valve formation, suggesting possible roles for fibronectin, PETA-3 and PA2.26 here.

Cardiac transcription factors play a key regulatory role in cardiac growth and patterning, and mutations in a number of cardiac transcription factors are associated with CHDs. The multifunctional gene RBMS1, which acts as both a cell cycle regulator (via binding to c-myc) and a transcription factor, was identified in the original P19 study [Ronksley, 2007]. RBMS1 has been shown to suppress transcription of  $\alpha$ -smooth muscle actin [Kimura et al., 1998], which has important functions in the

developing heart (section 7.4), suggesting a potential mode of action here. Other downstream targets of RBMS1 are largely unknown.

This microarray study led to the identification of an interesting and diverse group of genes which may be regulated by TBX5 and GATA-4. Some of these genes are already linked to the heart, including desmin,  $\alpha$ -tropomyosin, and fibronectin. Other genes such as PA2.26 and PETA-3 are involved in processes such as cell migration which are important in cardiac septation and valvulogenesis. RBMS1 is cell cycle regulator and transcription factor, and has not previously been implicated in cardiac development. FUCA1 encodes the exoglycosidase enzyme  $\alpha$ -L-fucosidase, and a role for this enzyme in cardiac development has not been postulated.

### **7.3 Development of a model system for assessment of the responsiveness of candidate genes to TBX5 and GATA-4**

At the time this part of the research was initiated (2008), there were no known *in vivo* studies looking at the effects of combined haploinsufficiency of TBX5 and GATA-4. In Chapter 4 of this thesis, the developing chick was selected as a model organism for study of candidate gene expression and responsiveness to TBX5 and GATA-4. The chick allows easy and rapid manipulation at selected time points since development occurs *in ovo* (as opposed to *in utero*), and morpholino antisense technology allows knockdown of up to two genes simultaneously. Seven genes were previously identified in the mouse P19 cell line as potential targets of TBX5 and GATA-4 and selected for further study in the developing chick embryo; *PA2.26*, *PETA-3*, *FUCA1*, *FN*, *TPM1*, *DES*, and *RBMS1*. As a starting point, expression of these genes was confirmed in the embryonic chick heart at HH12 - HH26.

#### **7.3.1 Development of an *in ovo* model of TBX5 and GATA-4 knockdown**

In order to assess candidate gene responsiveness to TBX5 and GATA-4 in the developing chick heart, an embryonic model of TBX5 / GATA-4 double knockdown was generated using AUG targeting morpholino antisense oligonucleotides. Five-

base mismatch morpholinos were originally tested as controls of specificity, but these were found to have an effect most likely due to retained target binding capability and were therefore subsequently replaced with 7-base mismatch controls. Morpholinos were applied at HH10 – HH16, encompassing key events such as dextral looping (HH10 – HH12), the early phase of s-looping (HH12 – HH17/18), and the initiation of atrial septation (HH14) [Anderson et al., 2003; Manner, 2000]. Previous studies have shown that complete mouse knockout of TBX5 results in embryonic lethality by E10.5, and hearts fail to undergo looping and display hypoplasia of the sinuatria and left ventricle [Bruneau et al., 2001]. Study of TBX5 heterozygous mice has demonstrated a regulatory role for TBX5 in chamber morphogenesis and cardiac septation [Bruneau et al., 2001]. In this study, *in ovo* knockdown of TBX5 resulted in abnormalities in heart shape, and a reduction in the size of the atrial septum, corresponding with the cardiac defects present in TBX5 heterozygote mice [Bruneau et al., 2001]. Mouse knockout of GATA-4 results in embryonic lethality at E7.0 – E9.5 due to defects in ventral morphogenesis and linear heart tube formation [Molkentin and Olson, 1997]. Early myocyte restricted deletion of GATA-4 by *Nkx2-5<sup>Cre</sup>* results in cardiac malformations including a single predominant ventricular chamber, myocardial hypoplasia, and small atrioventricular and OFT endocardial cushions due to defects in EMT [Rivera-Feliciano et al., 2006; Zeisberg et al., 2005]. Here, chick embryonic treatment with GATA-4 targeting morpholinos resulted in heart malformations and embryos displayed indications of a reduction in the size of the atrial septum, as would be expected based on the ASDs observed in humans with GATA-4 mutation [Garg et al., 2003; Nemer et al., 2006]. In parallel with this research, *Gata4<sup>+/-</sup> Tbx5<sup>+/-</sup>* compound heterozygote mice were generated by another research group and full phenotypic characterisation was performed [Maitra et al., 2009]. Almost 100% of embryos suffered postnatal lethality by day 7. Embryos displayed intrauterine growth retardation, a complete lack of AV septation due to defects in endocardial cushion maturation and modelling (not EMT), and myocardial thinning affecting both ventricles at E13.5, leading to subsequent heart failure and death [Maitra et al., 2009]. In this study, although it was not possible to quantify morpholino effect on protein levels upon

chick embryonic treatment with TBX5 and GATA-4 targeting morpholinos, these embryos displayed the expected phenotypes. Combined knockdown of TBX5 together with GATA-4 resulted in more severe cardiac defects than treatment with either alone, and a wider range of defects was observed. Double knockdown embryos displayed growth retardation, severe body kinking / twisting, and general malformations in comparison to control animals. A variety of heart defects including a reduction in heart size, constriction of the ventricle, high outflow tract, and most commonly abnormal looping of the heart were also observed. These observations correlate with the phenotype of *Gata4<sup>+/-</sup> Tbx5<sup>+/-</sup>* mice, and interestingly there are also some distinct features such as the defects in cardiac looping that were observed in the chick but not mouse [Maitra et al., 2009]. This may have been for a number of reasons including differences between species such as varying physiology and response to gene dosage (discussed further in section 7.7), the level of knockdown achieved, and the developmental stage of knockdown. Overall, morpholino knockdown of TBX5 and GATA-4 individually and in combination generated the expected phenotypes based on mouse knockouts performed by others.

### **7.3.2 Candidate gene responsiveness to combined knockdown of TBX5 and GATA-4**

In order to examine the responsiveness of candidate genes to TBX5 and GATA-4, QPCR expression analysis of these genes in double knockdown embryos was carried out using the Relative Standard Curve method. This method is ideal for the detection of small changes in expression as would be expected in an *in ovo* system, and was successfully developed and optimised for use. QPCR expression analysis showed knockdown of TBX5 and GATA-4 had no effect on expression of PETA-3, fibronectin,  $\alpha$ -tropomyosin, desmin, and RBMS1. It was not possible to accurately quantify expression of PA2.26 and  $\alpha$ -L-fucosidase due to low level expression. However, the level or presence of knockdown of TBX5 and GATA-4 at the protein level remains unknown. In addition, expression of MYH6 in these embryos was unaltered whilst this gene is down-regulated in *Gata4<sup>+/-</sup> Tbx5<sup>+/-</sup>* compound heterozygote mice [Maitra et al.,

2009]. If knockdown was occurring, this could be for a number of reasons; it is possible there are differences in the transcriptional regulation of MYH6 between the mouse and chick. The level of knockdown of TBX5 and GATA-4 in this system, whilst generating the expected cardiac phenotype, may not have been sufficient for down-regulation of MYH6. A low level of knockdown of TBX5 and GATA-4 may have resulted in very discrete changes in MYH6 expression which were not detected. The QPCR technique itself has limitations in its sensitivity, particularly since this study is attempting to quantify small reductions in gene expression. If this was the case, it could mean that the model generated may not have been sensitive enough to show differential regulation of candidate genes suggesting they may still be downstream targets of TBX5 and GATA-4. Establishment of knockdown and quantification of knockdown levels of TBX5 and GATA-4 knockdown achieved with these morpholinos has not been achieved and is an important factor when considering genome-wide effects. Despite the numerous technical difficulties associated with this, it is absolutely crucial for accurate interpretation of the data presented here. The research in this thesis took a two-pronged approach from this stage. One gene from the original study, RBMS1, was selected for further analysis (Chapter 5), and the *in ovo* model generated was used for identification of new synergistic targets of TBX5 and GATA-4 (Chapter 6).

#### **7.4 Investigation of the role of RBMS1 in cardiac development**

Both TBX5 and GATA-4 are involved in embryonic cardiac cell cycle progression, indicating a mechanism by which they can control cardiomyocyte proliferation [Rojas et al., 2008; Xiao et al., 2001]. RBMS1 is a cell cycle gene and transcription factor that was identified in the mouse P19 cell line as a potential downstream target of TBX5 and GATA-4. Little is currently known about the regulation of this gene other than the presence of a positive regulatory element that is necessary for transcriptional activation of RBMS1 [Fujimoto et al., 1998]. RBMS1 binds to DNA polymerase  $\alpha$  for activation of DNA replication [Niki et al., 2000a], and can induce apoptosis, mediated at least in part by positive transcriptional regulation of the Fas gene, which has an

important apoptotic role [Iida et al., 1997; Nomura et al., 2005]. *RBMS1* also suppresses transcription of  $\alpha$ -smooth muscle actin [Kimura et al., 1998], which is important in myofibrillogenesis [Sugi and Lough, 1992; Woodcock-Mitchell et al., 1988], EMT [Nakajima et al., 1997], and vascular contractility [Schildmeyer et al., 2000; Tomasek et al., 2006] which are all important in the heart. Mutations in  $\alpha$ -smooth muscle actin are associated with patent ductus arteriosus, which is thought to arise due to impaired SMC contractility [Guo et al., 2007]. *In ovo* attempts to assess the transcriptional regulation of *RBMS1* in the chick embryo left the link between this gene and *TBX5* / *GATA-4* unclear due to the limitations of the study. As *RBMS1* was considered to be potentially important in cardiogenesis based on the P19 study and previous work by others, investigation of this gene in the chick embryo was continued in Chapter 5. The chromosomal location of the chicken *RBMS1* gene was identified, and this gene was found to give rise to two highly similar splice variants (confirmed by EST evidence). Multispecies sequence alignments demonstrated that this gene is highly conserved.

#### 7.4.1 *RBMS1* expression

*RBMS1* expression has been studied by northern blot analysis in the adult mouse, where expression was detected in all tissues except testis [Fujimoto et al., 2000]. However, a more detailed spatial analysis of expression has not been performed, and the developmental expression of this gene is unknown. In order to determine the spatial and temporal expression pattern of *RBMS1* during chick embryonic development, *in situ* hybridisation was performed using two individual probes designed to detect both *RBMS1* transcripts. At HH16, heart expression was weak, and other regions of the embryo including the somites displayed strong expression. The HH19 embryo displayed widespread expression, and staining to the heart was stronger at this stage. At HH24, *RBMS1* displayed expression to the heart, and was highly expressed in the developing forelimb and hind limb buds, somites, and brain. As mentioned, *RBMS1* transcriptionally regulates expression of  $\alpha$ -smooth muscle actin [Kimura et al., 1998]. It is possible the  $\alpha$ -actin genes share common regulatory

elements, and it was hypothesised that RBMS1 may also transcriptionally regulate expression of  $\alpha$ -skeletal and/or  $\alpha$ -cardiac actin.

#### **7.4.2 Morpholino knockdown of RBMS1**

Mouse knockout of RBMS1 results in growth and developmental defects which can lead to embryonic lethality [Fujimoto et al., 2001]. Deficiency of the hormone progesterone occurs in adult female mice, and this is thought to contribute to the delay in development [Fujimoto et al., 2001]. However, the effect RBMS1 knockout has on the development of the heart has not specifically been studied. In order to assess the function of RBMS1 in the developing heart, morpholino knockdown studies in the chick were performed. Due to the possibility of individual translational start sites on each RBMS1 transcript, splice-blocking morpholinos were used to allow simultaneous knockdown of both. The first morpholino was designed to bind to the exon 2-intron 2 junction (E2I2). A corresponding 5-base mismatch morpholino was also designed as a specificity control, but experimental data indicated that this morpholino may still have been able to bind to the target region, which meant it could not be used. Consultation with Gene-Tools revealed that the use of mismatch morpholinos was no longer recommended due to a high likelihood of retained target binding capability or off-target effects (as observed in this thesis). Therefore, a second experimental morpholino to the same gene was recommended, for determination of specificity upon generation of a common phenotype by both. A second experimental morpholino was designed to bind to the exon8-intron 8 boundary (E8I8). Both morpholinos would most likely result in exon skipping, or alternatively intron retention, and all outcomes were expected to cause in a premature stop and produce a truncated protein. Morpholinos were applied at HH10 - HH16. Morpholino treated embryos were examined at HH19 and displayed normal body shape and size, and cardiac malformations particularly in heart looping were apparent upon external viewing of the heart. Histological analysis of internal heart structures showed defects in atrial septation, and in some cases, a complete absence of septum formation. Similar defects are seen as a result of knockdown of TBX5 and GATA-4. This data may indicate that RBMS1 is a transcriptional regulator

of genes involved in correct septation of the heart, possibly as a downstream target of TBX5 and GATA-4. This is a novel finding and if corroborated with further evidence, will contribute to our current knowledge of the genes and transcriptional pathways regulating heart development, opening up many possibilities for future research.

#### **7.4.3 Characterisation of morpholino effects**

The effect of RBMS1 knockdown on heart development is an interesting and novel finding. The two morpholinos used for knockdown of RBMS1 gave very similar phenotypes, implying morpholino specificity. However, it was not possible to identify an effect on mRNA splicing as alternatively spliced products were not detected by RT-PCR. Splice-modified mRNA transcripts are often undetectable by RT-PCR as nonsense mediated decay (NMD) can eliminate them from the cell (personal communication with Jon Moulton, Gene-Tools). Splicing of mRNA occurs in the nucleus, and NMD is a cytosolic process, which means that pre-mRNA transcripts persist for a shorter period than transcripts undergoing NMD. Additionally, there was no reduction in the quantity of the wild type transcript (measured by QPCR) as would be expected if NMD was causing degradation of aberrant transcripts. The sensitivity of the assay was not a contributing factor since pre-mRNA transcripts, which persist for a shorter period than transcripts undergoing NMD, were detectable. Western blotting was also attempted to quantify RBMS1 protein levels in knockdown embryos, but this was not successful. However, expression of  $\alpha$ -smooth muscle actin (a negatively regulated target of RBMS1) was up-regulated in RBMS1 E212 morpholino treated embryos, supporting the theory that RBMS1 knockdown was occurring. Time restrictions did not allow analysis of  $\alpha$ -smooth muscle actin expression in embryos treated with the RBMS1 E818 targeting morpholino. These conflicting data raise questions as to whether the phenotypes observed could be due to non-specific effects, and whether morpholinos were in fact inducing knockdown. Morpholino antisense technology is a relatively new advance, and is a highly useful tool for studying gene function by knockdown. However, the issue of controls is extremely important and it is not clear which serves as the best control of specificity. Mismatch

morpholinos may continue to display capability to bind to target sites, but if this issue can be resolved with 7-base mismatch morpholinos (i.e. if target binding does not occur and off-targets effects are also not seen), these may be suitable when attempting to re-create an already known and characterised effect, as in Chapter 4. However, when attempting to investigate novel gene function by knockdown, specificity controls are arguably of greater importance since the expected phenotype is unknown and thus there is no reference point (from an anatomical perspective). The use of two non-overlapping targeting morpholinos is now the recommended method and has advantages over mismatch controls, but is still an indirect means of demonstrating specificity. Whilst it is unlikely in this case that an identical cardiac effect was generated by two individual morpholinos through off-target RNA binding, and the known RBMS1 target  $\alpha$ -smooth muscle actin was up-regulated through such an interaction, the effect of morpholinos on RBMS1 needs to be investigated from new angles before a direct cause-effect relationship can be established. The mRNA rescue experiment, where mRNA coding for the protein being knocked down is co-injected with the morpholino, determines proof of specificity by restoration of the wild type phenotype. If this can be put into practice, this experiment provides good proof of principle. Alternatively, RBMS1 knockdown or knockout using an alternative model may be warranted. If the cardiac phenotype observed in this study can be confirmed to be an effect of RBMS1 knockdown, this opens up a range of possibilities for further research. Future directions may involve mutational analysis for investigation of RBMS1 as a causative gene of CHD, identification of upstream regulators and downstream targets, and functional study to determine the mechanisms by which a reduction in RBMS1 can lead to cardiac abnormalities.

### **7.5 Identification of new synergistic targets of TBX5 and GATA-4**

Known synergistic targets of TBX5 and GATA-4 include MYH6 [Ching et al., 2005; Huang et al., 1995; Maitra et al., 2009; Molkenin et al., 1994], ANF [Plageman and Yutzey, 2004], and connexin 40 [Linhares et al., 2004]. All three of these genes have been linked to cardiac defects; mutations in MYH6 are linked to atrial septal defects

[Ching et al., 2005], and mutations in connexin 40 and ANF are associated with atrial fibrillation [Gollob et al., 2006; Hodgson-Zingman et al., 2008]. In Chapter 6, the previously developed *in ovo* model of TBX5 and GATA-4 double knockdown was used for identification of new synergistic targets via microarray technology, allowing gene expression profiling on a genome-wide scale. Eighteen genes were identified displaying differential regulation in TBX5 / GATA-4 knockdown embryos but not in single knockdown embryos or controls (all were up-regulated by  $\geq 2$  fold). The majority of genes identified in the TBX5 / GATA-4 double knockdown group have known roles in embryonic development. Expression patterns of six identified genes were detailed in the online GEISHA resource (SOX3, ZIC1, FOXG1, NKX2-1, PAX6, and OTX2), and these did not display obvious expression to the heart so were not considered further. Based on current literature, some of the remaining twelve genes have been reported to display heart expression, such as the novel cytokine CYTL1 [Kim et al., 2007], and the growth factor FIGF (also called VEGFD) [Avantaggiato et al., 1998]. FIGF, in addition to displaying expression in the limb buds, ganglion, teeth, anterior pituitary, lung, kidney, derma, and vertebral column, is expressed in the presumptive endocardial cushions of the heart, potentially indicating a specific cardiac function here [Avantaggiato et al., 1998]. In addition, FIGF signalling is also important in angiogenesis [Marconcini et al., 1999; Veikkola et al., 2001]. However, the expression pattern of these twelve genes had not previously been characterised fully, and nine prioritised genes were selected for study including TFAP2B, PTPRZ1, FIGF, NR2E1, LOC420770, SUZ12, CRABP1, GOLGA4, and GPC3. Expression was examined by RT-PCR in the embryonic chick as a preliminary means of temporal and spatial characterisation of expression. With the exception of NR2E1, expression of all genes was detectable in the heart during development. LOC420770 displayed the most heart-restricted expression pattern and interestingly, once it was possible to differentiate between body and limb expression (at HH24), expression was observed to be more prominent in the limbs than body. This is suggestive of a heart/limb expression profile, similar to that of TBX5. Other genes such as TFAP2B, CRABP1 and PTPRZ1 displayed heart expression that appeared to be strongest during early

cardiac development. *TFAP2B* in particular was only detectable in the heart at HH16. Genes such as *SUZ12*, *GOLGA4*, *GPC3*, and *FIGF* displayed almost ubiquitous expression. It was not possible to study the expression patterns of *CYTL1*, *PLCH1* and *LOC419390* due to limited resources and time restrictions. Further studies need to be performed to determine the exact localisation of expression of genes of interest.

A number of the identified genes have established roles in cardiac development and disease. The small cytoplasmic protein *CRABP1* is important in the modulation of retinoic acid levels; this is very important developmentally and an excess of retinoic acid is associated with retinoic acid embryopathy (RAE), which is characterised by malformation of neural crest derived regions including conotruncal heart structures [Lammer et al., 1985]. Mutations in *CRABP1* are associated with the cerebrovascular condition Moyamoya disease [Suzuki and Takaku, 1969]. Mutations in *GPC3*, a cell surface heparan sulphate proteoglycan and component of the ECM, are linked to the overgrowth syndrome Simpson-Golabi-Behmel syndrome (SGBS) [Pilia et al., 1996]. SGBS is characterised by multiple congenital abnormalities including cardiovascular malformation such as VSDs, common AV canal, and DORV, cardiomyopathy, and conduction defects in the heart [Behmel et al., 1984; Golabi and Rosen, 1984; Lin et al., 1999; Neri et al., 1988]. *CRABP1* and *GPC3* are previously unknown targets of *TBX5* and *GATA-4*, and this is a novel finding. Mutations in the transcription factor *TFAP2B* are associated with Char syndrome, an autosomal dominant 'heart-hand' disorder whose anomalies arise in neural crest cell derived regions and include patent ductus arteriosus (PDA), facial dysmorphism and hand anomalies [Char, 1978]. It is likely that *TFAP2B* has a role in the migration or differentiation of neural crest cells. Little is currently known about the regulation of *TFAP2B*, and is interesting that this heart-hand gene may be transcriptionally co-regulated by another heart-hand gene, *TBX5*. This potentially provides a new link between cardiac transcription factors which have not previously been associated.

TBX5 and GATA-4 are known as master regulators of cardiac development, and the diverse nature of the identified genes in addition to the known roles of some of these in the heart is a demonstration of this. Further study is required to validate the link between these genes and the TBX5 / GATA-4 complex. Insight into the regulation of these genes may contribute to our current understanding of the transcriptional networks and pathways governing cardiac development, and the genetic basis of CHD. Study of identified genes was halted at this stage as a starting point for future PhD projects.

### **7.6 Summary of findings and implications of this research**

This thesis aimed to identify and investigate genes important in cardiac development, with focus on the synergistic targets of TBX5 and GATA-4. The results of two independent microarray studies were used as a basis for this research, and a diverse group of candidate genes was identified as a result, many of which have not previously been associated with a cardiac function.

Microarray expression analysis of TBX5 / GATA-4 double overexpression P19 cell lines led to the identification of a large number of candidate genes, of which seven were selected for further study - *PA2.26*, *PETA-3*, *FUCA1*, *FN*, *TPM1*, *DES*, and *RBMS1*. *In silico* promoter analysis identified the cell cycle gene and transcription factor RBMS1 as the gene with most putative TBX5 and GATA-4 binding sites, and this gene has not previously been associated with a cardiac function. RBMS1 was therefore selected for further study of its role in cardiac development. Chick embryonic treatment with RBMS1 targeting morpholinos for knockdown of expression resulted in defects in cardiac looping and atrial septation. This was an interesting and novel finding as this gene has not previously been implicated in cardiac development, and opened up a range of possibilities for future research into cardiac transcriptional networks. However further investigation is required to confirm the effect observed was a direct result of RBMS1 knockdown. Based on the P19 study, the roles of fibronectin and  $\alpha$ -tropomyosin in heart development were also investigated by Dr Christopher

Moore. Morpholino knockdown of fibronectin in the chick resulted in body twisting, growth retardation, abnormal looping of the heart, and a thickening of the cardiac jelly layer (unpublished data). Morpholino knockdown of  $\alpha$ -tropomyosin caused kinking of the body, abnormal heart looping, and upon internal analysis hearts showed defects in trabeculation and atrial septum formation (unpublished data). Other genes such as *PETA-3* and *PA2.26* remain to be investigated and this may be a basis for future research projects.

Microarray expression analysis using the *in ovo* model of TBX5 and GATA-4 double knockdown led to the identification of a number of interesting putative targets, including *TFAP2B*, *GPC3*, and *CRABP1*, which have established roles in cardiac development. *TFAP2B* is arguably the most interesting as mutations in this gene are associated with the heart-hand disorder Char syndrome [Satoda et al., 1999; Satoda et al., 2000]. Research into validating the link between genes of interest and TBX5 / GATA-4 may provide new insights into regulatory networks in the heart. *LOC420770*, a novel gene of unknown function, was also identified and displayed expression potentially indicative of a heart-limb profile. Further studies to attempt elucidation of the function of this gene may provide a novel candidate gene for CHD. Investigation of these genes will form the basis of future research, adding to our current knowledge of the complex network of genes involved in heart development.

### **7.7 Limitations of this approach**

The work in this thesis has been largely based on the chick. The many advantages of using the chick as a model of cardiac development, in terms of the structural similarity to the human heart, and ease of access and manipulation, have been discussed throughout this thesis. However, as with any model, this organism also has a number of limitations. As discussed, atrial septation in the chick differs from mammals; in the chick a single atrial septum is formed, whereas in higher vertebrates an additional septum (the septum secundum) also forms and contributes to atrial septation [Morse et al., 1984]. This means that atrial septal defects that arise from disrupted septum

secundum formation cannot be modelled in the chick. Since this study has focused on defects of the septum primum, this has not been a major concern here. Another limitation of this model is that due to the evolutionary diversity between the chick and human, homologues of candidate genes may not be present. An example of this is the gene encoding gamma filamin, which was of interest in this thesis but could not be studied in the chick. The differing physiology of organisms, and how this can manifest itself in many ways including a varied sensitivity to gene dosage, is of importance. Even within mammalian species, vast differences in the effect of equivalent levels of gene knockdown can be observed. For example, human mutations in *NKX2.5* (including those generating hypomorphic alleles) are associated with an array of congenital heart defects [Benson et al., 1999; Elliott et al., 2003; McElhinney et al., 2003; Pashmforoush et al., 2004; Schott et al., 1998]. In comparison, mouse heterozygotes of *NKX2.5* display only a mild cardiac phenotype [Biben et al., 2000]. A similar effect is seen with *TBX20*; hypomorphic mutations in this gene in humans lead to a diverse range of cardiac defects [Kirk et al., 2007], whilst in the mouse only a greater than 50% reduction will lead to heart defects [Stennard et al., 2005; Takeuchi et al., 2005]. This differing sensitivity and response to gene dosage is likely to be multi-factorial. Species-specific physiology is likely to be one contributing factor, and the genetic background, which is important in the manifestation of CHDs [Rajagopal et al., 2007], may be another. It is possible these differences are greater in the chick than mouse since the chick is more physiologically and evolutionary diverse from the human. In this thesis, knockdown of *TBX5* and *GATA-4* in the chick embryo had no effect on expression of *MYH6*. This may have been due to experimental factors, but a species-specific effect cannot be ruled out without further study. Unfortunately it is not possible to predict or quantify these effects, which means the use of any model organism has its limitations and these need to be considered when interpreting data.

**REFERENCES**

2004. Sequence and comparative analysis of the chicken genome provide unique perspectives on vertebrate evolution. *Nature* 432:695-716.
- Abdulla R, Blew GA, Holterman MJ. 2004. Cardiovascular embryology. *Pediatr Cardiol* 25:191-200.
- Abe J, Zhou W, Taguchi J, Takuwa N, Miki K, Okazaki H, Kurokawa K, Kumada M, Takuwa Y. 1994. Suppression of neointimal smooth muscle cell accumulation in vivo by antisense cdc2 and cdk2 oligonucleotides in rat carotid artery. *Biochem Biophys Res Commun* 198:16-24.
- Abu-Elmagd M, Ishii Y, Cheung M, Rex M, Le Rouedec D, Scotting PJ. 2001. cSox3 expression and neurogenesis in the epibranchial placodes. *Dev Biol* 237:258-69.
- Abu-Issa R, Waldo K, Kirby ML. 2004. Heart fields: one, two or more? *Dev Biol* 272:281-5.
- Acampora D, Mazan S, Lallemand Y, Avantaggiato V, Maury M, Simeone A, Brulet P. 1995. Forebrain and midbrain regions are deleted in *Otx2*<sup>-/-</sup> mutants due to a defective anterior neuroectoderm specification during gastrulation. *Development* 121:3279-90.
- Achen MG, Jeltsch M, Kukk E, Makinen T, Vitali A, Wilks AF, Alitalo K, Stacker SA. 1998. Vascular endothelial growth factor D (VEGF-D) is a ligand for the tyrosine kinases VEGF receptor 2 (Flk1) and VEGF receptor 3 (Flt4). *Proc Natl Acad Sci U S A* 95:548-53.
- Alsan BH, Schultheiss TM. 2002. Regulation of avian cardiogenesis by *Fgf8* signaling. *Development* 129:1935-43.
- Anderson RH, Webb S, Brown NA, Lamers W, Moorman A. 2003. Development of the heart: (2) Septation of the atriums and ventricles. *Heart* 89:949-58.

Andree B, Duprez D, Vorbusch B, Arnold HH, Brand T. 1998. BMP-2 induces ectopic expression of cardiac lineage markers and interferes with somite formation in chicken embryos. *Mech Dev* 70:119-31.

Ang SL, Jin O, Rhinn M, Daigle N, Stevenson L, Rossant J. 1996. A targeted mouse *Otx2* mutation leads to severe defects in gastrulation and formation of axial mesoderm and to deletion of rostral brain. *Development* 122:243-52.

Aoyagi M, Fukai N, Matsushima Y, Yamamoto M, Yamamoto K. 1993. Kinetics of <sup>125</sup>I-PDGF binding and down-regulation of PDGF receptor in arterial smooth muscle cells derived from patients with moyamoya disease. *J Cell Physiol* 154:281-8.

Aoyagi M, Fukai N, Sakamoto H, Shinkai T, Matsushima Y, Yamamoto M, Yamamoto K. 1991. Altered cellular responses to serum mitogens, including platelet-derived growth factor, in cultured smooth muscle cells derived from arteries of patients with moyamoya disease. *J Cell Physiol* 147:191-8.

Aravind L, Koonin EV. 2000. SAP - a putative DNA-binding motif involved in chromosomal organization. *Trends Biochem Sci* 25:112-4.

Ariani F, Hayek G, Rondinella D, Artuso R, Mencarelli MA, Spanhol-Rosseto A, Pollazzon M, Buoni S, Spiga O, Ricciardi S, Meloni I, Longo I, Mari F, Broccoli V, Zappella M, Renieri A. 2008. *FOXG1* is responsible for the congenital variant of Rett syndrome. *Am J Hum Genet* 83:89-93.

Armstrong EJ, Bischoff J. 2004. Heart valve development: endothelial cell signaling and differentiation. *Circ Res* 95:459-70.

Arsenian S, Weinhold B, Oelgeschlager M, Ruther U, Nordheim A. 1998. Serum response factor is essential for mesoderm formation during mouse embryogenesis. *EMBO J* 17:6289-99.

Aruga J, Minowa O, Yaginuma H, Kuno J, Nagai T, Noda T, Mikoshiba K. 1998. Mouse *Zic1* is involved in cerebellar development. *J Neurosci* 18:284-93.

- Aruga J, Mizugishi K, Koseki H, Imai K, Balling R, Noda T, Mikoshiba K. 1999. Zic1 regulates the patterning of vertebral arches in cooperation with Gli3. *Mech Dev* 89:141-50.
- Avantaggiato V, Orlandini M, Acampora D, Oliviero S, Simeone A. 1998. Embryonic expression pattern of the murine figf gene, a growth factor belonging to platelet-derived growth factor/vascular endothelial growth factor family. *Mech Dev* 73:221-4.
- Azpiazu N, Frasch M. 1993. tinman and bagpipe: two homeo box genes that determine cell fates in the dorsal mesoderm of Drosophila. *Genes Dev* 7:1325-40.
- Balchum OJ, Blount SG, Jr., Gensini G. 1956. The persistent ostium primum atrial septal defect. *Circulation* 13:499-509.
- Balducci-Silano PL, Suzuki K, Ohta M, Saito J, Ohmori M, Montani V, Napolitano G, Shong M, Taniguchi SI, Pietrarelli M, Lavaroni S, Mori A, Singer DS, Kohn LD. 1998. Regulation of major histocompatibility (MHC) class II human leukocyte antigen-DR alpha gene expression in thyrocytes by single strand binding protein-1, a transcription factor that also regulates thyrotropin receptor and MHC class I gene expression. *Endocrinology* 139:2300-13.
- Bamshad M, Lin RC, Law DJ, Watkins WC, Krakowiak PA, Moore ME, Franceschini P, Lala R, Holmes LB, Gebuhr TC, Bruneau BG, Schinzel A, Seidman JG, Seidman CE, Jorde LB. 1997. Mutations in human TBX3 alter limb, apocrine and genital development in ulnar-mammary syndrome. *Nat Genet* 16:311-5.
- Banerjee I, Fuseler JW, Price RL, Borg TK, Baudino TA. 2007. Determination of cell types and numbers during cardiac development in the neonatal and adult rat and mouse. *Am J Physiol Heart Circ Physiol* 293:H1883-91.
- Barron M, Gao M, Lough J. 2000. Requirement for BMP and FGF signaling during cardiogenic induction in non-precardiac mesoderm is specific, transient, and cooperative. *Dev Dyn* 218:383-93.

Basson CT, Bachinsky DR, Lin RC, Levi T, Elkins JA, Soultis J, Grayzel D, Kroumpouzou E, Traill TA, Leblanc-Straceski J, Renault B, Kucherlapati R, Seidman JG, Seidman CE. 1997. Mutations in human TBX5 [corrected] cause limb and cardiac malformation in Holt-Oram syndrome. *Nat Genet* 15:30-5.

Basson CT, Cowley GS, Solomon SD, Weissman B, Poznanski AK, Traill TA, Seidman JG, Seidman CE. 1994. The clinical and genetic spectrum of the Holt-Oram syndrome (heart-hand syndrome). *N Engl J Med* 330:885-91.

Basson CT, Huang T, Lin RC, Bachinsky DR, Weremowicz S, Vaglio A, Bruzzone R, Quadrelli R, Lerone M, Romeo G, Silengo M, Pereira A, Krieger J, Mesquita SF, Kamisago M, Morton CC, Pierpont ME, Muller CW, Seidman JG, Seidman CE. 1999. Different TBX5 interactions in heart and limb defined by Holt-Oram syndrome mutations. *Proc Natl Acad Sci U S A* 96:2919-24.

Baxter SC, Morales MO, Goldsmith EC. 2008. Adaptive changes in cardiac fibroblast morphology and collagen organization as a result of mechanical environment. *Cell Biochem Biophys* 51:33-44.

Begemann G, Ingham PW. 2000. Developmental regulation of Tbx5 in zebrafish embryogenesis. *Mech Dev* 90:299-304.

Behmel A, Plochl E, Rosenkranz W. 1984. A new X-linked dysplasia gigantism syndrome: identical with the Simpson dysplasia syndrome? *Hum Genet* 67:409-13.

Belaguli NS, Schildmeyer LA, Schwartz RJ. 1997. Organization and myogenic restricted expression of the murine serum response factor gene. A role for autoregulation. *J Biol Chem* 272:18222-31.

Bell E, Ensini M, Gulisano M, Lumsden A. 2001. Dynamic domains of gene expression in the early avian forebrain. *Dev Biol* 236:76-88.

Benson DW, Silberbach GM, Kavanaugh-McHugh A, Cottrill C, Zhang Y, Riggs S, Smalls O, Johnson MC, Watson MS, Seidman JG, Seidman CE, Plowden J, Kugler

JD. 1999. Mutations in the cardiac transcription factor NKX2.5 affect diverse cardiac developmental pathways. *J Clin Invest* 104:1567-73.

Bergman JE, Veenstra-Knol HE, van Essen AJ, van Ravenswaaij CM, den Dunnen WF, van den Wijngaard A, van Tintelen JP. 2007. Two related Dutch families with a clinically variable presentation of cardioskeletal myopathy caused by a novel S13F mutation in the desmin gene. *Eur J Med Genet* 50:355-66.

Bhagavatula MR, Fan C, Shen GQ, Cassano J, Plow EF, Topol EJ, Wang Q. 2004. Transcription factor MEF2A mutations in patients with coronary artery disease. *Hum Mol Genet* 13:3181-8.

Biben C, Harvey RP. 1997. Homeodomain factor Nkx2-5 controls left/right asymmetric expression of bHLH gene eHand during murine heart development. *Genes Dev* 11:1357-69.

Biben C, Weber R, Kesteven S, Stanley E, McDonald L, Elliott DA, Barnett L, Koentgen F, Robb L, Feneley M, Harvey RP. 2000. Cardiac septal and valvular dysmorphogenesis in mice heterozygous for mutations in the homeobox gene Nkx2-5. *Circ Res* 87:888-95.

Black BL, Olson EN. 1998. Transcriptional control of muscle development by myocyte enhancer factor-2 (MEF2) proteins. *Annu Rev Cell Dev Biol* 14:167-96.

Blom NA, Ottenkamp J, Jongeneel TH, DeRuiter MC, Gittenberger-de Groot AC. 2005. Morphogenetic differences of secundum atrial septal defects. *Pediatr.Cardiol.* 26:338-343.

Bodmer R. 1993. The gene tinman is required for specification of the heart and visceral muscles in *Drosophila*. *Development* 118:719-29.

Bongers EM, Duijf PH, van Beersum SE, Schoots J, Van Kampen A, Burckhardt A, Hamel BC, Losan F, Hoefsloot LH, Yntema HG, Knoers NV, van Bokhoven H. 2004.

- Mutations in the human TBX4 gene cause small patella syndrome. *Am J Hum Genet* 74:1239-48.
- Boogerd CJ, Dooijes D, Ilgun A, Hordijk R, van de Laar IM, Rump P, Veenstra-Knol HE, Moorman AF, Barnett P, Postma AV. Functional analysis of novel TBX5 T-box mutations associated with Holt-Oram syndrome. *Cardiovasc Res*.
- Boot MJ, Gittenberger-de Groot AC, van Iperen L, Poelmann RE. 2003. The myth of ventrally emigrating neural tube (VENT) cells and their contribution to the developing cardiovascular system. *Anat Embryol (Berl)* 206:327-33.
- Borg TK, Caulfield JB. 1980. Morphology of connective tissue in skeletal muscle. *Tissue Cell* 12:197-207.
- Bos JM, Ommen SR, Ackerman MJ. 2007. Genetics of hypertrophic cardiomyopathy: one, two, or more diseases? *Curr Opin Cardiol* 22:193-9.
- Bottcher RT, Niehrs C. 2005. Fibroblast growth factor signaling during early vertebrate development. *Endocr Rev* 26:63-77.
- Bowers SL, Banerjee I, Baudino TA. The extracellular matrix: at the center of it all. *J Mol Cell Cardiol* 48:474-82.
- Boyle BJ, Harris VK, Liaudet-Coopman ED, Riegel AT, Wellstein A. 2000. Differential regulation of a fibroblast growth factor-binding protein by receptor-selective analogs of retinoic acid. *Biochem Pharmacol* 60:1677-84.
- Brade T, Manner J, Kuhl M. 2006. The role of Wnt signalling in cardiac development and tissue remodelling in the mature heart. *Cardiovasc Res* 72:198-209.
- Breckenridge RA, Mohun TJ, Amaya E. 2001. A role for BMP signalling in heart looping morphogenesis in *Xenopus*. *Dev Biol* 232:191-203.

- Brown DD, Martz SN, Binder O, Goetz SC, Price BM, Smith JC, Conlon FL. 2005. Tbx5 and Tbx20 act synergistically to control vertebrate heart morphogenesis. *Development* 132:553-63.
- Bruneau BG. 2002. Transcriptional regulation of vertebrate cardiac morphogenesis. *Circ Res* 90:509-19.
- Bruneau BG, Logan M, Davis N, Levi T, Tabin CJ, Seidman JG, Seidman CE. 1999. Chamber-specific cardiac expression of Tbx5 and heart defects in Holt-Oram syndrome. *Dev Biol* 211:100-8.
- Bruneau BG, Nemer G, Schmitt JP, Charron F, Robitaille L, Caron S, Conner DA, Gessler M, Nemer M, Seidman CE, Seidman JG. 2001. A murine model of Holt-Oram syndrome defines roles of the T-box transcription factor Tbx5 in cardiogenesis and disease. *Cell* 106:709-21.
- Brutsaert DL. 2003. Cardiac endothelial-myocardial signaling: its role in cardiac growth, contractile performance, and rhythmicity. *Physiol Rev* 83:59-115.
- Budde BS, Binner P, Waldmuller S, Hohne W, Blankenfeldt W, Hassfeld S, Bromsen J, Dermintzoglou A, Wiczorek M, May E, Kirst E, Selignow C, Rackebrandt K, Muller M, Goody RS, Vosberg HP, Nurnberg P, Scheffold T. 2007. Noncompaction of the ventricular myocardium is associated with a de novo mutation in the beta-myosin heavy chain gene. *PLoS One* 2:e1362.
- Burkett EL, Hershberger RE. 2005. Clinical and genetic issues in familial dilated cardiomyopathy. *J Am Coll Cardiol* 45:969-81.
- Bussen M, Petry M, Schuster-Gossler K, Leitges M, Gossler A, Kispert A. 2004. The T-box transcription factor Tbx18 maintains the separation of anterior and posterior somite compartments. *Genes Dev* 18:1209-21.

Cai CL, Liang X, Shi Y, Chu PH, Pfaff SL, Chen J, Evans S. 2003. Isl1 identifies a cardiac progenitor population that proliferates prior to differentiation and contributes a majority of cells to the heart. *Dev Cell* 5:877-89.

Cano-Gauci DF, Song HH, Yang H, McKerlie C, Choo B, Shi W, Pullano R, Piscione TD, Grisaru S, Soon S, Sedlackova L, Tanswell AK, Mak TW, Yeger H, Lockwood GA, Rosenblum ND, Filmus J. 1999. Glypican-3-deficient mice exhibit developmental overgrowth and some of the abnormalities typical of Simpson-Golabi-Behmel syndrome. *J Cell Biol* 146:255-64.

Castier Y, Chemla E, Nierat J, Heudes D, Vasseur MA, Rajnoch C, Bruneval P, Carpentier A, Fabiani JN. 1998. The activity of c-myb antisense oligonucleotide to prevent intimal hyperplasia is nonspecific. *J Cardiovasc Surg (Torino)* 39:1-7.

Chapman DL, Garvey N, Hancock S, Alexiou M, Agulnik SI, Gibson-Brown JJ, Cebra-Thomas J, Bollag RJ, Silver LM, Papaioannou VE. 1996. Expression of the T-box family genes, Tbx1-Tbx5, during early mouse development. *Dev Dyn* 206:379-90.

Char F. 1978. Peculiar facies with short philtrum, duck-bill lips, ptosis and low-set ears--a new syndrome? *Birth Defects Orig Artic Ser* 14:303-5.

Chauhan AK, Li YS, Deuel TF. 1993. Pleiotrophin transforms NIH 3T3 cells and induces tumors in nude mice. *Proc Natl Acad Sci U S A* 90:679-82.

Chen CY, Croissant J, Majesky M, Topouzis S, McQuinn T, Frankovsky MJ, Schwartz RJ. 1996. Activation of the cardiac alpha-actin promoter depends upon serum response factor, Tinman homologue, Nkx-2.5, and intact serum response elements. *Dev Genet* 19:119-30.

Chen CY, Schwartz RJ. 1996. Recruitment of the tinman homolog Nkx-2.5 by serum response factor activates cardiac alpha-actin gene transcription. *Mol Cell Biol* 16:6372-84.

- Chen Y, Amende I, Hampton TG, Yang Y, Ke Q, Min JY, Xiao YF, Morgan JP. 2006. Vascular endothelial growth factor promotes cardiomyocyte differentiation of embryonic stem cells. *Am J Physiol Heart Circ Physiol* 291:H1653-8.
- Chin C, Gandour-Edwards R, Oltjen S, Choy M. 1992. Fate of the atrioventricular endocardial cushions in the developing chick heart. *Pediatr Res* 32:390-3.
- Ching YH, Ghosh TK, Cross SJ, Packham EA, Honeyman L, Loughna S, Robinson TE, Dearlove AM, Ribas G, Bonser AJ, Thomas NR, Scotter AJ, Caves LS, Tyrrell GP, Newbury-Ecob RA, Munnich A, Bonnet D, Brook JD. 2005. Mutation in myosin heavy chain 6 causes atrial septal defect. *Nat Genet* 37:423-8.
- Christoffels VM, Habets PE, Franco D, Campione M, de Jong F, Lamers WH, Bao ZZ, Palmer S, Biben C, Harvey RP, Moorman AF. 2000. Chamber formation and morphogenesis in the developing mammalian heart. *Dev Biol* 223:266-78.
- Coeshott CM, Smithson SL, Verderber E, Samaniego A, Blonder JM, Rosenthal GJ, Westerink MA. 2004. Pluronic F127-based systemic vaccine delivery systems. *Vaccine* 22:2396-405.
- Cogan JG, Sun S, Stoflet ES, Schmidt LJ, Getz MJ, Strauch AR. 1995. Plasticity of vascular smooth muscle alpha-actin gene transcription. Characterization of multiple, single-, and double-strand specific DNA-binding proteins in myoblasts and fibroblasts. *J Biol Chem* 270:11310-21.
- Colvin JS, White AC, Pratt SJ, Ornitz DM. 2001. Lung hypoplasia and neonatal death in Fgf9-null mice identify this gene as an essential regulator of lung mesenchyme. *Development* 128:2095-106.
- Consigli SA, Joseph-Silverstein J. 1991. Immunolocalization of basic fibroblast growth factor during chicken cardiac development. *J Cell Physiol* 146:379-85.
- Corda S, Samuel JL, Rappaport L. 2000. Extracellular matrix and growth factors during heart growth. *Heart Fail Rev* 5:119-30.

Crossley PH, Minowada G, MacArthur CA, Martin GR. 1996. Roles for FGF8 in the induction, initiation, and maintenance of chick limb development. *Cell* 84:127-36.

Davenport TG, Jerome-Majewska LA, Papaioannou VE. 2003. Mammary gland, limb and yolk sac defects in mice lacking *Tbx3*, the gene mutated in human ulnar mammary syndrome. *Development* 130:2263-73.

David G. 1993. Integral membrane heparan sulfate proteoglycans. *FASEB J* 7:1023-30.

Davis RL, Turner DL. 2001. Vertebrate hairy and Enhancer of split related proteins: transcriptional repressors regulating cellular differentiation and embryonic patterning. *Oncogene* 20:8342-57.

De La Cruz MV, Sanchez-Gomez C, Palomino MA. 1989. The primitive cardiac regions in the straight tube heart (Stage 9) and their anatomical expression in the mature heart: An experimental study in the chick embryo. *J Anat* 165:121-31.

de Lange FJ, Moorman AF, Anderson RH, Manner J, Soufan AT, de Gier-de Vries C, Schneider MD, Webb S, van den Hoff MJ, Christoffels VM. 2004. Lineage and morphogenetic analysis of the cardiac valves. *Circ Res* 95:645-54.

Dealy CN, Roth A, Ferrari D, Brown AM, Kosher RA. 1993. *Wnt-5a* and *Wnt-7a* are expressed in the developing chick limb bud in a manner suggesting roles in pattern formation along the proximodistal and dorsoventral axes. *Mech Dev* 43:175-86.

DeRossi C, Laiosa MD, Silverstone AE, Holdener BC. 2000. Mouse *fzd4* maps within a region of chromosome 7 important for thymus and cardiac development. *Genesis* 27:64-75.

Derynck RaM, K. 2008. The TGF- $\beta$  family. Cold Spring Harbor Laboratory Press, New York

- Diao A, Rahman D, Pappin DJ, Lucocq J, Lowe M. 2003. The coiled-coil membrane protein golgin-84 is a novel rab effector required for Golgi ribbon formation. *J Cell Biol* 160:201-12.
- Dodou E, Verzi MP, Anderson JP, Xu SM, Black BL. 2004. Mef2c is a direct transcriptional target of ISL1 and GATA factors in the anterior heart field during mouse embryonic development. *Development* 131:3931-42.
- Draper BW, Morcos PA, Kimmel CB. 2001. Inhibition of zebrafish fgf8 pre-mRNA splicing with morpholino oligos: a quantifiable method for gene knockdown. *Genesis* 30:154-6.
- Dreyfuss G, Swanson MS, Pinol-Roma S. 1988. Heterogeneous nuclear ribonucleoprotein particles and the pathway of mRNA formation. *Trends Biochem Sci* 13:86-91.
- Dyson E, Sucov HM, Kubalak SW, Schmid-Schonbein GW, DeLano FA, Evans RM, Ross J, Jr., Chien KR. 1995. Atrial-like phenotype is associated with embryonic ventricular failure in retinoid X receptor alpha  $-/-$  mice. *Proc Natl Acad Sci U S A* 92:7386-90.
- Edmondson DG, Lyons GE, Martin JF, Olson EN. 1994. Mef2 gene expression marks the cardiac and skeletal muscle lineages during mouse embryogenesis. *Development* 120:1251-63.
- Ehrman LA, Yutzey KE. 1999. Lack of regulation in the heart forming region of avian embryos. *Dev Biol* 207:163-75.
- Eisenberg CA, Eisenberg LM. 1999. WNT11 promotes cardiac tissue formation of early mesoderm. *Dev Dyn* 216:45-58.
- EI-Kamel AH. 2002. In vitro and in vivo evaluation of Pluronic F127-based ocular delivery system for timolol maleate. *Int J Pharm* 241:47-55.

- Elliott DA, Kirk EP, Yeoh T, Chandar S, McKenzie F, Taylor P, Grossfeld P, Fatkin D, Jones O, Hayes P, Feneley M, Harvey RP. 2003. Cardiac homeobox gene NKX2-5 mutations and congenital heart disease: associations with atrial septal defect and hypoplastic left heart syndrome. *J Am Coll Cardiol* 41:2072-6.
- Elliott DA, Solloway MJ, Wise N, Biben C, Costa MW, Furtado MB, Lange M, Dunwoodie S, Harvey RP. 2006. A tyrosine-rich domain within homeodomain transcription factor Nkx2-5 is an essential element in the early cardiac transcriptional regulatory machinery. *Development* 133:1311-22.
- Erickson SL, O'Shea KS, Ghaboosi N, Loverro L, Frantz G, Bauer M, Lu LH, Moore MW. 1997. ErbB3 is required for normal cerebellar and cardiac development: a comparison with ErbB2- and heregulin-deficient mice. *Development* 124:4999-5011.
- Faerman A, Shani M. 1993. The expression of the regulatory myosin light chain 2 gene during mouse embryogenesis. *Development* 118:919-29.
- Falk J, Drinjakovic J, Leung KM, Dwivedy A, Regan AG, Piper M, Holt CE. 2007. Electroporation of cDNA/Morpholinos to targeted areas of embryonic CNS in *Xenopus*. *BMC Dev Biol* 7:107.
- Fan C, Duhagon MA, Oberti C, Chen S, Hiroi Y, Komuro I, Duhagon PI, Canessa R, Wang Q. 2003. Novel TBX5 mutations and molecular mechanism for Holt-Oram syndrome. *J Med Genet* 40:e29.
- Farah CS, Reinach FC. 1995. The troponin complex and regulation of muscle contraction. *FASEB J* 9:755-67.
- Fedak PW, Verma S, Weisel RD, Li RK. 2005. Cardiac remodeling and failure From molecules to man (Part II). *Cardiovasc Pathol* 14:49-60.
- Ffrench-Constant C, Hynes RO. 1988. Patterns of fibronectin gene expression and splicing during cell migration in chicken embryos. *Development* 104:369-82.

- Ficker M, Powles N, Warr N, Pirvola U, Maconochie M. 2004. Analysis of genes from inner ear developmental-stage cDNA subtraction reveals molecular regionalization of the otic capsule. *Dev Biol* 268:7-23.
- Fidzianska A, Kotowicz J, Sadowska M, Goudeau B, Walczak E, Vicart P, Hausmanowa-Petrusewicz I. 2005. A novel desmin R355P mutation causes cardiac and skeletal myopathy. *Neuromuscul Disord* 15:525-31.
- Fijnvandraat AC, Lekanne Deprez RH, Christoffels VM, Ruijter JM, Moorman AF. 2003. TBX5 overexpression stimulates differentiation of chamber myocardium in P19C16 embryonic carcinoma cells. *J Muscle Res Cell Motil* 24:211-8.
- Finkelstein R, Boncinelli E. 1994. From fly head to mammalian forebrain: the story of *otd* and *Otx*. *Trends Genet* 10:310-5.
- Fiorella PD, Napoli JL. 1991. Expression of cellular retinoic acid binding protein (CRABP) in *Escherichia coli*. Characterization and evidence that holo-CRABP is a substrate in retinoic acid metabolism. *J Biol Chem* 266:16572-9.
- Firulli AB, McFadden DG, Lin Q, Srivastava D, Olson EN. 1998. Heart and extra-embryonic mesodermal defects in mouse embryos lacking the bHLH transcription factor *Hand1*. *Nat Genet* 18:266-70.
- Fischer S, Draper BW, Neumann CJ. 2003. The zebrafish *fgf24* mutant identifies an additional level of Fgf signaling involved in vertebrate forelimb initiation. *Development* 130:3515-24.
- Franco D, Lamers WH, Moorman AF. 1998. Patterns of expression in the developing myocardium: towards a morphologically integrated transcriptional model. *Cardiovasc Res* 38:25-53.
- Fries KM, Blieden T, Looney RJ, Sempowski GD, Silvera MR, Willis RA, Phipps RP. 1994. Evidence of fibroblast heterogeneity and the role of fibroblast subpopulations in fibrosis. *Clin Immunol Immunopathol* 72:283-92.

Fujimoto M, Iguchi-Ariga SM, Ariga H. 1998. Characterization of an element positively regulating the transcription of MSSP gene-2 which encodes C-MYC binding proteins. *Gene* 214:113-20.

Fujimoto M, Matsumoto K, Iguchi-Ariga SM, Ariga H. 2001. Disruption of MSSP, c-myc single-strand binding protein, leads to embryonic lethality in some homozygous mice. *Genes Cells* 6:1067-75.

Fujimoto M, Matsumoto KI, Iguchi-Ariga SM, Ariga H. 2000. Structures and comparison of genomic and complementary DNAs of mouse MSSP, a c-Myc binding protein. *Int J Oncol* 16:245-51.

Fujio Y, Matsuda T, Oshima Y, Maeda M, Mohri T, Ito T, Takatani T, Hirata M, Nakaoka Y, Kimura R, Kishimoto T, Azuma J. 2004. Signals through gp130 upregulate Wnt5a and contribute to cell adhesion in cardiac myocytes. *FEBS Lett* 573:202-6.

Gahlmann R, Kedes L. 1993. Tissue-specific restriction of skeletal muscle troponin C gene expression. *Gene Expr* 3:11-25.

Galvin KM, Donovan MJ, Lynch CA, Meyer RI, Paul RJ, Lorenz JN, Fairchild-Huntress V, Dixon KL, Dunmore JH, Gimbrone MA, Jr., Falb D, Huszar D. 2000. A role for smad6 in development and homeostasis of the cardiovascular system. *Nat Genet* 24:171-4.

Garcia-Calero E, Garda AL, Marin F, Puelles L. 2006. Expression of *Lrrn1* marks the prospective site of the zona limitans thalami in the early embryonic chicken diencephalon. *Gene Expr Patterns* 6:879-85.

Garg V. 2006. Insights into the genetic basis of congenital heart disease. *Cell Mol Life Sci* 63:1141-8.

Garg V, Kathiriya IS, Barnes R, Schluterman MK, King IN, Butler CA, Rothrock CR, Eapen RS, Hirayama-Yamada K, Joo K, Matsuoka R, Cohen JC, Srivastava D. 2003.

- GATA4 mutations cause human congenital heart defects and reveal an interaction with TBX5. *Nature* 424:443-7.
- Garg V, Muth AN, Ransom JF, Schluterman MK, Barnes R, King IN, Grossfeld PD, Srivastava D. 2005. Mutations in NOTCH1 cause aortic valve disease. *Nature* 437:270-4.
- Gassmann M, Casagrande F, Orioli D, Simon H, Lai C, Klein R, Lemke G. 1995. Aberrant neural and cardiac development in mice lacking the ErbB4 neuregulin receptor. *Nature* 378:390-4.
- Gaston-Massuet C, Henderson DJ, Greene ND, Copp AJ. 2005. Zic4, a zinc-finger transcription factor, is expressed in the developing mouse nervous system. *Dev Dyn* 233:1110-5.
- George EL, Georges-Labouesse EN, Patel-King RS, Rayburn H, Hynes RO. 1993. Defects in mesoderm, neural tube and vascular development in mouse embryos lacking fibronectin. *Development* 119:1079-91.
- Ghosh TK, Packham EA, Bonser AJ, Robinson TE, Cross SJ, Brook JD. 2001. Characterization of the TBX5 binding site and analysis of mutations that cause Holt-Oram syndrome. *Hum Mol Genet* 10:1983-94.
- Ghosh TK, Song FF, Packham EA, Buxton S, Robinson TE, Ronksley J, Self T, Bonser AJ, Brook JD. 2009. Physical interaction between TBX5 and MEF2C is required for early heart development. *Mol Cell Biol* 29:2205-18.
- Glaser T, Ton CC, Mueller R, Petzl-Erler ML, Oliver C, Nevin NC, Housman DE, Maas RL. 1994. Absence of PAX6 gene mutations in Gillespie syndrome (partial aniridia, cerebellar ataxia, and mental retardation). *Genomics* 19:145-8.
- Glaser T, Walton DS, Maas RL. 1992. Genomic structure, evolutionary conservation and aniridia mutations in the human PAX6 gene. *Nat Genet* 2:232-9.

- Golabi M, Rosen L. 1984. A new X-linked mental retardation-overgrowth syndrome. *Am J Med Genet* 17:345-58.
- Goldfarb LG, Park KY, Cervenakova L, Gorokhova S, Lee HS, Vasconcelos O, Nagle JW, Semino-Mora C, Sivakumar K, Dalakas MC. 1998. Missense mutations in desmin associated with familial cardiac and skeletal myopathy. *Nat Genet* 19:402-3.
- Gollob MH, Jones DL, Krahn AD, Danis L, Gong XQ, Shao Q, Liu X, Veinot JP, Tang AS, Stewart AF, Tesson F, Klein GJ, Yee R, Skanes AC, Guiraudon GM, Ebihara L, Bai D. 2006. Somatic mutations in the connexin 40 gene (GJA5) in atrial fibrillation. *N Engl J Med* 354:2677-88.
- Gonzalez P, Garcia-Castro M, Reguero JR, Batalla A, Ordonez AG, Palop RL, Lozano I, Montes M, Alvarez V, Coto E. 2006. The Pro279Leu variant in the transcription factor MEF2A is associated with myocardial infarction. *J Med Genet* 43:167-9.
- Goudeau B, Dagvadorj A, Rodrigues-Lima F, Nedellec P, Casteras-Simon M, Perret E, Langlois S, Goldfarb L, Vicart P. 2001. Structural and functional analysis of a new desmin variant causing desmin-related myopathy. *Hum Mutat* 18:388-96.
- Grepin C, Robitaille L, Antakly T, Nemer M. 1995. Inhibition of transcription factor GATA-4 expression blocks in vitro cardiac muscle differentiation. *Mol Cell Biol* 15:4095-102.
- Guo DC, Pannu H, Tran-Fadulu V, Papke CL, Yu RK, Avidan N, Bourgeois S, Estrera AL, Safi HJ, Sparks E, Amor D, Ades L, McConnell V, Willoughby CE, Abuelo D, Willing M, Lewis RA, Kim DH, Scherer S, Tung PP, Ahn C, Buja LM, Raman CS, Shete SS, Milewicz DM. 2007. Mutations in smooth muscle alpha-actin (ACTA2) lead to thoracic aortic aneurysms and dissections. *Nat Genet* 39:1488-93.
- Guo DC, Papke CL, Tran-Fadulu V, Regalado ES, Avidan N, Johnson RJ, Kim DH, Pannu H, Willing MC, Sparks E, Pyeritz RE, Singh MN, Dalman RL, Grotta JC, Marian AJ, Boerwinkle EA, Frazier LQ, LeMaire SA, Coselli JS, Estrera AL, Safi HJ,

Veeraraghavan S, Muzny DM, Wheeler DA, Willerson JT, Yu RK, Shete SS, Scherer SE, Raman CS, Buja LM, Milewicz DM. 2009. Mutations in smooth muscle alpha-actin (ACTA2) cause coronary artery disease, stroke, and Moyamoya disease, along with thoracic aortic disease. *Am J Hum Genet* 84:617-27.

Hailstones DL, Gunning PW. 1990. Characterization of human myosin light chains 1sa and 3nm: implications for isoform evolution and function. *Mol Cell Biol* 10:1095-104.

Hamburger V, Hamilton HL. 1992. A series of normal stages in the development of the chick embryo. 1951. *Dev Dyn* 195:231-72.

Han Y, Dennis JE, Cohen-Gould L, Bader DM, Fischman DA. 1992. Expression of sarcomeric myosin in the presumptive myocardium of chicken embryos occurs within six hours of myocyte commitment. *Dev Dyn* 193:257-65.

Hanashima C, Li SC, Shen L, Lai E, Fishell G. 2004. *Foxg1* suppresses early cortical cell fate. *Science* 303:56-9.

Hanson IM, Fletcher JM, Jordan T, Brown A, Taylor D, Adams RJ, Punnett HH, van Heyningen V. 1994. Mutations at the *PAX6* locus are found in heterogeneous anterior segment malformations including Peters' anomaly. *Nat Genet* 6:168-73.

Harrelson Z, Kelly RG, Goldin SN, Gibson-Brown JJ, Bollag RJ, Silver LM, Papaioannou VE. 2004. *Tbx2* is essential for patterning the atrioventricular canal and for morphogenesis of the outflow tract during heart development. *Development* 131:5041-52.

Harvey RP. 1996. NK-2 homeobox genes and heart development. *Dev Biol* 178:203-16.

Harvey RP, Lai D, Elliott D, Biben C, Solloway M, Prall O, Stennard F, Schindeler A, Groves N, Lavulo L, Hyun C, Yeoh T, Costa M, Furtado M, Kirk E. 2002. Homeodomain factor *Nkx2-5* in heart development and disease. *Cold Spring Harb Symp Quant Biol* 67:107-14.

- Hatada Y, Stern CD. 1994. A fate map of the epiblast of the early chick embryo. *Development* 120:2879-89.
- Hatcher CJ, Kim MS, Mah CS, Goldstein MM, Wong B, Mikawa T, Basson CT. 2001. TBX5 transcription factor regulates cell proliferation during cardiogenesis. *Dev Biol* 230:177-88.
- Hautmann MB, Madsen CS, Owens GK. 1997. A transforming growth factor beta (TGFbeta) control element drives TGFbeta-induced stimulation of smooth muscle alpha-actin gene expression in concert with two CArG elements. *J Biol Chem* 272:10948-56.
- Heinrich PC, Behrmann I, Muller-Newen G, Schaper F, Graeve L. 1998. Interleukin-6-type cytokine signalling through the gp130/Jak/STAT pathway. *Biochem J* 334 ( Pt 2):297-314.
- Hendrix MJ, Morse DE. 1977. Atrial septation. I. Scanning electron microscopy in the chick. *Dev Biol* 57:345-63.
- Hentze MW, Kulozik AE. 1999. A perfect message: RNA surveillance and nonsense-mediated decay. *Cell* 96:307-10.
- Herbert JM, Guy AF, Lamarche I, Mares AM, Savi P, Dol F. 1997. Intimal hyperplasia following vascular injury is not inhibited by an antisense thrombin receptor oligodeoxynucleotide. *J Cell Physiol* 170:106-14.
- Hermansson M, Sawaji Y, Bolton M, Alexander S, Wallace A, Begum S, Wait R, Saklatvala J. 2004. Proteomic analysis of articular cartilage shows increased type II collagen synthesis in osteoarthritis and expression of inhibin betaA (activin A), a regulatory molecule for chondrocytes. *J Biol Chem* 279:43514-21.
- Hinton RB, Jr., Lincoln J, Deutsch GH, Osinska H, Manning PB, Benson DW, Yutzey KE. 2006. Extracellular matrix remodeling and organization in developing and diseased aortic valves. *Circ Res* 98:1431-8.

- Hirayama-Yamada K, Kamisago M, Akimoto K, Aotsuka H, Nakamura Y, Tomita H, Furutani M, Imamura S, Takao A, Nakazawa M, Matsuoka R. 2005. Phenotypes with GATA4 or NKX2.5 mutations in familial atrial septal defect. *Am J Med Genet A* 135:47-52.
- Hiroi Y, Kudoh S, Monzen K, Ikeda Y, Yazaki Y, Nagai R, Komuro I. 2001. Tbx5 associates with Nkx2-5 and synergistically promotes cardiomyocyte differentiation. *Nat Genet* 28:276-80.
- Ho L, Crabtree GR. Chromatin remodelling during development. *Nature* 463:474-84.
- Hodgson-Zingman DM, Karst ML, Zingman LV, Heublein DM, Darbar D, Herron KJ, Ballew JD, de Andrade M, Burnett JC, Jr., Olson TM. 2008. Atrial natriuretic peptide frameshift mutation in familial atrial fibrillation. *N Engl J Med* 359:158-65.
- Hoffman JI, Kaplan S. 2002. The incidence of congenital heart disease. *J Am Coll Cardiol* 39:1890-900.
- Hojo M, Hoshimaru M, Miyamoto S, Taki W, Nagata I, Asahi M, Matsuura N, Ishizaki R, Kikuchi H, Hashimoto N. 1998. Role of transforming growth factor-beta1 in the pathogenesis of moyamoya disease. *J Neurosurg* 89:623-9.
- Holler KL, Hendershot TJ, Troy SE, Vincentz JW, Firulli AB, Howard MJ. Targeted deletion of Hand2 in cardiac neural crest-derived cells influences cardiac gene expression and outflow tract development. *Dev Biol* 341:291-304.
- Huang WY, Cukerman E, Liew CC. 1995. Identification of a GATA motif in the cardiac alpha-myosin heavy-chain-encoding gene and isolation of a human GATA-4 cDNA. *Gene* 155:219-23.
- Hudziak RM, Barofsky E, Barofsky DF, Weller DL, Huang SB, Weller DD. 1996. Resistance of morpholino phosphorodiamidate oligomers to enzymatic degradation. *Antisense Nucleic Acid Drug Dev* 6:267-72.

- Hume CR, Dodd J. 1993. Cwnt-8C: a novel Wnt gene with a potential role in primitive streak formation and hindbrain organization. *Development* 119:1147-60.
- Humphries JD, Byron A, Humphries MJ. 2006. Integrin ligands at a glance. *J Cell Sci* 119:3901-3.
- Hwang JI, Oh YS, Shin KJ, Kim H, Ryu SH, Suh PG. 2005. Molecular cloning and characterization of a novel phospholipase C, PLC-eta. *Biochem J* 389:181-6.
- Hynes RO. 1992. Integrins: versatility, modulation, and signaling in cell adhesion. *Cell* 69:11-25.
- Icardo JM, Nakamura A, Fernandez-Teran MA, Manasek FJ. 1992. Effects of injecting fibronectin and antifibronectin antibodies on cushion mesenchyme formation in the chick. An in vivo study. *Anat Embryol (Berl)* 185:239-47.
- Ieda M, Fu JD, Delgado-Olguin P, Vedantham V, Hayashi Y, Bruneau BG, Srivastava D. Direct reprogramming of fibroblasts into functional cardiomyocytes by defined factors. *Cell* 142:375-86.
- Iida M, Taira T, Ariga H, Iguchi-Ariga SM. 1997. Induction of apoptosis in HeLa cells by MSSP, c-myc binding proteins. *Biol Pharm Bull* 20:10-4.
- Iizuka M, Abe M, Shiiba K, Sasaki I, Sato Y. 2004. Down syndrome candidate region 1,a downstream target of VEGF, participates in endothelial cell migration and angiogenesis. *J Vasc Res* 41:334-44.
- Imbeaud S, Graudens E, Boulanger V, Barlet X, Zaborski P, Eveno E, Mueller O, Schroeder A, Auffray C. 2005. Towards standardization of RNA quality assessment using user-independent classifiers of microcapillary electrophoresis traces. *Nucleic Acids Res* 33:e56.
- Intra J, Perotti ME, Pavesi G, Horner D. 2006. Comparative and phylogenetic analysis of alpha-L-fucosidase genes. *Gene*.

- Isaac A, Rodriguez-Esteban C, Ryan A, Altabef M, Tsukui T, Patel K, Tickle C, Izpisua-Belmonte JC. 1998. Tbx genes and limb identity in chick embryo development. *Development* 125:1867-75.
- Jain N, Zhang T, Fong SL, Lim CP, Cao X. 1998. Repression of Stat3 activity by activation of mitogen-activated protein kinase (MAPK). *Oncogene* 17:3157-67.
- James TN. 1970. Cardiac conduction system: fetal and postnatal development. *Am J Cardiol* 25:213-26.
- Jane-Lise S, Corda S, Chassagne C, Rappaport L. 2000. The extracellular matrix and the cytoskeleton in heart hypertrophy and failure. *Heart Fail Rev* 5:239-50.
- Jaspard B, Couffinhal T, Dufourcq P, Moreau C, Duplaa C. 2000. Expression pattern of mouse sFRP-1 and mWnt-8 gene during heart morphogenesis. *Mech Dev* 90:263-7.
- Jay PY, Harris BS, Maguire CT, Buerger A, Wakimoto H, Tanaka M, Kupersmidt S, Roden DM, Schultheiss TM, O'Brien TX, Gourdie RG, Berul CI, Izumo S. 2004. Nkx2-5 mutation causes anatomic hypoplasia of the cardiac conduction system. *J Clin Invest* 113:1130-7.
- Jenuwein T, Allis CD. 2001. Translating the histone code. *Science* 293:1074-80.
- Jerome LA, Papaioannou VE. 2001. DiGeorge syndrome phenotype in mice mutant for the T-box gene, Tbx1. *Nat Genet* 27:286-91.
- Jiang Y, Evans T. 1996. The *Xenopus* GATA-4/5/6 genes are associated with cardiac specification and can regulate cardiac-specific transcription during embryogenesis. *Dev Biol* 174:258-70.
- Kadomatsu K, Hagihara M, Akhter S, Fan QW, Muramatsu H, Muramatsu T. 1997. Midkine induces the transformation of NIH3T3 cells. *Br J Cancer* 75:354-9.

- Kakinuma T, Ichikawa H, Tsukada Y, Nakamura T, Toh BH. 2004. Interaction between p230 and MACF1 is associated with transport of a glycosyl phosphatidyl inositol-anchored protein from the Golgi to the cell periphery. *Exp Cell Res* 298:388-98.
- Kaneda T, Naruse C, Kawashima A, Fujino N, Oshima T, Namura M, Nunoda S, Mori S, Konno T, Ino H, Yamagishi M, Asano M. 2008. A novel beta-myosin heavy chain gene mutation, p.Met531Arg, identified in isolated left ventricular non-compaction in humans, results in left ventricular hypertrophy that progresses to dilation in a mouse model. *Clin Sci (Lond)* 114:431-40.
- Kaplan R, Morse B, Huebner K, Croce C, Howk R, Ravera M, Ricca G, Jaye M, Schlessinger J. 1990. Cloning of three human tyrosine phosphatases reveals a multigene family of receptor-linked protein-tyrosine-phosphatases expressed in brain. *Proc Natl Acad Sci U S A* 87:7000-4.
- Kasahara H, Bartunkova S, Schinke M, Tanaka M, Izumo S. 1998. Cardiac and extracardiac expression of Csx/Nkx2.5 homeodomain protein. *Circ Res* 82:936-46.
- Kathiriya IS, Srivastava D. 2000. Left-right asymmetry and cardiac looping: implications for cardiac development and congenital heart disease. *Am J Med Genet* 97:271-9.
- Kaur A, Srivastava S, Lytrivi ID, Nguyen K, Lai WW, Parness IA. 2008. Echocardiographic evaluation and surgical implications of common atrioventricular canal defects with absent or diminutive ostium primum defect. *Am J Cardiol* 101:1648-51.
- Kawakami Y, Capdevila J, Buscher D, Itoh T, Rodriguez Esteban C, Izpisua Belmonte JC. 2001. WNT signals control FGF-dependent limb initiation and AER induction in the chick embryo. *Cell* 104:891-900.
- Kelley C, Blumberg H, Zon LI, Evans T. 1993. GATA-4 is a novel transcription factor expressed in endocardium of the developing heart. *Development* 118:817-27.

- Kelly R, Alonso S, Tajbakhsh S, Cossu G, Buckingham M. 1995. Myosin light chain 3F regulatory sequences confer regionalized cardiac and skeletal muscle expression in transgenic mice. *J Cell Biol* 129:383-96.
- Kelly RG, Brown NA, Buckingham ME. 2001. The arterial pole of the mouse heart forms from Fgf10-expressing cells in pharyngeal mesoderm. *Dev Cell* 1:435-40.
- Kelly RG, Buckingham ME. 2002. The anterior heart-forming field: voyage to the arterial pole of the heart. *Trends Genet* 18:210-6.
- Kerr MK, Martin M, Churchill GA. 2000. Analysis of variance for gene expression microarray data. *J Comput Biol* 7:819-37.
- Kim DK, Kim CH, Lamont SJ, Keeler CL, Jr., Lillehoj HS. 2009. Gene expression profiles of two B-complex disparate, genetically inbred Fayoumi chicken lines that differ in susceptibility to *Eimeria maxima*. *Poult Sci* 88:1565-79.
- Kim JS, Ryoo ZY, Chun JS. 2007. Cytokine-like 1 (Cyt11) regulates the chondrogenesis of mesenchymal cells. *J Biol Chem* 282:29359-67.
- Kim SK, Yoo JI, Cho BK, Hong SJ, Kim YK, Moon JA, Kim JH, Chung YN, Wang KC. 2003. Elevation of CRABP-I in the cerebrospinal fluid of patients with Moyamoya disease. *Stroke* 34:2835-41.
- Kimura K, Saga H, Hayashi K, Obata H, Chimori Y, Ariga H, Sobue K. 1998. c-Myc gene single-strand binding protein-1, MSSP-1, suppresses transcription of alpha-smooth muscle actin gene in chicken visceral smooth muscle cells. *Nucleic Acids Res* 26:2420-5.
- Kimura S, Hara Y, Pineau T, Fernandez-Salguero P, Fox CH, Ward JM, Gonzalez FJ. 1996. The T/eBP null mouse: thyroid-specific enhancer-binding protein is essential for the organogenesis of the thyroid, lung, ventral forebrain, and pituitary. *Genes Dev* 10:60-9.

- Kipp M, Gohring F, Ostendorp T, van Drunen CM, van Driel R, Przybylski M, Fackelmayer FO. 2000. SAF-Box, a conserved protein domain that specifically recognizes scaffold attachment region DNA. *Mol Cell Biol* 20:7480-9.
- Kirby ML. 1987. Cardiac morphogenesis--recent research advances. *Pediatr Res* 21:219-24.
- Kirby ML. 2002. Molecular embryogenesis of the heart. *Pediatr Dev Pathol* 5:516-43.
- Kirby ML, Gale TF, Stewart DE. 1983. Neural crest cells contribute to normal aorticopulmonary septation. *Science* 220:1059-61.
- Kirchhoff S, Nelles E, Hagendorff A, Kruger O, Traub O, Willecke K. 1998. Reduced cardiac conduction velocity and predisposition to arrhythmias in connexin40-deficient mice. *Curr Biol* 8:299-302.
- Kirk EP, Sunde M, Costa MW, Rankin SA, Wolstein O, Castro ML, Butler TL, Hyun C, Guo G, Otway R, Mackay JP, Waddell LB, Cole AD, Hayward C, Keogh A, Macdonald P, Griffiths L, Fatkin D, Sholler GF, Zorn AM, Feneley MP, Winlaw DS, Harvey RP. 2007. Mutations in cardiac T-box factor gene TBX20 are associated with diverse cardiac pathologies, including defects of septation and valvulogenesis and cardiomyopathy. *Am J Hum Genet* 81:280-91.
- Klamut HJ, Bosnoyan-Collins LO, Worton RG, Ray PN. 1997. A muscle-specific enhancer within intron 1 of the human dystrophin gene is functionally dependent on single MEF-1/E box and MEF-2/AT-rich sequence motifs. *Nucleic Acids Res* 25:1618-25.
- Knollmann BC, Kirchhof P, Sirenko SG, Degen H, Greene AE, Schober T, Mackow JC, Fabritz L, Potter JD, Morad M. 2003. Familial hypertrophic cardiomyopathy-linked mutant troponin T causes stress-induced ventricular tachycardia and Ca<sup>2+</sup>-dependent action potential remodeling. *Circ Res* 92:428-36.

- Kojima S, Muramatsu H, Amanuma H, Muramatsu T. 1995. Midkine enhances fibrinolytic activity of bovine endothelial cells. *J Biol Chem* 270:9590-6.
- Komuro I, Izumo S. 1993. Csx: a murine homeobox-containing gene specifically expressed in the developing heart. *Proc Natl Acad Sci U S A* 90:8145-9.
- Kos R, Tucker RP, Hall R, Duong TD, Erickson CA. 2003. Methods for introducing morpholinos into the chicken embryo. *Dev Dyn* 226:470-7.
- Koutsourakis M, Langeveld A, Patient R, Beddington R, Grosveld F. 1999. The transcription factor GATA6 is essential for early extraembryonic development. *Development* 126:723-32.
- Krauss S, Johansen T, Korzh V, Moens U, Ericson JU, Fjose A. 1991. Zebrafish pax[zf-a]: a paired box-containing gene expressed in the neural tube. *EMBO J* 10:3609-19.
- Krueger NX, Saito H. 1992. A human transmembrane protein-tyrosine-phosphatase, PTP zeta, is expressed in brain and has an N-terminal receptor domain homologous to carbonic anhydrases. *Proc Natl Acad Sci U S A* 89:7417-21.
- Kuisk IR, Li H, Tran D, Capetanaki Y. 1996. A single MEF2 site governs desmin transcription in both heart and skeletal muscle during mouse embryogenesis. *Dev Biol* 174:1-13.
- Ladd AN, Yatskievych TA, Antin PB. 1998. Regulation of avian cardiac myogenesis by activin/TGFbeta and bone morphogenetic proteins. *Dev Biol* 204:407-19.
- Lakdawala NK, Dellefave L, Redwood CS, Sparks E, Cirino AL, Depalma S, Colan SD, Funke B, Zimmerman RS, Robinson P, Watkins H, Seidman CE, Seidman JG, McNally EM, Ho CY. Familial dilated cardiomyopathy caused by an alpha-tropomyosin mutation: the distinctive natural history of sarcomeric dilated cardiomyopathy. *J Am Coll Cardiol* 55:320-9.

- Lamers WH, Moorman AF. 2002. Cardiac septation: a late contribution of the embryonic primary myocardium to heart morphogenesis. *Circ Res* 91:93-103.
- Lamers WH, Wessels A, Verbeek FJ, Moorman AF, Viragh S, Wenink AC, Gittenberger-de Groot AC, Anderson RH. 1992. New findings concerning ventricular septation in the human heart. Implications for maldevelopment. *Circulation* 86:1194-205.
- Lammer EJ, Chen DT, Hoar RM, Agnish ND, Benke PJ, Braun JT, Curry CJ, Fernhoff PM, Grix AW, Jr., Lott IT, et al. 1985. Retinoic acid embryopathy. *N Engl J Med* 313:837-41.
- Larkin JE, Frank BC, Gavras H, Sultana R, Quackenbush J. 2005. Independence and reproducibility across microarray platforms. *Nat Methods* 2:337-44.
- Latker CH, Feinberg RN, Beebe DC. 1986. Localized vascular regression during limb morphogenesis in the chicken embryo: II. Morphological changes in the vasculature. *Anat Rec* 214:410-7, 392-3.
- Laumonier F, Ronce N, Hamel BC, Thomas P, Lespinasse J, Raynaud M, Paringaux C, Van Bokhoven H, Kalscheuer V, Fryns JP, Chelly J, Moraine C, Briault S. 2002. Transcription factor SOX3 is involved in X-linked mental retardation with growth hormone deficiency. *Am J Hum Genet* 71:1450-5.
- Leachman RD, Cokkinos DV, Cooley DA. 1976. Association of ostium secundum atrial septal defects with mitral valve prolapse. *Am J Cardiol* 38:167-9.
- Lee KF, Simon H, Chen H, Bates B, Hung MC, Hauser C. 1995. Requirement for neuregulin receptor erbB2 in neural and cardiac development. *Nature* 378:394-8.
- Lee KJ, Hickey R, Zhu H, Chien KR. 1994. Positive regulatory elements (HF-1a and HF-1b) and a novel negative regulatory element (HF-3) mediate ventricular muscle-specific expression of myosin light-chain 2-luciferase fusion genes in transgenic mice. *Mol Cell Biol* 14:1220-9.

Lee ML, Kuo FC, Whitmore GA, Sklar J. 2000. Importance of replication in microarray gene expression studies: statistical methods and evidence from repetitive cDNA hybridizations. *Proc Natl Acad Sci U S A* 97:9834-9.

Lee Y, Shioi T, Kasahara H, Jobe SM, Wiese RJ, Markham BE, Izumo S. 1998. The cardiac tissue-restricted homeobox protein Csx/Nkx2.5 physically associates with the zinc finger protein GATA4 and cooperatively activates atrial natriuretic factor gene expression. *Mol Cell Biol* 18:3120-9.

Lee YM, Cope JJ, Ackermann GE, Goishi K, Armstrong EJ, Paw BH, Bischoff J. 2006. Vascular endothelial growth factor receptor signaling is required for cardiac valve formation in zebrafish. *Dev Dyn* 235:29-37.

Lehner R, Goharkhay N, Tringler B, Fasching C, Hengstschlager M. 2003. Pedigree analysis and descriptive investigation of three classic phenotypes associated with Holt-Oram syndrome. *J Reprod Med* 48:153-9.

Leonard MW, Lim KC, Engel JD. 1993. Expression of the chicken GATA factor family during early erythroid development and differentiation. *Development* 119:519-31.

Lepore JJ, Mericko PA, Cheng L, Lu MM, Morrissey EE, Parmacek MS. 2006. GATA-6 regulates semaphorin 3C and is required in cardiac neural crest for cardiovascular morphogenesis. *J Clin Invest* 116:929-39.

Li H, Capetanaki Y. 1994. An E box in the desmin promoter cooperates with the E box and MEF-2 sites of a distal enhancer to direct muscle-specific transcription. *EMBO J* 13:3580-9.

Li QY, Newbury-Ecob RA, Terrett JA, Wilson DI, Curtis AR, Yi CH, Gebuhr T, Bullen PJ, Robson SC, Strachan T, Bonnet D, Lyonnet S, Young ID, Raeburn JA, Buckler AJ, Law DJ, Brook JD. 1997. Holt-Oram syndrome is caused by mutations in TBX5, a member of the Brachyury (T) gene family. *Nat Genet* 15:21-9.

- Li S, Wang DZ, Wang Z, Richardson JA, Olson EN. 2003. The serum response factor coactivator myocardin is required for vascular smooth muscle development. *Proc Natl Acad Sci U S A* 100:9366-70.
- Li YS, Milner PG, Chauhan AK, Watson MA, Hoffman RM, Kodner CM, Milbrandt J, Deuel TF. 1990. Cloning and expression of a developmentally regulated protein that induces mitogenic and neurite outgrowth activity. *Science* 250:1690-4.
- Lickert H, Takeuchi JK, Von Both I, Walls JR, McAuliffe F, Adamson SL, Henkelman RM, Wrana JL, Rossant J, Bruneau BG. 2004. Baf60c is essential for function of BAF chromatin remodelling complexes in heart development. *Nature* 432:107-12.
- Lieu ZZ, Lock JG, Hammond LA, La Gruta NL, Stow JL, Gleeson PA. 2008. A trans-Golgi network golgin is required for the regulated secretion of TNF in activated macrophages in vivo. *Proc Natl Acad Sci U S A* 105:3351-6.
- Lin AE, Neri G, Hughes-Benzie R, Weksberg R. 1999. Cardiac anomalies in the Simpson-Golabi-Behmel syndrome. *Am J Med Genet* 83:378-81.
- Lin MH, Nguyen HT, Dybala C, Storti RV. 1996. Myocyte-specific enhancer factor 2 acts cooperatively with a muscle activator region to regulate *Drosophila* tropomyosin gene muscle expression. *Proc Natl Acad Sci U S A* 93:4623-8.
- Lin Q, Schwarz J, Bucana C, Olson EN. 1997. Control of mouse cardiac morphogenesis and myogenesis by transcription factor MEF2C. *Science* 276:1404-7.
- Linask KK, Lash JW. 1986. Precardiac cell migration: fibronectin localization at mesoderm-endoderm interface during directional movement. *Dev Biol* 114:87-101.
- Lincoln J, Alfieri CM, Yutzey KE. 2004. Development of heart valve leaflets and supporting apparatus in chicken and mouse embryos. *Dev Dyn* 230:239-50.
- Linden H, Williams R, King J, Blair E, Kini U. 2009. Ulnar Mammary syndrome and TBX3: expanding the phenotype. *Am J Med Genet A* 149A:2809-12.

- Lindsay EA. 2001. Chromosomal microdeletions: dissecting del22q11 syndrome. *Nat Rev Genet* 2:858-68.
- Lindsay EA, Vitelli F, Su H, Morishima M, Huynh T, Pramparo T, Jurecic V, Ogunrinu G, Sutherland HF, Scambler PJ, Bradley A, Baldini A. 2001. Tbx1 haploinsufficiency in the DiGeorge syndrome region causes aortic arch defects in mice. *Nature* 410:97-101.
- Lindsley A, Li W, Wang J, Maeda N, Rogers R, Conway SJ. 2005. Comparison of the four mouse fasciclin-containing genes expression patterns during valvuloseptal morphogenesis. *Gene Expr Patterns* 5:593-600.
- Linhares VL, Almeida NA, Menezes DC, Elliott DA, Lai D, Beyer EC, Campos de Carvalho AC, Costa MW. 2004. Transcriptional regulation of the murine Connexin40 promoter by cardiac factors Nkx2-5, GATA4 and Tbx5. *Cardiovasc Res* 64:402-11.
- Liu P, Wakamiya M, Shea MJ, Albrecht U, Behringer RR, Bradley A. 1999. Requirement for Wnt3 in vertebrate axis formation. *Nat Genet* 22:361-5.
- Liu X, Rapp N, Deans R, Cheng L. 2000. Molecular cloning and chromosomal mapping of a candidate cytokine gene selectively expressed in human CD34+ cells. *Genomics* 65:283-92.
- Livak KJ, Schmittgen TD. 2001. Analysis of relative gene expression data using real-time quantitative PCR and the 2<sup>(-Delta Delta C(T))</sup> Method. *Methods* 25:402-8.
- Logan CY, Nusse R. 2004. The Wnt signaling pathway in development and disease. *Annu Rev Cell Dev Biol* 20:781-810.
- Loose M, Patient R. 2004. A genetic regulatory network for *Xenopus* mesendoderm formation. *Dev Biol* 271:467-78.
- Lopez-Sanchez C, Climent V, Schoenwolf GC, Alvarez IS, Garcia-Martinez V. 2002. Induction of cardiogenesis by Hensen's node and fibroblast growth factors. *Cell Tissue Res* 309:237-49.

Lough J, Barron M, Brogley M, Sugi Y, Bolender DL, Zhu X. 1996. Combined BMP-2 and FGF-4, but neither factor alone, induces cardiogenesis in non-precardiac embryonic mesoderm. *Dev Biol* 178:198-202.

Lough J, Sugi Y. 2000. Endoderm and heart development. *Dev Dyn* 217:327-42.

Luscher B, Mitchell PJ, Williams T, Tjian R. 1989. Regulation of transcription factor AP-2 by the morphogen retinoic acid and by second messengers. *Genes Dev* 3:1507-17.

Lyn S, Giguere V. 1994. Localization of CRABP-I and CRABP-II mRNA in the early mouse embryo by whole-mount in situ hybridization: implications for teratogenesis and neural development. *Dev Dyn* 199:280-91.

Lyons GE, Schiaffino S, Sassoon D, Barton P, Buckingham M. 1990. Developmental regulation of myosin gene expression in mouse cardiac muscle. *J Cell Biol* 111:2427-36.

Lyons I, Parsons LM, Hartley L, Li R, Andrews JE, Robb L, Harvey RP. 1995. Myogenic and morphogenetic defects in the heart tubes of murine embryos lacking the homeo box gene *Nkx2-5*. *Genes Dev* 9:1654-66.

Ma L, Lu MF, Schwartz RJ, Martin JF. 2005. *Bmp2* is essential for cardiac cushion epithelial-mesenchymal transition and myocardial patterning. *Development* 132:5601-11.

Maeda N, Ichihara-Tanaka K, Kimura T, Kadomatsu K, Muramatsu T, Noda M. 1999. A receptor-like protein-tyrosine phosphatase PTPzeta/RPTPbeta binds a heparin-binding growth factor midkine. Involvement of arginine 78 of midkine in the high affinity binding to PTPzeta. *J Biol Chem* 274:12474-9.

Maeda N, Nishiwaki T, Shintani T, Hamanaka H, Noda M. 1996. 6B4 proteoglycan/phosphacan, an extracellular variant of receptor-like protein-tyrosine

- phosphatase zeta/RPTPbeta, binds pleiotrophin/heparin-binding growth-associated molecule (HB-GAM). *J Biol Chem* 271:21446-52.
- Maitra M, Schluterman MK, Nichols HA, Richardson JA, Lo CW, Srivastava D, Garg V. 2009. Interaction of Gata4 and Gata6 with Tbx5 is critical for normal cardiac development. *Dev Biol* 326:368-77.
- Malek AM, Connors S, Robertson RL, Folkman J, Scott RM. 1997. Elevation of cerebrospinal fluid levels of basic fibroblast growth factor in moyamoya and central nervous system disorders. *Pediatr Neurosurg* 27:182-9.
- Manduchi E, Grant GR, McKenzie SE, Overton GC, Surrey S, Stoeckert CJ, Jr. 2000. Generation of patterns from gene expression data by assigning confidence to differentially expressed genes. *Bioinformatics* 16:685-98.
- Mann DL, Spinale FG. 1998. Activation of matrix metalloproteinases in the failing human heart: breaking the tie that binds. *Circulation* 98:1699-702.
- Manner J. 2000. Cardiac looping in the chick embryo: a morphological review with special reference to terminological and biomechanical aspects of the looping process. *Anat Rec* 259:248-62.
- Manner J. 2009. The anatomy of cardiac looping: a step towards the understanding of the morphogenesis of several forms of congenital cardiac malformations. *Clin Anat* 22:21-35.
- Marconcini L, Marchio S, Morbidelli L, Cartocci E, Albini A, Ziche M, Bussolino F, Oliviero S. 1999. c-fos-induced growth factor/vascular endothelial growth factor D induces angiogenesis in vivo and in vitro. *Proc Natl Acad Sci U S A* 96:9671-6.
- Markwald RR, Fitzharris TP, Manasek FJ. 1977. Structural development of endocardial cushions. *Am J Anat* 148:85-119.

- Martin-Villar E, Scholl FG, Gamallo C, Yurrita MM, Munoz-Guerra M, Cruces J, Quintanilla M. 2005. Characterization of human PA2.26 antigen (T1alpha-2, podoplanin), a small membrane mucin induced in oral squamous cell carcinomas. *Int J Cancer* 113:899-910.
- Martinez-Morales JR, Signore M, Acampora D, Simeone A, Bovolenta P. 2001. Otx genes are required for tissue specification in the developing eye. *Development* 128:2019-30.
- Martinsen BJ. 2005. Reference guide to the stages of chick heart embryology. *Dev Dyn* 233:1217-37.
- Matsson H, Eason J, Bookwalter CS, Klar J, Gustavsson P, Sunnegardh J, Enell H, Jonzon A, Vikkula M, Gutierrez I, Granados-Riveron J, Pope M, Bu'Lock F, Cox J, Robinson TE, Song F, Brook DJ, Marston S, Trybus KM, Dahl N. 2008. Alpha-cardiac actin mutations produce atrial septal defects. *Hum Mol Genet* 17:256-65.
- McBurney MW. 1993. P19 embryonal carcinoma cells. *Int J Dev Biol* 37:135-40.
- McElhinney DB, Geiger E, Blinder J, Benson DW, Goldmuntz E. 2003. NKX2.5 mutations in patients with congenital heart disease. *J Am Coll Cardiol* 42:1650-5.
- McGrew MJ, Bogdanova N, Hasegawa K, Hughes SH, Kitsis RN, Rosenthal N. 1996. Distinct gene expression patterns in skeletal and cardiac muscle are dependent on common regulatory sequences in the MLC1/3 locus. *Mol Cell Biol* 16:4524-34.
- McKinsey TA, Zhang CL, Olson EN. 2002. MEF2: a calcium-dependent regulator of cell division, differentiation and death. *Trends Biochem Sci* 27:40-7.
- Meredith C, Herrmann R, Parry C, Liyanage K, Dye DE, Durling HJ, Duff RM, Beckman K, de Visser M, van der Graaff MM, Hedera P, Fink JK, Petty EM, Lamont P, Fabian V, Bridges L, Voit T, Mastaglia FL, Laing NG. 2004. Mutations in the slow skeletal muscle fiber myosin heavy chain gene (MYH7) cause laing early-onset distal myopathy (MPD1). *Am J Hum Genet* 75:703-8.

- Merscher S, Funke B, Epstein JA, Heyer J, Puech A, Lu MM, Xavier RJ, Demay MB, Russell RG, Factor S, Tokooya K, Jore BS, Lopez M, Pandita RK, Lia M, Carrion D, Xu H, Schorle H, Kobler JB, Scambler P, Wynshaw-Boris A, Skoultschi AI, Morrow BE, Kucherlapati R. 2001. TBX1 is responsible for cardiovascular defects in velo-cardio-facial/DiGeorge syndrome. *Cell* 104:619-29.
- Miano JM, Ramanan N, Georger MA, de Mesy Bentley KL, Emerson RL, Balza RO, Jr., Xiao Q, Weiler H, Ginty DD, Misra RP. 2004. Restricted inactivation of serum response factor to the cardiovascular system. *Proc Natl Acad Sci U S A* 101:17132-7.
- Mirza M, Robinson P, Kremneva E, Copeland O, Nikolaeva O, Watkins H, Levitsky D, Redwood C, El-Mezgueldi M, Marston S. 2007. The effect of mutations in alpha-tropomyosin (E40K and E54K) that cause familial dilated cardiomyopathy on the regulatory mechanism of cardiac muscle thin filaments. *J Biol Chem* 282:13487-97.
- Mitchell PJ, Timmons PM, Hebert JM, Rigby PW, Tjian R. 1991. Transcription factor AP-2 is expressed in neural crest cell lineages during mouse embryogenesis. *Genes Dev* 5:105-19.
- Miyazaki S, Suzuki S, Kawasaki N, Endo K, Takahashi A, Attwood D. 2001. In situ gelling xyloglucan formulations for sustained release ocular delivery of pilocarpine hydrochloride. *Int J Pharm* 229:29-36.
- Mjaatvedt CH, Nakaoka T, Moreno-Rodriguez R, Norris RA, Kern MJ, Eisenberg CA, Turner D, Markwald RR. 2001. The outflow tract of the heart is recruited from a novel heart-forming field. *Dev Biol* 238:97-109.
- Mohri T, Fujio Y, Maeda M, Ito T, Iwakura T, Oshima Y, Uozumi Y, Segawa M, Yamamoto H, Kishimoto T, Azuma J. 2006. Leukemia inhibitory factor induces endothelial differentiation in cardiac stem cells. *J Biol Chem* 281:6442-7.

- Molkentin JD, Kalvakolanu DV, Markham BE. 1994. Transcription factor GATA-4 regulates cardiac muscle-specific expression of the alpha-myosin heavy-chain gene. *Mol Cell Biol* 14:4947-57.
- Molkentin JD, Markham BE. 1993. Myocyte-specific enhancer-binding factor (MEF-2) regulates alpha-cardiac myosin heavy chain gene expression in vitro and in vivo. *J Biol Chem* 268:19512-20.
- Molkentin JD, Olson EN. 1997. GATA4: a novel transcriptional regulator of cardiac hypertrophy? *Circulation* 96:3833-5.
- Molkentin JD, Tymitz KM, Richardson JA, Olson EN. 2000. Abnormalities of the genitourinary tract in female mice lacking GATA5. *Mol Cell Biol* 20:5256-60.
- Monaghan AP, Bock D, Gass P, Schwager A, Wolfer DP, Lipp HP, Schutz G. 1997. Defective limbic system in mice lacking the tailless gene. *Nature* 390:515-7.
- Monaghan AP, Grau E, Bock D, Schutz G. 1995. The mouse homolog of the orphan nuclear receptor tailless is expressed in the developing forebrain. *Development* 121:839-53.
- Monserrat L, Hermida-Prieto M, Fernandez X, Rodriguez I, Dumont C, Cazon L, Cuesta MG, Gonzalez-Juanatey C, Peteiro J, Alvarez N, Penas-Lado M, Castro-Beiras A. 2007. Mutation in the alpha-cardiac actin gene associated with apical hypertrophic cardiomyopathy, left ventricular non-compaction, and septal defects. *Eur Heart J* 28:1953-61.
- Moorman A, Webb S, Brown NA, Lamers W, Anderson RH. 2003. Development of the heart: (1) formation of the cardiac chambers and arterial trunks. *Heart* 89:806-14.
- Moorman AF, Christoffels VM, Anderson RH, van den Hoff MJ. 2007. The heart-forming fields: one or multiple? *Philos Trans R Soc Lond B Biol Sci* 362:1257-65.

- Moorman AF, de Jong F, Lamers WH. 1997. Development of the conduction system of the heart. *Pacing Clin Electrophysiol* 20:2087-92.
- Morcos PA. 2007. Achieving targeted and quantifiable alteration of mRNA splicing with Morpholino oligos. *Biochem Biophys Res Commun* 358:521-7.
- Mori AD, Bruneau BG. 2004. TBX5 mutations and congenital heart disease: Holt-Oram syndrome revealed. *Curr Opin Cardiol* 19:211-5.
- Morita H, Seidman J, Seidman CE. 2005. Genetic causes of human heart failure. *J Clin Invest* 115:518-26.
- Morkin E. 2000. Control of cardiac myosin heavy chain gene expression. *Microsc Res Tech* 50:522-31.
- Morrissey EE, Ip HS, Tang Z, Lu MM, Parmacek MS. 1997a. GATA-5: a transcriptional activator expressed in a novel temporally and spatially-restricted pattern during embryonic development. *Dev Biol* 183:21-36.
- Morrissey EE, Ip HS, Tang Z, Parmacek MS. 1997b. GATA-4 activates transcription via two novel domains that are conserved within the GATA-4/5/6 subfamily. *J Biol Chem* 272:8515-24.
- Morrissey EE, Tang Z, Sigrist K, Lu MM, Jiang F, Ip HS, Parmacek MS. 1998. GATA6 regulates HNF4 and is required for differentiation of visceral endoderm in the mouse embryo. *Genes Dev* 12:3579-90.
- Morse DE, Hendrix MJ. 1980. Atrial septation. II. Formation of the foramina secunda in the chick. *Dev Biol* 78:25-35.
- Morse DE, Rogers CS, McCann PS. 1984. Atrial septation in the chick and rat: a review. *J Submicrosc Cytol* 16:259-72.
- Moser M, Ruschoff J, Buettner R. 1997. Comparative analysis of AP-2 alpha and AP-2 beta gene expression during murine embryogenesis. *Dev Dyn* 208:115-24.

- Muramatsu H, Muramatsu T. 1991. Purification of recombinant midkine and examination of its biological activities: functional comparison of new heparin binding factors. *Biochem Biophys Res Commun* 177:652-8.
- Muscat GE, Perry S, Prentice H, Kedes L. 1992. The human skeletal alpha-actin gene is regulated by a muscle-specific enhancer that binds three nuclear factors. *Gene Expr* 2:111-26.
- Nag AC. 1980. Study of non-muscle cells of the adult mammalian heart: a fine structural analysis and distribution. *Cytobios* 28:41-61.
- Nagai T, Aruga J, Takada S, Gunther T, Sporle R, Schughart K, Mikoshiba K. 1997. The expression of the mouse *Zic1*, *Zic2*, and *Zic3* gene suggests an essential role for *Zic* genes in body pattern formation. *Dev Biol* 182:299-313.
- Nagao K, Taniyama Y, Koibuchi N, Morishita R. 2007. Constitutive over-expression of VEGF results in reduced expression of Hand-1 during cardiac development in *Xenopus*. *Biochem Biophys Res Commun* 359:431-7.
- Nagase H, Woessner JF, Jr. 1999. Matrix metalloproteinases. *J Biol Chem* 274:21491-4.
- Naiche LA, Papaioannou VE. 2003. Loss of *Tbx4* blocks hindlimb development and affects vascularization and fusion of the allantois. *Development* 130:2681-93.
- Nakajima Y, Mironov V, Yamagishi T, Nakamura H, Markwald RR. 1997. Expression of smooth muscle alpha-actin in mesenchymal cells during formation of avian endocardial cushion tissue: a role for transforming growth factor beta3. *Dev Dyn* 209:296-309.
- Nakata K, Nagai T, Aruga J, Mikoshiba K. 1998. *Xenopus Zic* family and its role in neural and neural crest development. *Mech Dev* 75:43-51.

- Nakayama M, Stauffer J, Cheng J, Banerjee-Basu S, Wawrousek E, Buonanno A. 1996. Common core sequences are found in skeletal muscle slow- and fast-fiber-type-specific regulatory elements. *Mol Cell Biol* 16:2408-17.
- Nanba D, Kinugasa Y, Morimoto C, Koizumi M, Yamamura H, Takahashi K, Takakura N, Mekada E, Hashimoto K, Higashiyama S. 2006. Loss of HB-EGF in smooth muscle or endothelial cell lineages causes heart malformation. *Biochem Biophys Res Commun* 350:315-21.
- Naya FJ, Black BL, Wu H, Bassel-Duby R, Richardson JA, Hill JA, Olson EN. 2002. Mitochondrial deficiency and cardiac sudden death in mice lacking the MEF2A transcription factor. *Nat Med* 8:1303-9.
- Nemer G, Fadlalah F, Usta J, Nemer M, Dbaibo G, Obeid M, Bitar F. 2006. A novel mutation in the GATA4 gene in patients with Tetralogy of Fallot. *Hum Mutat* 27:293-4.
- Neri G, Marini R, Cappa M, Borrelli P, Opitz JM. 1988. Simpson-Golabi-Behmel syndrome: an X-linked encephalo-tropho-schisis syndrome. *Am J Med Genet* 30:287-99.
- Newbury-Ecob RA, Leanage R, Raeburn JA, Young ID. 1996. Holt-Oram syndrome: a clinical genetic study. *J Med Genet* 33:300-7.
- Ng A, Wong M, Viviano B, Erlich JM, Alba G, Pflederer C, Jay PY, Saunders S. 2009. Loss of glypican-3 function causes growth factor-dependent defects in cardiac and coronary vascular development. *Dev Biol* 335:208-15.
- Niki T, Galli I, Ariga H, Iguchi-Ariga SM. 2000a. MSSP, a protein binding to an origin of replication in the c-myc gene, interacts with a catalytic subunit of DNA polymerase alpha and stimulates its polymerase activity. *FEBS Lett* 475:209-12.
- Niki T, Izumi S, Saegusa Y, Taira T, Takai T, Iguchi-Ariga SM, Ariga H. 2000b. MSSP promotes ras/myc cooperative cell transforming activity by binding to c-Myc. *Genes Cells* 5:127-41.

- Nishida W, Nakamura M, Mori S, Takahashi M, Ohkawa Y, Tadokoro S, Yoshida K, Hiwada K, Hayashi K, Sobue K. 2002. A triad of serum response factor and the GATA and NK families governs the transcription of smooth and cardiac muscle genes. *J Biol Chem* 277:7308-17.
- Nishio H, Takeshima Y, Narita N, Yanagawa H, Suzuki Y, Ishikawa Y, Minami R, Nakamura H, Matsuo M. 1994. Identification of a novel first exon in the human dystrophin gene and of a new promoter located more than 500 kb upstream of the nearest known promoter. *J Clin Invest* 94:1037-42.
- Nomura J, Matsumoto K, Iguchi-Ariga SM, Ariga H. 2005. Mitochondria-independent induction of Fas-mediated apoptosis by MSSP. *Oncol Rep* 14:1305-9.
- Norris RA, Borg TK, Butcher JT, Baudino TA, Banerjee I, Markwald RR. 2008. Neonatal and adult cardiovascular pathophysiological remodeling and repair: developmental role of periostin. *Ann N Y Acad Sci* 1123:30-40.
- Obler D, Juraszek AL, Smoot LB, Natowicz MR. 2008. Double outlet right ventricle: aetiologies and associations. *J Med Genet* 45:481-97.
- Ohuchi H, Hayashibara Y, Matsuda H, Onoi M, Mitsumori M, Tanaka M, Aoki J, Arai H, Noji S. 2007. Diversified expression patterns of autotaxin, a gene for phospholipid-generating enzyme during mouse and chicken development. *Dev Dyn* 236:1134-43.
- Ohuchi H, Nakagawa T, Yamamoto A, Araga A, Ohata T, Ishimaru Y, Yoshioka H, Kuwana T, Nohno T, Yamasaki M, Itoh N, Noji S. 1997. The mesenchymal factor, FGF10, initiates and maintains the outgrowth of the chick limb bud through interaction with FGF8, an apical ectodermal factor. *Development* 124:2235-44.
- Oka T, Maillet M, Watt AJ, Schwartz RJ, Aronow BJ, Duncan SA, Molkenkin JD. 2006. Cardiac-specific deletion of Gata4 reveals its requirement for hypertrophy, compensation, and myocyte viability. *Circ Res* 98:837-45.

- Olive M, Armstrong J, Miralles F, Pou A, Fardeau M, Gonzalez L, Martinez F, Fischer D, Martinez Matos JA, Shatunov A, Goldfarb L, Ferrer I. 2007. Phenotypic patterns of desminopathy associated with three novel mutations in the desmin gene. *Neuromuscul Disord* 17:443-50.
- Olson EN. 2006. Gene regulatory networks in the evolution and development of the heart. *Science* 313:1922-7.
- Olson TM, Michels VV, Thibodeau SN, Tai YS, Keating MT. 1998. Actin mutations in dilated cardiomyopathy, a heritable form of heart failure. *Science* 280:750-2.
- Orlandini M, Marconcini L, Ferruzzi R, Oliviero S. 1996. Identification of a c-fos-induced gene that is related to the platelet-derived growth factor/vascular endothelial growth factor family. *Proc Natl Acad Sci U S A* 93:11675-80.
- Oshima Y, Fujio Y, Nakanishi T, Itoh N, Yamamoto Y, Negoro S, Tanaka K, Kishimoto T, Kawase I, Azuma J. 2005. STAT3 mediates cardioprotection against ischemia/reperfusion injury through metallothionein induction in the heart. *Cardiovasc Res* 65:428-35.
- Osugi T, Oshima Y, Fujio Y, Funamoto M, Yamashita A, Negoro S, Kunisada K, Izumi M, Nakaoka Y, Hirota H, Okabe M, Yamauchi-Takahara K, Kawase I, Kishimoto T. 2002. Cardiac-specific activation of signal transducer and activator of transcription 3 promotes vascular formation in the heart. *J Biol Chem* 277:6676-81.
- Ovcharenko I, Loots GG, Giardine BM, Hou M, Ma J, Hardison RC, Stubbs L, Miller W. 2005. Mulan: multiple-sequence local alignment and visualization for studying function and evolution. *Genome Res* 15:184-94.
- Packham EA, Brook JD. 2003. T-box genes in human disorders. *Hum Mol Genet* 12 Spec No 1:R37-44.
- Pandur P, Lasche M, Eisenberg LM, Kuhl M. 2002. Wnt-11 activation of a non-canonical Wnt signalling pathway is required for cardiogenesis. *Nature* 418:636-41.

- Papadimitriou E, Polykratis A, Courty J, Koolwijk P, Heroult M, Katsoris P. 2001. HARP induces angiogenesis in vivo and in vitro: implication of N or C terminal peptides. *Biochem Biophys Res Commun* 282:306-13.
- Parmacek MS, Ip HS, Jung F, Shen T, Martin JF, Vora AJ, Olson EN, Leiden JM. 1994. A novel myogenic regulatory circuit controls slow/cardiac troponin C gene transcription in skeletal muscle. *Mol Cell Biol* 14:1870-85.
- Pashmforoush M, Lu JT, Chen H, Amand TS, Kondo R, Pradervand S, Evans SM, Clark B, Feramisco JR, Giles W, Ho SY, Benson DW, Silberbach M, Shou W, Chien KR. 2004. Nkx2-5 pathways and congenital heart disease; loss of ventricular myocyte lineage specification leads to progressive cardiomyopathy and complete heart block. *Cell* 117:373-86.
- Pasini D, Bracken AP, Jensen MR, Lazzerini Denchi E, Helin K. 2004. Suz12 is essential for mouse development and for EZH2 histone methyltransferase activity. *EMBO J* 23:4061-71.
- Pawitan Y, Michiels S, Koscielny S, Gusnanto A, Ploner A. 2005. False discovery rate, sensitivity and sample size for microarray studies. *Bioinformatics* 21:3017-24.
- Pellegrini M, Pilia G, Pantano S, Lucchini F, Uda M, Fumi M, Cao A, Schlessinger D, Forabosco A. 1998. Gpc3 expression correlates with the phenotype of the Simpson-Golabi-Behmel syndrome. *Dev Dyn* 213:431-9.
- Perry SV. 2001. Vertebrate tropomyosin: distribution, properties and function. *J Muscle Res Cell Motil* 22:5-49.
- Peterkin T, Gibson A, Loose M, Patient R. 2005. The roles of GATA-4, -5 and -6 in vertebrate heart development. *Semin Cell Dev Biol* 16:83-94.
- Pfaffl MW. 2001. A new mathematical model for relative quantification in real-time RT-PCR. *Nucleic Acids Res* 29:e45.

- Pilia G, Hughes-Benzie RM, MacKenzie A, Baybayan P, Chen EY, Huber R, Neri G, Cao A, Forabosco A, Schlessinger D. 1996. Mutations in GPC3, a glypican gene, cause the Simpson-Golabi-Behmel overgrowth syndrome. *Nat Genet* 12:241-7.
- Pittenger MF, Kazzaz JA, Helfman DM. 1994. Functional properties of non-muscle tropomyosin isoforms. *Curr Opin Cell Biol* 6:96-104.
- Plageman TF, Jr., Yutzey KE. 2004. Differential expression and function of Tbx5 and Tbx20 in cardiac development. *J Biol Chem* 279:19026-34.
- Plouhinec JL, Leconte L, Sauka-Spengler T, Bovolenta P, Mazan S, Saule S. 2005. Comparative analysis of gnathostome Otx gene expression patterns in the developing eye: implications for the functional evolution of the multigene family. *Dev Biol* 278:560-75.
- Plumb M, Frampton J, Wainwright H, Walker M, Macleod K, Goodwin G, Harrison P. 1989. GATAAG; a cis-control region binding an erythroid-specific nuclear factor with a role in globin and non-globin gene expression. *Nucleic Acids Res* 17:73-92.
- Pohlenz J, Dumitrescu A, Zundel D, Martine U, Schonberger W, Koo E, Weiss RE, Cohen RN, Kimura S, Refetoff S. 2002. Partial deficiency of thyroid transcription factor 1 produces predominantly neurological defects in humans and mice. *J Clin Invest* 109:469-73.
- Polykratis A, Katsoris P, Courty J, Papadimitriou E. 2005. Characterization of heparin affin regulatory peptide signaling in human endothelial cells. *J Biol Chem* 280:22454-61.
- Powell DW, Mifflin RC, Valentich JD, Crowe SE, Saada JI, West AB. 1999. Myofibroblasts. I. Paracrine cells important in health and disease. *Am J Physiol* 277:C1-9.

- Puthenveedu MA, Bachert C, Puri S, Lanni F, Linstedt AD. 2006. GM130 and GRASP65-dependent lateral cisternal fusion allows uniform Golgi-enzyme distribution. *Nat Cell Biol* 8:238-48.
- Qayyum SR, Webb S, Anderson RH, Verbeek FJ, Brown NA, Richardson MK. 2001. Septation and valvar formation in the outflow tract of the embryonic chick heart. *Anat Rec* 264:273-83.
- Qi X, Yang G, Yang L, Lan Y, Weng T, Wang J, Wu Z, Xu J, Gao X, Yang X. 2007. Essential role of Smad4 in maintaining cardiomyocyte proliferation during murine embryonic heart development. *Dev Biol*.
- Ragge NK, Brown AG, Poloschek CM, Lorenz B, Henderson RA, Clarke MP, Russell-Eggitt I, Fielder A, Gerrelli D, Martinez-Barbera JP, Ruddle P, Hurst J, Collin JR, Salt A, Cooper ST, Thompson PJ, Sisodiya SM, Williamson KA, Fitzpatrick DR, van Heyningen V, Hanson IM. 2005. Heterozygous mutations of OTX2 cause severe ocular malformations. *Am J Hum Genet* 76:1008-22.
- Rajagopal SK, Ma Q, Obler D, Shen J, Manichaikul A, Tomita-Mitchell A, Boardman K, Briggs C, Garg V, Srivastava D, Goldmuntz E, Broman KW, Benson DW, Smoot LB, Pu WT. 2007. Spectrum of heart disease associated with murine and human GATA4 mutation. *J Mol Cell Cardiol* 43:677-85.
- Rao MV, Donoghue MJ, Merlie JP, Sanes JR. 1996. Distinct regulatory elements control muscle-specific, fiber-type-selective, and axially graded expression of a myosin light-chain gene in transgenic mice. *Mol Cell Biol* 16:3909-22.
- Rauvala H. 1989. An 18-kd heparin-binding protein of developing brain that is distinct from fibroblast growth factors. *EMBO J* 8:2933-41.
- Rawles ME. 1943. The heart-forming areas of the early chick blastoderm. *Physiological Zoology* 16:22-42.

- Reamon-Buettner SM, Ciribilli Y, Inga A, Borlak J. 2008. A loss-of-function mutation in the binding domain of HAND1 predicts hypoplasia of the human hearts. *Hum Mol Genet* 17:1397-405.
- Reamon-Buettner SM, Ciribilli Y, Traverso I, Kuhls B, Inga A, Borlak J. 2009. A functional genetic study identifies HAND1 mutations in septation defects of the human heart. *Hum Mol Genet* 18:3567-78.
- Redkar A, Montgomery M, Litvin J. 2001. Fate map of early avian cardiac progenitor cells. *Development* 128:2269-79.
- Rethinasamy P, Muthuchamy M, Hewett T, Boivin G, Wolska BM, Evans C, Solaro RJ, Wieczorek DF. 1998. Molecular and physiological effects of alpha-tropomyosin ablation in the mouse. *Circ Res* 82:116-23.
- Rivera-Feliciano J, Lee KH, Kong SW, Rajagopal S, Ma Q, Springer Z, Izumo S, Tabin CJ, Pu WT. 2006. Development of heart valves requires Gata4 expression in endothelial-derived cells. *Development* 133:3607-18.
- Rizzoti K, Brunelli S, Carmignac D, Thomas PQ, Robinson IC, Lovell-Badge R. 2004. SOX3 is required during the formation of the hypothalamo-pituitary axis. *Nat Genet* 36:247-55.
- Rojas A, De Val S, Heidt AB, Xu SM, Bristow J, Black BL. 2005. Gata4 expression in lateral mesoderm is downstream of BMP4 and is activated directly by Forkhead and GATA transcription factors through a distal enhancer element. *Development* 132:3405-17.
- Rojas A, Kong SW, Agarwal P, Gilliss B, Pu WT, Black BL. 2008. GATA4 is a direct transcriptional activator of cyclin D2 and Cdk4 and is required for cardiomyocyte proliferation in anterior heart field-derived myocardium. *Mol Cell Biol* 28:5420-31.
- Ronksley JN. 2007. Microarray analysis of P19CL6 cardiac differentiation. <sup>editor</sup>editors: University of Nottingham.

- Runyan RB, Markwald RR. 1983. Invasion of mesenchyme into three-dimensional collagen gels: a regional and temporal analysis of interaction in embryonic heart tissue. *Dev Biol* 95:108-14.
- Rutland C, Warner L, Thorpe A, Alibhai A, Robinson T, Shaw B, Layfield R, Brook JD, Loughna S. 2009. Knockdown of alpha myosin heavy chain disrupts the cytoskeleton and leads to multiple defects during chick cardiogenesis. *J Anat* 214:905-15.
- Ruzicka DL, Schwartz RJ. 1988. Sequential activation of alpha-actin genes during avian cardiogenesis: vascular smooth muscle alpha-actin gene transcripts mark the onset of cardiomyocyte differentiation. *J Cell Biol* 107:2575-86.
- Sachs N, Kreft M, van den Bergh Weerman MA, Beynon AJ, Peters TA, Weening JJ, Sonnenberg A. 2006. Kidney failure in mice lacking the tetraspanin CD151. *J Cell Biol* 175:33-9.
- Sadler TW. 2006. *Langman's Medical Embryology* 10th Edition. Lipincott Williams & Wilkins.
- Samson GR, Kumar SR. 2004. A study of congenital cardiac disease in a neonatal population--the validity of echocardiography undertaken by a neonatologist. *Cardiol Young* 14:585-93.
- Satoda M, Pierpont ME, Diaz GA, Bornemeier RA, Gelb BD. 1999. Char syndrome, an inherited disorder with patent ductus arteriosus, maps to chromosome 6p12-p21. *Circulation* 99:3036-42.
- Satoda M, Zhao F, Diaz GA, Burn J, Goodship J, Davidson HR, Pierpont ME, Gelb BD. 2000. Mutations in TFAP2B cause Char syndrome, a familial form of patent ductus arteriosus. *Nat Genet* 25:42-6.
- Schaper J, Speiser B. 1992. The extracellular matrix in the failing human heart. *Basic Res Cardiol* 87 Suppl 1:303-9.

- Schildmeyer LA, Braun R, Taffet G, DeBiasi M, Burns AE, Bradley A, Schwartz RJ. 2000. Impaired vascular contractility and blood pressure homeostasis in the smooth muscle alpha-actin null mouse. *FASEB J* 14:2213-20.
- Schinzel A. 1987. Ulnar-mammary syndrome. *J Med Genet* 24:778-81.
- Schlessinger J. 2000. Cell signaling by receptor tyrosine kinases. *Cell* 103:211-25.
- Scholl FG, Gamallo C, Vilar inverted question mark S, Quintanilla M. 1999. Identification of PA2.26 antigen as a novel cell-surface mucin-type glycoprotein that induces plasma membrane extensions and increased motility in keratinocytes. *J Cell Sci* 112 ( Pt 24):4601-13.
- Schott JJ, Benson DW, Basson CT, Pease W, Silberbach GM, Moak JP, Maron BJ, Seidman CE, Seidman JG. 1998. Congenital heart disease caused by mutations in the transcription factor NKX2-5. *Science* 281:108-11.
- Schröckel JW, Stockigt F, Krzyzak W, Paulin D, Li Z, Lubkemeier I, Fleischmann B, Sasse P, Linhart M, Lewalter T, Nickenig G, Lickfett L, Schröder R, Clemen CS. Cardiac conduction disturbances and differential effects on atrial and ventricular electrophysiological properties in desmin deficient mice. *J Interv Card Electrophysiol*.
- Schroeder A, Mueller O, Stocker S, Salowsky R, Leiber M, Gassmann M, Lightfoot S, Menzel W, Granzow M, Ragg T. 2006. The RIN: an RNA integrity number for assigning integrity values to RNA measurements. *BMC Mol Biol* 7:3.
- Seidman JG, Seidman C. 2001. The genetic basis for cardiomyopathy: from mutation identification to mechanistic paradigms. *Cell* 104:557-67.
- Selleck SB. 1999. Overgrowth syndromes and the regulation of signaling complexes by proteoglycans. *Am J Hum Genet* 64:372-7.

- Sepulveda JL, Vlahopoulos S, Iyer D, Belaguli N, Schwartz RJ. 2002. Combinatorial expression of GATA4, Nkx2-5, and serum response factor directs early cardiac gene activity. *J Biol Chem* 277:25775-82.
- Shelton EL, Yutzey KE. 2007. Tbx20 regulation of endocardial cushion cell proliferation and extracellular matrix gene expression. *Dev Biol* 302:376-88.
- Shimizu RT, Blank RS, Jervis R, Lawrenz-Smith SC, Owens GK. 1995. The smooth muscle alpha-actin gene promoter is differentially regulated in smooth muscle versus non-smooth muscle cells. *J Biol Chem* 270:7631-43.
- Shimura H, Shimura Y, Ohmori M, Ikuyama S, Kohn LD. 1995. Single strand DNA-binding proteins and thyroid transcription factor-1 conjointly regulate thyrotropin receptor gene expression. *Mol Endocrinol* 9:527-39.
- Shore P, Sharrocks AD. 1995. The MADS-box family of transcription factors. *Eur J Biochem* 229:1-13.
- Simeone A, Acampora D, Mallamaci A, Stornaiuolo A, D'Apice MR, Nigro V, Boncinelli E. 1993. A vertebrate gene related to orthodenticle contains a homeodomain of the bicoid class and demarcates anterior neuroectoderm in the gastrulating mouse embryo. *EMBO J* 12:2735-47.
- Simon AM, Goodenough DA. 1998. Diverse functions of vertebrate gap junctions. *Trends Cell Biol* 8:477-83.
- Simonson MS, Walsh K, Kumar CC, Bushel P, Herman WH. 1995. Two proximal CArG elements regulate SM alpha-actin promoter, a genetic marker of activated phenotype of mesangial cells. *Am J Physiol* 268:F760-9.
- Sincock PM, Mayrhofer G, Ashman LK. 1997. Localization of the transmembrane 4 superfamily (TM4SF) member PETA-3 (CD151) in normal human tissues: comparison with CD9, CD63, and alpha5beta1 integrin. *J Histochem Cytochem* 45:515-25.

- Sivak JM, Petersen LF, Amaya E. 2005. FGF signal interpretation is directed by Sprouty and Spred proteins during mesoderm formation. *Dev Cell* 8:689-701.
- Skerjanc IS, Petropoulos H, Ridgeway AG, Wilton S. 1998. Myocyte enhancer factor 2C and Nkx2-5 up-regulate each other's expression and initiate cardiomyogenesis in P19 cells. *J Biol Chem* 273:34904-10.
- Sletten LJ, Pierpont ME. 1996. Variation in severity of cardiac disease in Holt-Oram syndrome. *Am J Med Genet* 65:128-32.
- Small EM, Krieg PA. 2003. Transgenic analysis of the atrialnatriuretic factor (ANF) promoter: Nkx2-5 and GATA-4 binding sites are required for atrial specific expression of ANF. *Dev Biol* 261:116-31.
- Smith JC, Symes K, Hynes RO, DeSimone D. 1990. Mesoderm induction and the control of gastrulation in *Xenopus laevis*: the roles of fibronectin and integrins. *Development* 108:229-38.
- Snyder M, Huang XY, Zhang JJ. Stat3 directly controls the expression of Tbx5, Nkx2.5, and GATA4 and is essential for cardiomyocyte differentiation of P19CL6 cells. *J Biol Chem* 285:23639-46.
- Sodhi CP, Li J, Duncan SA. 2006. Generation of mice harbouring a conditional loss-of-function allele of Gata6. *BMC Dev Biol* 6:19.
- Sohda M, Misumi Y, Yoshimura S, Nakamura N, Fusano T, Sakisaka S, Ogata S, Fujimoto J, Kiyokawa N, Ikehara Y. 2005. Depletion of vesicle-tethering factor p115 causes mini-stacked Golgi fragments with delayed protein transport. *Biochem Biophys Res Commun* 338:1268-74.
- Somi S, Klein AT, Houweling AC, Ruijter JM, Buffing AA, Moorman AF, van den Hoff MJ. 2006. Atrial and ventricular myosin heavy-chain expression in the developing chicken heart: strengths and limitations of non-radioactive in situ hybridization. *J Histochem Cytochem* 54:649-64.

- Song L, Fassler R, Mishina Y, Jiao K, Baldwin HS. 2007. Essential functions of Alk3 during AV cushion morphogenesis in mouse embryonic hearts. *Dev Biol* 301:276-86.
- Sonnichsen B, Lowe M, Levine T, Jamsa E, Dirac-Svejstrup B, Warren G. 1998. A role for giantin in docking COPI vesicles to Golgi membranes. *J Cell Biol* 140:1013-21.
- Soto B, Becker AE, Moolaert AJ, Lie JT, Anderson RH. 1980. Classification of ventricular septal defects. *Br Heart J* 43:332-43.
- Sparrow DB, Guillen-Navarro E, Fatkin D, Dunwoodie SL. 2008. Mutation of Hairy-and-Enhancer-of-Split-7 in humans causes spondylocostal dysostosis. *Hum Mol Genet* 17:3761-6.
- Speiser B, Riess CF, Schaper J. 1991. The extracellular matrix in human myocardium: Part I: Collagens I, III, IV, and VI. *Cardioscience* 2:225-32.
- Speiser B, Weihrauch D, Riess CF, Schaper J. 1992. The extracellular matrix in human cardiac tissue. Part II: Vimentin, laminin, and fibronectin. *Cardioscience* 3:41-9.
- Sprague GF, Jr. 1990. Combinatorial associations of regulatory proteins and the control of cell type in yeast. *Adv Genet* 27:33-62.
- Srivastava D, Thomas T, Lin Q, Kirby ML, Brown D, Olson EN. 1997. Regulation of cardiac mesodermal and neural crest development by the bHLH transcription factor, dHAND. *Nat Genet* 16:154-60.
- Stalmans I, Lambrechts D, De Smet F, Jansen S, Wang J, Maity S, Kneer P, von der Ohe M, Swillen A, Maes C, Gewillig M, Molin DG, Hellings P, Boetel T, Haardt M, Compernelle V, Dewerchin M, Plaisance S, Vlietinck R, Emanuel B, Gittenberger-de Groot AC, Scambler P, Morrow B, Driscoll DA, Moons L, Esguerra CV, Carmeliet G, Behn-Krappa A, Devriendt K, Collen D, Conway SJ, Carmeliet P. 2003. VEGF: a modifier of the del22q11 (DiGeorge) syndrome? *Nat Med* 9:173-82.

- Stennard FA, Costa MW, Elliott DA, Rankin S, Haast SJ, Lai D, McDonald LP, Niederreither K, Dolle P, Bruneau BG, Zorn AM, Harvey RP. 2003. Cardiac T-box factor Tbx20 directly interacts with Nkx2-5, GATA4, and GATA5 in regulation of gene expression in the developing heart. *Dev Biol* 262:206-24.
- Stennard FA, Costa MW, Lai D, Biben C, Furtado MB, Solloway MJ, McCulley DJ, Leimena C, Preis JI, Dunwoodie SL, Elliott DE, Prall OW, Black BL, Fatkin D, Harvey RP. 2005. Murine T-box transcription factor Tbx20 acts as a repressor during heart development, and is essential for adult heart integrity, function and adaptation. *Development* 132:2451-62.
- Stewart AJ, Mukherjee J, Roberts SJ, Lester D, Farquharson C. 2005. Identification of a novel class of mammalian phosphoinositol-specific phospholipase C enzymes. *Int J Mol Med* 15:117-21.
- Sugi Y, Lough J. 1992. Onset of expression and regional deposition of alpha-smooth and sarcomeric actin during avian heart development. *Dev Dyn* 193:116-24.
- Sugi Y, Sasse J, Lough J. 1993. Inhibition of precardiac mesoderm cell proliferation by antisense oligodeoxynucleotide complementary to fibroblast growth factor-2 (FGF-2). *Dev Biol* 157:28-37.
- Summerton J, Weller D. 1997. Morpholino antisense oligomers: design, preparation, and properties. *Antisense Nucleic Acid Drug Dev* 7:187-95.
- Sun Rhodes LS, Merzdorf CS. 2006. The zic1 gene is expressed in chick somites but not in migratory neural crest. *Gene Expr Patterns* 6:539-45.
- Sung RK, Ursell PC, Rame JE, Bailey H, Caleshu C, Nussbaum RL, Scheinman MM. QTc Prolongation and Family History of Sudden Death in a Patient with Desmin Cardiomyopathy. *Pacing Clin Electrophysiol*.
- Suzuki J, Takaku A. 1969. Cerebrovascular "moyamoya" disease. Disease showing abnormal net-like vessels in base of brain. *Arch Neurol* 20:288-99.

- Szczesna D, Zhao J, Jones M, Zhi G, Stull J, Potter JD. 2002. Phosphorylation of the regulatory light chains of myosin affects  $Ca^{2+}$  sensitivity of skeletal muscle contraction. *J Appl Physiol* 92:1661-70.
- Tajsharghi H, Thornell LE, Lindberg C, Lindvall B, Henriksson KG, Oldfors A. 2003. Myosin storage myopathy associated with a heterozygous missense mutation in MYH7. *Ann Neurol* 54:494-500.
- Takada S, Stark KL, Shea MJ, Vassileva G, McMahon JA, McMahon AP. 1994. Wnt-3a regulates somite and tailbud formation in the mouse embryo. *Genes Dev* 8:174-89.
- Takai T, Nishita Y, Iguchi-Arigo SM, Ariga H. 1994. Molecular cloning of MSSP-2, a c-myc gene single-strand binding protein: characterization of binding specificity and DNA replication activity. *Nucleic Acids Res* 22:5576-81.
- Takeda Y, Kazarov AR, Butterfield CE, Hopkins BD, Benjamin LE, Kaipainen A, Hemler ME. 2007. Deletion of tetraspanin Cd151 results in decreased pathologic angiogenesis in vivo and in vitro. *Blood* 109:1524-32.
- Takeuchi JK, Bruneau BG. 2009. Directed transdifferentiation of mouse mesoderm to heart tissue by defined factors. *Nature* 459:708-11.
- Takeuchi JK, Koshiba-Takeuchi K, Suzuki T, Kamimura M, Ogura K, Ogura T. 2003. Tbx5 and Tbx4 trigger limb initiation through activation of the Wnt/Fgf signaling cascade. *Development* 130:2729-39.
- Takeuchi JK, Mileikovskaia M, Koshiba-Takeuchi K, Heidt AB, Mori AD, Arruda EP, Gertsenstein M, Georges R, Davidson L, Mo R, Hui CC, Henkelman RM, Nemer M, Black BL, Nagy A, Bruneau BG. 2005. Tbx20 dose-dependently regulates transcription factor networks required for mouse heart and motoneuron development. *Development* 132:2463-74.

- Tanaka M, Chen Z, Bartunkova S, Yamasaki N, Izumo S. 1999. The cardiac homeobox gene *Csx/Nkx2.5* lies genetically upstream of multiple genes essential for heart development. *Development* 126:1269-80.
- Taylor MR, Slavov D, Ku L, Di Lenarda A, Sinagra G, Carniel E, Haubold K, Boucek MM, Ferguson D, Graw SL, Zhu X, Cavanaugh J, Sucharov CC, Long CS, Bristow MR, Lavori P, Mestroni L. 2007. Prevalence of desmin mutations in dilated cardiomyopathy. *Circulation* 115:1244-51.
- ten Dijke P, Arthur HM. 2007. Extracellular control of TGFbeta signalling in vascular development and disease. *Nat Rev Mol Cell Biol* 8:857-69.
- Thierfelder L, Watkins H, MacRae C, Lamas R, McKenna W, Vosberg HP, Seidman JG, Seidman CE. 1994. Alpha-tropomyosin and cardiac troponin T mutations cause familial hypertrophic cardiomyopathy: a disease of the sarcomere. *Cell* 77:701-12.
- Thomas PS, Kasahara H, Edmonson AM, Izumo S, Yacoub MH, Barton PJ, Gourdie RG. 2001. Elevated expression of *Nkx-2.5* in developing myocardial conduction cells. *Anat Rec* 263:307-13.
- Thornell L, Carlsson L, Li Z, Mericskay M, Paulin D. 1997. Null mutation in the desmin gene gives rise to a cardiomyopathy. *J Mol Cell Cardiol* 29:2107-24.
- Timmerman LA, Grego-Bessa J, Raya A, Bertran E, Perez-Pomares JM, Diez J, Aranda S, Palomo S, McCormick F, Izpisua-Belmonte JC, de la Pompa JL. 2004. Notch promotes epithelial-mesenchymal transition during cardiac development and oncogenic transformation. *Genes Dev* 18:99-115.
- Togi K, Yoshida Y, Matsumae H, Nakashima Y, Kita T, Tanaka M. 2006. Essential role of *Hand2* in interventricular septum formation and trabeculation during cardiac development. *Biochem Biophys Res Commun* 343:144-51.

- Tomanek RJ, Ishii Y, Holifield JS, Sjogren CL, Hansen HK, Mikawa T. 2006. VEGF family members regulate myocardial tubulogenesis and coronary artery formation in the embryo. *Circ Res* 98:947-53.
- Tomasek JJ, Haaksma CJ, Schwartz RJ, Vuong DT, Zhang SX, Ash JD, Ma JX, Al-Ubaidi MR. 2006. Deletion of smooth muscle alpha-actin alters blood-retina barrier permeability and retinal function. *Invest Ophthalmol Vis Sci* 47:2693-700.
- Ton CC, Hirvonen H, Miwa H, Weil MM, Monaghan P, Jordan T, van Heyningen V, Hastie ND, Meijers-Heijboer H, Drechsler M, et al. 1991. Positional cloning and characterization of a paired box- and homeobox-containing gene from the aniridia region. *Cell* 67:1059-74.
- Torres MA, Yang-Snyder JA, Purcell SM, DeMarais AA, McGrew LL, Moon RT. 1996. Activities of the Wnt-1 class of secreted signaling factors are antagonized by the Wnt-5A class and by a dominant negative cadherin in early *Xenopus* development. *J Cell Biol* 133:1123-37.
- Toyofuku T, Hong Z, Kuzuya T, Tada M, Hori M. 2000. Wnt/frizzled-2 signaling induces aggregation and adhesion among cardiac myocytes by increased cadherin-beta-catenin complex. *J Cell Biol* 150:225-41.
- Trelles RD, Leon JR, Kawakami Y, Simoes S, Izpisua Belmonte JC. 2002. Expression of the chick vascular endothelial growth factor D gene during limb development. *Mech Dev* 116:239-42.
- Turnpenny PD, Alman B, Cornier AS, Giampietro PF, Offiah A, Tassy O, Pourquie O, Kusumi K, Dunwoodie S. 2007. Abnormal vertebral segmentation and the notch signaling pathway in man. *Dev Dyn* 236:1456-74.
- Ueno S, Weidinger G, Osugi T, Kohn AD, Golob JL, Pabon L, Reinecke H, Moon RT, Murry CE. 2007. Biphasic role for Wnt/beta-catenin signaling in cardiac specification in zebrafish and embryonic stem cells. *Proc Natl Acad Sci U S A* 104:9685-90.

- Ueyama T, Kasahara H, Ishiwata T, Nie Q, Izumo S. 2003. Myocardin expression is regulated by Nkx2.5, and its function is required for cardiomyogenesis. *Mol Cell Biol* 23:9222-32.
- Ulrich F, Krieg M, Schotz EM, Link V, Castanon I, Schnabel V, Taubenberger A, Mueller D, Puech PH, Heisenberg CP. 2005. Wnt11 functions in gastrulation by controlling cell cohesion through Rab5c and E-cadherin. *Dev Cell* 9:555-64.
- van den Hoff MJ, Kruithof BP, Moorman AF. 2004. Making more heart muscle. *Bioessays* 26:248-61.
- van Gijn ME, Blankesteyn WM, Smits JF, Hierck B, Gittenberger-de Groot AC. 2001. Frizzled 2 is transiently expressed in neural crest-containing areas during development of the heart and great arteries in the mouse. *Anat Embryol (Berl)* 203:185-92.
- Vanderwinden JM, Mailleux P, Schiffmann SN, Vanderhaeghen JJ. 1992. Cellular distribution of the new growth factor pleiotrophin (HB-GAM) mRNA in developing and adult rat tissues. *Anat Embryol (Berl)* 186:387-406.
- Veeman MT, Axelrod JD, Moon RT. 2003. A second canon. Functions and mechanisms of beta-catenin-independent Wnt signaling. *Dev Cell* 5:367-77.
- Veikkola T, Jussila L, Makinen T, Karpanen T, Jeltsch M, Petrova TV, Kubo H, Thurston G, McDonald DM, Achen MG, Stacker SA, Alitalo K. 2001. Signalling via vascular endothelial growth factor receptor-3 is sufficient for lymphangiogenesis in transgenic mice. *EMBO J* 20:1223-31.
- Vernengo L, Chourbagi O, Panuncio A, Lilienbaum A, Batonnet-Pichon S, Bruston F, Rodrigues-Lima F, Mesa R, Pizzarossa C, Demay L, Richard P, Vicart P, Rodriguez MM. Desmin myopathy with severe cardiomyopathy in a Uruguayan family due to a codon deletion in a new location within the desmin 1A rod domain. *Neuromuscul Disord* 20:178-87.

- Voiculescu O, Papanayotou C, Stern CD. 2008. Spatially and temporally controlled electroporation of early chick embryos. *Nat Protoc* 3:419-26.
- von Both I, Silvestri C, Erdemir T, Lickert H, Walls JR, Henkelman RM, Rossant J, Harvey RP, Attisano L, Wrana JL. 2004. Foxh1 is essential for development of the anterior heart field. *Dev Cell* 7:331-45.
- Vrabie A, Goldfarb LG, Shatunov A, Nagele A, Fritz P, Kaczmarek I, Goebel HH. 2005. The enlarging spectrum of desminopathies: new morphological findings, eastward geographic spread, novel exon 3 desmin mutation. *Acta Neuropathol* 109:411-7.
- Waldo K, Miyagawa-Tomita S, Kumiski D, Kirby ML. 1998. Cardiac neural crest cells provide new insight into septation of the cardiac outflow tract: aortic sac to ventricular septal closure. *Dev Biol* 196:129-44.
- Waldo KL, Kumiski DH, Wallis KT, Stadt HA, Hutson MR, Platt DH, Kirby ML. 2001. Conotruncal myocardium arises from a secondary heart field. *Development* 128:3179-88.
- Waldo KL, Lo CW, Kirby ML. 1999. Connexin 43 expression reflects neural crest patterns during cardiovascular development. *Dev Biol* 208:307-23.
- Walther C, Gruss P. 1991. Pax-6, a murine paired box gene, is expressed in the developing CNS. *Development* 113:1435-49.
- Wang D, Chang PS, Wang Z, Sutherland L, Richardson JA, Small E, Krieg PA, Olson EN. 2001. Activation of cardiac gene expression by myocardin, a transcriptional cofactor for serum response factor. *Cell* 105:851-62.
- Wang G, Yeh HI, Lin JJ. 1994. Characterization of cis-regulating elements and trans-activating factors of the rat cardiac troponin T gene. *J Biol Chem* 269:30595-603.

- Wang L, Fan C, Topol SE, Topol EJ, Wang Q. 2003a. Mutation of MEF2A in an inherited disorder with features of coronary artery disease. *Science* 302:1578-81.
- Wang YK, Sporle R, Paperna T, Schughart K, Francke U. 1999. Characterization and expression pattern of the frizzled gene *Fzd9*, the mouse homolog of FZD9 which is deleted in Williams-Beuren syndrome. *Genomics* 57:235-48.
- Wang YX, Qian LX, Liu D, Yao LL, Jiang Q, Yu Z, Gui YH, Zhong TP, Song HY. 2007. Bone morphogenetic protein-2 acts upstream of myocyte-specific enhancer factor 2a to control embryonic cardiac contractility. *Cardiovasc Res* 74:290-303.
- Wang Z, Wang DZ, Pipes GC, Olson EN. 2003b. Myocardin is a master regulator of smooth muscle gene expression. *Proc Natl Acad Sci U S A* 100:7129-34.
- Waterman RE, Balian G. 1980. Indirect immunofluorescent staining of fibronectin associated with the floor of the foregut during formation and rupture of the oral membrane in the chick embryo. *Anat Rec* 198:619-35.
- Weber KT. 1989. Cardiac interstitium in health and disease: the fibrillar collagen network. *J Am Coll Cardiol* 13:1637-52.
- Weng L, Kavaslar N, Ustaszewska A, Doelle H, Schackwitz W, Hebert S, Cohen JC, McPherson R, Pennacchio LA. 2005. Lack of MEF2A mutations in coronary artery disease. *J Clin Invest* 115:1016-20.
- Wessels A, Anderson RH, Markwald RR, Webb S, Brown NA, Viragh S, Moorman AF, Lamers WH. 2000. Atrial development in the human heart: an immunohistochemical study with emphasis on the role of mesenchymal tissues. *Anat Rec* 259:288-300.
- Winnier G, Blessing M, Labosky PA, Hogan BL. 1995. Bone morphogenetic protein-4 is required for mesoderm formation and patterning in the mouse. *Genes Dev* 9:2105-16.

- Woodcock-Mitchell J, Mitchell JJ, Low RB, Kieny M, Sengel P, Rubbia L, Skalli O, Jackson B, Gabbiani G. 1988. Alpha-smooth muscle actin is transiently expressed in embryonic rat cardiac and skeletal muscles. *Differentiation* 39:161-6.
- Wright MD, Geary SM, Fitter S, Moseley GW, Lau LM, Sheng KC, Apostolopoulos V, Stanley EG, Jackson DE, Ashman LK. 2004. Characterization of mice lacking the tetraspanin superfamily member CD151. *Mol Cell Biol* 24:5978-88.
- Wunsch AM, Little CD, Markwald RR. 1994. Cardiac endothelial heterogeneity defines valvular development as demonstrated by the diverse expression of JB3, an antigen of the endocardial cushion tissue. *Dev Biol* 165:585-601.
- Xiao G, Mao S, Baumgarten G, Serrano J, Jordan MC, Roos KP, Fishbein MC, MacLellan WR. 2001. Inducible activation of c-Myc in adult myocardium in vivo provokes cardiac myocyte hypertrophy and reactivation of DNA synthesis. *Circ Res* 89:1122-9.
- Xin M, Davis CA, Molkentin JD, Lien CL, Duncan SA, Richardson JA, Olson EN. 2006. A threshold of GATA4 and GATA6 expression is required for cardiovascular development. *Proc Natl Acad Sci U S A* 103:11189-94.
- Xu H, Morishima M, Wylie JN, Schwartz RJ, Bruneau BG, Lindsay EA, Baldini A. 2004. Tbx1 has a dual role in the morphogenesis of the cardiac outflow tract. *Development* 131:3217-27.
- Xuan S, Baptista CA, Balas G, Tao W, Soares VC, Lai E. 1995. Winged helix transcription factor BF-1 is essential for the development of the cerebral hemispheres. *Neuron* 14:1141-52.
- Xuan YT, Guo Y, Han H, Zhu Y, Bolli R. 2001. An essential role of the JAK-STAT pathway in ischemic preconditioning. *Proc Natl Acad Sci U S A* 98:9050-5.

- Yamada M, Revelli JP, Eichele G, Barron M, Schwartz RJ. 2000. Expression of chick Tbx-2, Tbx-3, and Tbx-5 genes during early heart development: evidence for BMP2 induction of Tbx2. *Dev Biol* 228:95-105.
- Yamagishi T, Ando K, Nakamura H. 2009. Roles of TGFbeta and BMP during valvulo-septal endocardial cushion formation. *Anat Sci Int* 84:77-87.
- Yang Y, Wang J, Zhang X, Lu W, Zhang Q. 2009. A novel mixed micelle gel with thermo-sensitive property for the local delivery of docetaxel. *J Control Release* 135:175-82.
- Yatskievych TA, Ladd AN, Antin PB. 1997. Induction of cardiac myogenesis in avian pregastrula epiblast: the role of the hypoblast and activin. *Development* 124:2561-70.
- Yutzey KE, Kirby ML. 2002. Wherefore heart thou? Embryonic origins of cardiogenic mesoderm. *Dev Dyn* 223:307-20.
- Zak R. 1974. Development and proliferative capacity of cardiac muscle cells. *Circ Res* 35:suppl II:17-26.
- Zeisberg EM, Ma Q, Juraszek AL, Moses K, Schwartz RJ, Izumo S, Pu WT. 2005. Morphogenesis of the right ventricle requires myocardial expression of Gata4. *J Clin Invest* 115:1522-31.
- Zhang H, Bradley A. 1996. Mice deficient for BMP2 are nonviable and have defects in amnion/chorion and cardiac development. *Development* 122:2977-86.
- Zhang Z, Huynh T, Baldini A. 2006. Mesodermal expression of Tbx1 is necessary and sufficient for pharyngeal arch and cardiac outflow tract development. *Development* 133:3587-95.
- Zhao B, Etter L, Hinton RB, Jr., Benson DW. 2007. BMP and FGF regulatory pathways in semilunar valve precursor cells. *Dev Dyn* 236:971-80.

Zhu L, Vranckx R, Khau Van Kien P, Lalande A, Boisset N, Mathieu F, Wegman M, Glancy L, Gasc JM, Brunotte F, Bruneval P, Wolf JE, Michel JB, Jeunemaitre X. 2006. Mutations in myosin heavy chain 11 cause a syndrome associating thoracic aortic aneurysm/aortic dissection and patent ductus arteriosus. *Nat Genet* 38:343-9.

Zhu X, Sasse J, McAllister D, Lough J. 1996. Evidence that fibroblast growth factors 1 and 4 participate in regulation of cardiogenesis. *Dev Dyn* 207:429-38.

Zuber ME, Gestri G, Viczian AS, Barsacchi G, Harris WA. 2003. Specification of the vertebrate eye by a network of eye field transcription factors. *Development* 130:5155-67.

## APPENDIX

### **APPENDIX A: An overview of cardiac development in the chick**

Chick development is described from a cardiological perspective from HH 1 – HH 36. The HH 1 chick embryo is at the pre-primitive streak stage [Hamburger and Hamilton, 1992], with cardiac precursor cells identifiable in the epiblast cell layer [Yutzey and Kirby, 2002]. At HH 2 (6 – 7 hrs) cardiac progenitor cells exist in the postero-lateral epiblast and primitive streak formation begins. An intermediate primitive streak is visible at HH 3 (12 – 13 hrs). The HH 4 embryo (18 – 19 hours) displays a definitive primitive streak and precardiac cells are found either side of Hensen's node and in the anterior mesoderm. Gastrulation takes place at HH 5. At HH 5 / 6 (19 – 25 hrs) the cells that will form the heart move into two bilateral regions in the anterolateral region of the embryo, the primary heart field. Cardiac precursor cells are at a higher level of commitment at HH 6, and expression of cardiac genes is initiated at this stage [van den Hoff et al., 2004]. At HH 7 (23 – 26 hrs, 1 somite), markers of terminal myocardial differentiation can be detected in the primary heart fields [Han et al., 1992]. At HH 8 (26 – 29 hrs, 4 somites), endocardial tube formation begins. Embryonic folding leads to formation the primary heart tube at the embryonic ventral midline [Moorman et al., 2003]. Prior to looping, the heart is centrally positioned and undergoes rapid elongation by addition of myocardial cells to both ends of the heart tube along the craniocaudal axis of the embryo to form a long nearly symmetrical tube at HH9. At HH 9 (29 – 33 hrs, 7 somites), cardiac neural crest (CNC) cells undergo epithelial-to-mesenchymal transition (EMT) and migrate away from the neural tube towards the mesenchyme, outflow tract aorticopulmonary septum, and pharyngeal arch arteries [Boot et al., 2003]. The primitive tubular heart begins to beat at HH 10. Dextral looping, where the linear heart tube loops to the right to become c-shaped and asymmetric, begins at this stage and is completed at HH 12 (45 – 49 hrs, 16 somites) [Manner, 2000]. The early phase of s-looping begins at HH 13 (48 – 52 hours, 19 somites), and this phase is characterised by transformation of the heart from a c-

shape to an immature s-shaped structure. Development of the interatrial septum begins at HH 14 (50 – 53 hours, 22 somites), and the septum primum grows from the dorsal cranial wall of the common atrium into the atrial lumen, towards the endocardial cushions in the AV canal [Anderson et al., 2003]. The early phase of s-looping is completed at HH 17 – HH 18 (52 – 72 hrs, 29 – 36 somites). The late phase of s-looping occurs at HH 19 – HH 24, and ballooning of the chambers also occurs at this stage [Christoffels et al., 2000]. At HH 21 – 23 (3.5 – 4 days, 43 – 44 somites) two pairs of endocardial cushions, one proximal and one distal, are found in the outflow tract [Qayyum et al., 2001]. At HH 24 (4 days), the atrial septum becomes fused with dorsal and ventral endocardial cushions in the AV canal, and small perforations (foramina secunda) form in the septum [Morse and Hendrix, 1980]. The foramina secunda increase in size and number during days 5 and 6, creating cords of endocardium covered tissue [Morse and Hendrix, 1980]. This cord tissue thickens during days 8 to 15, reducing the size of the foramina secunda, will close to complete atrial septation by day 2 post hatching. At HH 25 – HH 26 (4.5 – 5 days), a third distal endocardial cushion (required for AV canal septation) has formed in the outflow tract. The aorticopulmonary septum, which divides the truncus into aortic and pulmonary channels, forms as a result of fusion of the left and right superior truncus swellings. Mitral and tricuspid valve primordia are present and the muscular interventricular septum, which septates the left and right ventricles, begins to grow at this stage. At HH 28 (5.5 days) division of the semilunar valve region results from formation of the aorticopulmonary septum, and AV valve development begins. At HH 34 (8.0 days), ventricular and outflow tract septation is completed. Fusion of the dorsal and ventral endocardial cushions results in septation of the AV canal. At HH 35 – HH 36 (8 – 10 days), development of AV valves is nearly complete.

## Appendix B: QPCR assays designed to candidate genes in the mouse

Gene	Accession ID	Primer name	Primer sequence (5' – 3')	Position	Probe*
Neurofilament 3	NM_008691.2	Neurofilament F	GGTGCGAGGCACTAAGGAG	1024 – 1042	1
		Neurofilament R	ATTTTCCAAGTCTGGATGG	1110 - 1129	
PMM2	NM_016881.2	PMM2 F	ATGGATGGGACCCTGACTG	77 - 95	29
		PMM2 R	TCTGACCCACCTACCACTCC	164 - 183	
VEGFB	BC046303.1	VEGFB F	CAACACCAAGTCCGAATGC	498 – 516	76
		VEGFB R	GGCTTCACAGCACTCTCCTT	603 - 622	
$\alpha$ 2-macroglobulin	NM_175628.3	$\alpha$ 2-macroglobulin F	TGAGGAGGCGGTAAAAGAAG	3575 - 3594	93
		$\alpha$ 2-macroglobulin R	TGGCACTCTGGTTTCTGA	3620 – 3638	
Galanin R2	NM_010254.4	Galanin R2 F	GAGAGGCATTTGCTTCTTGG	735 - 754	1
		Galanin R2 R	AGTACAGCTCAGTCCTAAGCCTAAA	787 - 811	
Glutaredoxin	AB013137.1	Glutaredoxin F	TGGAGCTCTGCAGTTATAAAAGG	355 - 377	13
		Glutaredoxin R	GCCATCAGCATGGTTAGACA	408 - 427	
S100A10	NM_009112.2	S100A10 F	AGTTCCTGGGTTTTTGGGA	228 – 246	76
		S100A10 R	CACTGGTCCAGGTCCTTCAT	281 - 300	
AP4e1	BC042530.1	AP4e1 F	TGGCATCATCGCTGTTTG	531 – 548	93
		AP4e1 R	AACATCTGCTTTCCCAACAA	578 – 598	
mRbap46	NM_009031.3	mRbap46 F	ACGCAAGATGGCGAGTAAAG	227 - 246	25
		mRbap46 R	TCCAGATTTTATACTCTTCGTTGATG	278 - 303	
Gamma Filamin	BC060276.1	Gamma Filamin F	GGGTACACACACCCTCAGGA	3698 - 3717	25
		Gamma Filamin R	TGAAGCGGATGGTATGCTTAT	3755 - 3775	
HNRPDL	NM_016690.4	HNRPDL F	AACCAGCAGGATGACGGTA	145 - 163	13
		HNRPDL R	ATTCAGTCAGATCTTCTTGCTTG	194 - 217	
Calreticulin	NM_007591.3	Calreticulin F	TGAAGCTGTTCCGAGTGGT	401 – 420	93
		Calreticulin R	GATGACATGAACCTTCTGGTG	492 - 513	
Annexin A4	BC055871.1	Annexin A4 F	AGGCTCTACGGGAAGTCTTTG	944 - 964	25
		Annexin A4 R	GCGGCGTCTTGTTAATC	1034 - 1052	
RBMS1	BC057866.1	RBMS1 F	GAAGCAAGTGGCCAGCAG	1461 - 1478	76
		RBMS1 R	GAATCCCTTCGGTACATCTCA	1542 - 1563	
$\alpha$ -tropomyosin	M22479.1	$\alpha$ -tropomyosin F	TCGTGCTCAGGAGCGTCT	354 - 371	25
		$\alpha$ -tropomyosin R	TTCAATGACTTTCATGCCTCTC	426 - 447	

Fibronectin	X93167.1	Fibronectin F	TGATTGGGAGGAAGAAGACAG	3531 - 3551	93
		Fibronectin R	TGTGGAGGGAACATCCAAG	3607 - 3625	
FUCA1	NM_024243.4	FUCA1 F	GCCAGAGCTGTATGACCTTGT	640 - 660	93
		FUCA1 R	GGAGTCCAGTACGTGTCCAGG	710 - 730	
PETA-3	AF033620.1	PETA-3 F	CTCCATGATAACCCACCATGT	211 - 231	76
		PETA-3 R	GCATTCCAGGAACCTTATG	267 - 286	
PA2.26	AJ250246.1	PA2.26 F	CAGTGTGTTCTGGGTTTTGG	52 - 72	95
		PA2.26 R	TGGGGTCACAATATCATCTTCA	122 - 143	
nono	NM_023144.1	Nono F	GGTTATGCTAATGAGGCAGGA	1058 - 1078	25
		Nono R	TTCGCTTCTGAACCTCTTGG	1127 - 1146	
$\beta$ -tubulin	BC003825.1	$\beta$ -tubulin 5 F	GCTGGACCGAATCTCTGTGT	283 - 302	95
		$\beta$ -tubulin 5 R	GACCTGAGCGAACGGAGTC	374 - 392	
Rpl13a	NM_009438.3	Rpl13a F	GCCCCACAAGACCAAGAG	285 - 302	1
		Rpl13a R	GACCACCATCCGCTTTTTTC	363 - 381	
Bola2	NM_175103.3	Bola2 F	GATTACCTCCGCGAGAAGC	53 - 71	13
		Bola2 R	AACGGTTCAGAGTCGTGTCC	109 - 128	
dynactin	NM_007835.2	Dynactin F	TCCTCATCAGCAGATGAAC	2968 - 2987	76
		Dynactin R	CTGCGTCATACTCGCCTTCT	3008 - 3027	
tmem131	NM_018872.2	tmem131 F	AGTTCAGCTCCCAACC	5502 - 5519	76
		tmem131 R	GAGCTGCTGAATGGAGTGGT	5565 - 5584	

\*Probe identifiers refer to pre-designed Universal ProbeLibrary probes (Roche). Each probe binds to a specific nucleotide sequence. Probe sequence information can be found online at <https://www.roche-applied-science.com>).

**Appendix C: IUPAC-IUB consensus nucleotide definitions**

IUPAC-IUB consensus nucleotide definitions	
IUB	Base
A	A
C	C
G	G
T	T
M	A or C
R	A or G
W	A or T
S	C or G
Y	C or T
K	G or T
V	A or C or G
H	A or C or T
D	A or G or T
B	C or G or T
N	G or A or C or T

**Appendix D Cell transfection and luciferase reporter assays**

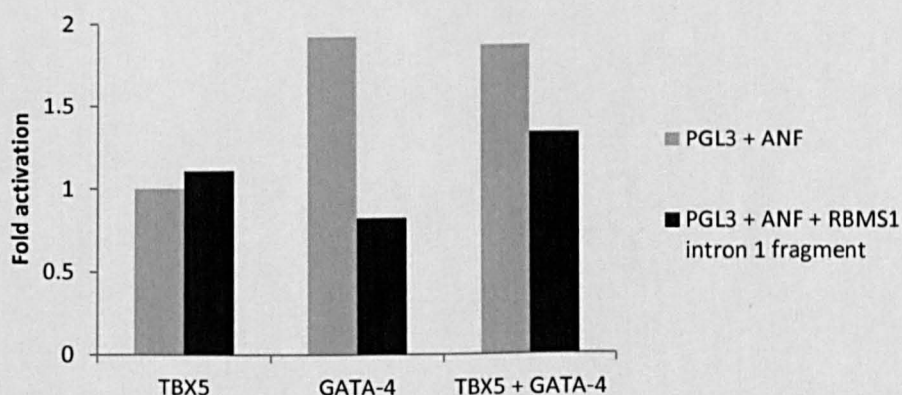
Cell transfection and luciferase reporter assays were performed by Dr Tushar Ghosh. COS7 cells were transfected (using Polyfect) with 1 µg expression plasmids (pcDNA-TBX5 and / or pcDNA-GATA-4), and 1.5 µg reporter plasmid. Cells were harvested 24 hours after transfection for measurement of cell lysate luciferase activity using the Dual Luciferase Reporter Assay system. Transfections were performed in duplicate, and each experiment carried out twice. Cells transfected with reporter plasmid but neither expression plasmid were used for normalisation.

The results of reporter assays performed in the pGL3-basic vector containing the human ANF promoter are displayed in Table 3.7 and Figure 3.9. Luciferase activity of vectors with and without the intronic fragment was very similar in the presence of TBX5. This suggests that TBX5 does not bind to this region for regulation of promoter activity. In the presence of GATA-4, luciferase activity was over 2-fold lower in the PGL3/ANF vector containing the intronic fragment compared to the PGL3/ANF vector lacking it i.e. GATA-4 has a strong repressive effect via this region. There was a 28% reduction in luciferase activity in the presence of both TBX5 and GATA-4, smaller than the effect of GATA-4 alone, ruling out synergistic repression by both transcription factors via this region. Reporter assays were also performed using the pGL3-promoter vector, but luciferase activity was too low for accurate quantification.

**Effect of the RBMS1 intron 1 fragment on promoter activity**

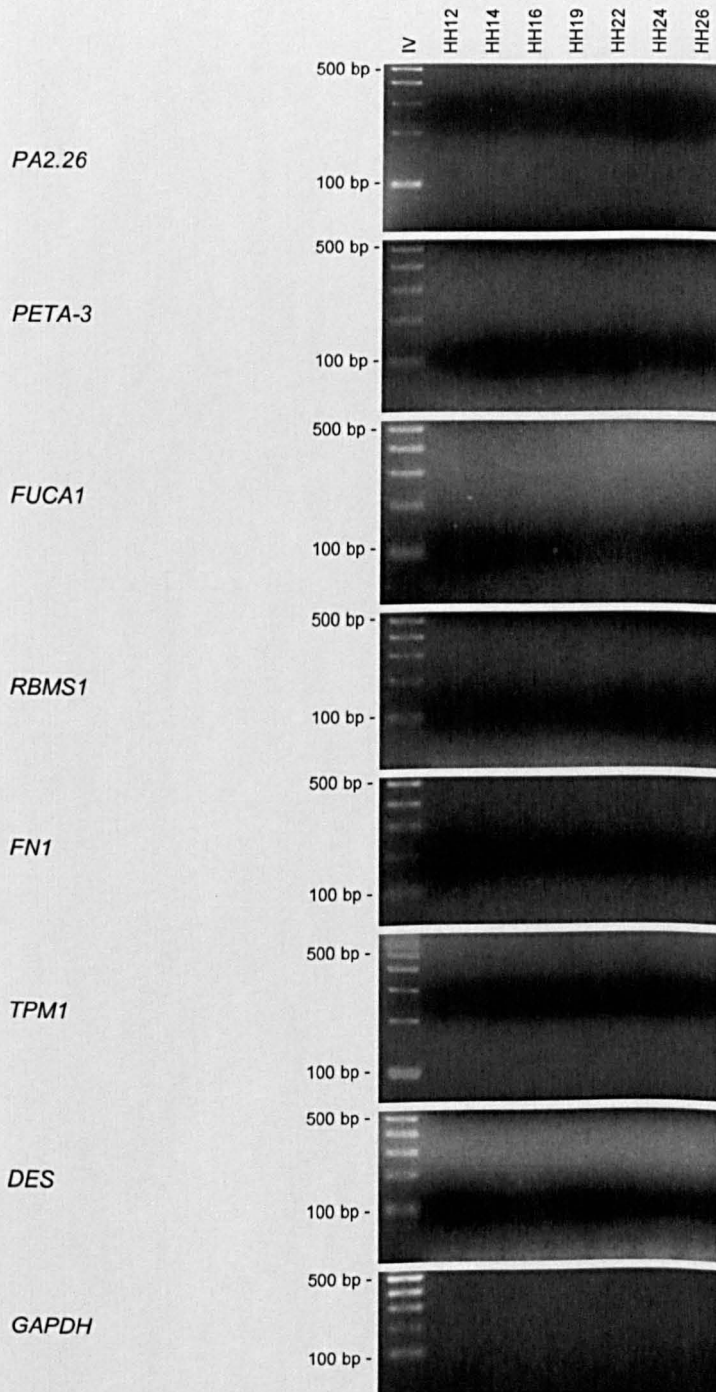
Expression plasmid	Fold Activation	
	PGL3 + ANF	PGL3 + ANF + RBMS1 intron 1 fragment
TBX5	1.00	1.11
GATA-4	1.91	0.82
TBX5 + GATA-4	1.86	1.33

COS7 cells were transfected with 1  $\mu$ g expression plasmids (pcDNA-TBX5 and / or pcDNA-GATA-4), and 1.5  $\mu$ g reporter plasmid. Cells were harvested 24 hours after transfection for measurement of luciferase activity. Each transfection was performed in duplicate, and each experiment carried out twice. Cells transfected with reporter plasmid, but neither expression plasmid, were used for normalisation.

**Effect of the RBMS1 intron 1 fragment on promoter activity**

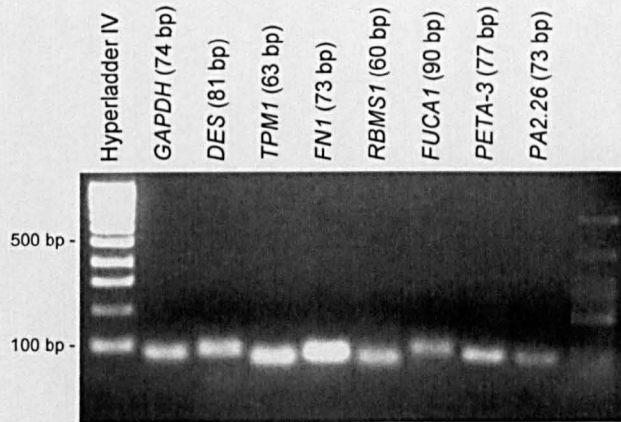
COS7 cells were transfected with 1  $\mu$ g expression plasmids (pcDNA-TBX5 and / or pcDNA-GATA-4), and 1.5  $\mu$ g reporter plasmid. Cells were harvested 24 hours after transfection for measurement of luciferase activity. Each transfection was performed in duplicate, and each experiment carried out twice. Cells transfected with reporter plasmid, but neither expression plasmid, were used for normalisation.

**Appendix E: Negative RT controls performed in parallel to expression profiling of candidate genes in the chick heart**



Samples were electrophoresed on 2% agarose gels using Hyperladder IV as a size marker (500 bp and 100 bp bands are indicated). Negative RT controls (where reverse transcriptase enzyme was not added) did not display amplification for any of the assays. All products assays spanned a 60 – 90 bp region.

**Appendix F: Relative sizes of products amplified for expression profiling of candidate genes in the chick heart**

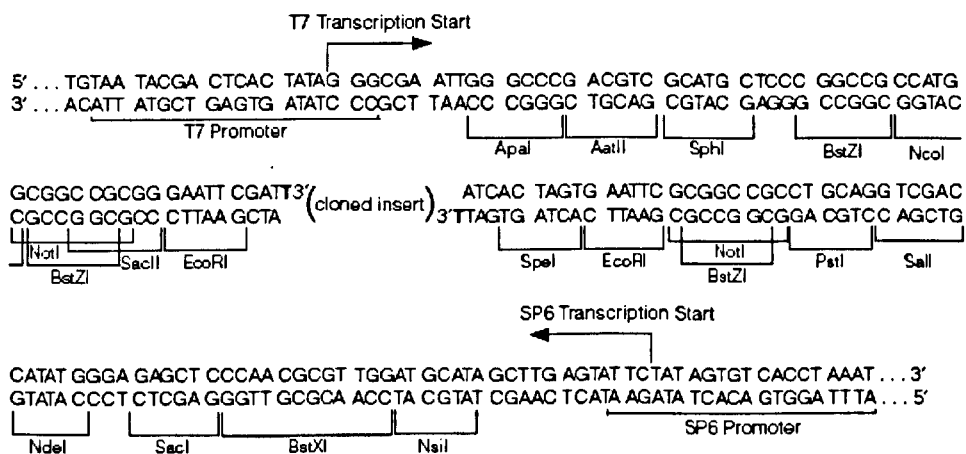
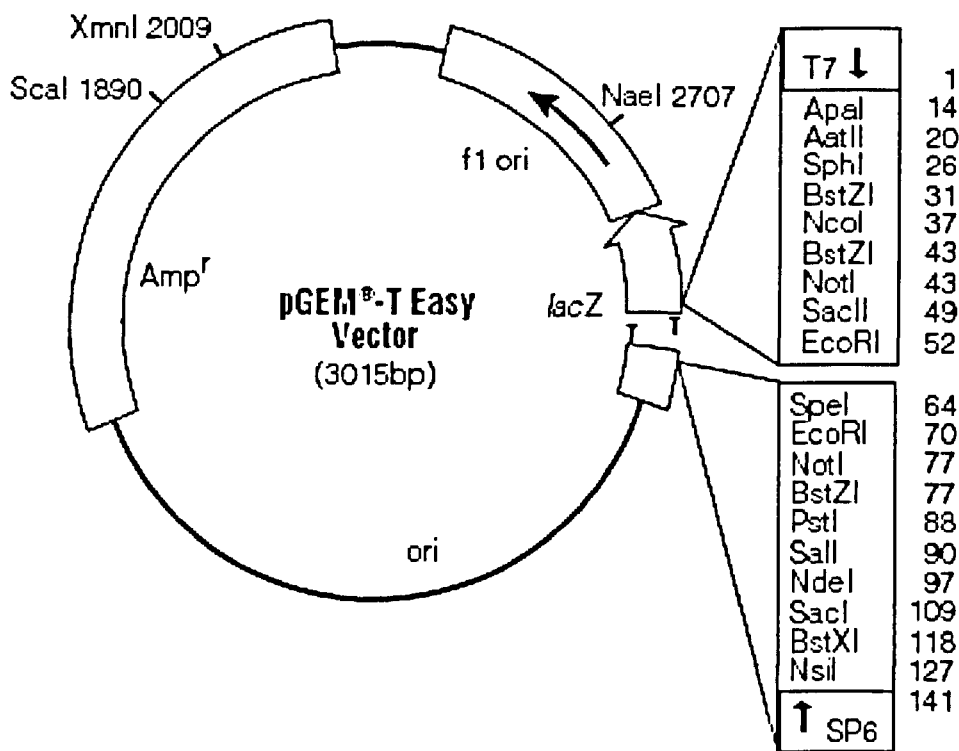


Samples were electrophoresed on 2% agarose gels using Hyperladder IV as a size marker (500 bp and 100 bp bands are indicated).

**Appendix G: Standard amino acid abbreviations**

Amino acid	3-letter abbreviation	1-letter abbreviation
Alanine	Ala	A
Arginine	Arg	R
Asparagine	Asn	N
Aspartic acid	Asp	D
Cysteine	Cys	C
Glutamic acid	Glu	E
Glutamine	Gln	Q
Glycine	Gly	G
Histidine	His	H
Isoleucine	Ile	I
Leucine	Leu	L
Lysine	Lys	K
Methionine	Met	M
Phenylalanine	Phe	F
Proline	Pro	P
Serine	Ser	S
Threonine	Thr	T
Tryptophan	Trp	W
Tyrosine	Tyr	Y
Valine	Val	V
Selenocysteine	Sec	U
Pyrrolysine	Pyl	O

Appendix H Map of the pGEM-T Easy vector



The position of the T7 and SP6 transcription start sites are marked in addition to restriction sites. T7 RNA polymerase was used for synthesis of antisense RNA probes from SpeI linearised plasmid DNA, and SP6 RNA polymerase used for synthesis of sense control probes from SacII linearised plasmid DNA (both inserts in forward orientation).

## **Appendix I Genes identified in microarray analysis of TBX5 and GATA-4 knockdown**

### **SOX3**

SOX3 (SRY (sex determining region Y)-box 3) is a member of the SOX family of transcription factors that are important in embryonic development and determination of cell fate. This gene was up-regulated by 2-fold in double knockdown embryos. SOX3 null mice displayed a range of defects including craniofacial abnormalities, midline CNS defects, growth retardation, reduced fertility, and hypopituitarism [Rizzoti et al., 2004]. Human mutations in SOX3 are associated with X-linked hypopituitarism and mental retardation [Laumonnier et al., 2002].

### **ZIC1**

ZIC1 (Zic family member 1) is a member of the conserved ZIC family of C2H2-type zinc finger transcription factors which are important in early development. Transcripts of this gene displayed 2.6 and 26.6-fold up-regulation in TBX5 / GATA-4 knockdown embryos. ZIC1 is expressed in regions that give rise to the dorsal neural tube and neural crest [Nakata et al., 1998], but not in migratory neural crest cells [Sun Rhodes and Merzdorf, 2006]. Whole mount *in situ* hybridisation expression analysis in the mouse embryo (E9.5 – E11.5) showed that ZIC1 is expressed along the dorsal midline of the cranial and spinal neural tube, and expression was not detected in the heart [Gaston-Massuet et al., 2005; Nagai et al., 1997]. ZIC1 is involved in cerebellar development, and mouse knockout of this gene results in brain and axial skeletal abnormalities [Aruga et al., 1998; Aruga et al., 1999].

### **PAX6**

PAX6 (paired box 6) is a transcription factor which contains a paired box domain and homeodomain, with a crucial role in the development of the eyes, nose, central nervous system, and pancreas. This gene was up-regulated 2.7 fold in TBX5 / GATA-4 double knockdown embryonic hearts. PAX6 is expressed in the developing nervous

system [Krauss et al., 1991; Walther and Gruss, 1991] and eyes [Ton et al., 1991]. Mutations in this gene are linked to an array of ocular disorders including aniridia [Glaser et al., 1992], Gillespie syndrome [Glaser et al., 1994] and Peter's anomaly [Hanson et al., 1994].

## **OTX2**

OTX2 (orthodenticle homeobox 2) is a member of the bicoid family of homeodomain transcription factors, and a homologue of the drosophila gene orthodenticle which is involved in formation of the brain and eyes [Finkelstein and Boncinelli, 1994]. OTX2 transcripts displayed 2.8 and 16 fold up-regulation in TBX5 / GATA-4 double knockdown embryos. This gene is expressed in the developing nose, ear, eyes, and brain [Martinez-Morales et al., 2001; Simeone et al., 1993]. Mouse knockout of this gene results in embryonic lethality due to defects in gastrulation which cause severe brain malformations including deletion of large regions [Acampora et al., 1995; Ang et al., 1996]. Human mutations in OTX2 are associated with a range of ocular disorders including microphthalmia syndromic type 5 (MCOPS5) [Ragge et al., 2005]. There is evidence that OTX2 interacts with other ocular transcription factors including PAX6 [Zuber et al., 2003].

## **FOXP1**

FOXP1 (forkhead box G1) belongs to the forkhead family of transcription factors. FOXP1 displayed 2.8 fold up-regulation in TBX5 / GATA-4 double knockdown embryos. This gene is expressed in the brain and testis where it acts as a transcriptional repressor crucial in brain development [Xuan et al., 1995]. Mouse knockout of FOXP1 results in hypoplasia of the cerebral hemispheres and lethality at birth [Hanashima et al., 2004; Xuan et al., 1995]. Mutations in this gene are associated with the congenital variant of Rett syndrome, a neurodevelopmental disorder [Ariani et al., 2008].

**NKX2-1**

NKX2-1 (NK2 homeobox 1), also called thyroid transcription factor 1 (TTF1), is a developmentally important homeodomain transcription factor which regulates expression of thyroid specific genes. NKX2-1 displayed 11.4 fold up-regulation in response to double knockdown of TBX5 and GATA-4. NKX2-1 null mice lack thyroid glands, lungs, and pituitary glands, and display defects of the ventral forebrain [Kimura et al., 1996]. Mutations or deletions in this gene in both humans and mice are associated with neurological defects [Pohlentz et al., 2002].

**CYTL1**

CYTL1 (cytokine-like 1) is a secreted peptide classed as a novel cytokine based on its predicted secondary structure which indicates it contains four alpha helices, a common characteristic of cytokines [Liu et al., 2000]. This gene was up-regulated 2.3 fold in TBX5 / GATA-4 double knockdown embryos. The function of CYTL1 is not well characterised. It is expressed in the cartilage tissue of the mouse inner ear [Ficker et al., 2004] and articular cartilage in humans [Hermansson et al., 2004], and has a function in chondrogenesis [Kim et al., 2007]. RT-PCR expression studies in the adult mouse show CYTL1 expression is highest in cartilage and lungs, and is also observed in the heart, trachea, and testis [Kim et al., 2007].

**PLCH1**

PLCH1 (phospholipase C, eta 1) is a member of the phosphoinositide-specific phospholipase C family of enzymes which are important in intracellular signal transduction (via release of inositol 1,4,5-triphosphate (IP3) and diacylglycerol (DAG)), intracellular Ca<sup>2+</sup> release, and protein kinase C activation [Hwang et al., 2005]. PLCH1 displayed 2.8-fold up-regulation in response to TBX5 / GATA-4 double knockdown. This gene displays expression in several cell types and has a variety of functions [Stewart et al., 2005].

**TFAP2B**

TFAP2B (transcription factor AP-2 beta (activating enhancer binding protein 2 beta)) is a member of the AP-2 family of transcription factors which are important in retinoic acid-induced differentiation [Luscher et al., 1989; Mitchell et al., 1991]. This gene displayed 2.3-fold up-regulation in TBX5 / GATA-4 double knockdown embryos. TFAP2B is expressed in migrating neural crest cells which move into the aortic arches and contribute to the formation of a number of structures including the ductus arteriosus [Moser et al., 1997; Satoda et al., 2000]. Mutations in this gene are associated with Char syndrome in humans, an autosomal dominant disorder whose anomalies arise in neural crest cell derived regions [Satoda et al., 1999; Satoda et al., 2000]. These include patent ductus arteriosus (PDA), facial dysmorphism and hand abnormalities [Char, 1978]. Char syndrome is one of a number of 'heart-hand' disorders to include congenital heart defects and hand anomalies.

**PTPRZ1**

PTPRZ1 (protein tyrosine phosphatase, receptor-type, Z polypeptide 1) is a member of the receptor type protein tyrosine phosphatase family, encoding a single pass type I membrane protein. This gene displayed 6.1-fold up-regulation in response to double knockdown of TBX5 and GATA-4. PTPRZ1 expression has been reported in the brain [Kaplan et al., 1990; Krueger and Saito, 1992] and human umbilical vein cells (HUVEC) [Polykratis et al., 2005], and binds the developmentally regulated proteins midkine [Maeda et al., 1999] and pleiotrophin [Maeda et al., 1996]. These are heparin-binding growth factors with roles in neurite outgrowth [Li et al., 1990; Muramatsu and Muramatsu, 1991; Rauvala, 1989], plasminogen activity [Kojima et al., 1995], and oncogenic transformation [Chauhan et al., 1993; Kadomatsu et al., 1997]. Pleiotrophin has also been implicated in neuronal migration and EMT based on its expression pattern [Vanderwinden et al., 1992], and stimulates angiogenesis [Papadimitriou et al., 2001].

**FIGF**

FIGF (c-fos induced growth factor) or vascular endothelial growth factor D (VEGF-D) is a member of the PDGF/VEGF superfamily whose expression is induced by the nuclear oncogene c-fos [Orlandini et al., 1996]. In this study FIGF was up-regulated by 2.2-fold in response to double knockdown of TBX5 and GATA-4. FIGF acts via VEGFR2 and VEGFR3 receptors [Achen et al., 1998] to stimulate angiogenesis and lymphangiogenesis [Marconcini et al., 1999; Veikkola et al., 2001]. Studies of limb development in the chick have shown that FIGF is highly expressed in this region during embryogenesis [Trelles et al., 2002]. Broader studies in the developing mouse embryo have identified expression in various regions including the limbs, lungs, kidneys, liver, and presumptive endocardial cushions of the heart [Avantaggiato et al., 1998].

**NR2E1**

NR2E1 (nuclear receptor subfamily 2, group E, member 1) was up-regulated 2.8-fold in double knockdown embryos. This gene is a member of the orphan nuclear receptor gene superfamily and is required for cellular proliferation and differentiation of forebrain progenitor cells [Monaghan et al., 1997; Monaghan et al., 1995]. Mouse knockout of this gene results in impaired development of forebrain derived structures.

**LOC420770**

LOC420770 is a hypothetical chicken gene supported by EST evidence (GenBank ID: CR390114), up-regulated by 2.6 fold in response to TBX5 and GATA-4 double knockdown. The mRNA of this gene is 648 nucleotides in length and encodes a protein of 108 amino acids. A function has not yet been assigned to this gene.

**LOC419390**

LOC419390 is a hypothetical chicken gene supported by EST evidence (GenBank ID: CD740249), with similarity to hairy-and-enhancer-of-split related protein-7 (HES7) [Kim et al., 2009]. This gene was up-regulated by 2.7-fold in double knockdown

embryos. Hairy-and-enhancer-of-split genes belong to the basic helix-loop-helix superfamily, and the HES7 gene in humans acts as a repressor protein in Notch signalling [Davis and Turner, 2001]. Mutations in the human HES7 gene are associated with spondylocostal dystosis (SCD) [Sparrow et al., 2008], a congenital disorder characterised by abnormal vertebral segmentation (AVS) [Turnpenny et al., 2007]. LOC419390 may be a transcriptional repressor with a developmental function in the heart.

### **SUZ12**

SUZ12 (suppressor of zeste 12 homolog) was up-regulated by 2-fold following double knockdown of TBX5 / GATA-4. It encodes a zinc finger protein, recently classified as a member of the Polycomb group (PcG) of proteins which form multi-protein complexes that can regulate transcription through chromatin modification [Jenuwein and Allis, 2001]. SUZ12 is required for cell proliferation, and mouse knockout of this gene results in embryonic lethality [Pasini et al., 2004].

### **CRABP1**

CRABP1 (cellular retinoic acid binding protein 1) is a small cytoplasmic protein which binds to and can modulate levels of retinoic acid [Fiorella and Napoli, 1991]. This gene displayed 4.9-fold up-regulation in response to TBX5 / GATA-4 knockdown. CRABP1 expression in the mouse embryo is observed in regions derived from the neural crest [Lyn and Giguere, 1994]. Retinoic acid is a teratogen, and an excess leads to retinoic acid embryopathy (RAE), whose abnormalities include malformation of neural crest derived regions i.e. craniofacial, thymic and CNS structures, and conotruncal heart defects [Lammer et al., 1985]. CRABP1 levels are elevated in the cerebrospinal fluid of sufferers of Moyamoya disease (MMD) [Kim et al., 2003], a cerebrovascular condition characterised by progressive occlusion of the carotid artery (as a result of fibrosis and excess proliferation of smooth muscle cells) and formation of abnormal collateral vessels at the base of the brain [Suzuki and Takaku, 1969]. Retinoid signalling has been implicated in ventricular formation [Dyson et al., 1995].

There is evidence that retinoids can modulate expression of growth factors [Boyle et al., 2000], and a number of growth factors are elevated in MMD including basic fibroblast growth factor (bFGF) [Malek et al., 1997], transforming growth factor  $\beta$  (TGF $\beta$ ) [Hojo et al., 1998], and platelet derived growth factor (PDGF) [Aoyagi et al., 1993; Aoyagi et al., 1991].

### **GOLGA4**

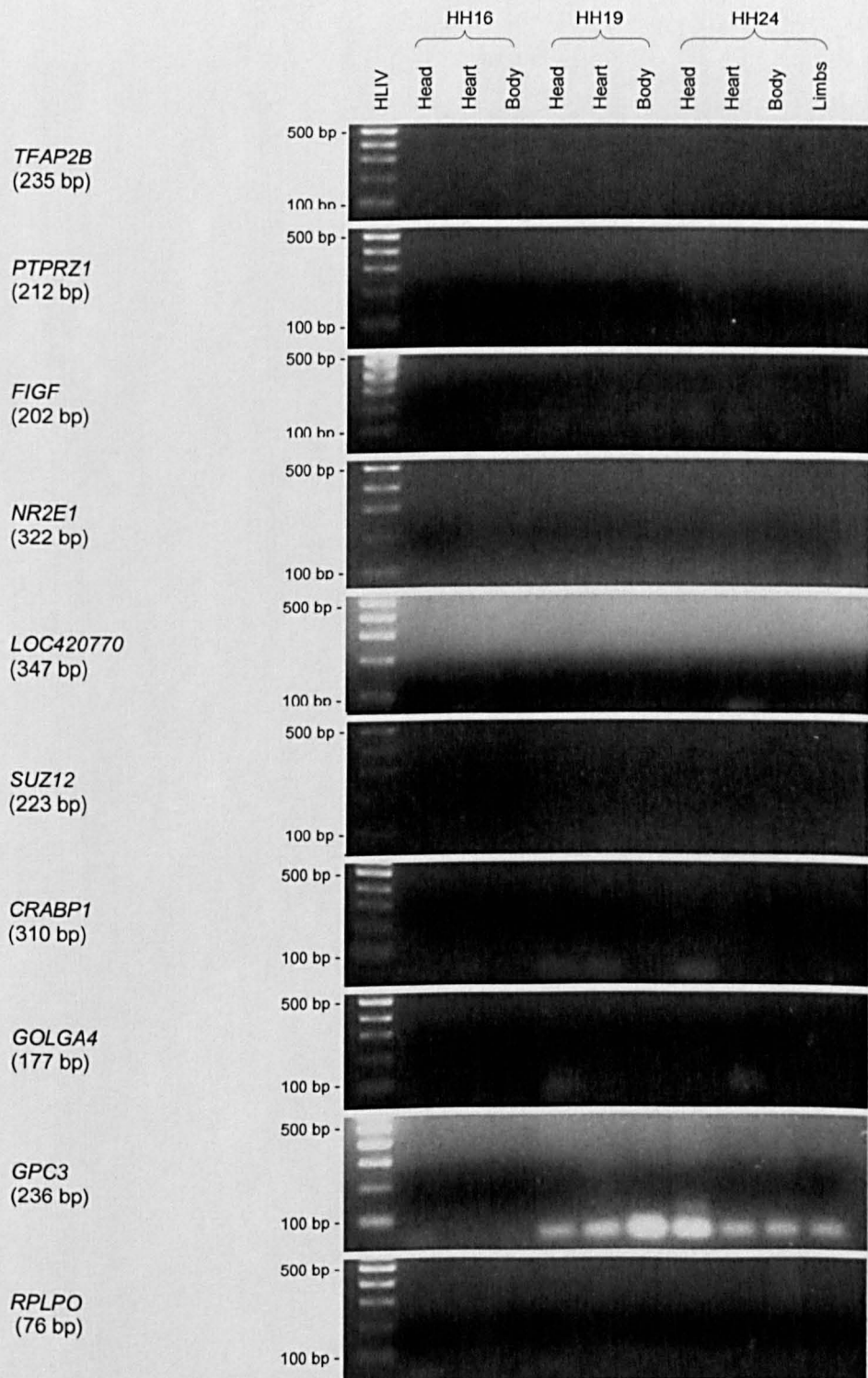
GOLGA4 (golgi autoantigen, golgin subfamily a, 4) is a member of the golgin protein family which localise with the golgi apparatus, helping to maintain its structure [Diao et al., 2003; Puthenveedu et al., 2006; Sohda et al., 2005], with an additional role in vesicle tethering [Sonnichsen et al., 1998]. GOLGA4 expression was up-regulated 2-fold in TBX5 / GATA-4 double knockdown embryos. GOLGA4 is important in protein transport [Kakinuma et al., 2004; Lieu et al., 2008].

### **GPC3**

GPC3 (glypican 3) is a member of the glypican family of cell surface heparan sulphate proteoglycans [David, 1993], which have roles in regulation of developmental growth and signalling [Selleck, 1999]. GPC3 was up-regulated 2.4-fold in TBX5 / GATA-4 double knockdown embryos. Mutations in this gene are associated with Simpson-Golabi-Behmel syndrome (SGBS) in humans [Pilia et al., 1996], an X linked disorder characterised by pre- and post-natal overgrowth, a characteristic facial appearance, and multiple congenital abnormalities including cardiac defects [Behmel et al., 1984; Golabi and Rosen, 1984; Neri et al., 1988]. Cardiac anomalies occur in approximately 50% of SGBS cases and include cardiovascular malformation, cardiomyopathy, and conduction defects [Lin et al., 1999]. Developmental expression of GPC3 in the mouse is observed in the organs that overgrow in SGBS, correlating with the phenotype of this disorder [Pellegrini et al., 1998]. GPC3 null mice display several of the clinical features of SGBS including developmental overgrowth, perinatal death, kidney malformations, and lung abnormalities [Cano-Gauci et al., 1999]. Congenital cardiac malformations such as VSDs, common AV canal, and DORV are also

observed, along with coronary vasculature defects [Ng et al., 2009]. There is evidence that GPC3 acts as a receptor for FGF9, a growth factor with a crucial role in mesenchymal differentiation [Colvin et al., 2001].

**Appendix J: Negative RT controls performed in parallel to expression profiling of candidate genes chick embryonic segments at HH16, HH19 and HH24**



Samples were electrophoresed on 2% agarose gels using Hyperladder IV as a size marker (500 bp and 100 bp bands are indicated). Negative RT controls (where reverse transcriptase enzyme was not added) did not display amplification for any of the assays.